



King's Research Portal

DOI:

[10.1152/physrev.00041.2017](https://doi.org/10.1152/physrev.00041.2017)

Document Version

Peer reviewed version

[Link to publication record in King's Research Portal](#)

Citation for published version (APA):

Keeley, T. P., & Mann, G. E. (2019). Defining physiological normoxia for improved translation of cell physiology to animal models and humans. *Physiological Reviews*, 99(1), 161-234.
<https://doi.org/10.1152/physrev.00041.2017>

Citing this paper

Please note that where the full-text provided on King's Research Portal is the Author Accepted Manuscript or Post-Print version this may differ from the final Published version. If citing, it is advised that you check and use the publisher's definitive version for pagination, volume/issue, and date of publication details. And where the final published version is provided on the Research Portal, if citing you are again advised to check the publisher's website for any subsequent corrections.

General rights

Copyright and moral rights for the publications made accessible in the Research Portal are retained by the authors and/or other copyright owners and it is a condition of accessing publications that users recognize and abide by the legal requirements associated with these rights.

- Users may download and print one copy of any publication from the Research Portal for the purpose of private study or research.
- You may not further distribute the material or use it for any profit-making activity or commercial gain
- You may freely distribute the URL identifying the publication in the Research Portal

Take down policy

If you believe that this document breaches copyright please contact librarypure@kcl.ac.uk providing details, and we will remove access to the work immediately and investigate your claim.

1
2
3
4
5
6
7
8
9
10
11
12
13
14
15
16
17
18
19
20
21
22
23

Defining physiological normoxia for improved translation of cell physiology to animal models and man

Thomas P. Keeley and Giovanni E. Mann

King's British Heart Foundation Centre of Research Excellence, School of Cardiovascular Sciences & Medicine, Faculty of Life Sciences & Medicine, King's College London, SE1 9NH, UK

Short title: Redefining hyperoxia, normoxia and hypoxia *in vitro*

Author for manuscript correspondence:
Prof Giovanni E. Mann, King's British Heart Foundation Centre of Research Excellence, School of Cardiovascular Sciences & Medicine, Faculty of Life Sciences & Medicine, King's College London, 150 Stamford Street, London SE1 9NH, U.K.

Correspondence:
Thomas P. Keeley, Email: thomas.keeley@ndm.ox.ac.uk
Giovanni E. Mann, Email: giovanni.mann@kcl.ac.uk

24 **Abstract**

25 The extensive oxygen gradient between the air we breathe (PO₂ ~21 kPa) and its ultimate
26 distribution within mitochondria (as low as ~0.5-1 kPa) is testament to the efforts expended in
27 limiting its inherent toxicity. It has long been recognised that cell culture undertaken under room air
28 conditions falls short of replicating this protection *in vitro*. Despite this, difficulty in accurately
29 determining the appropriate O₂ level(s) in which to culture cells, coupled with a lack of the
30 technology to replicate and maintain a physiological O₂ environment *in vitro*, has hindered
31 addressing this issue thus far. In this review, we aim to address the current understanding of tissue
32 PO₂ distribution *in vivo*, and summarize the attempts made to replicate these conditions *in vitro*.
33 The state-of-the-art techniques employed to accurately determine O₂ levels, as well as the issues
34 associated with reproducing physiological O₂ levels *in vitro*, are also critically reviewed. We aim to
35 provide the framework for researchers to undertake cell culture under O₂ levels relevant to specific
36 tissues and organs. We envisage that this review will facilitate a paradigm shift, enabling
37 translation of findings under physiological conditions *in vitro* to disease pathology and the design of
38 novel therapeutics.
39
40

41 **Table of Contents**

42 **I. Introduction3**

43 **II. Techniques to measure oxygen in cells and tissues4**

44 **III. Oxygen delivery *in vivo*.....8**

45 **IV. Understanding oxygenation *in vitro*.....12**

46 **V. Cellular oxygen sensing - when is low O₂ hypoxic?18**

47 **VI. Replicating normoxia *in vitro*.....22**

48 **VII. Conclusions and future research53**

49

50

51 **I. Introduction**

52 Although most organisms on Earth possess a carbon-based skeleton, oxygen fuels life. The
53 conversion of a CO₂-rich atmosphere to one containing precious O₂, initially by photosynthesising
54 cyanobacteria and later by plants, was the pivotal step in the evolution of multicellular life on
55 Earth (324). However, O₂ is an inherently dangerous molecule, and hence its utilization as a
56 metabolic substrate is closely associated with the development of highly efficient detection (e.g.
57 hypoxia inducible factors (516, 630)), defense (glutathione (195, 387) and antioxidant
58 enzymes (261)) systems. Despite this, the damage caused by a lifetime breathing O₂ may
59 ultimately affect lifespan (222, 324). Several excellent and comprehensive reviews have discussed
60 the various roles played by O₂ in mammalian physiology (59, 119, 333, 565, 594, 679, 699), and
61 thus these will not form the primary focus of this review article. Nevertheless, a brief overview is
62 important to inform the themes addressed herein.

63
64 The principle role of O₂ in mammalian physiology is as the terminal electron acceptor in the
65 electron transport chain. In this capacity, a single oxygen atom is reduced to H₂O in the presence
66 of 2 protons and 2 electrons. Such reductive/oxidative (redox) reactions are fundamental in O₂
67 physiology and are utilized by cytosolic enzymatic systems in addition to mitochondria. Aside from
68 molecular O₂, oxygen strongly influences cellular physiology through the formation of reactive
69 oxygen species (ROS). First considered merely as unwanted by-products of oxidative
70 phosphorylation and dysfunctional enzymatic reactions (222), reactive oxygen species are now
71 considered to play functional and non-redundant roles in cell signaling in physiology as reviewed
72 previously (119).

73
74 Our increased understanding of oxygen's role in human physiology is paralleled by the growing
75 number of primary research publications (see Figure 1). To date, over half a million research
76 articles reference oxygen as a keyword, and the number per year has steadily increased over the
77 last century. Attention has shifted from initial interests in the mechanisms of cellular O₂ utilization to
78 consequences associated with dysfunction in these processes leading ultimately to the production
79 of reactive oxygen species (Figure 1). Another key theme to have emerged is the concept of
80 hypoxia, a pathological reduction in O₂ availability now accepted as a hallmark of disease
81 conditions (522). Indeed, a significant proportion of O₂-related research still focuses on the
82 consequences of O₂ deprivation (Figure 1). In view of the importance of maintaining O₂ levels
83 within a finite range at the whole organism level, we here *readdress* the role of O₂ in mammalian
84 cell culture.

85
86 The invention of an O₂ sensitive electrodes (87), and in recent years phosphorescent
87 dyes (116, 610), has enabled researchers to resolve tissue O₂ distribution *in vivo*. Whilst incredibly
88 heterogeneous, at no point beyond the mouth is PO₂ equivalent to room air (20.9 kPa). Despite

89 this, the culture of mammalian cells is routinely conducted under atmospheric O₂, conditions
90 hyperoxic with respect to the tissue of origin. Although this discrepancy has been widely
91 acknowledged (215, 455, 633), only in recent years have primary research publications addressed
92 this issue directly (Figure 1 inset). A consensus approach to tackling this concept is still lacking,
93 largely plagued by incorrect nomenclature and widely differing experimental conditions. This
94 review aims to provide an insight into the current knowledge regarding tissue O₂ distribution *in*
95 *vivo*, and in doing so to redefine the term normoxia for more appropriate use in *in vitro*
96 experiments. Techniques used to monitor O₂ levels both *in vivo* and *in vitro* will be described
97 initially, followed by an overview of experimental issues associated with varying O₂ levels *in vitro*.
98 Physiological O₂ levels in numerous tissues and the existing literature concerning replication of
99 these conditions *in vitro* are summarised and critically discussed. The development of cell culture
100 techniques revolutionized medical science in the 1950s, yet maintenance of cultured cells or
101 tissues under non-physiological O₂ levels limits translation from bench to bedside. In many fields,
102 cell culture under atmospheric, room air O₂ levels has been assumed to reflect 'normoxia' largely
103 due to the complexity of conducting experiments in an oxygen-regulated workstation. This review
104 aims to readdress the conditions in which all mammalian cells should be cultured with the aim of
105 more effective translation of *in vitro* science into potentially life-saving therapies.

106

107 **II. Techniques to measure oxygen in cells and tissues**

108 Necessity often dictates that improvements in experimental techniques frequently precede
109 advances in scientific knowledge, and such is the case with oxygen related physiology (Figure 1).
110 The study of the physiology and biochemistry of molecular O₂ was aided immensely in the 1950's
111 by the development of O₂-sensitive electrodes, which allowed the direct quantification of O₂ levels
112 in biological fluids (87). A number of innovative techniques have since been developed, facilitating
113 more advanced experimental measurements with greater spatial and temporal resolution. Wire
114 electrodes can offer excellent spatial definition over a very small sample area, whereas
115 phosphorescence imaging techniques can offer greater stability over time and over a greater
116 sampling size. Notably, these techniques rarely monitor O₂ concentration directly but rather PO₂,
117 which is directly proportional to concentration, or hemoglobin saturation. The following section
118 outlines the basic principles of the most well established techniques currently used to monitor
119 cellular and tissue PO₂, providing a basis for discussion of data obtained using such equipment in
120 later sections.

121

122 **A. Oxygen sensitive electrodes**

123 The chemical reduction of molecular O₂ on a polarized (usually 0.6-7V) platinum cathode
124 generates a current proportional to the concentration of O₂ present. This concept led to the
125 development of O₂ sensitive electrodes in the early 1950's, consisting of a polarised platinum
126 cathode and non-polarizable silver anode (see Figure 2A). Although effective in determining

127 dissolved O₂, these early electrodes were not suitable for measuring tissue or blood O₂ due to the
128 accumulation of cells/proteins on the cathode limiting reactivity. This problem was solved by
129 Leland Clark and colleagues who, in 1953, described the fabrication of a platinum electrode with
130 an O₂-permeable cellophane coating (87)(Figure 2Ai). The addition of a selectively permeable
131 membrane permitted the measurement of PO₂, as O₂ must now diffuse across its partial pressure
132 gradient to react on the cathode. These electrodes, commonly referred to now as 'Clark
133 Electrodes', were greatly utilized for the measurement of liquid PO₂ for blood gas analysis and
134 early mitochondrial respiration experiments (73), yet their relatively large size (<1mm) prevented
135 accurate measurements of tissue PO₂. Efforts during the 1960's culminated in the introduction of
136 the 'Whalen' type electrode; a recessed-tip gold alloy cathode with a diameter of 1-
137 3µm (644)(Figure 2Aii). By attaching an O₂-electrode to a micromanipulator, tissue PO₂ histograms
138 were easily obtainable and rapidly became the preferred method for reporting PO₂ (see Section
139 VI). In recent decades, the use of electrodes has decreased in favor of newer techniques
140 (discussed below) due to the following disadvantages: (i) by virtue of their chemistry, electrodes
141 consume O₂ (proportional to their diameter) and therefore may be considered less reliable
142 especially when attempting to measure very low levels of O₂, (ii) the small sampling area means
143 measuring large areas of tissue is tedious, and (iii) many have shown that tissue penetration by
144 electrodes produces artefactual changes in tissue PO₂ resulting from blood vessel rupture or cell
145 disruption (266). The second point has been partially addressed through the development of the
146 'multiwire' platinum electrode (296), in which eight independent Clark type electrodes are housed
147 within a hemispherical structure of roughly ~50µm diameter. Whilst greatly increasing the sampling
148 area, these electrodes are confined to surface PO₂ measurements and hence their use is limited.

149

150 B. Hemo/myoglobin spectroscopy

151 Prior to the invention of O₂-sensitive electrodes, the only readout of blood oxygenation available
152 was the spectrophotometric analysis of hemoglobin (Hb), although this was only employed
153 clinically in the late 1970's following the development of the pulse oximeter by Aoyagi and
154 colleagues (13). This technique relies on the change in absorbance spectrum of hemoglobin upon
155 binding to O₂ (see Figure 2B), characterised by a reduction in absorbance in the red region (650-
156 700nm) and an increase in the near-infrared (900-1000nm) region. Isolation of the hemoglobin-
157 derived signal from intrinsic signals of the surrounding tissues and venous blood is achieved by
158 only measuring the pulsatile changes in absorbance. So called Pulse oximeters are extensively
159 used clinically to monitor peripheral arterial blood O₂ saturation, which is 95-99% in normoxic
160 patients. In the laboratory, a technique to measure Hb saturation in the microvasculature was
161 developed by Pittman and Duling in 1975 (460, 461), in which the effects of light scattering by red
162 blood cells was accounted for. A similar technique has also been used to measure myoglobin
163 saturation in cardiac and skeletal muscle (89, 252). In the context of defining tissue PO₂, Hb
164 saturation can be converted into approximate PO₂ based on the known Hb saturation curves for

165 the appropriate species (594), although this conversion is subject to changes in local pH/PCO₂ and
166 temperature and hence should be used with caution.

167

168 C. Fluorescent and phosphorescent probes

169 Optical techniques to monitor cellular and tissue PO₂ were developed by David Wilson and
170 colleagues in the late 1980's, who introduced platinum (Pt^{II}) and palladium (Pd^{II})-porphyrin based
171 probes which exhibit quenched phosphorescence in the presence of molecular O₂ (497, 610). These
172 have been complemented by similar complexes utilizing ruthenium (Ru^{II}) (348, 366, 580) or iridium
173 (Ir^{III}) (108), all of which can be conjugated to various macromolecular carriers or polymers to
174 improve solubility or phosphorescence yield. A complete description of O₂-sensitive lumiphores
175 can be found elsewhere (115). In principle, complexes are excitable in the UV range (350-410 nm)
176 and emit in the far red (630-700 nm) region, allowing excellent resolution in biological media, with
177 decay lifetimes in the μ s range. Typically, measurements are taken using time-resolved
178 phosphorescence, whereby the probe is excited and the O₂-sensitive decay in resultant emission
179 intensity resolved over time (see Figure 2C). First generation phosphorescent complexes were
180 hydrophilic and hence measurements were confined to the vasculature (535, 583), but subsequent
181 variations have generated hydrophobic equivalents that can penetrate the cell membrane, such as
182 Oxyphor G4 (136) or MitoXpress® INTRA (151). The addition of other chemical moieties to the
183 basic metal-porphyrin structure has also alleviated issues with non-specific protein binding that
184 altered the spectral properties of first generation compounds *in vivo* (115). With these,
185 simultaneous measurements of blood and tissue PO₂ have been reported (9), as well as
186 intracellular PO₂ within monolayers in culture (75, 151, 615). Ru^{II} complexes have largely been
187 utilized in the OxyLite™ probe, where they are immobilized in a sensor tip (~200 μ m in diameter)
188 and excited via a fibre-optic cable, functioning in an analogous manner to a traditional electrode.

189

190 D. Magnetic, paramagnetic and electron spin resonance

191 Positron emission tomography (PET), magnetic resonance imaging (MRI) and electron spin
192 resonance (ESR) techniques have been developed to image regions of hypoxia *in vivo*, as
193 reviewed elsewhere (60). Imaging using PET employs traditional biochemical markers of tissue
194 hypoxia, such as the imidazole compounds (see below), containing the radionucleotide ¹⁸F as a
195 short-lived source of protons. These compounds accumulate within regions of hypoxia and have
196 been useful in imaging tumor PO₂ in animal models and in the clinical setting (356). More recently,
197 ⁶⁴Cu containing bisthiosemicarbozones have been targeted as potentially useful markers of
198 hypoxia, with ⁶⁴Cu-ATSM showing high selectivity for regions of relative hypoxia in the ischemic
199 Langendorff heart (169) and atherosclerotic lesions in rodents (426), as well as tumors in
200 man (602). An example of ⁶⁴Cu-ATSM accumulation in the myocardial ischemic core is provided in
201 Figure 2D. MRI oximetry emerged in the late 1980s following the discovery that rates of relaxation
202 to perfluorocarbon (PFC) compounds were linearly related to PO₂ (572). When combined with

203 traditional ^1H MRI anatomical imaging, MRI oximetry can provide useful spatial resolution in both
204 animals and man (680). In the lungs, PO_2 distribution can also be monitored by MRI using inhaled
205 hyperpolarized ^3He , the decay of which is increased in the presence of O_2 (127) (see Figure 7). In
206 addition to using exogenous probes, deoxy-hemoglobin is a paramagnetic species itself, and its
207 relative proportion to oxyhemoglobin can be visualized as a disturbance in the transverse
208 relaxation time (T_2^*) of the surrounding protons in water. This led to the development of blood-
209 oxygen level dependent MRI imaging (BOLD-MRI) (436, 577) which uses standard MRI protocols
210 to monitor changes in hemoglobin saturation, and is widely used clinically. One major advantage of
211 BOLD-MRI over PFC-MRI and PET is that it does not require the introduction of an exogenous
212 probe, mitigating fears over chemical or radioactive toxicity. Unfortunately, BOLD-MRI is not
213 capable of determining absolute fluid PO_2 and hence cannot be used to monitor tissue PO_2 .
214 Molecular O_2 is weakly paramagnetic itself, and can be detected as a small but definitive increase
215 in the longitudinal relaxation time (T_1) of the surrounding protons, first identified using NMR (590)
216 and later confirmed using MRI (267, 432, 656). Notably, changes in T_1 rates occur under
217 conditions in which very limited increases in Hb saturation (and therefore T_2^* rates) were
218 detected (656). Whilst this technique has been used to determine absolute increases in O_2 content
219 (ml/L blood) following hyperoxic inspiration, it has had limited application to determine absolute
220 physiological tissue O_2 concentration. Varying T_1 times were reported in the liver, kidney and
221 muscle of rabbits which, when combined with simultaneous measurements of T_2^* rates, may be
222 indicative of tissue PO_2 (432, 656).

223

224 Much like PET and PFC-MRI, ESR oximetry relies on the interaction between a probe and
225 molecular O_2 . The most commonly used probes to measure PO_2 using ESR are lithium based
226 cyanines (LiXC) and india ink (8), which are biocompatible particulate probes and have been used
227 to report tissue PO_2 in liver (275), heart (487), lungs (487), digestive tract (228) and bone (360).
228 The presence of O_2 in close proximity to the ESR probe causes a broadening of the probe
229 spectrum, measurable in the line-width, which is directly proportional to PO_2 . Hence, unlike PET
230 and MRI, ESR permits the direct quantification of tissue PO_2 , and can be used for long periods of
231 time due to the inert and stable nature of the spin probes (8). Unfortunately, the complex and
232 costly equipment required to detect spin resonance limits the application of ESR to specialized
233 facilities.

234

235 E. Immunohistochemical methods

236 The techniques discussed so far have been developed to monitor relative or absolute tissue PO_2 .
237 Complimentary to these has been the immunohistochemical identification of hypoxic areas using
238 exogenous dyes like pimonidazole or EF5 (357, 474) or antibodies raised against known hypoxia-
239 inducible target proteins such as HIF or CA9, which rely on the cellular response to lowered O_2
240 levels rather than the absolute PO_2 . Pimonidazole and EF5 are 2-nitromidazole derivatives

241 containing a NO₂ group attached to an imidazole ring, which undergoes rapid reduction to produce
242 a highly reactive intermediate species that will react with any macromolecule in the vicinity. At a
243 PO₂ ~>1.5 kPa O₂, this reduction is prevented and thus 2-nitromidazole staining is selective for
244 regions of severe hypoxia. When sections of hypoxic tissue are co-stained with pimonidazole and
245 a hypoxia-inducible protein such as HIF-1α or CA9, distinct and mildly overlapping regions are
246 observed (see Figure 2E), suggesting that the two probes are marking areas of differing severity of
247 hypoxia (253, 545). Although the nature of pimonidazole O₂ sensitivity has been considered
248 reasonably binary (staining is either present or absent), gradients in intensity corresponding to
249 measurable gradients in PO₂ have been reported across the intestinal wall (294). This tissue is
250 reported to be severely hypoxic (see Section VI-G-2), and hence it is possible that differences in
251 staining intensity may be resolved within the reported range (PO₂ 0-1.5 kPa). A disadvantage in
252 the use of 2-nitromidazole compounds to identify hypoxic tissue is that staining requires live cells,
253 thus the dye must be injected prior to samples being collected. This limits its use in retrospectively
254 identifying hypoxic areas in tissue specimens already collected or in patient samples. A caveat to
255 the use of immunostaining members of the HIF pathway as a marker of tissue hypoxia is the well-
256 described potential of HIF-1α to be stabilized under oxygenated conditions, most notably during
257 inflammation due to crosstalk with NFκB and direct effects of reactive oxygen species (44, 607).
258 Hence, results obtained using HIF-based immunostaining should always be confirmed with an
259 alternative method.

260 261 **III. Oxygen delivery *in vivo***

262 A basic understanding of the delivery of O₂ from the atmosphere to the cytosol is fundamental for
263 interpreting specific tissue O₂ distribution. Moreover, insights into O₂ transport *in vivo* provide a
264 useful perspective for some of the challenges associated with oxygenation of cell monolayers *in*
265 *vitro*. A point worth clarifying prior to any detailed further discussion is the difference between the
266 terms saturation, concentration and content as commonly used throughout physiology, and partial
267 pressure used universally. In mammals O₂ is transported in two forms: bound to hemoglobin (Hb)
268 and dissolved in blood. Saturation refers to the **percentage** of total number of Hb bindings sites
269 saturated with O₂ (4 moles O₂ bind to 1 mole Hb), noting that Hb saturation occurs in continuum
270 until all molecules are saturated. This unit does not strictly measure the concentration of O₂
271 present (although this can be inferred), but is a good measurement of total blood O₂ content.
272 Although convention is to express components of a chemical reaction as a concentration (in moles
273 per L, for example), O₂ should be reported as **partial pressure** (in mmHg, torr or kPa, Figure 5A)
274 in physiology, noting the final dissolved gaseous concentration in a liquid is proportional to its
275 partial pressure within the corresponding gas phase (Henry's Law (235), taking into account
276 changes in temperature and solubility, Section IV-B). This is because the chemical potential of
277 physiological gases is determined by their partial pressure, and as such they will diffuse down
278 pressure, not concentration, gradients. Content refers to the total amount of O₂, in **ml/100ml**, that

blood can carry, combining that bound to hemoglobin with that dissolved in plasma according to the following equation:

$$cO_2 = ([O_2]_{max} \times [Hb] \times SO_2 \times 0.01) + (H \times PO_2) \quad (1)$$

where the maximal O₂ carrying capacity of blood ([O₂]_{max}) is 1.31-1.36 ml O₂/g hemoglobin, otherwise known as Hüfner's constant (110, 194), and *H* is the Henry's Law constant for O₂ (0.023 ml/kPa/100ml blood). Human blood contains on average 14-15 g hemoglobin per 100 ml (194, 604), therefore the O₂ content (cO₂) of fully O₂-saturated (SO₂ ~100%) arterial blood = (1.34 x 15 x 100 x 0.01) + (0.023 x 13) = 20.4 ml/100 ml blood. Note that O₂ content is also expressed in units of concentration (ml/100ml), but differs from the traditional use of O₂ concentration which typically refers to only dissolved O₂ in solution.

With these three terms defined, the disparity between O₂ delivery *in vivo* and *in vitro* becomes readily apparent. In the absence of hemoglobin *in vitro*, O₂ delivery to the cell monolayer is defined largely by the PO₂ of the culture medium directly adjacent and therefore the total available O₂ is considerably lower, e.g. cO₂ = 0.48 ml/100 ml medium under standard atmospheric conditions. The issue of O₂ delivery *in vitro* will be discussed in more detail in Section IV. As cells cannot access O₂ bound to Hb, total O₂ content is not a particularly useful unit to use when comparing *in vivo* and *in vitro* O₂ conditions at the cellular level. Ideally, [O₂] should be defined in units of partial pressure (mmHg or kPa) in compliance with Henry's Law (235). However, the majority of biologists prefer to express gas concentrations *in vitro* as % of atmospheric composition, i.e. *cultured in a standard 37°C, 5% CO₂ incubator*. As O₂ expressed as % ≈ kPa at sea level (see Figure 5A), we have standardized the expression of [O₂] in kPa units in this review.

A. From air to blood

Even before entering the circulation, humidification of incoming air within the trachea reduces PO₂, and the introduction of CO₂ (~5 kPa) within the alveoli reduces this further (Figure 3A). Hence the gradient between atmosphere and alveoli can be described according to the following equations:

$$PO_{2(trachea)} = (P_{atm} - P_{H_2O}) \times F_iO_2 \quad (2)$$

$$PO_{2(alveoli)} = PO_{2(trachea)} - (PCO_2 / RQ) \quad (3)$$

where atmospheric pressure (P_{atm}) is 101.325 kPa at sea level, normal water vapor partial pressure (P_{H₂O}) is ~6.2 kPa and the fraction of O₂ in inspired air (F_iO₂) is 0.209. Thus PO_{2(trachea)} is normally ~19.9 kPa. As this inspired air mixes with expired air containing CO₂ (PCO₂ ~5 kPa) when respiring with mixed carbohydrate/fat fuel (RQ, respiratory quotient 0.8), the PO₂ is reduced further to ~13.3 kPa. A proportion of venous (deoxygenated) blood from the microvasculature supplying the larger airway and lung adventitia drains into the pulmonary vein rather than the bronchial vein (19, 76). Because of this nuance in lung perfusion, known as pulmonary venous admixture or

320 shunt, a small gradient exists between the alveoli and arterial PO_2 (usually <1.3 kPa) in healthy
321 adults), spoiling an otherwise remarkably efficient exchange. Taken together, the passage of O_2
322 from air to the blood results in a gradient of ~ 9 kPa, the largest such gradient in mammalian
323 physiology.

324

325 B. From blood to cytosol

326 1. Longitudinal gradients within the vasculature

327 The subject of intravascular O_2 gradients has been reviewed elegantly by Tsai et al. (2003), and as
328 such will only be described briefly in this review. Duling and Berne (1970) were the first to
329 demonstrate experimentally a significant loss of oxygen from the arteriolar circulation. They and
330 many others subsequently established that (i) there is a significant decrease in O_2 between the
331 systemic arterial circulation and arteriolar vessels (43, 123, 124, 263, 325, 459), which is
332 proportional to luminal diameter (124, 500) and inversely proportional to red blood cell
333 velocity/blood flow (295, 584); (ii) the difference between terminal arteriolar and post-capillary
334 venular O_2 is minimal (325, 534), as is the gradient between capillary and tissue O_2 (43, 325); (iii)
335 the next largest tissue compartment outside the lungs in which a significant O_2 gradient is
336 observed is the vascular wall of arterioles (99, 124, 428, 507, 532, 592), which is proportional to
337 the thickness of the arteriolar wall (124); and (iv) A post-capillary diffusional shunt occurs in most
338 microvascular beds, in which a portion of O_2 from saturated arterioles diffuses into venules running
339 parallel (131, 534). Furthermore, measurements of O_2 saturation in red blood cells by absorption at
340 555 nm (460, 461) confirm that Hb saturation falls proportionally with dissolved O_2 (457). Based on
341 these observations, the arteriolar network appears to play more of a role in the delivery of O_2 to
342 the tissue than previously considered (500), and there may even be a role for post-capillary
343 venules in homogenizing tissue PO_2 (328). This was first noted following the observation that the
344 relationship between venular diameter and luminal PO_2 was opposite to that described for
345 arteriolar vessels. In other words, blood PO_2 increases between post-capillary and collecting
346 venules (43, 131, 295, 325, 532, 534, 622). However, it must be noted that blood entering the
347 arteriolar network has a PO_2 above the steepest part of the O_2 dissociation curve of hemoglobin
348 (see Figure 4B), and therefore it is hard to reconcile how so much O_2 is transferred to the
349 surrounding tissues from these vessels unless only the transfer of dissolved O_2 is being measured.
350 Moreover, one must also weigh up the influence of the magnitude of the vascular wall PO_2 gradient
351 (the argument in favour of arteriolar O_2 delivery) against the raw number of vessels (capillaries
352 vastly out-number arterioles) when concluding the relative contribution of each type of vessel to
353 tissue O_2 delivery.

354

355 2. Radial gradients across and within the vascular wall

356 The evidence for longitudinal O_2 gradients within the vasculature is complimented by the finding of
357 significant radial, or transmural, gradients across the vascular wall. Radial gradients have been

358 reported in the rabbit aortic wall (99, 428, 508), cat pial vessels (124), dog carotid arteries (507),
359 dog femoral arteries (410) rat mesenteric arterioles (592) and rat cortical microvessels (622).
360 Elegant work by Niinikoski et al. (428) and Santilli et al. (507, 508) using electrode penetration of
361 the vascular wall demonstrated the existence of a substantial drop in O_2 between the lumen and a
362 very thin tissue layer directly adjacent, attributed by the authors to the endothelium, although the
363 magnitude of this drop has been questioned subsequently (see Section VI-B-1). Nevertheless, a
364 mismatch between intimal and luminal PO_2 would suggest inefficient transfer of O_2 from blood to
365 cell. A physical barrier at the tissue level seems highly unlikely since a high O_2 diffusion resistance
366 of the vascular wall would result in higher downstream PO_2 than observed (592), and O_2 is freely
367 soluble in the plasma membrane (562).

368
369 The transfer of O_2 between the lumen and the endothelial cell initially involves the dissociation of
370 O_2 from hemoglobin. Considering the well-characterized O_2 dissociation curve for hemoglobin
371 (Figure 4B), it is clear that arterial blood exists at a sufficiently high PO_2 to prevent substantial O_2
372 dissociation from hemoglobin, as intended in such conduit vessels. Although this relationship can
373 vary with changes in local pH/ CO_2 (the Bohr Shift), it is unlikely that such changes would lead to
374 large dissociations at such a high blood PO_2 (see Figure 4B). Moreover, measurements of luminal
375 PO_2 as referenced above reflect *dissolved* PO_2 rather than that stored in hemoglobin (total O_2
376 content). Thus the large drop in PO_2 between lumen and endothelial cell cannot be explained by
377 limited dissociation from hemoglobin. The relative contribution of vascular wall/tissue O_2
378 consumption to this large decline is not fully agreed upon, as reviewed elegantly
379 elsewhere (456, 594, 603). There is general disagreement as to whether the vascular wall can
380 consume enough O_2 to account for the large radial gradient detected, with large differences
381 between cultured cells, tissue segments and *in vivo* measurements clouding any consensus
382 (summarised elegantly by Vadapalli and colleagues (603)). Differences in experimental technique
383 and interpretation can certainly account for some of this variation (see Section VI-B-1 for a more
384 detailed discussion), leading to the conclusion that many reported measurements of vascular wall
385 O_2 consumption may be overestimated (456, 603). It therefore seems unlikely that this alone is
386 sufficient to drive the large radial gradients alone. Recent evidence indicates that the major barrier
387 to the transfer of O_2 from the lumen to tissue may in fact be the plasma phase of blood. This was
388 first proposed by Hellums (231) who hypothesised that plasma (in which O_2 is poorly soluble)
389 represents a significant barrier between the red blood cell and endothelium. In this model dissolved
390 O_2 fluctuates as a function of hematocrit, with so-called erythrocyte-associated transients
391 increasing PO_2 near red blood cells and gradients extending in-between. Such theories were
392 corroborated by others (148, 405) and later demonstrated experimentally (22, 184, 328). In large
393 vessels with wall thickness large enough to prevent efficient oxygenation of the vascular cells by
394 diffusion alone, O_2 is supplied via the vasa vasorum as opposed to directly from the
395 lumen (58, 230, 410), as discussed in detail in Section VI-B-1.

396

397 *3. From vessel to cytosol*

398 The largest O_2 gradient in the vascular network is across the arteriolar wall, implicating these
399 vessels as primary sites for O_2 delivery. However, the smaller overall area of arteriolar networks
400 compared to capillaries dictates that large heterogeneity should therefore exist in tissue PO_2 , with
401 large gradients extending between arteriolar vessels. O_2 transport between the capillary and tissue
402 was first addressed by Krogh (316), in his now seminal description of the cylinder model. These
403 relatively simple models tend to oversimplify, since microvascular networks are rarely uniformly
404 distributed (except perhaps in skeletal muscle), but rather display a more 'disorganised' network.
405 Moreover, Krogh's model assumed that longitudinal gradients occur along the length of capillaries,
406 which we now know not necessarily the case. The presence of both longitudinal and radial
407 gradients in the vasculature, and diffusional transfer of O_2 between neighbouring arterioles,
408 capillaries and venules, results in a reasonably narrow Gaussian tissue PO_2 distribution (593). The
409 lack of substantial intra-tissue PO_2 heterogeneity is of physiological significance, since an
410 implication of Krogh's model of tissue O_2 distribution is that tissue close to the venular end of the
411 microvascular network would be at a distinct disadvantage in terms of PO_2 . Of course, this
412 viewpoint is still over-simplified as neither tissue perfusion, i.e. the number of microvascular
413 vessels per cm^3 tissue, nor is cellular O_2 demand generally homogeneous, and thus tissue PO_2
414 gradients can still form especially in larger organs and under uncontrolled tumor growth (as will be
415 discussed in Section VI). PO_2 distribution in different organs/tissues will be discussed in later
416 sections.

417

418 **IV. Understanding oxygenation *in vitro***

419 A reoccurring theme throughout this review will be the complex nature of cellular oxygenation *in*
420 *vitro*. The combined effects of a static layer of medium above an O_2 consuming monolayer of cells,
421 and poor solubility of O_2 leads to the formation of a gradient between the atmosphere and
422 intracellular environment (10, 75, 420). In some cases, this gradient can be substantial enough to
423 significantly reduce intracellular PO_2 below ambient, used herein analogously to head-space to
424 refer to the gas phase immediately adjacent to the medium. Thus intracellular oxygenation, and not
425 ambient PO_2 , is the key parameter to consider when designing research under low O_2
426 environments. This section will address some of the nuances associated with achieving the
427 desired *intracellular* O_2 level *in vitro* to recapitulate levels *in vivo*.

428

429 A. What is the PO_2 in room air?

430 The often quoted 20.9 kPa refers strictly to standard 'dry' atmospheric air (see Figure 5B).
431 However, most cell culture is conducted within a controlled atmosphere of 95% air: 5% CO_2 .
432 Moreover, incubators are normally run at 75% humidity (compared to ~50% at room air) to prevent
433 excessive evaporation of medium. Considering this, the actual PO_2 within a standard cell culture

incubator is ~18.5 kPa (at sea level, Figure 5) (377, 420). This value is even lower at high altitude, as the water vapor and CO₂ components are a constant ~47/35 mmHg even under reduced atmospheric pressure. Most atmosphere-regulated cell culture chambers used to perform research under O₂ conditions different from atmospheric alter the PO₂ at the expense of nitrogen, thereby maintaining atmospheric pressure. Moreover, many are engineered to run at slightly higher atmospheric pressure at sea level (101.33-101.78 kPa) to obviate fluctuations in PO₂ due to changes in altitude.

B. Achieving the appropriate dissolved O₂ level *in vitro*

Modulating the gaseous atmosphere with respect to O₂ is straightforward, yet cells do not exist in contact with O₂ in the gas phase, with the possible exception of lung epithelial cells (see Section VI-A). The evolution of red cells as an intricate and highly efficient O₂ transporter bears testament to the poor solubility of this gas in solution. In contrast to CO₂, which reaches equilibrium in solution within minutes, O₂ dissolves too slowly to be overlooked in experimental protocols.

1. Factors affecting O₂ solubility

Efforts to determine O₂ solubility are spear-headed by oceanography and hydrometallurgy communities, with O₂ in solution used for numerous industrial processes. Initially defined by Henry's Law (235) (see Section III-A), the solubility of a gas in pure water is related to the temperature of water and the gaseous pressure. Such relationships have been confirmed more recently, both experimentally and computationally (see Battino (1981) (25) and Ming and Zhenhao (2010) (399) for a review), and are illustrated in Figure 5C. The relationship between temperature, pressure and O₂ solubility is further defined by the Bunsen adsorption coefficient (α , measured in dm³.dm⁻³.kPa⁻¹). From α , the solubility of O₂ (S_{O2}) is defined here in $\mu\text{mol}.\text{dm}^{-3}.\text{kPa}^{-1}$ by:

$$\begin{aligned} S_{O_2} &= \alpha / (\text{molar volume} \times 101.325) [O_2 \text{ molar volume} = 22.393] \\ S_{O_2} &= \alpha / 2269.9 \end{aligned} \quad (4)$$

This initial equation was refined further by Benson and Krause (32, 33), in their proposal of *units of standard concentration* (c^*), defined as the concentration of dissolved O₂ per volume of solution. As such, cO₂^{*} in pure water under standard atmospheric conditions is defined as:

$$cO_2^* = S_{O_2} \times (P_{\text{atm}} - P_{\text{H}_2\text{O}}) \times FO_2 \quad (5)$$

Temperature also strongly impacts the PH₂O of a given atmosphere, with higher temperature increasing evaporation and thus increasing PH₂O at the expense of O₂. The salinity of a solution also impacts O₂ solubility, as demonstrated in pioneering work from Sechenov (524) and tabulated for convenience elsewhere (399). With relevance to physiology, the vast majority of experimental work is conducted in solutions of a reasonably similar salinity and thus this factor can be assumed constant. As shown in Figure 5C, the solubility of O₂ in pure water at 37°C is approximately 77% that at 20°C, resulting in ~30% less O₂ in solution. This merits consideration when comparing

475 experimental data derived at room temperature with that at 37°C. Moreover, with relevance to
476 Section IV-B-2, the equilibration of culture medium from room air to physiological O₂ levels is
477 significantly more time-efficient when the solutions are cooled to 4°C.

478

479 2. *Equilibration in solution*

480 Mass diffusion was first described by Fick in 1855, in a seminal piece of work from which we now
481 derive Fick's laws of diffusion (153). In the absence of cells, O₂ equilibration between atmosphere
482 and medium follows Fick's second law, and can therefore be estimated using a one-dimension,
483 single compartment diffusion model. This is described by the equation $Q=AK((C_s-C)/d)$ (458),
484 where Q is the rate of O₂ diffusion ($\mu\text{M min}^{-1}$), A is the surface area (cm^2), K is Krogh's constant,
485 derived from the diffusivity and solubility of O₂, C_s and C are the saturating and desired PO₂ (kPa),
486 respectively, and d is the depth of the medium (cm). To frame this scenario in the context of *in vitro*
487 cell culture, imagine a 90 mm petri dish filled with 20 ml medium and placed within a sealed
488 chamber at a PO₂ of 5 kPa. Using Fick's laws, we can estimate that this medium will take ~2 h to
489 equilibrate to 5 kPa, as shown in Figure 5D, in agreement with experimentally derived
490 values (10, 420). This rate can be increased by dividing the 20 ml into two 90 mm petri dishes,
491 thereby doubling the effective surface area for diffusion. Dissolved O₂ levels achieved in culture
492 medium are a critical and often under-estimated factor in conducting experiments under low O₂
493 conditions aimed at recapitulating O₂ levels *in vivo*. Thus, addition of poorly equilibrated, overly
494 oxygenated medium to cells pre-adapted to low O₂ conditions may generate a reaction akin to the
495 reoxygenation phenomena observed during stroke and myocardial infarction.

496

497 3. *Accounting for plastic leaching*

498 The equations described above assume that the only path by which O₂ equilibrates in solution is
499 through the gas-liquid interface. Whilst by far the most important source, plastic is not completely
500 impermeable to O₂, and hence O₂ can diffuse through the sides and bottom of culture dishes to
501 varying degrees. This is largely deemed negligible by most researchers based on the extremely
502 low diffusivity and solubility coefficients of standard polystyrene culture-ware (see Table 1-1). The
503 effect of substrate O₂ permeability on pericellular PO₂, specifically comparing 'impermeable'
504 polystyrene with permeable substrates such as silicone rubber or Teflon membranes, has been
505 demonstrated mathematically (274, 466) and experimentally (659, 690). Notably, Powers et
506 al. (466) incorporated substrate permeability into the most widely adopted mathematical model to
507 determine pericellular PO₂ (672), accounting for the surface area in contact with cells and
508 substrate O₂ diffusivity and solubility. This was intentionally left out in Table 1-2 for greater clarity,
509 but essentially involves an additional α value for the substrate. When monolayer O₂ consumption
510 substantially outweighs O₂ diffusion capacity, using a gas-permeable culture substrate can be an
511 effective way to minimise unintentionally hypoxic conditions. On a separate note, plastic-ware left
512 at room air (PO₂ 20 kPa) will accumulate a significant amount of O₂ and this will eventually leach

out when placed in an environment of lower PO_2 , thus acting as a O_2 source (558). When plastic equilibrated to 20 kPa was placed within an anoxic water solution, dissolved PO_2 reached ~12 kPa after 60 h (558). Although specific rates of leaching will depend on the plastic composition and its mass/surface, it is highly advised that when working with cells pre-adapted to a specific low PO_2 , all plastic-ware (pipette tips, stripettes, petri dishes, culture flasks) be pre-equilibrated at the appropriate PO_2 prior to use. This is of particular importance when working with near anoxic conditions, where even small amounts of O_2 leaching can severely compromise experiments, and we would always recommend measuring PO_2 in the medium/monolayer under such conditions to be confident a sufficiently low PO_2 is achieved and maintained.

C. Accommodating O_2 diffusion and monolayer consumption

One of the most common, and incorrect, assumptions made during *in vitro* research is that intracellular PO_2 and ambient PO_2 are synonymous. The consumption of O_2 by cells, coupled to the poor solubility of O_2 in solution, generates a gradient between the head-space and monolayer proportional to the rate of monolayer O_2 consumption (389). Without compensation, cell cultures may inadvertently experience 'culture-induced' hypoxia by consuming O_2 faster than it can diffuse, as discussed in Section IV-D. Under these conditions, it may become difficult to differentiate the cellular response to physiological and hypoxic O_2 levels, resulting in incorrect interpretations. Compounding this problem has been the lack of technology to accurately monitor intracellular O_2 levels in living cells (see Section II). In lieu of physical measurements, many have relied on an derivation of Fick's second law to predict pericellular PO_2 in monolayers cultured under static conditions (26, 199, 371, 384, 389, 421, 466, 559, 596, 659, 672). By considering oxygen diffusion within a culture dish as a one-dimensional diffusion-reaction, cell boundary O_2 levels can be predicted and, given that O_2 can freely diffuse across the plasma membrane (562), this approximately equates to generalised intracellular O_2 levels (Figure 6A). Although exact equations differ between studies (summarized in Table 1-2), the common critical variables in determining pericellular PO_2 were always, as expected, ambient PO_2 , cell density, cellular O_2 consumption and medium height. The most comprehensive equation to date has been put forward by Powers et al. (466), in which the equation by Yarmush and colleagues (672) was adapted to reflect the change in cellular O_2 consumption as a function of ambient PO_2 . Common to a number of such studies was the conclusion that hepatocyte monolayers (rabbit (559), human (672) and HepG2/3B cell lines (389)) are most likely severely hypoxic even when cultured under room air, which has subsequently been demonstrated experimentally (see Section VI-E).

These theoretical observations have been corroborated using electrode and fluorescence based probes to experimentally determine pericellular PO_2 in monolayer cultures. Increased cell density has been shown to decrease pericellular PO_2 in monolayers of rat hepatocytes (250, 421), human dermal fibroblasts (581), T-47D breast cancer cells (453), and peripheral blood mononuclear

551 cells (64). Notably, comparisons between cell types (389) revealed the importance of considering
552 cell-type specific differences in density at confluence in addition to O₂ consumption rate per cell.
553 Although mesangial cells had similar O₂ consumption rates to Hep3B cells (~9 nmol/min/mg
554 protein), vastly different pericellular PO₂ (14.6 vs ~0 kPa at room air) results from differences in
555 monolayer protein content, reflecting morphological differences in cell types (389). The other
556 significant variable, fluid height, has also been confirmed experimentally (77, 371, 389, 421, 581)
557 and is likely the most easily controlled to maintain the appropriate pericellular PO₂. Using the
558 equation first described by Stevens in 1965 (559), one can calculate the required medium height to
559 achieve the desired pericellular PO₂ as recently reviewed (462). Other methods to control
560 pericellular PO₂ include varying the permeability of the base substrate (466, 659) to bypass the
561 need for O₂ to diffuse through the medium, and increasing ambient PO₂ to compensate for
562 monolayer consumption and poor diffusivity (75).

563
564 As illustrated in Figure 6B, cellular O₂ consumption rates vary considerably between cell types;
565 from 4×10^{-5} -0.02 amol O₂ cell⁻¹ s⁻¹ in red blood cells (179, 510) to as high as 200-500 in
566 cardiomyocytes and hepatocytes (20, 165, 200, 478). These differences between cell types most
567 likely arise from differences in metabolic activity and mitochondrial content/density. As monolayer
568 O₂ consumption is a major determinant of O₂ diffusion and ultimately pericellular PO₂, low
569 consuming cell types are likely to experience much greater intracellular PO₂ than those that
570 consume O₂ more rapidly when placed in the same environment. Sekine and colleagues (521)
571 illustrate this concept by comparing pericellular PO₂ values and oxygen consumption rates in
572 monolayers of hiPSC-cardiomyocytes, rat cardiomyocytes, human aortic smooth muscle cells and
573 cardiac fibroblasts. Cardiomyocyte monolayers consume significantly more O₂ than the non-
574 cardiomyocyte cell types and this is reflected in a much steeper gradient between ambient and
575 pericellular PO₂ (see Figure 6B). Similar results were obtained when comparing medium PO₂ in
576 monolayers of human umbilical vein endothelial cells (HUVEC, low consuming, large size) and
577 human embryonic stem cells (hESC, high consuming, small size) (2). If cellular O₂ consumption
578 significantly outweighs O₂ diffusion capacity, a condition of 'self-inflicted hypoxia' may arise at
579 sufficiently low ambient PO₂ (77, 421)(Figure 6B). In reality, since cellular O₂ consumption
580 decreases with ambient PO₂ (88, 211, 441, 443), the accuracy of many of the predictions (which
581 assume a constant rate of O₂ consumption) are limited under extreme hypoxia. It is more likely that
582 under these conditions, intracellular O₂ levels in high-consuming cell types range around a value
583 more conducive to viability, under the control of negative feedback mechanisms orchestrated by
584 HIF (178). In support of this, rat hepatocytes cultured at a PO₂ of 4 kPa stain strongly with the
585 hypoxic marker hypoxypoint (indicating cytosolic PO₂ below 1 kPa) but retain reasonable viability,
586 suggesting a sufficient supply of O₂ to maintain function (421).

587

588 One technique used extensively to alleviate problems associated with poor oxygenation *in vitro*
589 has been the use of 'bioreactor' type culture conditions, in which medium is continuously stirred.
590 Under these conditions cellular oxygenation can occur through convection in addition to diffusion,
591 greatly increasing O₂ supply (172). Medium agitation also forms a critical component of a
592 successful microbial culture system, where bacterial or fungal cells are cultured in suspension at
593 very high densities and therefore require additional oxygenation. Such conditions are not generally
594 appropriate for the majority of adherent cell lines without prior immobilization (see bio-artificial
595 livers for an example (579)), although some success has been obtained using roller bottle
596 technology, in which adherent cells are cultured on the side of a cylindrical device placed
597 horizontally on an orbital shaker (175, 462). Furthermore, microfluidic perfusion has received
598 increasing attention in recent years and also solves several problems associated with monolayer
599 oxygenation, especially when constructed using plastic with a high O₂ permeability coefficient.
600 Many of these techniques can create adequate monolayer oxygenation even though more effort
601 and expense is required,, and thereby provide more accessible means of altering existing culture
602 conditions to improve oxygenation.

603

604 D. Evidence for compromised oxygen delivery *in vitro*

605 As eluded to above, the concept of 'self-inflicted' hypoxia is not restricted to theory. Confluent
606 HepG2 cultures rapidly (within 1 h) deplete medium PO₂ to <0.1 kPa even at an ambient PO₂ of
607 ~20 kPa. In these studies, an hypoxic status was confirmed by continuous secretion of the HIF-
608 target protein erythropoietin and an increase in lactate production, indicative of a switch from
609 oxidative phosphorylation to glycolysis (659). Similar observations were made by Metzen et
610 al. (389) and Bhatia et al. (421) in HepG2 and rat hepatocytes, respectively. Compromised O₂
611 delivery *in vitro* is not confined to hepatocyte cultures, since large culture O₂ gradients have been
612 reported using a number of different cell types under standard culture conditions and low ambient
613 PO₂ (see Table 1-3). Traditional micro-manipulator mounted electrode methodologies have largely
614 been superseded by fluorescence and phosphorescence-based techniques, which can provide a
615 more accurate determination of pericellular PO₂ in culture dishes. Using immobilized luminescent
616 dyes (see Section II-C), large culture gradients have been demonstrated in cultures of human
617 embryonic stem cells (hESC) (2, 320) and Caco-2 intestinal epithelial cells (690). Meanwhile, cell-
618 permeable phosphorescent nanoparticles have been used to monitor intracellular (cytosolic) PO₂ in
619 mouse embryonic fibroblasts (MEFs) (151), cortical neurons (114), and in HUVEC (75). Hence
620 intracellular or pericellular PO₂ provides a more accurate parameter when translating *in vitro*
621 experiments to an *in vivo* setting.

622

623 E. Maintaining the appropriate environment for the duration of culture
624 Culture of mammalian cells under reduced O₂ environments has generally been undertaken using
625 three types of equipment; (i) an airtight, gassed chamber placed within a standard CO₂ incubator,
626 (ii) a tri-gas incubator, or (iii) a dedicated O₂-regulated workstation, with cost and infrastructure
627 requirements increasing accordingly. The former is most widely used due to the relatively low price
628 and ease with which it can be accommodated into existing culture infrastructure, although
629 dedicated chambers generally have limited multi-user space and accessibility. Tri-gas incubators
630 are variations of standard CO₂-regulated cell culture incubators in which an additional N₂ gas input
631 is provided, with which the PO₂ can be manipulated to a required level. Tri-gas incubators offer
632 increased capacity for multi-users, especially units equipped with independent, modular
633 compartments. However, both these types of equipment suffer from an important disadvantage
634 when used for long-term culture of cells under defined low O₂ conditions. Cells need to be removed
635 from the chamber or tri-gas incubator in order to feed, monitor and perform any required sub-
636 culture or experimental treatments. Thus, cells are re-exposed to hyperoxic atmospheric levels of
637 O₂. Such fluctuations in the resultant pericellular PO₂ induce a phenotype distinct from that of cells
638 maintained long-term under a defined level of O₂ (289, 437, 640). Indeed, direct comparisons
639 between culture in tri-gas incubators and dedicated O₂-regulated workstations demonstrate that
640 repeated re-exposure to atmospheric O₂ levels during culture is detrimental to human
641 mesenchymal stem cell growth (289). Medium and pericellular PO₂ require hours to re-equilibrate
642 to a required PO₂ level even when only transiently exposed (~5min) to atmospheric
643 levels (320, 404, 690). Such technical problems associated with *in vitro* cell culture mimic
644 'reperfusion injury' common following restoration of cerebral or myocardial blood after infarction.
645 Re-exposure to atmospheric PO₂ can be avoided completely by using a dedicated O₂-regulated
646 workstation, where access to cells for sub-culture and treatment is permitted through gas-tight
647 glove ports and transfer chambers. It is for this reason that we strongly recommend that any work
648 investigating the effects of prolonged culture under well-defined low PO₂ be conducted using a
649 dedicated O₂-regulated workstation.

650

651 **V. Cellular oxygen sensing - when is low O₂ hypoxic?**

652 Having established the difficulties in accurately predicting and controlling monolayer oxygenation *in*
653 *vitro*, a consideration for how cells sense the difference between normoxic and hypoxic PO₂ is now
654 relevant. The question posed relates to the understanding that physiological oxygenation varies by
655 so much *in vivo* that the use of terminology like hyperoxia, normoxia and hypoxia should be used
656 contextually rather than absolutely, and should always be defined quantitatively for better
657 interpretation. Each cell type has unique responses to a reduction in available O₂. For example,
658 endothelial cells release vascular endothelium-derived growth factor (VEGF) and nitric oxide (NO)
659 to initiate vasodilation and angiogenesis in an attempt to increase local blood flow, thereby
660 normalising tissue O₂ distribution (351, 536, 630). A more generalised 'hypoxic' response is

orchestrated predominantly by hypoxic-inducible factors (HIFs), with additional contributions from less well defined pathways. The relevance of these mechanisms in the context of *in vitro* normoxia remains to be defined fully, since they have evolved to respond to acute reductions in PO₂ within (patho)physiological levels, and not the substantial reductions imposed in the majority of studies *in vitro* (room air to 1-3 kPa). Thus the study of cellular phenotypes under low O₂ generally requires culturing cells for a sufficient period to allow *adaptation* to the new baseline [O₂]. Several excellent articles have reviewed the general and state-of-the-art literature concerning how cells sense O₂ (476, 516, 522, 575), and as such only the most well established cellular O₂ sensors will be covered here. Particular emphasis will be placed on their relevance under physiological O₂ levels in terms of the PO₂ at which they have been shown to be active. This will be followed by a brief discussion of how the duration of exposure to low O₂ can influence the interpretation of experimental data.

673

674 A. Cellular oxygen sensors

675 1. Hypoxia-inducible factors

Several excellent reviews have been published on the physiology and biochemistry of HIFs (472, 504, 516, 522), and therefore HIFs will only be briefly discussed. HIFs are evolutionarily conserved transcription factors expressed in all eukaryotic organisms as 3 α isoforms (HIF1-3) and a β subunit. The vast majority of research to date has focussed on HIF-1, which regulates the acute and reactive phase of the hypoxic response in most cell types (257, 549). Whilst the β subunit is constitutively expressed and not actively degraded, the α subunit is post-translationally modified through O₂-dependent hydroxylation at prolyl residues (by prolyl hydroxylases, PHD), which targets the subunit for degradation (35, 134), or at asparagine residues by factor inhibiting HIF-1 (FIH) which interferes with its binding to transcriptional co-activators (238, 322, 323). Thus, when intracellular O₂ availability decreases these enzymes are no longer able to hydroxylate HIF α subunits resulting in the formation of a transcriptionally competent stable α/β dimer. This can then translocate to the nucleus where it binds hypoxia-response elements initiating the transcription of hypoxia-sensitive genes. Such genes encode proteins such as vascular endothelium-derived growth factor (VEGF) (162, 536), erythropoietin (EPO) (630) and glucose transporter 1 (GLUT1) (128), which function collectively to either increase O₂ delivery or reduce cellular O₂ consumption. It was traditionally considered that a large degree of redundancy exists between HIF-1 α and -2 α (549, 667), which itself has fewer selective targets (120, 193, 257, 444, 569, 599, 634). However, recent pan-genomic screens (503, 514, 515) have identified a large number of HRE binding sites with distinct isoform binding affinities, despite an identical core recognition sequence (RCGTG). Such variance may represent different topographical chromatin binding locations, affinity for HIF- β binding partner and/or the involvement of other transcription factors, most notably AP-1 (321, 503). Comparatively little is known about HIF-3 α , but it is thought to act as a negative regulator of HIF-1 and -2 (219).

700 The K_m for O_2 of the reaction catalysed by PHD ranges between 140-250 μ M (~10-20
 701 kPa) (243, 517), and thus O_2 may be a rate-limiting substrate under atmospheric O_2 conditions.
 702 Despite this, HIFs are not constitutively stabilized in cells at physiologically normoxic levels (on
 703 average 5 kPa), otherwise organisms would have no reactive response to further reductions during
 704 genuine hypoxia. Persistent stabilization is prevented by HIF-dependent negative feedback
 705 mechanisms, including specific interactions with microRNA 210 (631) and reactive oxygen
 706 species (254), upregulation of prolyl hydroxylases 2 and 3 (36, 106, 178, 372) and the global
 707 impact of HIF-induced proteins to increase intracellular O_2 levels. Thus, any reduction in O_2
 708 availability is addressed by transient stabilization of HIF-1 α , and the upregulation of associated
 709 regulated proteins, followed by pathway normalization at a new baseline reflecting the altered O_2
 710 levels. A question that remains unsolved in HIF hydroxylation is the concept of 'range finding'; that
 711 oxygen-dependent regulation of HIF is observed in a variety of tissues existing across a huge
 712 variety of O_2 levels (476). The high K_m of PHD enzymes for O_2 has led many to conclude that
 713 absolute O_2 levels are perhaps of secondary importance in the mechanism by which cells sense
 714 O_2 , and that complimentary signals may further modulate hydroxylase activity. To date, alternative
 715 signals include reactive oxygen species (74, 378), intracellular $[Fe^{2+}]$ (306), and competing
 716 hydroxylase substrates (91). Inclusion of these additional parameters in the mechanism of HIF O_2
 717 sensing creates an increasingly complex model which may offer insight into the 'range finding'
 718 capabilities of the system (476), a concept critical for defining physiological normoxia.

719

720 *2. Mitochondria and/or superoxide*

721 Given their central role in O_2 homeostasis and intracellular signaling, mitochondria are prime
 722 candidates for intracellular O_2 sensors. Mechanisms by which these organelles are thought to
 723 transduce changes in O_2 levels revolve around changes in either intracellular redox or energy
 724 states (or both) (74, 633). Limitations in O_2 supply would logically lead to reductions in
 725 mitochondrial ATP generation which subsequently activates AMP-dependent protein kinase
 726 (AMPK), a cellular energy sensor (220, 556), although some have argued this occurs due to
 727 reactive oxygen species generation and not changes in ADP/ATP (132). AMPK in turn targets
 728 several transcription factors to repress fatty acid biosynthesis and upregulate proteins involved in
 729 glycolysis, resulting in a metabolic shift away from O_2 consuming oxidative phosphorylation (221)
 730 Pharmacological inhibition of the electron transport chain (ETC) can mimic hypoxic
 731 responses (121, 392), although others report an abolition in O_2 sensing following ETC
 732 inhibition (635). One major limitation to the energy state hypothesis of mitochondrial O_2 sensing is
 733 that the P_{50} of cytochrome C oxidase for O_2 is ~0.07 kPa (181), and thus ATP production would
 734 not be expected to decrease until cytosolic PO_2 fall very low. However, some have suggested that
 735 the affinity of cytochrome C oxidase for O_2 is modified substantially by cellular reducing agents
 736 (GSH and NAD(P)H), suggesting that O_2 may become rate-limiting at much higher levels than

previously predicted (633, 653). The generation of superoxide anions by the ETC has formed the basis of intense debate in the context of mitochondrial O_2 sensing, with both decreases and increases in mitochondrial superoxide ($O_2^{\cdot-}$) generation reported to mediate O_2 sensing. On one side, reductions in O_2 availability would logically result in reductions in $O_2^{\cdot-}$ production, which in turn would cause the cytosolic environment to become more reduced, affecting many redox-sensitive pathways (15, 480, 641). Conversely, others have reported a paradoxical increase in superoxide generation in mitochondria during hypoxia (74, 206, 207, 373, 450, 609, 636), resulting from enhanced electron leak within the ETC.

Mitochondria are not the only source of reactive oxygen species within the cytosol, and indeed other enzymatic sources have been implicated as O_2 sensors. Since NAD(P)H oxidases (NOX) function to generate reactive oxygen species with a reported P50 for O_2 of ~ 1.7 kPa (31), it is tempting to speculate that NOX serve as a key cytosolic O_2 sensors (633). Indeed, mice lacking an essential subunit of the NOX2 isoform (gp91^{phox}) exhibit impaired O_2 sensing (168), although this remains controversial (14, 633). Both increases (229, 375) and decreases (100) in NOX-derived reactive oxygen species generation have been reported during hypoxia.

3. Gaseous messengers

A new O_2 sensing mechanism has emerged in recent years focusing on the interplay between two physiological gaseous messenger molecules, carbon monoxide (CO) and hydrogen sulphide (H_2S) (468). The effects of CO on hypoxia-induced ventilation have been well known for 50 years (352), yet the finding that it is produced endogenously highlighted its possible involvement in O_2 sensing. CO is produced by heme oxygenases, of which there are two principle isoforms: inducible (HO-1) and constitutively expressed (HO-2) (369, 542). Importantly, production of CO is O_2 dependent (652) with a P50 of 8.7 kPa (683), placing this potential sensor within the physiological range. CO was found to inhibit the activity of cystathionine- γ -lyase (CSE), the enzyme responsible for H_2S synthesis, and hence H_2S production is increased when HO-2 becomes substrate limited during hypoxia (683). In archetypical O_2 sensing cells, e.g. type I cells of the carotid body, it is proposed that H_2S initiates depolarisation through inhibition of Ca^{2+} -activated K^+ channels (340) and increasing Ca^{2+} influx (56). Less is known about the role this CO- H_2S sensing system functions in non-excitabile, non-specialised cell types.

B. Exposure or adaptation – Does timing matter?

With the exception of the HIFs, the above O_2 sensing mechanisms have been described in the context of whole body physiological reactions to hypoxia, and therefore have an implied negative feedback loop whereby a plethora of actions instigated by the sensing of hypoxia act in conjunction to increase tissue PO_2 , to alleviate input stimuli. There is little information on how these mechanisms function in chronically hypoxic environments. The general consensus is that HIF-1 α

actions peak after 12-16 h exposure to low O₂, and then normalize by 24 h to a new set-point (62, 178, 249, 630). In contrast, any stabilization of HIF-2 α has been shown to require considerably longer (>72 h) (249, 355). Since these transient responses to reduced O₂ availability are unavoidable during transfer from room air to physiological normoxia, it is critical that experiments aimed at recapitulating physiological conditions enable cells to adapt long-term. Importantly, this should include the time required for the expression of any induced protein to also normalize. A global analysis of protein half-life reveals a mean half-life of 46 h (520), and thus the adaptation time required to circumvent these initial responses to reduced O₂ can be estimated. We have observed that at least 5 days are required for a phenotype to stabilize in human endothelial cells when transferred from room air to a PO₂ of 5 kPa during culture (75, 290), with culture beyond this period inducing no further alterations in cell phenotype (75). To avoid misinterpretation of experimental data, we suggest that cells are cultured for as long as possible (at least 5 days) under physiological normoxic conditions.

VI. Replicating normoxia *in vitro*

Significant efforts have been undertaken to better recapitulate a physiological milieu *in vitro*, with particular focus on the physical environment in which cells are cultured. For example, numerous studies have characterized the phenotype of endothelial cells exposed to laminar flow (80), or vascular smooth muscle cells (481) and renal mesangial cells (198) exposed to cyclic biaxial stretch, or dermal fibroblasts in 3D extracellular matrix culture (197). However, few studies have carefully considered the gaseous composition of the culture environment. The following sections provide an overview of current understanding of PO₂ in specific tissues *in vivo* and summarize the key studies aimed at replicating these conditions *in vitro*. We focus specifically on investigations in mammalian cells under quasi-physiological PO₂ (not hypoxia) and long-term culture conditions (2-12 kPa, >24 h) to avoid confusing physiological phenotypes with those associated with relatively rapid adaptive responses to reduced O₂ availability. However, it is worth noting that when reviewing this literature, in most cases only ambient PO₂ is considered and therefore many observations may not describe the ideal physiologically normoxic phenotype. Furthermore, tissue PO₂ distribution is considerably heterogeneous in both space (regional differences in perfusion or consumption) and time (changes in metabolic activity). The data quoted herein therefore often represent one observation across a range of potential values, and should be interpreted accordingly. All measurements of tissue PO₂ discussed in this review have, to the best of our knowledge, been performed on intact preparations kept *in situ* to maintain the endogenous blood supply and minimise interference from the atmosphere.

A. Lungs

In the airways, PO₂ in the gaseous phase can be predicted accurately, and thus concentrations within the respiratory tract are known with high certainty (see Section III-A and Figure 3).

813 Consistent with the large area occupied by the bronchi, bronchioles and alveoli, whole organ PO₂
814 maps (see Figure 7B) conducted with MRI scanning using ³He polarisation (3) reveal average PO₂
815 values of 14.5 (107), 13.4 (649), 13.6 (396), 14 (216), ~12.7 (217), and 13.5 kPa (407) in human
816 subjects, largely reflecting inspired air PO₂. Whole lung PO₂ is lower in chronic smokers (216), but
817 does not differ in patients with heart failure, although the alveolar-arterial gradient (see Section III-
818 A) is significantly higher in these patients suggesting a less efficient gaseous transfer (407). These
819 values closely reflect values obtained in experimental animal models, where mean PO₂ values of
820 11 (156), 14.7 (682) and 19.6 kPa (107) have been reported in porcine lung, 17.1 kPa in rat
821 lung (85) and 14.7 kPa in rabbit lung (681). Regional heterogeneity in PO₂ measurements
822 throughout the lung was common in all the above studies, consistent with the known variability in
823 lung perfusion and gas exchange. This, coupled with a small image acquisition field of view, can
824 lead to lung PO₂ values skewed by sampling in highly or poorly perfused regions. Encouragingly,
825 lung or alveolar PO₂ values determined by ³He-MRI correlate very well with traditional methods
826 used to determine alveolar PO₂, in which PO₂ in the expired gas is related to arterial PO₂ and
827 PCO₂ using equations 2/3 (see Section III-A) (217, 407).

828

829 The need to transition into the aqueous phase within the airway surface liquid (ASL) for
830 bioavailability make estimates of how a gaseous PO₂ of 13-18 kPa translates into cytosolic PO₂
831 within airway epithelial cells ambiguous. The average ASL depth in healthy human bronchi is 15-
832 80µm (273) and is therefore unlikely to present a significant barrier to O₂ diffusion. To our
833 knowledge, no measurements of ASL PO₂ in healthy bronchi have been reported, and thus we are
834 left to interpolate lung epithelial PO₂ based on ASL depth. Worlitzsch et al. (664) elegantly
835 demonstrated that increased ASL depth (up to 800µm) in patients with cystic fibrosis resulted in a
836 mean mucosal PO₂ of 2.5mmHg (0.3 kPa). Such hypoxic conditions were associated not only with
837 increased ASL, but also with increased epithelial cell O₂ consumption, and facilitated the early
838 pathogenesis of anaerobic *P. aeruginosa* infections (664).

839

840 Beyond the epithelia, the lung connective tissue largely consists of fibroblasts whose role it is to
841 maintain the structural integrity of the organ. Intriguingly, adventitial PO₂ has been reported
842 significantly lower than the average lung PO₂ (13-14 kPa) as measured by ³He-inhalation. Using
843 microelectrode penetration, 'peribronchial' PO₂ values of 5.7 kPa were recorded in patients
844 inspiring >50% FiO₂ (326). Similar values have been described in porcine (5.1 kPa (236), 5.8
845 kPa (205)), canine (~6.5 kPa (282)) and rat (5.1 kPa (487)) experimental models. In the latter
846 study (487), an implantable EPR resonator was used in conjunction with O₂-sensitive EPR probes
847 to monitor deep tissue PO₂ in real time, confirming measurements using microelectrodes.
848 Anatomically, the site most often sampled by microelectrode penetration lies ~1cm distal to the
849 tracheal bifurcation, near to the peribronchial lymph node. Kamler and colleagues (282)
850 demonstrated that ligation of the aortic stem of the bronchial artery dramatically reduces

peribronchial PO₂ in this region, even when breathing was maintained (Figure 7C). This, coupled with the observation that peribronchial PO₂ does not increase proportionally with FiO₂ (unlike arterial PO₂) (236), suggests that lung adventitial PO₂ is critically dependent on blood perfusion from the bronchial artery, and does not receive O₂ supply directly from the airways. How representative this highly sampled region is of non-airway lung tissue as a whole remains to be established, although it has been used as a measure of overall tissue oxygenation following lung transplant and correlates well with improved outcomes (282, 425, 431).

858

Unlike most other cell types, lung epithelial cells experience a high PO₂ physiologically and are only separated from gaseous O₂ by a thin layer of ASL. These conditions have been recapitulated *in vitro* in the form of air-liquid interface culture, as illustrated in Figure 7D. First introduced in the late 1980's by Wu, Kim and colleagues (6, 7, 645), this technique has been shown to be essential in maintaining primary cultures of tracheal and bronchial epithelial cells in a differentiated state *in vitro*. Principally, the pseudostratified phenotype observed *in vivo* can be recapitulated *in vitro* after ~7 days culture at the air-liquid interface (5, 645), with cells typically differentiating into ciliated and granulated mucus-secreting epithelial cells. Other responses to culture at the air-liquid interface include: increased Na⁺ transport via short-circuit current (*I*_{sc}) (278), restoration of epithelial barrier function (190) and a transcriptional profile more comparative with fresh tracheal/bronchial epithelial cells *in vivo* (126, 454), even in response to cigarette smoke inhalation (381). More recently, culture at the air-liquid interface has been used as a tool to differentiate inducible pluripotent stem cells into mature airway epithelial cells (470, 662). This method of culture clearly has profound impact on the phenotype of airway epithelial cells, very accurately recapitulating that observed *in vivo*. However, we could not identify a publication employing air-liquid interface culture in which the PO₂ was implicitly defined. When the immortalised epithelial A549 cell line was cultured long-term at a PO₂ of 13 kPa, an increased sensitivity to copper oxide nanoparticles was observed paralleled by a decrease in cellular antioxidant defences (317). Although pericellular PO₂ may be lower than 13 kPa in this model, thus poorly representing physiological normoxia, this study provides important insight into the potential of employing culture under physiological normoxia to evaluate environmental toxicity in models of airway damage. Standard incubator conditions (~18.5 kPa, 5 kPa CO₂) reasonably reflect upper tracheal PO₂, but bronchiolar PO₂ can drop as low as 13 kPa. Thus careful control of ambient PO₂ during air-liquid interface culture may yield interesting insights into phenotypic differences related to PO₂ between epithelial cells along the length of the respiratory tract.

884

885 B. The vasculature

The mechanics of O₂ distribution in the vasculature have already been covered in Section III-B, and this section aims to further discuss the absolute PO₂ values measured in the vascular network. In estimating PO₂ values experienced by different cell types in the vascular wall (endothelial,

smooth muscle, fibroblasts), it is critical to assess the level of O₂ within the wall tissue itself. An excellent review by Tsai, Johnson and Intaglietta (594) summarizes the distribution and gradients of O₂ in the microvasculature, and we have here integrated their summaries and conclusions with recent research findings. Current understanding of the PO₂ levels in vessels related to specific tissues will be discussed in the context of the relevant tissue.

894

895 1. *The macrovascular wall*

896 Section III-B-2 introduced the concept of radial gradients across the vascular wall, which are
897 particularly prominent in larger arteries such as the aorta and carotid arteries. O₂ supply to the
898 endothelial layer occurs largely by diffusion from the lumen (containing oxygenated blood PO₂ ~12
899 kPa), noting that the thickness of the walls of such vessels can severely limit adequate delivery. As
900 such, vessel wall PO₂ decreases significantly between the luminal and medial layers, as first
901 reported nearly 50 years ago (410, 428). By advancing a tissue-penetrating Clark-type electrode
902 perpendicular to the vessel wall, as illustrated in Figure 8B, a pattern of wall oxygenation in large
903 arterial vessels such as the aorta, femoral and carotid arteries is clearly evident. Penetrating the
904 intimal layer was associated with a prominent, rapid reduction in PO₂ in the rabbit infrarenal
905 aorta (237, 330, 428, 509) and abdominal aorta (505, 506, 508), pigeon abdominal aorta (214),
906 and dog carotid artery (507). In such studies, PO₂ in the intimal layer reached an average of 3-5
907 kPa, representing a drop of 5-7 kPa from the lumen. Others reported no such sudden drop in
908 similarly sized vessels and preparations (23, 57, 97, 99, 279, 691), instead reporting gradual
909 declines in PO₂ across the inner third of the wall, reaching a similar nadir within the medial layer.
910 Such discrepancies have been attributed largely to differences in methodology, including (i) the
911 nature of vessel preparation and maintenance, with contrasting PO₂ profiles observed when the
912 vessel is left *in situ* (237) versus superfused with physiological solution at a controlled PO₂ (97)
913 and (ii) the method of electrode advancing, with many using 'vibration mounting' apparatus to
914 minimize tissue distortion. Some (509) have postulated that the resonance created by such
915 devices can interfere with the laminar flow patterns close to the vessel wall, considered critical in
916 forming the aforementioned O₂ diffusion barrier. In contrast, others (98) have suggested that the
917 sharp decline in PO₂ at the intimal layer is an artefact resulting from the use of large-diameter
918 electrodes. Whether sharp or gradual, experimental evidence is clear that vessel wall PO₂ declines
919 proportional to distance from the lumen (in vessels devoid of vasa vasorum, see below).

920

921 Aside from this discrepancy, remarkable conformity exists in the reported minimal vessel wall PO₂.
922 The nadir within the medial layer shown in Figure 8B-C occurs at 50-70% of the wall thickness
923 away from the adventitia (~200µm in a rabbit thoracic aorta) and reaches a PO₂ of 3-4
924 kPa (23, 237, 279, 330, 428, 505, 506, 507, 508, 509). This value has been shown to correlate
925 negatively with total wall thickness (97, 279), and hence conditions in which vessel wall
926 hyperplasia occurs can result in significant reductions in medial PO₂, as observed in alloxan-

927 induced diabetes (505), atherosclerosis (279), hypertension (99, 506), after insertion of vascular
928 grafts (330, 509) or stents (508) and after balloon de-endothelialization (691). Reduced medial PO₂
929 in such conditions has been attributed to an altered bioenergetic profile in resident (and migrating)
930 cells (330) as well as biophysical considerations such as increased wall stress (508) and
931 compression of the vasa vasorum (57, 508). Medial hypoxia has been demonstrated *in vivo* in
932 rabbits with late-stage atherosclerotic plaques in the aortic arch and thoracic aorta using the
933 biochemical hypoxia marker 7-(4'-(2-nitroimidazol-1-yl)-butyl)-theophylline (NITP) (41). In this
934 study, plaques >400µm diameter exhibited hypoxic regions ~200µm in diameter and 200-300µm
935 from the endothelial/intimal surface, with an estimated PO₂ of 0.5 kPa. Using similar probes ([¹⁸F]
936 EF5 and [⁶⁴Cu]ATSM), hypoxic regions have been visualized within the media of athero-
937 susceptible transgenic mice (427, 537) and rabbits (426). Atherosclerotic plaques occur
938 preferentially in regions of the vasculature that experience oscillatory blood flow, such as the inner
939 curvature of the aortic arch and carotid bifurcation (370) and lower medial PO₂ has been measured
940 in such regions using microelectrodes (507). It is therefore possible that medial hypoxia precedes
941 and facilitates atherogenesis in such regions, rather than occurring subsequent to plaque
942 development and wall thickening.

943

944 Limited data are available on PO₂ profiles in large arteries in humans, as measurements are
945 invasive and difficult to perform in humans. However, Vorp and colleagues (620, 621) performed
946 microelectrode measurements of PO₂ within the abdominal aortic wall of patients with aneurysms.
947 Although reported measurements were normalized to luminal PO₂, interpolation based on an
948 average aortic luminal PO₂ of ~11 kPa suggests that the aortic aneurysm wall PO₂ was ~7 kPa in
949 the absence of intraluminal thrombi, falling to ~2.5 kPa when a thick thrombus was evident (620).
950 Although the exact topographical location of the PO₂ sampling point was not reported, an aortic
951 wall PO₂ of ~7 kPa is similar to values measured in animal models (279, 505, 506, 508).

952

953 The walls of large blood vessels can be thick enough in diameter to merit their own blood supply,
954 and in arteries these vessels are termed the vasa vasorum. The extent and nature of such vessels
955 is critically dependent on the wall thickness. Peri-adventitial vasa can exist in moderately sized
956 arteries such as the femoral or carotid, whereas vasa penetrating into the media are thought only
957 to occur beyond a critical threshold diameter (>500µm or 29 lamellar units, irrespective of species
958 or vessel characteristics) (661). In the context of vessel wall PO₂ distribution, the presence of vasa
959 vasorum is critical in defining adventitial PO₂, as outlined in Figure 8C. An upward inflection
960 beyond the 'medial nadir' in the PO₂ profile of a vessel wall is characteristic of a second source of
961 O₂ diffusion from the outer layers. Arteries confirmed histologically to be devoid of adventitial vasa
962 demonstrate a continuous decline in PO₂ between the lumen and adventitia (97, 99, 279), and
963 experimental disruption of vasa vasorum patency (surgical or resulting from increased wall stress
964 secondary to increased blood pressure) in those vessels possessing peri-adventitial vasa results in

965 a significant reduction in adventitial PO₂ (23, 57, 330, 508, 509, 691). Moreover, increases in aortic
966 tissue PO₂ in response to vasodilatory compounds (adenosine and epinephrine) applied to the
967 adventitia have been attributed to vasa vasorum vasodilation (58). Notably, adventitial and medial
968 neovascularization often occurs in response to vessel injury (413), and Lee et al. (330) showed
969 that decreased adventitial PO₂ following insertion of an anastomotic graft can resolve over time in
970 conjunction with the histological appearance of new medial vasa.

971

972 2. The microvasculature

973 The vascular network between an artery and vein, encompassing arterioles, capillaries and
974 venules, is the prime region for O₂ exchange, as evidenced by the significant difference in blood
975 PO₂ between an artery and vein (~6-7 kPa). This longitudinal gradient was first highlighted in
976 Section III-B-1, and is the focus of previous reviews (456, 594). As such, only an overview of blood
977 PO₂ within the microvascular network will be included here. Microvascular networks are present in
978 all organs, and we provide an overview of blood PO₂ in an 'idealised' microvascular network
979 comprised of (i) a feeding artery, (ii) 1st, 2nd and 3rd order arterioles, (iii) a capillary bed, (iv) 1st, 2nd
980 and 3rd order venules and (v) a collecting vein (Figure 9A). The majority of studies of microvascular
981 PO₂ distribution have focused on 3 experimental preparations: the hamster skinfold/cheek window,
982 rat cremaster/spinotrapezius muscle and rat pial/cortical microvasculature. Their minimally invasive
983 nature and the ability to monitor intravascular PO₂ in live animals are major advantages of such
984 models. A summary of studies for each experimental model is provided in Figure 9B. Blood enters
985 the microvascular network at an average PO₂ of ~9 kPa and rapidly declines along the arterioles to
986 reach a capillary PO₂ ~5 kPa. As described by Tsai et al. (594), such a finding suggests that
987 arterioles, and not capillaries, are the major source of O₂ delivery in most microvascular beds. This
988 may be true for hamster cheek pouch and rat muscle preparations, but reports in rat pial
989 microvessels indicate that intravascular PO₂ in pre-capillary arterioles is still ~7-9 kPa, and only
990 falls substantially once it has entered the capillary networks (622). However, recent evidence using
991 2-photon time resolved phosphorescence (500) has refuted such claims, demonstrating that
992 arterioles in the mouse cerebral cortex are responsible for ~50% of O₂ delivered to the underlying
993 parenchyma. These authors postulated that the expansive capillary network may act as a reserve
994 mechanism for O₂ delivery during times of increased activity (500).

995

996 Unlike large vessels, the presence of radial gradients and their contribution to tissue PO₂ in
997 arterioles is less well defined. Many studies report differences between intravascular and peri-
998 arteriolar PO₂ (260, 531, 585, 591) which appear proportional to the blood PO₂ and luminal
999 diameter (594). Such differences are in the order of 2.5-3.5 kPa in large (A1) arterioles (531, 591)
1000 and ~1.5 kPa in moderately sized (~40µm diameter) arterioles (260, 531, 585). In contrast, others
1001 have observed an arteriolar wall O₂ gradient of only a few mmHg (1.4 mmHg/0.2 kPa per
1002 µm (122, 123), 1.2 mmHg/0.16 kPa per µm (527, 623)). Pittman (456) proposed a possible

1003 explanation for this discrepancy, citing misinterpretation of phosphorescence quenching data due
1004 to O₂ consumption by the probe itself. Attempts to remedy these differences have subsequently
1005 been made by adapting the methodology (182, 183, 185). Unusually high vascular wall
1006 consumption, the reasoning put forward to explain large radial arteriolar gradients (594), was also
1007 refuted by Vadapalli et al. (603). With relevance to estimating physiological normoxia for cells
1008 resident within the microvascular wall, we believe that intravascular (blood) PO₂ most appropriately
1009 represents this value.

1010

1011 3. *The human umbilical vein*

1012 One of the most well studied and widely utilized vascular cell type *in vitro* are human umbilical vein
1013 endothelial cells (HUVEC). However, its unique physiology (fetal, venous tissue carrying
1014 oxygenated blood at a low flow rate) means it does not reflect normal artery/vein,
1015 macro/microvascular characteristics. Unlike many other tissues in the human body, the umbilical
1016 cord can be accessed relatively easily/non-invasively for blood collection and gas analysis, albeit
1017 *ex vivo*. It is therefore fortunate that endothelial cells isolated from these vessels have been used
1018 extensively in vascular biology *in vitro*, allowing for an accurate and well characterised transition to
1019 physiologically normoxic cell culture. A meta-analysis of data extracted from a number of studies
1020 reporting umbilical blood PO₂ (102, 109, 298, 313, 347, 376, 465, 486, 576, 605, 675) reveals a
1021 mean blood PO₂ of 3.8 and 2.4 kPa within umbilical veins and arteries, respectively. Although
1022 collected *ex vivo* under room air, this has been shown not to increase measured O₂ levels in
1023 umbilical blood (382). Interestingly, umbilical vein PO₂ decreases throughout gestation from ~6
1024 kPa at 20 weeks to ~4 kPa at 36 weeks (639), and final PO₂ at birth is significantly affected by the
1025 method of delivery (spontaneous vaginal vs caesarean) (109, 313) and position of the fetus
1026 (breech) (102). The human umbilical vein is a macrovessel of 2-3 mm diameter with an average
1027 wall thickness of 430µm and a moderate adventitial layer (344). Although not studied, based on
1028 these dimensions, it seems likely that a significant radial gradient would be apparent across the
1029 length of the wall (Section III-B-2), and thus physiological normoxia in smooth muscle cells in these
1030 vessels may be lower than that measured in the endothelium (~3.5 kPa (75)).

1031

1032 4. *Endothelial cells*

1033 The physiological response to hypoxic tissue O₂ levels is an initial vasodilation followed by the
1034 induction of angiogenesis, with both responses increasing O₂ delivery and thereby alleviating the
1035 harmful effects of hypoxia (536, 571). Given the primary role of endothelial cells in orchestrating
1036 such responses, it is no surprise this cell type has received considerable attention in the context of
1037 low O₂ physiology (393, 472, 523) as summarized in Table 1-4. We recently described a well-
1038 defined model to recapitulate physiological normoxia in cultured human venous and arterial
1039 endothelial cells (75, 290, 291). Using a phosphorescent nanoparticle probe to monitor intracellular
1040 PO₂ in living cells (Figure 10A), we established that culture at a PO₂ of 5 kPa was required to

1041 compensate for monolayer O₂ consumption and recapitulate a physiologically normoxic
1042 intracellular environment of 3.5-4 kPa (measured in umbilical venous blood, see above). In order to
1043 maintain such conditions in different culture apparatus (6-, 24- or 96-well plates) with varying
1044 surface area, volume was adjusted to achieve similar surface area: medium depth ratios. For
1045 example, 100μL in a 96-well plate has roughly the same surface area: medium depth as 500μL in
1046 a 24-well plate.

1047

1048 The importance of distinguishing between ambient and intracellular PO₂ was further highlighted by
1049 the different absolute P₅₀ (akin to E/IC₅₀) (633) values for HIF-1α stabilization when plotted against
1050 each O₂ parameter (Figure 10C) (290). When ambient PO₂ is used, the resulting P₅₀ value (4.3
1051 kPa) is not consistent with the known PO₂ distribution in the majority of the microvasculature nor in
1052 tissues, where a PO₂ 4-5 kPa would be considered normoxic and hence minimal HIF-1α
1053 stabilization should be apparent. In contrast, use of intracellular O₂ levels results in a P₅₀ value of
1054 2.3 kPa, a level more consistent with what one may expect to observe in the hypoxic vasculature *in*
1055 *vivo*. Under these defined conditions, we have shown that the induction of nuclear factor E2-
1056 regulated factor 2 (Nrf2) regulated antioxidant gene expression in response to oxidative stress was
1057 markedly attenuated in HUVEC (Figure 10D). Similar findings have been reported in RAW 264.7
1058 macrophages cultured at 5 kPa (208), and in human diploid fibroblasts upon re-exposure to
1059 atmospheric PO₂ following long-term culture at 3 kPa (21). Notably, this phenotype was only
1060 observed following long-term adaptation (>5 days) to physiological normoxia (75). Glutathione-
1061 based defense systems remained intact, and this alone conferred sufficient protection to maintain
1062 cell viability (69). In line with this, basal levels of apoptosis are lower in HUVEC (1) and rat liver
1063 sinusoidal endothelial cells (377) cultured at 5 kPa for 3 and 5 days, respectively. We have
1064 recently shown that HUVEC cultured at a PO₂ of 5 kPa exhibited significantly less sensitivity to
1065 Ca²⁺ overload induced cell death (291), which we attributed this enhanced sarco/endoplasmic
1066 reticulum Ca²⁺ ATPase activity sparing the mitochondria from Ca²⁺ overload.

1067

1068 There are conflicting reports on the effects of physiological O₂ levels on endothelial cell
1069 proliferation *in vitro*. In the context of angiogenesis, the consensus is that a higher proliferative
1070 rates occur in endothelial cells cultured under physiological O₂ levels, and indeed this has been
1071 demonstrated in HUVEC (2, 276, 277, 695) and HDMVEC (697). However, we observed a
1072 significant reduction in HUVEC proliferation following culture at 5 kPa for more than 5 days (75), in
1073 line with the quiescent nature of endothelial cells *in vivo* (133, 244). Moreover, production of
1074 extracellular matrix proteins type IV collagen (49, 697), fibronectin, CD105, CD31 and
1075 laminin (695) is significantly higher in human dermal microvascular endothelial cells (HDMVEC)
1076 and HUVEC cultured at 5 kPa levels. Differentiating between endothelial cell responses to
1077 physiological and hypoxic O₂ levels is especially relevant given their unique and highly regulated
1078 response to pathological hypoxia. For example, different HUVEC phenotypes are observed when

1079 cultured at a PO₂ of 3 (277) and 5 kPa (2, 75), largely due to increased stabilization of HIF-1α
1080 under the lower O₂ level. We have recently demonstrated that the synthesis of nitric oxide (NO) is
1081 significantly altered when endothelial cells are cultured at 5 kPa (Figure 10E) (290). Importantly,
1082 these processes were still functional, yet under more strict regulatory control by protein
1083 phosphatase 2A. This is in stark contrast to the phenotype observed in hypoxic (1 kPa) cells,
1084 where stimulation of NO synthesis is largely abolished. In many respects, cells cultured at hypoxic
1085 O₂ levels more closely resemble those maintained at room air than those cultured at physiological
1086 O₂ levels, further highlighting the importance of this distinction.

1087

1088 5. Circulating and immune cells

1089 As for endothelial and smooth muscle cells, no single O₂ level can be described as normoxic for
1090 circulating cells. This does not preclude the study of circulating cells under physiologically relevant
1091 O₂ levels *in vitro*, since even the highest O₂ levels encountered *in vivo* (~13 kPa within the
1092 pulmonary circulation) are still much lower than atmospheric. Whilst circulating cells are exposed
1093 to the full dynamic range of blood physiological O₂ (~5-13 kPa) over a relatively short period of
1094 time, the majority of blood at any given time resides in the venous and microvascular
1095 compartments (~60-75%) (24, 47), in which PO₂ averages 5 kPa (594). Moreover, most monocytes
1096 reside within the spleen at rest (564), where PO₂ ranges from 2-5 kPa in rodents (48, 61, 67, 266)
1097 and swine (573), and 7-8 kPa in rabbits (613, 614). Such variance likely reflects the heterogeneous
1098 perfusion of the spleen, with pronounced gradients extending away from the splenic artery in
1099 mice (61).

1100

1101 Several studies have investigated the effects of isolation and culture of human peripheral blood
1102 mononuclear cells (PBMC) under physiological O₂ (as summarised in Table 1-5). Basal
1103 proliferation of human CD4+/CD8+ PBMC (16, 17, 315) and murine CD4+ T cells (259) was largely
1104 unchanged during culture at a PO₂ of 5 kPa, whereas proliferation stimulated by concanavalin A or
1105 CD3/CD28 crosslinking was markedly lower (16, 17). Interestingly, growth stimulated by another
1106 lectin, phytohemagglutinin (PHA), was unaffected by culture at 5 kPa (16, 17, 315). Another
1107 common observation during culture at 5 kPa is enhanced T-cell differentiation and activation, with
1108 increased early expression of the activated-lymphocyte marker CD69 on PBMC (17, 210, 315),
1109 activation of PBMC-matured human dendritic cells (171) and murine splenocyte-differentiated T
1110 cell CD4:CD8 maturation (61). Indeed, a transcriptional array of human PBMC samples cultured at
1111 5 kPa for 15 days revealed significant upregulation of genes important for lymphocyte biology,
1112 whereas expansion at room air highlighted upregulation of gene clusters associated with stress
1113 responses, cell death and repair mechanisms (210). Expansion of human PBMC under
1114 atmospheric conditions reduces intracellular glutathione (GSH) levels due oxidative stress
1115 associated with prolonged hyperoxia. This artefact can be reduced by expansion of PMBC
1116 expanded at a PO₂ of 5 kPa (146). Associated with atmospheric-culture induced GSH depletion is

the induction of antioxidant and defense proteins such as superoxide dismutase, catalase (CAT) and glutathione peroxidase-1 (146), resulting in lower basal cytosolic reactive oxygen species (146, 315). One potentially significant consequence of the altered human PBMC phenotype at a PO₂ of 5 kPa was reported by Sahaf and colleagues (499). The HIV-Transactivator of transcription (Tat) protein, previously understood to induce apoptosis in *ex vivo* T-cell preparations, caused rapid proliferation and primed cells for subsequent infection more rapidly than PHA (499). This novel finding highlights the possibility of drawing misinformed conclusions based on *in vitro* experiments performed under hyperoxic conditions. In summary, culture of PBMC and similar cells under physiological PO₂ conditions has significant consequences on cell proliferation, redox status and differentiation capacity. It remains to be investigated whether changes in PO₂ within the physiological range (2-5 kPa), e.g. as would occur when monocytes enter the systemic circulation from the spleen, have functional consequences on their physiology.

Human peripheral blood neutrophils undergo rapid (within 24h) and constitutive apoptosis after isolation and culture under standard culture conditions (PO₂ 18-20 kPa). This can be reduced significantly by isolation in a low PO₂ (0-3 kPa) environment (218) and with inhibitors of HIF-1 α hydroxylation (628). Moreover, hyperoxia-induced apoptosis was also reduced in peripheral neutrophils isolated from patients with VHL syndrome (627), although this was further reduced by hypoxic incubation, suggesting a role for both HIF-1 α -dependent and independent pathways. Despite enhanced survival, neutrophils maintained at a PO₂ of 3 kPa exhibited defective respiratory burst activity and hence killing ability against *S. aureus* infection, seemingly through the limitation of molecular O₂ as a substrate for the generation of ROS (383). This may result from sub-optimal O₂ diffusion/supply capacity *in vitro*, as elegantly demonstrated recently (63), rather than true substrate limitation. The effects of low PO₂ culture on neutrophils has been summarised elsewhere (354, 574) and so will not be discussed in further detail here. Whilst a PO₂ of 3 kPa may be considered 'sub physiological' in the general context of this article, one must consider that inflammation can produce localised areas of profound tissue hypoxia (63, 189, 331, 367, 538, 588) and therefore it may be more appropriate to study neutrophil physiology under such conditions, especially if these cells cannot survive at higher PO₂ for more than a few hours. Active neutrophils consume high amounts of O₂ and can actually create or exacerbate a hypoxic environment *in vivo* and *in vitro* (63), which can accelerate the resolution of tissue inflammation.

C. Heart

The heart is second only to the lungs in terms of exposure to O₂, yet in contrast to the lungs is a highly metabolically active tissue with a large O₂ requirement. Although the coronary artery branches directly from the ascending aorta in which blood is at its most oxygenated, measurements of cardioplegic solution PO₂ sampled from numerous coronary artery branches in patients undergoing revascularisation or aortic valve replacement surgery reveal levels of 5

1155 kPa (202). We could not find any measurements of coronary artery PO_2 in healthy humans or
1156 experimental animal models, and thus whether these measurements reflect normal physiology or
1157 are lower as a result of disease remains unclear. Interestingly, PO_2 values not much lower than
1158 these are reported within the coronary sinus in humans (2.7-4.4 kPa (385, 624, 646)), canine (2.9
1159 kPa (69)) and in the great cardiac vein of patients undergoing coronary artery bypass surgery (3.5
1160 kPa (651)). Using a blood-borne phosphorescent probe, Rumsy and colleagues (496) measured
1161 the PO_2 distribution in the epicardial microvasculature of the porcine heart prior to and during
1162 infarction. An average PO_2 of 2.2 kPa was recorded in non-infarcted tissue, with a gradient
1163 observed towards the ischemic core. The coronary microvasculature penetrates the myocardium
1164 superficially, and compression of microvessels during systole means perfusion of the deep
1165 myocardial tissue is intermittent. As a result, a gradient of PO_2 has been observed between the
1166 superficial epicardium, the deep myocardium and individual myocytes, as illustrated in Figure 11.
1167 Such levels range from 4.1-6.1 kPa at the epicardial surface (245, 543) to 3.4 kPa in the
1168 subepicardium (3 mm depth in the canine heart) (654) and 2-3 kPa in the myocardial
1169 tissue (11, 40, 72, 150, 297, 358, 487, 648, 654). Hence, coronary microvascular PO_2 (2.2
1170 kPa (496)) closely matches the average adjacent tissue PO_2 , supporting the concept that a
1171 significant portion of O_2 diffusion must occur upstream of the capillary bed.

1172
1173 The increase in O_2 between the endocardium and coronary sinus reflects the increasingly
1174 acknowledged arteriolar-venular shunting hypothesis of O_2 distribution (328, 594). Generally,
1175 excellent corroboration exists in cardiac PO_2 measurements using a variety of techniques,
1176 including the use of implantable EPR probes which can be used to monitor cardiac PO_2 with
1177 impressive temporal resolution (72, 339, 487) and are stable for at least 112 days *in situ* (297),
1178 though these typically do not offer great spatial resolution. Anatomical complexity in O_2 delivery is
1179 compounded by the extremely high O_2 consumption rate of cardiomyocytes (see Section IV-C),
1180 resulting in very low intracellular PO_2 (1-1.6 kPa (84, 252)), though this low O_2 does not limit
1181 aerobic respiration in these cells (84). Myoglobin, present within the cytosol of skeletal and
1182 cardiomyocytes, has a greater affinity for O_2 than hemoglobin (P50 of ~0.3 vs ~3.5 kPa (12)) and is
1183 thought to facilitate O_2 delivery to respiring mitochondria (567, 568). It may do this simply by
1184 providing a store of O_2 within the cell, that can be made available during periods of increased
1185 activity, or perhaps by 'removing' dissolved O_2 from the cytosol thereby increasing the
1186 concentration gradient from the blood to cell in a process of facilitated
1187 diffusion (90, 234, 281, 657, 658). Hence, actual O_2 content within a cardiomyocyte *in vitro* will be
1188 higher than the detected dissolved PO_2 , complicating interpretations of relative monolayer
1189 oxygenation.

1190
1191 Stem cells derived from human myocardial biopsies cultured at a PO_2 of 5 kPa exhibit greater
1192 chromosomal stability and fewer karyotypic defects over 1-2 months of culture than their room air

1193 counterparts (343). Moreover, a greater yield was achieved per biopsy, with a higher reparative
1194 capacity when subsequently transplanted into a mouse infarcted heart (342). Interestingly, Puente
1195 et al. (471) recently demonstrated that the dramatic rise in cardiac tissue PO₂ in the fetal heart at
1196 birth induces growth arrest through oxidative damage. This elegant study may explain the
1197 enhanced proliferative and reparative potential of cardiac stem cells under physiological O₂ levels,
1198 especially when one considers that the true intracellular O₂ level in these cells may be
1199 considerably lower than 5 kPa.

1200

1201 Murine cardiac fibroblasts cultured at a PO₂ of 3 kPa were also found to proliferate more rapidly,
1202 which was attributed to reduced expression of p21 and a less oxidised environment (494).
1203 However, since intracellular PO₂ in these cells are likely to be considerably lower than the ambient
1204 (and physiological) 3 kPa, these results more accurately represent a hypoxic phenotype
1205 acknowledged by the authors. In line with this, human cardiac fibroblasts cultured under perfused
1206 conditions at a PO₂ of 5 kPa exhibit decreased growth relatively to room air and hypoxic (1 kPa)
1207 cultures (600), suggesting hypoxia and hyperoxia, but not physiological normoxia, are potent
1208 triggers for fibroblast proliferation *in vitro*. In this recent study, a clear delineation between the
1209 cellular response to normoxia (5 kPa) and hypoxia (1 kPa) is demonstrated, with hypoxia strongly
1210 associated with markers of pathological cardiac remodeling (600). However, cells were subjected
1211 to altered ambient PO₂ for only 24 h in this study, and hence may not represent truly 'adapted'
1212 cells. Rat neonatal cardiomyocytes isolated and maintained at a PO₂ of 5 kPa release higher
1213 concentrations of adenosine but rapidly release the vasoconstrictive angiotensin II when exposed
1214 to higher O₂ levels (655). Although limited, these studies collectively demonstrate that culture of
1215 cardiac-derived cells under physiological O₂ levels robustly alters their phenotype, with significant
1216 therapeutic implications.

1217

1218 D. Brain

1219 The brain receives blood from mainly the common carotid artery and to a lesser extent the
1220 vertebral artery, both of which branch directly from the ascending aortic arch. In line with
1221 microvascular O₂ distribution outlined above, oxygen levels of ~8 kPa have been measured in
1222 rat (70, 527) and mouse (501) pial arterioles. Moreover, a PO₂ of ~3.5 kPa in the pial parenchyma
1223 (at depth of ~50µm) (390, 527), indicate a significant loss of O₂ across the pial arteriolar wall (527).
1224 Similar to other major organs, the cerebral vasculature extends superficially throughout the brain
1225 with fewer vessels penetrating the inner layers of the cortex. Accordingly, PO₂ within the cortex
1226 decrease proportional to the depth: from ~5 kPa the superficial
1227 cortex (70, 111, 247, 248, 351, 688) to ~3 kPa in the deep white matter (70, 111, 390, 501, 544),
1228 as illustrated in Figure 12. This gradient further extends into the deeper regions associated with
1229 CNS function (hypothalamus, hippocampus, midbrain). Surprisingly, PO₂ levels within these
1230 regions have been measured as low as 0.5 kPa (0.5-1 kPa midbrain (70), 0.4 kPa pons (70), 1.5-2

1231 kPa hypothalamus (70), 0.8-3.5 kPa caudate nucleus (525)). However, Lyons and
1232 colleagues (364) have challenged this concept recently. Using 2-photon PQM (phosphorescence
1233 quenching method, Section II-C), they observed no change in intravascular PO₂ in either arterioles
1234 or venules of the somatosensory cortex with increasing depth from the surface (364). These
1235 authors proposed that anesthesia and associated stressful handling during the experiment setup
1236 may artificially alter brain activity and hence tissue PO₂ (364). Prior measurements were made
1237 using the surgical insertion of a microelectrode, and therefore revisiting brain tissue PO₂ levels
1238 using 2-photon light microscopy could provide further insights (501, 502). Indeed, Lecoq and
1239 colleagues (328) were able to measure neuronal PO₂ in the mouse olfactory bulb during odour
1240 stimulation, in which average microvascular PO₂ increased from ~6 kPa to 7.5 kPa, simultaneous
1241 with similar increases in red blood cell velocity and intracellular Ca²⁺ (328). Notably, neuropil PO₂
1242 was substantially lower than the surrounding microvasculature (~3 kPa), yet still increased upon
1243 odour stimulation. In subsequent studies, a mean interstitial PO₂ of 3-4 kPa was found in the
1244 murine olfactory bulb and somatosensory cortex (364, 445), consistent with previous studies using
1245 implanted ESR probes (125, 350, 439). Changes in brain oxygenation during stimulation or
1246 disease have become the focus of increased experimental and clinical studies, the former spurred
1247 on by the development of BOLD-MRI (see Section II-D). Whilst blood-oxygen level dependent
1248 functional MRI imaging has established clinically that changes in blood saturation correlate with
1249 changes in neuronal activity within the predicted area (as reviewed (164)), this technique cannot
1250 be used to quantify absolute changes in PO₂ in the brain. However, several recent studies using
1251 microelectrode and phosphorescence-quenching techniques have demonstrated quantitative
1252 changes in brain tissue PO₂ (either in the microvasculature or surrounding neurons) upon sensory
1253 stimulation (256, 328, 445, 692). In these studies, stimulation of neuronal activity was associated
1254 with a transient reduction in tissue PO₂, likely representing localized increases in O₂ consumption,
1255 followed by increases in local blood PO₂ and flow, confirming similar observations using fMRI.

1256

1257 Neurons isolated from rat striatum (578) and cortex (698), human fetal neurons and the neuronal
1258 cell line SH-SY5Y (617), as well as mouse astrocytes (95), have all been studied under
1259 physiological normoxia (defined by authors as an ambient PO₂ of 3-5 kPa). A common phenotypic
1260 change was observed in all these cell types following normoxic culture, characterised by a
1261 hyperpolarized mitochondrial membrane potential, reduced reactive oxygen species generation
1262 and greater survival during prolonged culture. The latter two features may result from enhanced
1263 activity of manganese superoxide dismutase under low O₂ (617). The most significant impact to be
1264 uncovered following culture under normoxia is on neuronal mitochondria. In addition to
1265 mitochondrial hyperpolarization (578, 698), more dense mitochondrial networks have been
1266 observed (578). Moreover, a proteomic screen of SH-SY5Y cells maintained at a PO₂ of 5 kPa
1267 revealed significant induction of mitochondrial complex I proteins, most notably NADH:ubiquinone

oxidoreductase subunit 3, which was associated with greater sensitivity to the complex I inhibitor rotenone (617).

1270

Neuronal stem cells (NSC), otherwise known as neuronal precursor cells, are adult stem cells which differentiate into neurons, astrocytes and glial within the CNS. Neurogenesis generally occurs in regions of the inner brain, such as the hippocampus and dentate gyrus (135), and as such occurs within a physiological PO_2 range of 0.5-3 kPa (see Figure 12). Neuronal stem cells from the embryo (554), sciatic nerve (409), cortex (555), midbrain (561) and ganglionic eminence (255, 258) all exhibit higher proliferation, survival and differentiation potential when cultured at 3 kPa. These effects were associated with enhanced HIF-2 α stabilization and downstream protein expression (258, 554), resulting in an increased transplantation potential following *in vitro* expansion (554, 555). NSC from whole mouse brain homogenates cultured at 5 kPa also exhibit a higher differentiation potential associated with greater mitochondrial oxidative phosphorylation and reduced production of reactive oxygen species (563). Though informative, this latter study makes no justification for the level of O_2 used, instead opting for the arbitrary use of 5 kPa as physiological normoxia. Whilst not necessarily incorrect, the numerous studies listed above suggest that NSC may rarely experience a PO_2 of 5 kPa. Nonetheless, these and other studies have led many to propose a causal relationship between O_2 concentration and stem cell differentiation potential (625), with numerous cell types displaying enhanced differentiation potential under lower O_2 levels. This is corroborated by the anatomical topology of neurogenesis, which occurs predominantly in the brain regions containing lower O_2 (Figure 12).

1289

E. Liver

The liver is a highly vascularized and metabolically active tissue, and as such is relatively well oxygenated as illustrated in Figure 13. Blood entering the hepatic artery is fully saturated and rich in O_2 (human 12.2 kPa (526)). Processed blood exiting the hepatic vein reportedly has a PO_2 between 4-6.5 kPa (526, 598, 660), whilst blood entering through the portal vein is at ~6.5 kPa (526, 598, 660). This dramatic gradient likely reflects the mixing of hepatic arterial blood with venous portal vein blood (at a ratio of 1:3) before entering the hepatic triad, as well as a high metabolic demand of the underlying tissue. Indeed, blood PO_2 within the portal triad is already reduced compared to that of the hepatic artery (8.7 kPa (660). This level is further reduced within the liver parenchyma, where a PO_2 of between 4-7 kPa has been reported (54, 55, 103, 312, 327, 546, 608). Using the oxygen-sensitive EPR probes India ink and lithium phthalocyanine, Jiang et al. (275) were able to measure PO_2 localized to Kupffer cells and whole liver PO_2 , respectively, and demonstrated that Kupffer cells experience a lower PO_2 than the average liver parenchyma (2 vs 3.2 kPa). These values are lower than expected within the liver, possibly reflecting differences in experimental technique. The gradient between the portal triad and vein creates a functional polarization of the underlying hepatocytes, wherein nitrogen metabolism

1306 and albumin secretion are proportional to cell surface O_2 level (37). This allows a similar effluent
1307 composition under conditions of flow reversal. Clearly, although a significant loss of O_2 occurs
1308 during passage through the liver, this organ is still extremely well oxygenated in relation to other
1309 similarly active tissues such as the heart or brain (377).

1310

1311 Studies *in vitro* have provided some explanation for the abnormally high oxygen levels in liver
1312 tissue. In contrast to the majority of cell types, hepatocytes isolated from rat livers and maintained
1313 under low O_2 (4-10 kPa) for the duration of culture (3-9 days) responded adversely. This included
1314 reduced viability (37, 345, 669) and diminished liver-specific gene expression (299, 345) and
1315 functions such as nitrogen metabolism and albumin excretion (37, 669). Moreover, several reports
1316 have highlighted the enhanced infectivity of liver-associated pathogens such as Hepatitis C and
1317 *Plasmodium berghei* (during liver stage malaria) in hepatocytes under low O_2 conditions *in*
1318 *vitro* (421, 612). Interestingly, acetaminophen toxicity was less pronounced in mouse hepatocytes
1319 cultured at a PO_2 of 5 kPa relative to room air (668), although significantly higher basal LDH
1320 release was observed in these cells. Part of this adverse response can be attributed to the very
1321 high O_2 consumption rate of primary hepatocytes which, during static cell culture *in vitro*, can
1322 create an extensive O_2 gradient between air and cytosol (see Section IV-C) (75, 671). In this
1323 context, culture under previously regarded physiological PO_2 (4-10 kPa) may actually expose the
1324 cell monolayer to a PO_2 as low as 0.5 kPa (421). In corroboration, exposure to relatively high (but
1325 still lower than ambient) PO_2 (13-17 kPa) proved beneficial for cell yield (345, 368) and the
1326 response to phenobarbital challenge (299). HepG3 and Hep3B cells cultured at 8 kPa for up to 30
1327 days had higher intracellular, but not mitochondrial, reactive oxygen species generation with
1328 severely reduced intracellular GSH levels (587). Despite this, SOD activity and expression were
1329 significantly higher in these cells, and they exhibited greater resistance to oxidative challenge.
1330 These studies in hepatocytes emphasize the need to understand monolayer oxygenation more
1331 closely. Ambient PO_2 during *in vitro* culture must be accurately tailored to the cell type to avoid
1332 exposing high O_2 -demanding cells to cellular hypoxia (204).

1333

1334 F. Kidneys

1335 The kidneys comprise only 1% of total body mass, yet filter ~20% of cardiac output (4.2 mL/min/g
1336 tissue), and as such are disproportionately perfused compared to the other organs. Indeed, renal
1337 cortical blood flow is the highest recorded per g tissue within the body (386), and the metabolic
1338 requirements are relatively low under normal conditions, yet increase linearly with glomerular
1339 filtration rate, renal blood flow and Na^+ transport (479, 642). Considering such hyperperfusion,
1340 renal tissue should be extremely well oxygenated as with other well-perfused organs such as the
1341 liver (see above). Counter-intuitively however, renal cortical PO_2 has been measured at 4.7 kPa in
1342 the dog (28), 5-7 kPa in the rat (50, 51, 203, 334, 349, 362, 519, 642), 6 kPa in the pig and 4-9.5
1343 kPa in human (411, 541). When the measuring electrode is advanced beyond ~3mm (in the rat

1344 kidney), a sharp reduction in tissue PO_2 is observed corresponding to entry into the medulla (see
1345 Figure 14), where O_2 levels are between 1 kPa in the dog (28), 1.3-4.2 kPa in the
1346 rat (50, 51, 203, 334, 349, 362, 519, 642), 3.3 kPa in the pig (693) and 2 kPa in human (693). In
1347 elegant work by Lübbers and Baumgärtl, a large heterogeneity in cortical PO_2 was observed
1348 whereby some regions experienced near-arterial PO_2 values (~ 11 kPa) (334, 362). Such
1349 heterogeneity was not apparent within the medulla, prompting these authors to conclude that the
1350 highly vascularized anatomy of the cortex results in the formation of large intra-renal PO_2
1351 gradients. Using ultramicroelectrodes (diameter 3-5 μ m), Welch and colleagues achieved
1352 measurements of PO_2 in the nephrons of rats (642). In line with previous data, a significant drop in
1353 PO_2 was reported between the renal artery and efferent arterioles (10.7 to 6 kPa), and tubular PO_2
1354 remained around 6 kPa before increasing within the renal vein to 6.7 kPa (see Figure 14). Kidney
1355 PO_2 values determined by Clark electrode penetration were corroborated by recent measurements
1356 using BOLD MRI (395, 451, 693), confirming the validity of both techniques. Notably,
1357 measurement of kidney PO_2 using a dual laser-Doppler blood flow/ O_2 electrode technique
1358 consistently demonstrated lower cortical PO_2 values than the corresponding single O_2 electrode
1359 (1.3 (434) and 2.1 (463) vs 5.3-6.7 kPa). This disparity was attributed to the larger diameter O_2
1360 electrode required in the dual electrode array compared to that used in tissue penetration studies
1361 (350-500 μ m vs $<20\mu$ m), potentially resulting in damage to the delicate kidney architecture (434).

1362
1363 The substantial drop in PO_2 between the renal artery and cortical tissue prompted many to
1364 postulate the existence of a pre-glomerular O_2 shunt (28, 334, 338). This was confirmed by
1365 Schurek and colleagues who demonstrated that inspiration of gas at 100 kPa PO_2 led to minimal
1366 changes in glomerular PO_2 (5.6 to 9 kPa) despite a robust increase in systemic PO_2 (12 to 74.6
1367 kPa) (519). The close anatomical relationship between interlobular arteries and veins, and the
1368 absence of surrounding capillaries (141, 422), is thought to be responsible for such a shunt in line
1369 with the arterio-venous O_2 transfer theory proposed by Duling and Berne (123). Indeed, renal vein
1370 PO_2 is unusually high compared to systemic venous PO_2 (measured at 6.5 and 7.8 kPa in the
1371 rat (642) and dog (201), respectively, vs ~ 5 kPa), further corroborating renal arterio-venous O_2
1372 transfer. Moreover, whilst whole kidney O_2 consumption is second only to the heart (10 vs 15
1373 ml/min/g), renal blood flow far exceeds myocardial blood flow (750 vs 250 ml/min) and thus renal
1374 O_2 extraction is only $\sim 10\%$ vs 55% in the heart (452, 479, 485, 687). Taken together, these
1375 observations led O'Connor and colleagues to hypothesize that renal tissue is maintained at a low
1376 PO_2 level relative to blood flow to prevent over-oxygenation and excessive oxidative stress (433).
1377 Unfortunately, the side-effect of this proposed adaptation is that segments of the papillae within the
1378 medulla (in particular the S3 proximal tubule and medullary thick ascending limb) are exquisitely
1379 sensitivity to reductions in blood flow, and are the first sites damaged during acute renal
1380 ischemia (46, 130).

1381

1382 Considering the prominent role of hypoxia-inducible factor signaling in the kidney (209) and its
1383 sensitivity to low oxygen (167, 398), relatively little has been published on the long-term culture of
1384 kidney-derived cells under physiological normoxia. This may, in part, be complicated by the
1385 significant differences in what may constitute normoxia in this tissue, with medullary PO₂ values
1386 often 4-5 kPa O₂ lower than corresponding cortical tissue (see above). Much like the
1387 gastrointestinal tract (see Section VI-G), parts of the renal medulla may exist in a state of
1388 'physiological hypoxia'. In intestinal epithelia, cellular phenotypes characterised at a PO₂ of 1 kPa
1389 appear a better reflection of their *in vivo* counterparts than those cultured under room air. However,
1390 exposure of renal tubular epithelial cells to hypoxia (1-3 kPa) results in robust HIF downstream
1391 target protein (VEGF and EPO) induction (129, 209, 337, 417), phenotypes not observed in their
1392 counterparts *in vivo* (491). This discrepancy may reflect the artifactual baseline cellular PO₂ prior to
1393 hypoxic exposure (room air, PO₂ ~18 kPa), potentially exacerbating the subsequent hypoxic
1394 response. It would be interesting to explore whether small reductions in cellular PO₂ around
1395 physiological normoxic values (from 1.5/2 to 1 kPa) can elicit more physiologically relevant
1396 responses in these cells. Such experiments may identify additional, more subtle roles for the HIF in
1397 renal cells, and in doing so shed further light on the renal cell specificity of von Hippel-Lindau
1398 syndrome (29, 419, 503).

1399

1400 G. The digestive system

1401 The discovery of anaerobic bacterium resident within the intestinal lumen led to the concept of
1402 'physiological hypoxia' within the adjacent intestinal tissue (696), with important implications for our
1403 understanding of host-microbiome interactions (292). This section aims to review the literature,
1404 with an overview of digestive system PO₂ and discussion of the importance of considering the O₂
1405 environment during culture of cells derived from the digestive tract *in vitro*. The digestive tract is
1406 characterised by an adventitial (serosa) layer, a muscular middle layer and an epithelial (mucosal)
1407 layer. Large arterioles run longitudinally along the serosa and the microvasculature (mesentery)
1408 penetrating towards the mucosal layer. Although the digestive tract receives a high proportion of
1409 blood flow, only 25% of this perfuses the mucosal and muscular layers at rest (81, 191).
1410 Measurements of digestive tract PO₂ have been divided into luminal, mucosal and serosal tissue,
1411 and the gradient between these values discussed where evident.

1412

1413 1. Stomach

1414 The stomach, similar to the lungs and skin, can come into direct contact with atmospheric levels of
1415 O₂. As a result, PO₂ measurements at the submucosal aspect of the gastric fundus using micro-
1416 electrodes are in the range of 6-10.2 kPa in humans undergoing
1417 esophagectomy (94, 264, 265, 529) and 7.6 kPa in experimental canine models (318), with
1418 similar values (8.4 kPa) reported in canine serosa (353). Using activated charcoal as an EPR
1419 probe (see Section II-D), He and colleagues (228) determined a luminal PO₂ of 7.7 kPa at the level

1420 of the fundus/pylorus. Since PO_2 values are roughly equal across the gastric wall
1421 (lumen>mucosa>serosa, Figure 15C), and such a level is not dissimilar from what might be
1422 expected in the arteriolar circulation (see Section VI-B-2 and Figure 9), we might conclude neither
1423 the contents of the stomach or the cells of the gastric wall represent a significant source of O_2
1424 consumption, at least under basal conditions.

1425

1426 2. Intestines

1427 As illustrated in Figure 15A, a longitudinal gradient in luminal PO_2 is observed during passage
1428 along the gastrointestinal tract. From a luminal PO_2 of 7.7 kPa in the stomach (228), luminal PO_2 in
1429 the small intestine decreases to between 4.2-4.6 kPa (312), and decreases even further to 0.4-1.5
1430 kPa in the large intestine (9, 228, 294, 346). Importantly, the techniques used to obtain such data,
1431 including EPR and 2-photon phosphorescent quenching, are non-invasive and therefore avoid
1432 contaminating the bowel environment with atmospheric air and preserve the integrity of the bowel
1433 wall. A similar longitudinal gradient is observed in mucosal PO_2 (Figure 15A); from 6-10 kPa in the
1434 stomach to values of 3.5 kPa (rat (42)), 5.8 kPa (dog (353)), 2.6-5 kPa
1435 (pig (212, 213, 305, 429, 540, 611)) and 4.5-4.8 kPa (humans (529)) in the small intestine and
1436 values less than 1 kPa in the colon (9, 294). A similar longitudinal gradient is present, albeit less
1437 pronounced, at the serosal aspect (Figure 15A). Small intestine serosal PO_2 is 5.6 kPa
1438 (rabbit (163)), 7.2-8.4 kPa (pig (157, 213, 429, 540)) and 8.1 kPa in humans (570). In the large
1439 intestine, PO_2 at the serosal layer is reported at 4.6 kPa (rabbit, (163)), 3.7-4.5 kPa (pig, corrected
1440 for FiO_2 0.21, (301, 388)), 5.3 kPa (mouse, (9)) and 3.9-5.5 kPa (human, (412, 529, 530)).

1441

1442 From such data, it is clear that O_2 levels show a general decline along the length of the
1443 gastrointestinal tract, being highest in the stomach and lowest in the colon. It is perhaps of more
1444 interest to note that the radial gradient across the intestinal wall (lumen to serosa) does not behave
1445 proportionally. No detectable difference is observed between the lumen and serosa of the
1446 stomach, whereas the lumen of the large intestine is ~5 kPa lower than the serosal layer (Figure
1447 15A). This radial gradient has been demonstrated directly in the small intestine using the
1448 penetrating microelectrode technique (42, 212, 429), by 2-photon PQM (540), and by pimonidazole
1449 staining (157), and also in the colon (294) (representative immunohistochemical images from the
1450 latter studies are shown in Figure 15B). Data from the study by Bohlen indicates a difference of as
1451 much as 2.3 kPa O_2 between the apex and base of a villus (42), whilst a difference of 4.6-9 kPa is
1452 reported between the mucosa and serosa (212, 429, 540). This is corroborated by a gradient in
1453 pimonidazole staining along the villus length (157, 294). It was originally proposed that this
1454 gradient occurs due to an arteriolar-venular O_2 shunt at the base of the villus, where vessels reside
1455 in close proximity to each other (42). However, the finding that this gradient is abolished by
1456 antibiotic treatment and is absent in germ-free mice (294) would suggest the O_2 consumption by
1457 the gut microbiome is wholly responsible. Upon reflection, this is logical given that the bacterial

1458 population increases along the gastrointestinal tract, whereas there is no evidence to suggest the
1459 proposed arteriolar-venular shunt shows similar topographical changes.

1460

1461 The extremely low physiological PO_2 experienced by intestinal epithelium *in vivo* creates an
1462 interesting scenario whereby there is probably no real distinction between hypoxia and normoxia,
1463 but rather a state of 'physiological hypoxia' exists in the intestinal mucosa (92, 696). Hence those
1464 pathways traditionally important in coordinating a cellular response to pathological hypoxia, such
1465 as the HIFs (see Section V-A-1), may have more importance in defining the phenotype of intestinal
1466 epithelia *in vivo*. Indeed, a healthy gut epithelium respiring on their preferred substrate butyrate
1467 exhibits profound HIF response element (HRE)-luciferase activity and HIF-1 α
1468 stabilization (64, 294), indicating a persistent activation of the pathway. This constitutive activity
1469 was found to be essential for the production of defensins, key endogenous antimicrobial peptides
1470 secreted by the intestinal epithelium and accumulated within the mucus layer (293), which itself is
1471 regulated by HIF-1 α at a number of levels (170, 359). Moreover, expression of the multidrug-
1472 resistance protein 1 (P-glycoprotein) was also found to be dependent on constitutive HIF-1 α
1473 activity in the intestine (93). HIF activity is also crucial in maintaining intestinal barrier integrity, with
1474 key junctional proteins such as claudin-1 and creatine kinases M and B regulated by HIF-1 and
1475 HIF-2, respectively (180, 498). Notably, a key role for constitutive HIF-2 α activity in maintaining
1476 iron absorption has also been identified in the mouse duodenum, the epithelium of which also
1477 exhibits strong basal pimonidazole staining (379). Hence, the state of physiological hypoxia is
1478 important in maintaining host defence, barrier integrity and iron absorption throughout the
1479 gastrointestinal tract.

1480

1481 Importantly in the context of replicating normoxia *in vitro*, experiments in which intestinal epithelial
1482 cell lines (Caco-2 and T84) are exposed to physiological normoxia (PO_2 1-2 kPa) generally
1483 corroborate such observations (see Table 1-6 for summary). Notably, although few studies have
1484 extended the period of normoxic culture beyond 24 h, a number did demonstrate a stable
1485 phenotype after up to 4 days of normoxia (93, 566). A point worth discussing is the apparent
1486 discrepancy between the effects of low O_2 exposure on transepithelial resistance (TER) *in vitro* and
1487 *in vivo*. Exposure of Caco-2 and T84 cells to a PO_2 of 1-2 kPa induces no change or increases in
1488 TER *in vitro* (170, 284, 566), a characteristic unique to intestinal epithelial cells (170). In contrast,
1489 intestinal permeability is consistently decreased in mice breathing low O_2 (8
1490 kPa) (170, 284, 408, 566). Aside from technical differences, there are two possible explanations for
1491 these observations. Firstly, hypoxic exposure does not alter TER *in vitro* relative to room air
1492 cultured cells, a condition wholly artificial in the context of physiology. Moreover, if mucosal PO_2 is
1493 normally physiologically hypoxic (see above) then a reduction in inspiratory PO_2 (from 20.9 to 8
1494 kPa) may create a genuinely pathologically hypoxic/near anoxic environment within the mucosal
1495 intestinal epithelium. Similar conditions are observed during inflammatory bowel disease and

ulcerative colitis (64, 284), conditions associated with increased intestinal permeability. Thus fundamental differences in the context and degree of 'hypoxia' under these experimental conditions make comparisons difficult to interpret. Secondly, whole body hypoxia undoubtedly has effects beyond the intestines, and it is therefore difficult to isolate the actions of any paracrine mediators released by other tissues also responding to reduced systemic arterial PO_2 . Notably, work by Zeitouni and colleagues (689, 690), using O_2 -sensitive chips immobilized on the bottom of standard culture plates, indicates that exposure of Caco-2 cells to an ambient PO_2 of ~ 1 kPa results in a near anoxic medium PO_2 after 6 days (690). However, it should be noted that the authors used 1 mL of medium in a 24-well plate, double the recommended volume for such dishes. Using the example discussed in a previous section (Section IV-C), these conditions would generate a value for d double that commonly used (0.2 mm), facilitating 'self-inflicted hypoxia' in this scenario. Ideally, the correct *in vitro* experiment to accompany *in vivo* hypoxia models would be exposure of intestinal epithelial cells to very low ($PO_2 \sim 0$ -0.5 kPa) O_2 from a baseline of 1-3 kPa to more accurately reflect conditions generated *in vivo*.

1510

1511 3. The Pancreas

Interest in pancreatic PO_2 distribution arose largely out of the need to understand the oxygenation of endogenous islets in order to match this when implanted elsewhere. Using a microelectrode, Harper and colleagues (226) reported a PO_2 of 3.3 kPa in the acinar/exocrine region of the exteriorised rat pancreas. This was corroborated by more detailed measurements by Carlsson and colleagues (66, 67), who reported a gradient from 4.6 to 2.7 kPa O_2 between the surface and interior of the exocrine pancreas. Kinnala and colleagues used a technique termed suffusion tonometry to monitor whole organ PO_2 in the porcine pancreas. Briefly, a silicone tube is implanted into the tissue and equilibrated with anoxic saline. After a subsequent period of equilibration with the tissue, fluid is extracted from the tube and PO_2 determined using a standard electrode. Using this technique, they reported pancreatic PO_2 values of 5.3 (302) and 5.6 (303), thus reasonably matching reported values using microelectrode techniques. The Islets of Langerhans are important anatomical features of the pancreas wherein insulin and glucagon are synthesized and secreted. These tiny collections of cells constitute only 1-2% of total pancreatic tissue, yet receive 10-15% of organ blood flow (268). This extensive perfusion is reflected in a PO_2 level considerably higher than the surrounding parenchyma, between 5-6 kPa in the rat (66, 67).

1527

The high rates of O_2 consumption in pancreatic β cells has presented a unique problem during their isolation, culture and implantation. Isolated β cells typically exist in culture as suspended spheroids, and pimonidazole staining illustrates that such conditions produced severe hypoxia (113, 438) which is proportional to medium PO_2 and islet size (310). This also extends to monolayer cultures of the pancreatic cell line MIN6, in which intracellular PO_2 (based on pimonidazole staining) was far below ambient (511). Moreover, exogenously implanted islets

1534 rapidly develop hypoxia regardless of their anatomical location (66, 67), reflecting an inability of
1535 neo-vascularisation to counteract islet O₂ consumption. Attempts to address this problem have
1536 included the use of permeably culture supports, such as silicone membranes (18, 304)
1537 perfluorocarbon (PFC)-based culture dishes (166) or O₂ leaching materials (96), as well as culture
1538 under hyperoxic ambient PO₂ (50 kPa) (309). Using a PFC-PDMS construct, Fraker and
1539 colleagues elegantly demonstrated that the combination of high substrate solubility and lower
1540 ambient PO₂ (~12.6 kPa) produced the greatest volume of physiologically oxygenated (predicted
1541 pericellular PO₂ of ~5.5 kPa) β-cells and almost no anoxic cells compared to culture under room air
1542 on traditional plastic ware (166). This translated into greater β-cell viability and function following
1543 isolation and a trend towards greater *in vivo* survivability once transplanted.

1544

1545 H. Bone and cartilage

1546 1. Bone and bone marrow

1547 Typical bone consists of an outer cortical/compact layer, a spongy/cancellous inner layer and the
1548 medulla, containing the bone marrow (Figure 16A). The outer mineralized layers are sparsely
1549 populated with cells and are effectively avascular, and the only vessels found within this layer are
1550 the superficial periosteal arteries and penetrating nutrient arteries perfusing the bone marrow. As
1551 such, mineralized bone tissue exists at relatively low PO₂. In the only known publication measuring
1552 bone extravascular PO₂, Brighton and Heppenstall reported a steep gradient in PO₂ between the
1553 diaphyseal and metaphyseal regions (14.5 to 2.6 kPa) of the rabbit proximal tibial epiphyses (52).
1554 Since the reported PO₂ in the diaphyseal region is beyond the physiological arterial range (12-13
1555 kPa), the accuracy of these values necessitates further study. The concept of a steep gradient
1556 between regions of mineralized bone has been predicted mathematically (685). More recently,
1557 measurement of PO₂ distribution in the mouse tibia was partially accomplished using implantable
1558 LiPc crystal EPR probes (see Section II-D) (360, 361). PO₂ at the periosteum of normal tibia was 6
1559 kPa (360), whereas localized PO₂ within the bone upon fracturing decreased significantly to ~1.5
1560 kPa immediately after injury (361). Subsequent angiogenesis and healing resulted in a robust
1561 increase in bone PO₂ (from 1.5 to ~7 kPa), indicating that neovascularization of damaged bone
1562 can restore normal O₂ distribution (361). Notably, periosteal PO₂ values reported by Lu and
1563 colleagues match closely the intravascular PO₂ values in microvessels of the periosteum (6.6
1564 kPa (552)), suggesting a limited radial gradient in this tissue which is consistent with the sparsely
1565 populated nature of mineralized bone.

1566

1567 The isolation and maintenance of human stem cells under low O₂ has generated promising
1568 advances in their clinical application. Whilst effects of culture under physiological O₂ levels on
1569 partially differentiated precursor stem cells have already been discussed under the auspice of their
1570 respective tissue origin, bone marrow is a primary source of adult pluripotent stem cells.
1571 Furthermore, this tissue is also the source of hemopoietic stem cells which give rise to all

1572 circulating blood cells. As such, a detailed understanding of their physiological environment is of
1573 clinical relevance. PO₂ has been determined in human sternum (5.4 kPa (192)), and iliac crest
1574 marrow (6.8 (262), 7.2 (227), 6.1 kPa (154)), canine femoral medulla (6.4 kPa (308)) and mouse
1575 femoral marrow (~4 kPa (71)). These measurements were largely obtained from blood-gas
1576 analysis following the aspiration of marrow. Recently, detailed *in situ* measurements of marrow O₂
1577 levels in living mice have been obtained using the more advanced 2PLM method (see Section
1578 C) (552), with impressive resolution. Spencer and colleagues (502) reported an intravascular PO₂
1579 gradient between vessels in the periosteum (6.6 kPa), cortical bone (4.2 kPa) and marrow (3 kPa).
1580 By comparing intravascular and extravascular PO₂ within the bone marrow, these authors
1581 identified a significant radial gradient (~1.5 kPa) in these vessels which could be abolished by sub-
1582 lethal irradiation or chemotherapy. Indeed, localized bone marrow hypoxia was associated with
1583 large clusters of cells within the marrow, indicating that O₂ consumption maintains a low PO₂
1584 environment in the bone marrow.

1585

1586 Whilst elegant and informative, the study by Spencer and colleagues reports bone marrow PO₂
1587 values considerably lower than values reported by numerous other laboratories (~2 vs ~5 kPa).
1588 Tissue trauma associated with bone marrow aspiration or microelectrode penetration may lead to
1589 artificially high marrow O₂ level estimations and hence the non-invasive measurements by Spencer
1590 et al. may be physiologically representative. Species differences are an unlikely explanation, since
1591 Ceradini et al. (71) reported a bone marrow PO₂ of ~4 kPa in the mouse femoral marrow. Instead,
1592 regional differences in bone PO₂ may provide some clarification, with Spencer et al. opting to study
1593 the calvaria (skull cap) in contrast to the femur, sternum or iliac crest. Similarly, PO₂ distribution in
1594 the brain microvasculature differs subtly from other microvascular beds (Figure 9).

1595

1596 2. Cartilage and synovial fluid

1597 Many bones are connected via a synovial joint consisting of a fluid filled synovial cavity and
1598 articular cartilage lining the epiphyses of the bone (Figure 16A). In addition to providing mechanical
1599 support during movement, synovial fluid is also crucial in supplying nutrients, including O₂, to the
1600 articular cartilage, which itself is completely avascular. Chondrocyte physiology is strongly
1601 influenced by O₂ tension, during development and in adult life (513), and increases in O₂
1602 consumption are observed during rheumatoid arthritis-associated inflammation (332). For these
1603 reasons, understanding PO₂ distribution within the synovial joint is of great interest. Of the studies
1604 reporting synovial PO₂ values, only two investigated synovial fluid PO₂ in healthy tissue. Ferrell
1605 and Najafipour (1992) reported a mean PO₂ of 6.4 kPa in the rabbit knee (152). Using
1606 microelectrode penetration, these authors also demonstrated a gradient in PO₂ between the
1607 superficial synovial membrane and articular cartilage, at which point mean PO₂ reached ~1.5 kPa,
1608 a value corroborated in human septal cartilage more recently (482). Although such PO₂ distribution
1609 traces are commonly reported in numerous tissues, the study of a synovial joint under immobile

1610 anesthetised conditions may create an artifactual gradient which would not otherwise be present in
1611 a mobile joint (152). Indeed, Etherington and colleagues (137) reported a transient increase in
1612 knee synovial PO₂ upon mobilisation of the joint. A number of studies have reported synovial fluid
1613 PO₂ in the human arthritic knee, with values ranging from 2.6 (38), 3.5 (363), 3.7 (143), 4.1 (589),
1614 5.7 (363) to 7.3 kPa (484). Inflammatory arthritis was also associated with a decline in knee
1615 synovial PO₂ in rabbits (416) and mice (137). In general, synovial PO₂ correlated negatively with
1616 the severity of inflammation (589), with relationships to blood flow (416) and white blood cell
1617 count (484) observed. Furthermore, patients with osteoarthritis had significantly higher synovial
1618 fluid PO₂ than those with rheumatoid arthritis (363). Hence it is likely that the inflamed nature of the
1619 arthritic joint produces a pathophysiologically 'hypoxic' environment relative to the normal joint, and
1620 thus PO₂ values derived from the study of such joints likely underestimate physiological normoxia.

1621

1622 3. Resident bone cells

1623 As described in Sections H-1 and H-2, the avascular nature of mineralised bone and cartilage
1624 creates a physiological milieu containing relatively little O₂ (~1.5 kPa in deep cortical bone and
1625 articular cartilage) for resident cells. Table 1-7 provides an overview of studies conducted to
1626 investigate the effects of culture at physiological normoxia on bone cell physiology. Long-term
1627 culture (>72 h) of osteoblasts at the lower end of this physiological range (PO₂ 2 kPa) is associated
1628 with a significant reduction in mineralization (Ca²⁺ deposition as measured by Alizarin red staining)
1629 and alkaline phosphatase activity compared to room air cultures (329, 423, 435, 601, 686). This
1630 was reportedly due to a delayed (601) or reduced (423) expression of the osteocyte markers
1631 osteocalcin and procollagen lysine dioxygenase, and was associated with a reduced ability to
1632 synthesize and deposit collagen (435). Indeed, microarray analysis of human osteoblastic cells
1633 (SV-HFO) cultured at 2 kPa for up to 3 weeks revealed the greatest impact of low O₂ on the
1634 mineralization phase of differentiation (424). However, culture under an ambient PO₂ of 2 kPa
1635 would result in a much lower intracellular PO₂ and hence this phenotype is likely representative of
1636 a reactive, hypoxic cell rather than the physiological norm. This hypothesis is corroborated by the
1637 observation that pre-osteoblastic cell lines (MC3T3-E1 and MLOA5) cultured long-term at a PO₂ of
1638 2 kPa exhibit marked HIF-1 α stabilization (686), pimonidazole staining and HRE luciferase
1639 activity (329), indicating a classical hypoxic phenotype. In contrast, paired cultures maintained at a
1640 PO₂ of 5 kPa showed no such HIF-1 α activity (329), consistent with our findings in human
1641 endothelial cells maintained >5 days under similar conditions (see Figure 10). Under this more
1642 physiologically relevant PO₂ (accommodating for monolayer consumption), MC3T3-E1 cells
1643 exhibited earlier and more robust mineralization and alkaline phosphatase activity, which was
1644 associated with increased expression of the osteocytic markers osteocalcin, Dmp1, Mepe and
1645 Fgf23 (241). Similar findings were reported in murine calvarial organ cultures maintained under 5
1646 kPa O₂ (241). These findings suggest that higher O₂ levels may stimulate osteocyte maturation
1647 and mineral bone formation *in vivo*, supported by the knowledge that the highest intraosseal PO₂

values (6-7 kPa) recorded are in the periosteal layers of diaphyseal bone (52, 552). Thus, the appropriate intracellular O₂ level *in vitro* should be defined based on the differentiation state to be studied.

4. Chondrocytes

Grimshaw and Mason (2000) (196) attributed the unusual ability of chondrocytes to withstand severe hypoxia to a very low mitochondrial mass *in vivo* (53) and low O₂ consumption rates *in vivo* and *in vitro* (240). As chondrocytes experience very low O₂ levels *in vivo* (~1.5 kPa, see Figure 16A), O₂ conservation may be necessary. There are numerous studies of chondrocytes during culture under normoxic conditions *in vitro*, as summarised in Table 1-8. Such studies have largely focused on culture techniques to reverse the de-differentiation of primary chondrocytes that occurs following isolation and monolayer culture *in vitro*. De-differentiation is characterised by a switch in collagen production from type II to type I (34), with concomitant downregulation of key chondrocyte markers aggrecan and SOX9. Whilst very low O₂ (<1.5 kPa) levels exist in deep articular cartilage, new cartilage is formed at the superficial layer adjacent to the synovial fluid where PO₂ values are closer to 5 kPa (see Figure 16A). When cultured on alginate beads at a PO₂ of 5 kPa for 2-4 weeks, the phenomenon of redifferentiation is accelerated and enhanced in human (287, 414, 518), bovine (117, 118, 239, 415), mouse (242) and rabbit (233) chondrocytes. In addition to the expression of *Col2a1*, *Aggrecan* and SOX9, increased deposition of collagen and GAG was frequently observed in alginate 3D bead cultures (518). Furthermore, enlarged matrix area was noted in E14.5 murine forelimbs cultured *ex vivo* at 5 kPa (242), indicating this effect is not confined to isolated cells.

Culture in 3D alginate beads presents a particular problem concerning O₂ diffusion and ultimately intracellular PO₂. Li et al. (341) addressed this question using a combination of experimentally determined O₂ consumption rates and PO₂ distribution modeling in scaffold-free aggregate cultures seeded at varying densities. They reported a 'critical' threshold of ~8 kPa, at which point cells no longer synthesized collagen and preferentially produced proteoglycans. How this relates to previous studies is unclear, given that the majority of the studies cited above use cells cultured in pellet or alginate 3D conditions at 5 kPa and report increased collagen deposition relative to room air cultures. Based on the PO₂ profiles published by Li et al., average pellet PO₂ may be closer to 8 kPa when cultured at room air (~18.5 kPa) than under 5 kPa, and therefore one might expect increased collagen deposition in these pellets. Despite this, gradients in collagen deposition have been observed in alginate beads under 5 kPa, with the highest collagen-associated staining apparent at the periphery (117). Thus, the concept of a critical threshold for collagen deposition may have some merit, but discrepancies in the actual PO₂ value are expected given differences in O₂ diffusion between scaffold free and alginate cultures.

1686 5. Marrow-derived stem cells

1687 The concept of a stem cell niche within the bone marrow and its influence on mesenchymal and
1688 hematopoietic stem cell fate are front-and-centre in our understanding of the physiology of these
1689 cells. Elegant imaging-based investigations have demonstrated that hematopoietic stem cells
1690 (HSC) preferentially localize to small arterioles within the endosteal marrow (319) and that
1691 variations from this niche induce a proliferative and 'hypoxic' phenotype (319, 430). Given our
1692 knowledge that the steepest O₂ gradients outside the lungs exist across the walls of arterioles
1693 (Section III-B and Figure 9), it is likely that steep gradients in PO₂ also exist in between arterioles
1694 within the bone marrow. Such heterogeneity in marrow PO₂ may be confounded by regional
1695 heterogeneity in cell populations, with varying degrees of cellular activity and thus O₂
1696 consumption (552). Measurements of marrow PO₂ range from 1.7 to 7.2 kPa (Figure 16A), yet no
1697 study has directly addressed the concept of localized regions of lower PO₂. Moreover,
1698 mesenchymal stem cells (MSC) and hematopoietic stem cells (HSC) may originate from the bone
1699 marrow, but their sites of action extend throughout the body. Indeed, many have postulated that
1700 changes in PO₂ as cells exit the marrow into the systemic blood stream serve as a key trigger for
1701 terminal differentiation (402). In light of this, defining physiological normoxia for marrow-derived
1702 stem cells is difficult. Here, we will consider 3-5 kPa as normoxia but will discuss select studies in
1703 which cells were cultured under 2 kPa for comparative purposes. A full summary of papers
1704 meeting these criteria is provided in Table 1-9.

1705
1706 Expansion at a PO₂ of 3-5 kPa has repeatedly demonstrated greater colony formation or
1707 proliferation of mesenchymal stem cells (MSC) isolated from human (149, 528, 616) and
1708 sheep (700) bone marrow, although conflicting evidence has also been reported (449). A number
1709 of studies have identified an enhanced chondrogenic differentiation potential in MSC colonies
1710 expanded at 5 kPa (336, 374, 391, 528, 700), as characterised by the expression of *Col2a1* (see
1711 above) and quantitative analysis of glycosaminoglycan deposition. One study of human MSC
1712 cultured at 5 kPa reported no change in chondrogenic or osteogenic differentiation (449). This
1713 could be related to the source of cells used, as the latter study sourced human MSC from a
1714 commercial supplier whereas the majority of studies obtain cells directly from donors. A common
1715 observation reported by Pattappa et al. and others (149, 700) is a reduced level of cellular
1716 senescence after long-term expansion at 5 kPa. This finding may be related to the increased level
1717 of 'stemness' or differentiation potential in these cells, and supports the notion of a more
1718 physiologically relevant phenotype under physiological PO₂ *in vitro*. Fewer studies have focused on
1719 hematopoietic (CD44+) stem cells (HSC) within the marrow. Reykdal et al. observed less nitrite
1720 accumulation in cultures of human CD34+ HSC isolated and expanded at 5 kPa for 7 days. These
1721 authors attributed this to reduced induction of the inducible isoform of nitric oxide synthase,
1722 although they did not investigate the contributions of other isoforms. Similar to MSC, HSC
1723 proliferate more rapidly under 5 kPa and form larger colonies (483).

1724

1725 I. Skin

1726 The measurement of transcutaneous PO_2 using non-invasive techniques has long been used
1727 experimentally and clinically as a readout of peripheral perfusion/oxygenation. This procedure
1728 involves placing a housed electrode onto the skin surface heated to 41-44°C to encourage
1729 microvascular vasodilation, thus increasing local blood supply which creates a local excess of O_2
1730 delivered by the arteriolar circulation (Figure 17A). Transcutaneous PO_2 is directly proportional to
1731 cutaneous blood flow (647) and inversely proportional to epidermal thickness (144). Heating the
1732 skin from 37-45°C increases blood flow 3-4-fold (269), thus temperature intimately influences the
1733 reported PO_2 value. For example, transcutaneous PO_2 in the human forearm was recorded as 9.3
1734 kPa at 44°C by Falstie-Jensen et al., yet only 5.1 kPa at 41°C by Spence et al. (550). Whilst a
1735 useful readout of arterial oxygenation clinically, such artefactual conditions result in relatively poor
1736 correlation with *bone fide* measurements of skin PO_2 (see Figure 17B). Using penetrating
1737 electrodes, PO_2 has been determined in the human abdominal, forearm, thigh and fingernail
1738 cuticular dermis, as well as in rat abdomen. At a generalised subcutaneous level, PO_2 has been
1739 reported to range between 3 (266), 4.1 (626), 5 (551), 5.3 (632), 6.3 (637) and 8 kPa (138). More
1740 detailed investigations by Evans and Naylor (140), Baumgärtl et al. (27) and Wang *et al.* recorded
1741 PO_2 profiles at varying dermal depths (see Figure 17C). Evans and Naylor reported PO_2 values of
1742 6.1, 6.2 and 7.4 kPa at depths of 1-2, 3 and 5 mm respectively, and similar profiles are also
1743 reported at equivalent depths in other areas of skin (27, 632). Clearly, the skin has two distinct
1744 sources of O_2 diffusion, the atmosphere and microvasculature, and a nadir exists in which cells
1745 receive little O_2 from either. One apparent pitfall in skin PO_2 measurements using penetrating
1746 electrodes is the potential for overestimated values resulting from damage to the dense
1747 microvasculature. Jamieson and Brenk demonstrated that larger electrodes (330µm vs 60µm
1748 diameter) produced higher average subcutaneous PO_2 values in the rat abdomen (alongside
1749 similar measurements in liver, kidney, and splenic tissue), with evidence of macroscopic tissue
1750 damage.

1751

1752 More recently, significant efforts have been made to develop techniques to non-invasively monitor
1753 cutaneous PO_2 using phosphorescence quenching. Unlike the methods discussed in Section II-C,
1754 in which a synthetic porphyrin-type dye is administered exogenously as an O_2 -sensitive probe, a
1755 technique developed by Mik and colleagues (223) employs 5-aminolevulinic acid (ALA), a
1756 precursor to the endogenously produced protoporphyrin IX. ALA cream is administered topically to
1757 the skin and results in accumulation of protoporphyrin IX in the mitochondria of epidermal cells
1758 within ~3 h (224). Using this technique, a PO_2 of between 6.3-8 kPa was reported in cutaneous
1759 mitochondria of the rat abdomen (223, 225, 637), which correlates well with similar measurements
1760 using microelectrodes (138, 139). By co-injection of the hydrophilic Oxyphor G4 dye, simultaneous
1761 measurement of mitochondrial and microvascular PO_2 was possible (223). A gradient of ~2.7 kPa

1762 between blood and mitochondria was reported in the rat abdominal cutis, which was abolished by
1763 topical application of cyanide. Notably, a microvascular PO₂ of 10 kPa measured in this study is
1764 well within the range of reported transcutaneous PO₂ values (9.3-11.2 kPa (144, 560, 647)),
1765 confirming that transcutaneous measurements accurately reflect microvascular PO₂. In a more
1766 recent study, mitochondrial PO₂ was found to be a very sensitive indicator of the limit of
1767 hemodilution in pigs (489). However, the average baseline mitochondrial PO₂ value reported in this
1768 study (2.7 kPa) is far lower than that recorded in rats in previous investigations (7.3-8
1769 kPa (223, 225)), a discrepancy that remains unexplained.

1770

1771 Fibroblasts isolated from mouse embryos, tail and human dermis have all been cultured at 3-5 kPa
1772 (Table 1-10). Common to many of these independent reports is the observation that cells
1773 maintained at low O₂ exhibit markedly less chromosomal instability/breakage (78, 283, 446) and
1774 senescence (78, 446). This was particularly apparent in mouse derived fibroblasts (446) which
1775 appear highly sensitive to the damaging effects of atmospheric conditions. Mouse embryonic
1776 fibroblasts (MEF) cultured at 3 kPa had higher and persistent expression of the p53-related
1777 proteins p19^{ARF} and p16, yet senescence could be rapidly induced by re-exposure to 20 kPa (446).
1778 Notably, this sensitivity appears specific to laboratory rodent strains and is not observed in wild
1779 animals of the same species (448). This could reflect the longer telomeres observed in laboratory
1780 species (232) that are thought to occur in the absence of evolutionary selection for short telomeres
1781 in the wild. In human keratinocytes, isolation and culture at 4 kPa O₂ results in enhanced migration
1782 rates associated with reduced superoxide generation compared to cells cultured under 20
1783 kPa (493).

1784

1785 Carrera et al. (68) reported increased HIF-1 α activity in primary keratinocyte populations cultured
1786 at a PO₂ of 5 kPa for up to 4 days. This was reduced by inhibition of the MAPK cascade and with
1787 certain DNA damaging compounds such doxorubicin, with minimal effects on proliferation. It is
1788 likely that these observations can be attributed to the phenomenon of 'self-inflicted hypoxia' (see
1789 Section IV-D), based on the following observations: (i) HIF-1 α protein levels were still minimal at 5
1790 kPa compared to those observed at 1 kPa. Since monolayer oxygenation decreases with cell
1791 density (see Section IV-C), HIF-1 α protein may only be stabilized at confluency and may therefore
1792 only affect proliferation in its latter stages; (ii) prominent HIF-1 α protein expression and HRE-
1793 luciferase was observed in monolayers of the colon cancerous cell line HCT116 under the same
1794 conditions. Oxygen consumption rates are reportedly higher in these cells compared to primary
1795 human keratinocytes (25 vs 8 amol/min/cell (147, 619, 638)), and thus would have a lower
1796 intracellular PO₂ and hence higher HIF-1 α activity; and finally (iii) inhibition of HIF-1 α stabilization
1797 was observed when cellular activity was reduced by MAPK inhibitors or by DNA damaging agents.
1798 A reduction in cellular activity may result in decreased O₂ consumption rates, thereby increasing
1799 intracellular PO₂. As discussed in Section IV-D, an understanding of O₂ dynamics in monolayer

1800 cultures is critical in interpreting experimental data, and should be considered when designing a
1801 model of *in vitro* normoxia.

1802

1803 J. Adipose tissue

1804 Interest in PO₂ distribution in adipose tissue has increased in the last 2 decades (246) based on
1805 the observations that tissue from obese patients or animals can be hypoxic, although this is not
1806 fully accepted (188). In lean mice, PO₂ values have been reported between 6.4-7.7 kPa in
1807 epididymal fat pads (673, 676) and 5.6 kPa in the perigonadal white adipose tissue (477). Parallel
1808 measurements in the *ob/ob* transgenic obese mouse revealed a consistently lower adipose tissue
1809 PO₂ (2-4.6 kPa, decreasing with age), with strong histochemical evidence for tissue hypoxia
1810 through pimonidazole staining (477, 673, 676). In humans, subcutaneous adipose tissue PO₂ was
1811 measured at 7.6 kPa in the arm (280) and 7.3-7.9 kPa in in abdomen (187, 447) of lean patients. In
1812 contrast to rodent models of obesity, adipose tissue PO₂ in obese patients has been shown to be
1813 both higher (187, 618) and lower (280, 447) compared to matched lean patients. Pasarica and
1814 colleagues (447) were able to demonstrate that adipose tissue PO₂ correlated negatively with
1815 percentage fat composition and the expression of the inflammatory marker CD68, whilst correlating
1816 positively with capillary density. Based on these correlative relationships and the known
1817 histological characteristics of adipose tissue from obese patients (582), a lower PO₂ in tissue from
1818 obese patients seems logical. The work by Goossens and colleagues (39, 187, 618) reports a
1819 higher fasting adipose tissue PO₂ in obese patients compared with matched lean (~9 vs ~6 kPa)
1820 subjects (187) and that weight loss in obese patients is associated with a significant reduction in
1821 mean adipose PO₂ (6.8 to 5.5 kPa) (618). It was demonstrated that increasing and decreasing
1822 adipose tissue blood flow (using isoprenaline and angiotensin II infusion, respectively) leads to
1823 corresponding changes in tissue PO₂, corroborating claims by Pasarica et al. (447) concerning the
1824 relationship between adipose tissue PO₂ and perfusion/vascularization. As adipose tissue blood
1825 flow is reduced in obese patients (187), one would expect a lower PO₂. These discrepancies could
1826 be due to either differences in technique used to monitor PO₂, with Goossens and colleagues
1827 using a custom-designed microdialysis technique as opposed to the more commonly used
1828 electrode/fiberoptic probe, or physiological state in which measurements were made (fasting (187)
1829 vs normal (280, 447)).

1830

1831 As discussed and reviewed in by Trayhurn (586), a large body of work exists examining the effects
1832 of hypoxia (PO₂ of 1-2 kPa) on adipocyte function *in vitro* to better understand the pathophysiology
1833 of obesity. However, as highlighted by Trayhurn, culture at 20 kPa followed by a dramatic drop to
1834 1-2 kPa has limited physiological significance, as neither the starting PO₂ nor 'hypoxic' value are
1835 physiological for adipocytes. It is far more likely that adipocytes experience a PO₂ of around 6-7
1836 kPa *in vivo*, and to date two studies have attempted to address this issue. The first by Wood and
1837 colleagues (663) exposed primary human adipocytes to PO₂ values of 1, 3, 5, 10, 15 and 20 kPa

for 24 h and measured expression and release of the key adipokines leptin and adiponectin, as well as IL-6 and VEGF. A strong negative correlation was observed between leptin, VEGF and IL-6 mRNA expression and PO₂, whereas the opposite was observed for adiponectin and glucose uptake (663). Notably, the steepest part of the O₂ concentration response curve was between 3-10 kPa, the (patho)physiological range of PO₂ in adipose tissue (see above). However, adipocytes were only exposed to different PO₂ environments for 24 h, which may induce a response more representative of a response to low O₂ and less indicative of their physiology *in vivo*. This problem was addressed in a subsequent study, in which Famulla and colleagues (145) cultured adipocytes at 5 and 10 kPa for 14 days before measuring key adipocyte functions. Corroborating observations by Wood et al. (663), leptin expression and secretion were decreased at lower O₂ and associated with increased triglyceride content and glycerol release. Interestingly, peak responses were observed at a PO₂ of 10 kPa (145), conditions in which intracellular PO₂ is likely to be ~7 kPa based on known O₂ consumption rates of cultured adipocytes (694).

In addition to adipocytes and vascular cells, adipose tissue also contains a population of multipotent stem cells known as stromal cells (177). A number of studies have investigated the effects of long-term culture of these adipose-derived multipotent stem cells at low O₂ levels, as summarised in Table 1-11. Similar to other types of stem cells (see Sections H-5 and K-3), culture at either 2 (606) or 5 (464, 512, 533) kPa for the duration of culture/differentiation resulted in increased adipogenic (512, 606) and/or osteogenic/chondrogenic (464, 606) differentiation *in vitro*. Notably, enhanced differentiation potential *in vitro* did not translate into increased chondrogenesis when explanted *in vivo* (464). Whilst informative, the rationale behind culturing adipose derived stem cells at 2-5 kPa is unclear in light of the known distribution of PO₂ in such tissue *in vivo* (mean tissue PO₂ ~7 kPa). It is possible that populations of stem cells exist in localized regions of lower PO₂ within the tissue, although no evidence for this has been put forward to date. It seems more likely that 2 or 5 kPa O₂ was chosen as a 'best-guess' based on similar publications in cells of different origin. Although the matter may appear trivial, the work of Wood et al. (663) discussed above illustrates a steep relationship between ambient PO₂ and adipocyte function between 3-10 kPa, and thus selecting the most appropriate ambient PO₂ at which to culture such cells is absolutely critical.

K. Uterus and embryo

1. Uterus and oviduct

The uterus is a highly dynamic organ that experiences gross changes in physiology and function throughout the menstrual cycle, with surges in hormone secretion closely linked to contractile function and blood flow. In seminal work during the late 1960's, Mitchell and Yochim described periodic fluctuations in luminal (intrauterine) PO₂ that were rhythmic from hour to hour (401), and also changed dramatically according to stage of the menstrual cycle (400). During estrous,

1876 intrauterine PO₂ has been reported at between 3 (677) and 3.4 kPa (288, 400, 401) in the rat, 2.7
1877 kPa in the guinea pig (174), 4.9 kPa in hamster (155), 5.7 kPa in rabbit, 1.7 kPa in Rhesus
1878 monkeys (155) and between 2 (674) and 2.4-2.5 kPa in humans (440, 488). In experimental rodent
1879 models, intrauterine PO₂ peaked during the diestrous-1 period (288) and was strongly associated
1880 with similar increases in blood flow (174, 400). Such changes were not observed in primates (155).
1881 Upon conception, intrauterine PO₂ rises dramatically in rats (677) and rabbits (155) simultaneous
1882 with increases in progesterin and decreases in estrogen secretion (677). Indeed, ovariectomy to
1883 mimic estrogen depletion also caused large increases in intrauterine PO₂ in rats (from 3.4 to 8.2
1884 kPa) which were reversed by concomitant estrogen treatment (401). Unfortunately, no data exist to
1885 our knowledge concerning intrauterine PO₂ across the menstrual cycle in humans, nor are there
1886 direct measurements prior to and post conception. Endometrial PO₂ was measured by Rodesch
1887 and colleagues (488) in patients undergoing elective termination procedures at 8-10 weeks and in
1888 those at 12-13 weeks. These authors report an increase from a mean PO₂ of 5.3 kPa in the early
1889 termination to 6.2 kPa at 12-13 weeks. Similarly, Jauniaux and colleagues (271) measured PO₂ in
1890 coelomic/amniotic fluid and in the decidual lining in pregnancies between 7-10 weeks and 11-16
1891 weeks. Whilst intrauterine fluid PO₂ was similar (2.5 kPa, similar to that reported by Ottosen et
1892 al. (440) and Yedwab et al. (674)), PO₂ in the decidual lining was significantly higher in late
1893 pregnancies (8.6 vs 9.8 kPa) (271). Thus, intrauterine PO₂ is relatively low prior to pregnancy and
1894 during estrous, especially in primates and humans, but rises rapidly within the uterine wall
1895 (myometrium/decidua) upon conception or during diestrous in line with increases in blood flow.

1896

1897 In the fallopian tubes, a dichotomy exists between mammalian species according to whether
1898 ovulation is cyclic or initiated by copulation. In rodent species (non-cycling), PO₂ within the
1899 fallopian tubes/oviducts remains constant and is relatively high, ranging from 6.8-8 kPa in
1900 rabbits (155, 380) and 5.6 kPa in hamsters (155). In contrast, PO₂ in the oviduct of rhesus
1901 monkeys is incredibly low when ovulation is not occurring (<1 kPa O₂) but increases dramatically
1902 during ovulation to between 7-10 kPa (155, 365). During passage to the uterus, the oocyte
1903 receives nutrients and O₂ directly from the fallopian tube lumen, and thus it is postulated that
1904 rodent oviduct PO₂ is maintained at a high level to ensure it can accommodate an oocyte at any
1905 point (365).

1906

1907 2. *In vitro* fertilization

1908 One of the earliest adoptions of in vitro culture under physiological normoxia was in the field of in
1909 vitro fertilization, where the first successful culture of a human embryo to the blastocyst stage was
1910 achieved only under 5 kPa (557). Since then, working under a reduced ambient PO₂ (usually 5
1911 kPa) has become reasonably common both in research and clinical IVF (45, 186, 285, 314, 418).
1912 Given the demand for improved clinical outcomes with IVF procedures, a large number of clinical
1913 trials have been performed to investigate whether culturing early-stage embryos at 5 kPa is

1914 beneficial. These have been reviewed extensively in several meta-analyses (45, 186, 418), and as
1915 such this topic will not be discussed in detail. In two reviews published in 2011, (45, 186)
1916 conflicting conclusions were drawn. Bontekoe and colleagues (45) reported a statistically
1917 significant improvement in live birth rate when embryos were cultured at 5-6 kPa O₂ which equated
1918 to an increase in success rate from 30% to between 32-43%. In contrast, Gomes-Sobrinho and
1919 colleagues (186) were unable to conclude that culture at low O₂ improved outcomes, although they
1920 did state that many results seemed promising. Notably, 7 studies were retrieved in both reviews
1921 based on their respective selection criteria, yet these were not the same 7 studies. Differences in
1922 selection criteria, with those applied by Bontekoe et al. (45) appearing stricter, are likely to explain
1923 the discrepancy in outcomes. In a later review by Nastri and colleagues (418), a small (5%) but
1924 significant improvement was detected in live birth rates when embryos were cultured at 5-6 kPa,
1925 corroborating the findings of Bontekoe et al. (45). Common to all reviews was the criticism of study
1926 quality; especially related to investigator bias and differences in equipment/technique.

1927

1928 More recently, some have challenged the dogma that 5 kPa represents the ideal physiological PO₂
1929 at which IVF should be conducted (286, 406, 670). This is based on the observation that PO₂
1930 drops substantially between the oviduct and uterine lining; from ~6 to 2-3 kPa (see Figure 18), and
1931 thus the early blastocyst may experience a decrease in ambient PO₂ during implantation. To model
1932 this *in vitro*, embryos have been cultured at room air (670) or 5 kPa (286) until day 3, at which point
1933 ambient PO₂ was reduced to 2 kPa and blastocyst yield and quantity assessed at day 5. Cell yield
1934 increased 2-fold when embryos were cultured at 2 kPa between days 3 and 5 only when they were
1935 previously cultured at 5 kPa (286), with no significant effect detected if the embryo was previously
1936 kept at room air (670). In light of the significant effort and expense invested in improving IVF
1937 outcomes by utilising the concept of physiological normoxia, these more intricate efforts to better
1938 match physiological conditions are a logical progression.

1939

1940 3. *Embryonic stem cells*

1941 Embryonic stem cells (ESC) are pluripotent stem cells derived from the inner cell mass of the early
1942 blastocyst, pre-implantation into the uterine wall, and receives nutrients and O₂ from the fallopian
1943 tube/uterine fluid. As such, they propagate in an environment containing low O₂, ranging between
1944 2-5 kPa depending on the species (see above). Much like in IVF procedures, the derivation of ESC
1945 from the early blastocyst has long been conducted under low O₂ conditions (see (397) and (539)
1946 for reviews, and Table 1-12 for an up-to-date summary). This has largely been driven by enhanced
1947 proliferation or colony/embryonic body formation, consistently observed in both mouse and human
1948 ESC expanded at a PO₂ of 2-5 kPa (30, 142, 161, 173, 176, 300, 403, 467, 469, 473, 475, 629). A
1949 second advantage is a higher degree of pluripotency and less spontaneous differentiation; whether
1950 determined by expression of the OCT4/NANOG/SOX2 triad or downstream targets (643, 678), by
1951 SSEA-1 expression (142, 469), or morphological analysis (161, 469). Interestingly, although

maintained in an undifferentiated state, ESC at low O₂ can also more readily differentiate and to a higher degree when stimulated. More efficient differentiation into cardiomyocyte (30), vascular (320, 473) pulmonary (173), chondrocyte (307) and most often neuronal (300, 403, 404, 666) lineages has been reported. Differentiation into neural precursor cells appears to occur preferentially at very low PO₂ (2-3.5 kPa) under the control of HIF-1/2 (666).

Genomic stability has often been assessed in ESC cultured at low O₂ and compared with those exposed to room air. Forsyth et al. (161) showed that hESC exhibited greater spontaneous chromosomal aberrations after 20 passages at room air compared to those maintained for the equivalent time at 2 kPa, which had very few additional aberrations. Lengner et al. (335) subsequently demonstrated that culture at room air is responsible for the premature and irreversible inactivation of an X-chromosome frequently observed during hESC culture, through demethylation of the *XIST* gene promoter region. Similarly, hyper-methylation of the DLK1-DIO3 cluster at room air results in silencing of this gene region which can be prevented by maintenance at physiological PO₂ levels (5 kPa).

Embryonic stem cells are known to be highly metabolically active, preferring glycolysis as their source of ATP generation (79). This phenotype appears accentuated when ESC are cultured at low O₂, with higher rates of glucose consumption and lactate production frequency observed (83, 158, 596). In their most recent paper, Christensen and colleagues (83) propose that increased glycolysis is facilitated by enhanced expression of glucose transporter 3 (GLUT3) which correlated positively with OCT4 mRNA expression, thus relating glycolytic activity to pluripotency. ESC are also known to consume a large amount of O₂, which creates a concern regarding self-inflicted hypoxia during culture (see Section IV). It has been demonstrated on a number of occasions that O₂ can be severely limited in monolayer cultures of ESC especially at low ambient PO₂ (320, 466, 467, 596). Hence, as proposed by Turner et al. (596), confluent cultures kept at a PO₂ of 2 kPa (and even perhaps at 5 kPa (2, 320)) are inevitably encroaching on anoxia. This issue, whilst acknowledged, is yet to be satisfactorily addressed and thus calls into question the physiological validity of using very low (2-5 kPa) ambient PO₂ in ESC culture, with an intracellular PO₂ ~2-5 kPa being the actual desired outcome. Limit studies have been conducted with ESC cultured at higher (6-10 kPa) O₂ levels, which may counteract O₂ consumption to produce a more physiological intracellular PO₂. In mouse ESC, similar levels of proliferation and pluripotency (OCT4/NANOG/SOX2 mRNA) (467) and VEGF production (473) were observed between ~4-10 kPa ambient PO₂. However, human ESC differentiated to a higher degree during colony growth at 10 vs 5 kPa ambient PO₂ (469). Thus there may well be physiological consequences to the 'self-inflicted' hypoxia occurring following culture at 2-5 kPa, although this needs further investigation.

4. Placental tissue and trophoblasts

1990 Placental development and subsequently the health of the tissue and fetus are closely linked to
1991 changes in PO_2 (270, 597, 650). During embryogenesis, rapid proliferation of trophoblastic tissue
1992 creates thick villus membranes which result in reduced diffusion of O_2 from the maternal arterial
1993 blood to the surrounding tissue. As such intervillous PO_2 is reportedly as low as 2-3 kPa in human
1994 placenta at 8-10 weeks gestation (271, 272, 488), which has been shown to modulate the
1995 proliferative and angiogenic trophoblastic phenotype required to establish a patent intervillous
1996 circulation (65, 270, 597). Once adequate perfusion is established (>12 weeks gestation), a rapid
1997 rise in villous/placental tissue PO_2 is observed, reaching 7-8 kPa (271, 272, 488, 548), where
1998 placental tissue PO_2 remains largely stable for the duration of gestation (597).

1999

2000 The issue of oxygenation *in vitro* has long been considered important in the culture of trophoblasts
2001 and placental tissue explants, and a large amount of the literature has already been elegantly
2002 reviewed by Tuuli and colleagues (597). Numerous studies have attempted to understand the
2003 impact of changes in PO_2 on trophoblast phenotype, largely through comparative studies on
2004 cultures maintained at ambient PO_2 values ranging from 20 to <1 kPa. However, measurement of
2005 pericellular PO_2 in primary human trophoblast cultures using a microelectrode revealed that cells
2006 were experiencing near anoxic (PO_2 of 0.1-0.6 kPa) conditions even when cultured under ambient
2007 (20 kPa) PO_2 (77). This gradient was medium-depth dependent and abolished by methanol fixation
2008 of the cells, confirming evidence discussed previously (Section IV-C). Although not confirmed by
2009 others to date, these data clearly call into question the validity of using standard culture conditions
2010 to study primary trophoblasts *in vitro*.

2011

2012 VII. Conclusions and future prospects

2013 The concept that oxygen is critical for normal cellular function is unanimously accepted. However,
2014 for scientists O_2 may represent more of a double-edged sword, in view of the numerous damaging
2015 effects associated with reactive species produced from O_2 . Despite this, traditional methods used
2016 extensively in the culture of mammalian cells result in the exposure to undefined, uncontrolled O_2
2017 levels which are often at either extreme of the quasi-physiological range, i.e. either hyperoxic or
2018 hypoxic with respect to the physiological milieu. In this review, we have provided an up-to-date
2019 assessment of the current understanding of PO_2 distribution in tissues and organs *in vivo*, and
2020 discussed some examples of where this knowledge has been implemented to enhance the
2021 physiological relevance of cell culture conditions *in vitro*. In collating and critically discussing this
2022 information, we hope to provide a reference source for future research aimed at designing novel
2023 and physiologically relevant experiments to address ever-more complex scientific questions.

2024

2025 As highlighted throughout this review, accurately recapitulating physiological normoxia *in vitro* is far
2026 more complex than simply adjusting the ambient 'head-space' PO_2 . An understanding of the
2027 physical conditions in which cells are cultured (i.e. plastic permeability, volume of medium used

and rates of O₂ equilibration in solution) should underpin the choice of the final desired pericellular PO₂ determined using mathematical models and/or experimental data to predict pericellular versus ambient PO₂. Such careful experimental design informed by our review of the literature should provide researchers with the ‘closest representation’ of likely tissue PO₂ levels *in vivo*. Differences in experimental conditions and protocols for cell culture, when sufficient detail is reported, and concerns about the definition of physiological normoxia have may limit collective advances for translational research.

Powerful tools are now available to better predict and measure PO₂ in culture, with accumulating studies highlighting their necessity. We thus hope that the contents of this review will help unify experimental approaches used by basic and clinical researchers. In this context, we propose the following guidelines for researchers who wish to culture their cells under defined physiological normoxia *in vitro*:

1. **Define the conditions appropriately.** Oxygen levels should be measured and defined in terms of PO₂ whenever possible. Often reported as ‘room air’ or 20% O₂, most cell culture experiments are conducted in incubators in which the ambient PO₂ is closer to 18.5 kPa, and sometimes below.
2. **Start the experiment properly.** Always pre-equilibrate all culture media and solutions for a minimum of 2 hours, and considerably longer for large volumes, at the appropriate ambient PO₂ prior to use on cells. It is advisable to store all culture plasticware at the desired PO₂ to avoid O₂ leaching.
3. **Controlling monolayer oxygenation.** We have highlighted throughout this review that appropriately controlling monolayer oxygenation is a consistent problem. There are several parameters that can be easily altered to maintain control over monolayer oxygenation, listed here according to relative ease:
 - i. *Use of O₂-permeable plastic:* this creates a new and much more efficient way in which O₂ can be delivered to the monolayer, alleviating problems due to static medium.
 - ii. *Varying medium height: surface area:* by minimising the ratio between medium height and culture surface area, one reduces the distance for O₂ diffusion and thereby maximise delivery. Simply reducing the volume of medium can achieve this.
 - iii. *Varying ambient PO₂:* if medium volume cannot be reduced, one can increase the ambient PO₂ to compensate for monolayer O₂ consumption.
 - iv. *Continuous perfusion:* To completely alleviate issues associated with O₂ delivery, continuous perfusion of well oxygenated medium is an elegant way to control intracellular O₂ precisely even in response to large increases in O₂ consumption.

Results should always be interpreted in the context of pericellular or intracellular PO₂ rather than ambient PO₂. Mathematical models have proved a useful tool to predict such values,

and recent advances in experimental techniques have allowed the direct monitoring of intracellular PO₂.

4. **Consider a range of PO₂ values.** Oxygenation *in vivo* is heterogeneous in both space and time, and thus no single value can be described as normoxia for a given cell type. Moreover, the expression and activity of many proteins are not linearly related to the intracellular PO₂. It is for these reasons that we find it far more informative to conduct preliminary studies under a range of 'physiological' O₂ levels (2-10 kPa, for example), which offer a far more relevant comparison than 21 vs 1 kPa.

Can culture under physiological normoxia improve the translation of cell physiology to animal models and the clinic? There are several excellent studies (342, 499, 553, 578) that have already provided convincing evidence in favor of this hypothesis, and the concept is already implemented clinically in IVF clinics around the world. Despite this, we believe there is still significant scope to demonstrate that culturing cells under their respective physiologically normoxic conditions genuinely recapitulates their native phenotype and improves outcomes of clinical relevance. Moving forward, we believe it is critical for this field of research to avoid isolated phenotypic comparisons between cells at room air and those at normoxia, instead focusing on whether culture under physiological conditions can reveal novel insights into disease pathology, or pharmacodynamics and kinetics of existing and novel therapeutics. Moreover, it is perhaps overly simplistic to consider only one normoxic value within a given tissue, when there is clearly considerably complexity in tissue oxygenation. Thus, the oxygen-sensitivity of a pathway of interest may be more accurately assessed over a small range of normoxic values, such as that between the renal medulla and cortex (Section VI-F) or from the inner bone marrow to the associated vasculature (Section VI-H). Furthermore, whilst critically important, O₂ represents just one component of the physiological milieu that is altered during standard culture practice, with other factors such as biomechanics, 3D co-culture and substrate matrix contributing equally to the cellular phenotype. Moving forward, it is essential to better model all these factors together to truly begin recapitulating the physiological environment *in vitro*.

ACKNOWLEDGEMENTS

We thank Professor Sir Peter Ratcliffe, FRS (The Francis Crick Institute, London, and University of Oxford, U.K.) for his helpful comments and discussion of this article. Correspondence to Dr Thomas P. Keeley (e-mail: thomas.keeley@ndm.ox.ac.uk) and Prof Giovanni E. Mann (e-mail: giovanni.mann@kcl.ac.uk)

GRANTS

This work was supported by research grants from the British Heart Foundation (FS/13/66/30445, PG/13/1/29801) and Heart Research UK (Novel Emerging Technologies NET RG2633).

2104

2105 **DISCLOSURES**

2106 GE Mann and TP Keeley have no conflicts of interest, financial or otherwise.

2107

2108 References

- 2109 1. Abaci HE, Shen Y-I, Tan S, and Gerecht S. Recapitulating physiological and pathological
2110 shear stress and oxygen to model vasculature in health and disease. *Sci Rep* 4: 4951,
2111 2014.
- 2112 2. Abaci HE, Truitt R, Luong E, Drazer G, and Gerecht S. Adaptation to oxygen deprivation in
2113 cultures of human pluripotent stem cells, endothelial progenitor cells, and umbilical vein
2114 endothelial cells. *Am J Physiol Cell Physiol* 298: C1527-1537, 2010.
- 2115 3. Adamson E, Ludwig K, Mummy D, and Fain SB. Magnetic resonance imaging with
2116 hyperpolarized agents: methods and applications. *Phys Med Biol* 2017.
- 2117 4. Adesida AB, Grady LM, Khan WS, Millward-Sadler SJ, Salter DM, and Hardingham TE.
2118 Human meniscus cells express hypoxia inducible factor-1 α and increased SOX9 in
2119 response to low oxygen tension in cell aggregate culture. *Arthritis research & therapy*
2120 9: R69, 2007.
- 2121 5. Adler KB, Cheng P-W, and Kim KC. Characterization of guinea pig tracheal epithelial cells
2122 maintained in biphasic organotypic culture: cellular composition and biochemical analysis of
2123 released glycoconjugates. *Am J Respir Cell Mol Biol* 2: 145-154, 1990.
- 2124 6. Adler KB, Khosla J, and Kim KC. Morphometric and biochemical characterization of a
2125 chamber system for maintaining differentiated guinea pig respiratory mucosal cells between
2126 air and liquid phases. *Am Rev Respir Dis* 137: 14, 1988.
- 2127 7. Adler KB, Schwarz JE, Whitcutt MJ, and Wu R. A new chamber system for maintaining
2128 differentiated guinea pig respiratory epithelial cells between air and liquid phases.
2129 *Biotechniques* 5: 462-466, 1987.
- 2130 8. Ahmad R, and Kuppusamy P. Theory, instrumentation, and applications of electron
2131 paramagnetic resonance oximetry. *Chem Rev* 110: 3212-3236, 2010.
- 2132 9. Albenberg L, Esipova TV, Judge CP, Bittinger K, Chen J, Laughlin A, Grunberg S,
2133 Baldassano RN, Lewis JD, and Li H. Correlation between intraluminal oxygen gradient and
2134 radial partitioning of intestinal microbiota. *Gastroenterology* 147: 1055-1063, 2014.
- 2135 10. Allen CB, Schneider BK, and White CW. Limitations to oxygen diffusion and equilibration in
2136 in vitro cell exposure systems in hyperoxia and hypoxia. *Am J Physiol Lung Cell Mol*
2137 *Physiol* 281: L1021-1027, 2001.
- 2138 11. Angell CS, Lakatta EG, Weisfeldt ML, and Shock NW. Relationship of intramyocardial
2139 oxygen tension and epicardial ST segment changes following acute coronary artery
2140 ligation: effects of coronary perfusion pressure. *Cardiovasc Res* 9: 12-18, 1975.
- 2141 12. Antonini E, and Brunori M. *Hemoglobin and myoglobin in their reactions with ligands*.
2142 North-Holland Pub. Co., 1971.
- 2143 13. Aoyagi T, Kishi M, Yamaguchi K, and Watanabe S. Improvement of the earpiece oximeter.
2144 *Japanese Society of Medical Electronics and Biological Engineering* 974: 90-91, 1974.
- 2145 14. Archer SL, Reeve HL, Michelakis E, Puttagunta L, Waite R, Nelson DP, Dinauer MC, and
2146 Weir EK. O₂ sensing is preserved in mice lacking the gp91 phox subunit of NADPH
2147 oxidase. *Proceedings of the National Academy of Sciences* 96: 7944-7949, 1999.
- 2148 15. Archer SL, Will JA, and Weir EK. Redox status in the control of pulmonary vascular tone.
2149 *Herz* 11: 127-141, 1986.
- 2150 16. Atkuri KR, Herzenberg LA, and Herzenberg LA. Culturing at atmospheric oxygen levels
2151 impacts lymphocyte function. *Proc Natl Acad Sci U S A* 102: 3756-3759, 2005.
- 2152 17. Atkuri KR, Herzenberg LA, Niemi A-K, Cowan T, and Herzenberg LA. Importance of
2153 culturing primary lymphocytes at physiological oxygen levels. *Proc Natl Acad Sci U S A*
2154 104: 4547-4552, 2007.
- 2155 18. Avgoustiniatos ES, Hering BJ, Rozak PR, Wilson JR, Tempelman LA, Balamurugan AN,
2156 Welch DP, Weegman BP, Suszynski TM, and Papas KK. Commercially available gas-
2157 permeable cell culture bags may not prevent anoxia in cultured or shipped islets. In:
2158 *Transplantation proceedings* 2008, p. 395-400.
- 2159 19. AVIADO DM, DALY MD, LEE CY, and SCHMIDT CF. The contribution of the bronchial
2160 circulation to the venous admixture in pulmonary venous blood. *J Physiol* 155: 602-622,
2161 1961.
- 2162 20. Balis UJ, Behnia K, Dwarakanath B, Bhatia SN, Sullivan SJ, Yarmush ML, and Toner M.
2163 Oxygen consumption characteristics of porcine hepatocytes. *Metab Eng* 1: 49-62, 1999.

- 2164 21. Bannai S, Sato H, Ishii T, and Sugita Y. Induction of cystine transport activity in human
2165 fibroblasts by oxygen. *J Biol Chem* 264: 18480-18484, 1989.
- 2166 22. Barker MC, Golub AS, and Pittman RN. Erythrocyte-associated transients in capillary PO₂:
2167 an isovolemic hemodilution study in the rat spinotrapezius muscle. *Am J Physiol Heart Circ*
2168 *Physiol* 292: H2540-2549, 2007.
- 2169 23. Barker SG, Talbert A, Cottam S, Baskerville PA, and Martin JF. Arterial intimal hyperplasia
2170 after occlusion of the adventitial vasa vasorum in the pig. *Arteriosclerosis, thrombosis, and*
2171 *vascular biology* 13: 70-77, 1993.
- 2172 24. Barrett KE, Barman SM, and Boitano S. *Ganong's review of medical physiology*. New Delhi:
2173 McGraw Hill, 2010, 2010.
- 2174 25. Battino R. Oxygen and ozone. IUPAC solubility data series. Vol. 7. Oxford, UK: Pergamon
2175 Press, 1981.
- 2176 26. Baumgardner JE, and Otto CM. In vitro intermittent hypoxia: challenges for creating
2177 hypoxia in cell culture. *Respir Physiol Neurobiol* 136: 131-139, 2003.
- 2178 27. Baumgärtl H, Ehrly AM, Saeger-Lorenz K, and Lübbers DW editors. *Clinical oxygen*
2179 *pressure measurement*. Springer, 1987, p. 121-128.
- 2180 28. Baumgärtl H, Leichtweiss HP, Lübbers DW, Weiss C, and Huland H. The oxygen supply of
2181 the dog kidney: measurements of intrarenal pO₂. *Microvasc Res* 4: 247-257, 1972.
- 2182 29. Bausch B, Jilg C, Gläsker S, Vortmeyer A, Lützen N, Anton A, Eng C, and Neumann HP.
2183 Renal cancer in von Hippel-Lindau disease and related syndromes. *Nature Reviews*
2184 *Nephrology* 9: 529-538, 2013.
- 2185 30. Bauwens C, Yin T, Dang S, Peerani R, and Zandstra PW. Development of a perfusion fed
2186 bioreactor for embryonic stem cell-derived cardiomyocyte generation: oxygen-mediated
2187 enhancement of cardiomyocyte output. *Biotechnol Bioeng* 90: 452-461, 2005.
- 2188 31. Bedard K, and Krause K-H. The NOX family of ROS-generating NADPH oxidases:
2189 physiology and pathophysiology. *Physiol Rev* 87: 245-313, 2007.
- 2190 32. Benson BB, and Krause D. The concentration and isotopic fractionation of gases dissolved
2191 in freshwater in equilibrium with the atmosphere. 1. Oxygen. *Limnology and Oceanography*
2192 25: 662-671, 1980.
- 2193 33. Benson BB, Krause D, and Peterson MA. The solubility and isotopic fractionation of gases
2194 in dilute aqueous solution. I. Oxygen. *Journal of Solution Chemistry* 8: 655-690, 1979.
- 2195 34. Benya PD, Padilla SR, and Nimni ME. Independent regulation of collagen types by
2196 chondrocytes during the loss of differentiated function in culture. *Cell* 15: 1313-1321, 1978.
- 2197 35. Berra E, Benizri E, Ginouvès A, Volmat V, Roux D, and Pouyssegur J. HIF prolyl-
2198 hydroxylase 2 is the key oxygen sensor setting low steady-state levels of HIF-1α in
2199 normoxia. *EMBO J* 22: 4082-4090, 2003.
- 2200 36. Berra E, Richard DE, Gothié E, and Pouyssegur J. HIF-1-dependent transcriptional activity
2201 is required for oxygen-mediated HIF-1α degradation. *FEBS letters* 491: 85-90, 2001.
- 2202 37. Bhatia SN, Toner M, Foy BD, Rotem A, ONeil KM, Tompkins RG, and Yarmush ML. Zonal
2203 liver cell heterogeneity: effects of oxygen on metabolic functions of hepatocytes. *Cell Eng*
2204 1: 125-135, 1996.
- 2205 38. Biniecka M, Kennedy A, Fearon U, Ng CT, Veale DJ, and O'Sullivan JN. Oxidative damage
2206 in synovial tissue is associated with in vivo hypoxic status in the arthritic joint. *Ann Rheum*
2207 *Dis* 69: 1172-1178, 2010.
- 2208 39. Bizzarri A, Koehler H, Cajlakovic M, Pasic A, Schaupp L, Klimant I, and Ribitsch V.
2209 Continuous oxygen monitoring in subcutaneous adipose tissue using microdialysis. *Anal*
2210 *Chim Acta* 573-574: 48-56, 2006.
- 2211 40. Bjerrum JT, Perko MJ, and Beck B. Myocardial oxygen tension during surgical
2212 revascularization. A clinical comparison between blood cardioplegia and crystalloid
2213 cardioplegia. *Eur J Cardiothorac Surg* 29: 181-185, 2006.
- 2214 41. Björnheden T, Levin M, Evaldsson M, and Wiklund O. Evidence of hypoxic areas within the
2215 arterial wall in vivo. *Arteriosclerosis, thrombosis, and vascular biology* 19: 870-876, 1999.
- 2216 42. Bohlen HG. Intestinal tissue PO₂ and microvascular responses during glucose exposure.
2217 *Am J Physiol* 238: H164-171, 1980.
- 2218 43. Bohlen HG. Tissue PO₂ in the intestinal muscle layer of rats during chronic diabetes. *Circ*
2219 *Res* 52: 677-682, 1983.

- 2220 44. Bonello S, Zahringer C, BelAiba RS, Djordjevic T, Hess J, Michiels C, Kietzmann T, and
2221 Gorlach A. Reactive oxygen species activate the HIF-1alpha promoter via a functional
2222 NFkappaB site. *Arterioscler Thromb Vasc Biol* 27: 755-761, 2007.
- 2223 45. Bontekoe S, Mantikou E, van Wely M, Seshadri S, Repping S, and Mastenbroek S. Low
2224 oxygen concentrations for embryo culture in assisted reproductive technologies. *Cochrane*
2225 *Database Syst Rev* 7: 2011.
- 2226 46. Bonventre JV, and Zuk A. Ischemic acute renal failure: an inflammatory disease? *Kidney*
2227 *Int* 66: 480-485, 2004.
- 2228 47. Brandis K. The Physiology Viva. *Australia Print and Copy, Southport* 2002.
- 2229 48. Braun RD, Lanzen JL, Snyder SA, and Dewhirst MW. Comparison of tumor and normal
2230 tissue oxygen tension measurements using OxyLite or microelectrodes in rodents.
2231 *American Journal of Physiology* 280: H2533-H2544, 2001.
- 2232 49. Brevig T, Røhrmann JH, and Riemann H. Oxygen reduces accumulation of type IV
2233 collagen in endothelial cell subcellular matrix via oxidative stress. *Artif Organs* 30: 915-921,
2234 2006.
- 2235 50. Brezis M, Heyman SN, Dinour D, Epstein FH, and Rosen S. Role of nitric oxide in renal
2236 medullary oxygenation. Studies in isolated and intact rat kidneys. *J Clin Invest* 88: 390-395,
2237 1991.
- 2238 51. Brezis M, Heyman SN, and Epstein FH. Determinants of intrarenal oxygenation. II.
2239 Hemodynamic effects. *Am J Physiol* 267: F1063-1068, 1994.
- 2240 52. Brighton CT, and Heppenstall RB. Oxygen Tension in Zones of the Epiphyseal Plate, the
2241 Metaphysis and Diaphysis: AN in Vitro AND in Viro STUDY IN RATS AND RABBITS. *JBJs*
2242 53: 719-728, 1971.
- 2243 53. Brighton CT, Kitajima T, and Hunt RM. Zonal analysis of cytoplasmic components of
2244 articular cartilage chondrocytes. *Arthritis & Rheumatism* 27: 1290-1299, 1984.
- 2245 54. Brooks AJ, Eastwood J, Beckingham IJ, and Girling KJ. Liver tissue partial pressure of
2246 oxygen and carbon dioxide during partial hepatectomy. *Br J Anaesth* 92: 735-737, 2004.
- 2247 55. Brooks AJ, Hammond JS, Girling K, and Beckingham IJ. The effect of hepatic vascular
2248 inflow occlusion on liver tissue pH, carbon dioxide, and oxygen partial pressures: defining
2249 the optimal clamp/release regime for intermittent portal clamping. *J Surg Res* 141: 247-251,
2250 2007.
- 2251 56. Buckler KJ. Effects of exogenous hydrogen sulphide on calcium signalling, background
2252 (TASK) K channel activity and mitochondrial function in chemoreceptor cells. *Pflügers*
2253 *Archiv-European Journal of Physiology* 463: 743-754, 2012.
- 2254 57. Buerk DG, and Goldstick TK. Arterial wall oxygen consumption rate varies spatially. *Am J*
2255 *Physiol* 243: H948-958, 1982.
- 2256 58. Buerk DG, and Goldstick TK. Oxygen tension changes in the outer vascular wall supplied
2257 by vasa vasorum following adenosine and epinephrine. *Blood Vessels* 23: 9-21, 1986.
- 2258 59. Bunn HF, and Poyton RO. Oxygen sensing and molecular adaptation to hypoxia.
2259 *Physiological reviews* 76: 839-885, 1996.
- 2260 60. C Gaertner F, Souvatzoglou M, Brix G, and J Beer A. Imaging of hypoxia using PET and
2261 MRI. *Current pharmaceutical biotechnology* 13: 552-570, 2012.
- 2262 61. Caldwell CC, Kojima H, Lukashev D, Armstrong J, Farber M, Apasov SG, and Sitkovsky
2263 MV. Differential effects of physiologically relevant hypoxic conditions on T lymphocyte
2264 development and effector functions. *The Journal of Immunology* 167: 6140-6149, 2001.
- 2265 62. Calvani M, Rapisarda A, Uranchimeg B, Shoemaker RH, and Melillo G. Hypoxic induction
2266 of an HIF-1alpha-dependent bFGF autocrine loop drives angiogenesis in human
2267 endothelial cells. *Blood* 107: 2705-2712, 2006.
- 2268 63. Campbell EL, Bruyninckx WJ, Kelly CJ, Glover LE, McNamee EN, Bowers BE, Bayless AJ,
2269 Scully M, Saeedi BJ, Golden-Mason L, Ehrentraut SF, Curtis VF, Burgess A, Garvey JF,
2270 Sorensen A, Nemenoff R, Jedlicka P, Taylor CT, Kominsky DJ, and Colgan SP.
2271 Transmigrating neutrophils shape the mucosal microenvironment through localized oxygen
2272 depletion to influence resolution of inflammation. *Immunity* 40: 66-77, 2014.
- 2273 64. Campbell EL, Bruyninckx WJ, Kelly CJ, Glover LE, McNamee EN, Bowers BE, Bayless AJ,
2274 Scully M, Saeedi BJ, Golden-Mason L, Ehrentraut SF, Curtis VF, Burgess A, Garvey JF,
2275 Sorensen A, Nemenoff R, Jedlicka P, Taylor CT, Kominsky DJ, and Colgan SP.

Transmigrating neutrophils shape the mucosal microenvironment through localized oxygen depletion to influence resolution of inflammation. *Immunity* 40: 66-77, 2014.

65. Caniggia I, Winter J, Lye SJ, and Post M. Oxygen and placental development during the first trimester: implications for the pathophysiology of pre-eclampsia. *Placenta* 21 Suppl A: S25-30, 2000.

66. Carlsson PO, Liss P, Andersson A, and Jansson L. Measurements of oxygen tension in native and transplanted rat pancreatic islets. *Diabetes* 47: 1027-1032, 1998.

67. Carlsson PO, Palm F, Andersson A, and Liss P. Markedly decreased oxygen tension in transplanted rat pancreatic islets irrespective of the implantation site. *Diabetes* 50: 489-495, 2001.

68. Carrera S, Senra J, Acosta MI, Althubiti M, Hammond EM, de Verdier PJ, and Macip S. The role of the HIF-1 α transcription factor in increased cell division at physiological oxygen tensions. *PloS one* 9: e97938, 2014.

69. Case RB, Greenberg H, and Moskowitz R. Alterations in coronary sinus pO₂ and O₂ saturation resulting from pCO₂ changes. *Cardiovasc Res* 9: 167-177, 1975.

70. Cater DB, Garattini S, Marina F, and Silver IA. Changes of oxygen tension in brain and somatic tissues induced by vasodilator and vasoconstrictor drugs. *Proceedings of the Royal Society of London Series B Biological Sciences* 155: 136-158, 1961.

71. Ceradini DJ, Kulkarni AR, Callaghan MJ, Tepper OM, Bastidas N, Kleinman ME, Capla JM, Galiano RD, Levine JP, and Gurtner GC. Progenitor cell trafficking is regulated by hypoxic gradients through HIF-1 induction of SDF-1. *Nat Med* 10: 858-864, 2004.

72. Chacko SM, Khan M, Kuppusamy ML, Pandian RP, Varadharaj S, Selvendiran K, Bratasz A, Rivera BK, and Kuppusamy P. Myocardial oxygenation and functional recovery in infarct rat hearts transplanted with mesenchymal stem cells. *American Journal of Physiology-Heart and Circulatory Physiology* 296: H1263-H1273, 2009.

73. CHANCE B. THE ENERGY-LINKED REACTION OF CALCIUM WITH MITOCHONDRIA. *J Biol Chem* 240: 2729-2748, 1965.

74. Chandel NS, Maltepe E, Goldwasser E, Mathieu CE, Simon MC, and Schumacker PT. Mitochondrial reactive oxygen species trigger hypoxia-induced transcription. *Proc Natl Acad Sci U S A* 95: 11715-11720, 1998.

75. Chapple SJ, Keeley TP, Mastronicola D, Arno M, Vizcay-Barrena G, Fleck R, Siow RCM, and Mann GE. Bach1 differentially regulates distinct Nrf2-dependent genes in human venous and coronary artery endothelial cells adapted to physiological oxygen levels. *Free Radic Biol Med* 92: 152-162, 2016.

76. Charan NB, Thompson WH, and Carvalho P. Functional anatomy of bronchial veins. *Pulm Pharmacol Ther* 20: 100-103, 2007.

77. Chen B, Longtine MS, and Nelson DM. Pericellular oxygen concentration of cultured primary human trophoblasts. *Placenta* 34: 106-109, 2013.

78. Chen Q, Fischer A, Reagan JD, Yan L-J, and Ames BN. Oxidative DNA damage and senescence of human diploid fibroblast cells. *Proceedings of the National Academy of Sciences* 92: 4337-4341, 1995.

79. Chen X, Chen A, Woo TL, Choo AB, Reuveny S, and Oh SK. Investigations into the metabolism of two-dimensional colony and suspended microcarrier cultures of human embryonic stem cells in serum-free media. *Stem Cells and Development* 19: 1781-1792, 2010.

80. Chiu J-J, and Chien S. Effects of disturbed flow on vascular endothelium: pathophysiological basis and clinical perspectives. *Physiol Rev* 91: 327-387, 2011.

81. Chou CC, and Coatney RW. Nutrient-induced changes in intestinal blood flow in the dog. *Br Vet J* 150: 423-437, 1994.

82. Christensen DR, Calder PC, and Houghton FD. Effect of oxygen tension on the amino acid utilisation of human embryonic stem cells. *Cell Physiol Biochem* 33: 237-246, 2014.

83. Christensen DR, Calder PC, and Houghton FD. GLUT3 and PKM2 regulate OCT4 expression and support the hypoxic culture of human embryonic stem cells. *Sci Rep* 5: 17500, 2015.

84. Chung Y. Myocardial Po₂ does not limit aerobic metabolism in the postischemic heart. *American journal of physiology Heart and circulatory physiology* 310: H226-238, 2016.

- 2332 85. Cieřlar K, Stupar V, Canet-Soulas E, Gaillard S, and Cr millieux Y. Alveolar oxygen partial
2333 pressure and oxygen depletion rate mapping in rats using 3He ventilation imaging. *Magn*
2334 *Reson Med* 57: 423-430, 2007.
- 2335 86. Clark CC, Tolin BS, and Brighton CT. The effect of oxygen tension on proteoglycan
2336 synthesis and aggregation in mammalian growth plate chondrocytes. *J Orthop Res* 9: 477-
2337 484, 1991.
- 2338 87. Clark LC, Wolf R, Granger D, and Taylor Z. Continuous recording of blood oxygen tensions
2339 by polarography. *J Appl Physiol* 6: 189-193, 1953.
- 2340 88. Clementi E, Brown GC, Foxwell N, and Moncada S. On the mechanism by which vascular
2341 endothelial cells regulate their oxygen consumption. *Proc Natl Acad Sci U S A* 96: 1559-
2342 1562, 1999.
- 2343 89. Coburn RF, Ploegmakers F, Gondrie P, and Abboud R. Myocardial myoglobin oxygen
2344 tension. *American Journal of Physiology--Legacy Content* 224: 870-876, 1973.
- 2345 90. Cole RP, Sukanek PC, Wittenberg JB, and Wittenberg BA. Mitochondrial function in the
2346 presence of myoglobin. *J Appl Physiol Respir Environ Exerc Physiol* 53: 1116-1124, 1982.
- 2347 91. Coleman ML, McDonough MA, Hewitson KS, Coles C, Mecinovic J, Edelmann M, Cook
2348 KM, Cockman ME, Lancaster DE, Kessler BM, Oldham NJ, Ratcliffe PJ, and Schofield CJ.
2349 Asparaginyl hydroxylation of the Notch ankyrin repeat domain by factor inhibiting hypoxia-
2350 inducible factor. *J Biol Chem* 282: 24027-24038, 2007.
- 2351 92. Colgan SP, and Taylor CT. Hypoxia: an alarm signal during intestinal inflammation. *Nat*
2352 *Rev Gastroenterol Hepatol* 7: 281-287, 2010.
- 2353 93. Comerford KM, Wallace TJ, Karhausen J, Louis NA, Montalto MC, and Colgan SP.
2354 Hypoxia-inducible factor-1-dependent regulation of the multidrug resistance (MDR1) gene.
2355 *Cancer Res* 62: 3387-3394, 2002.
- 2356 94. Cooper GJ, Sherry KM, and Thorpe JA. Changes in gastric tissue oxygenation during
2357 mobilisation for oesophageal replacement. *Eur J Cardiothorac Surg* 9: 158-160; discussion
2358 160, 1995.
- 2359 95. Copin JC, Gasche Y, Li Y, and Chan PH. Prolonged hypoxia during cell development
2360 protects mature manganese superoxide dismutase-deficient astrocytes from damage by
2361 oxidative stress. *FASEB J* 15: 525-534, 2001.
- 2362 96. Coronel MM, Geusz R, and Stabler CL. Mitigating hypoxic stress on pancreatic islets via in
2363 situ oxygen generating biomaterial. *Biomaterials* 129: 139-151, 2017.
- 2364 97. Crawford DW, Back LH, and Cole MA. In vivo oxygen transport in the normal rabbit femoral
2365 arterial wall. *J Clin Invest* 65: 1498-1508, 1980.
- 2366 98. Crawford DW, and Blankenhorn DH. Arterial wall oxygenation, oxyradicals, and
2367 atherosclerosis. *Atherosclerosis* 89: 97-108, 1991.
- 2368 99. Crawford DW, and Kramsch DM. The oxygen environment of the arterial media in early
2369 rabbit hypertension. *Exp Mol Pathol* 49: 215-233, 1988.
- 2370 100. Cross AR, Henderson L, Jones OT, Delpiano MA, Hentschel J, and Acker H. Involvement
2371 of an NAD(P)H oxidase as a pO2 sensor protein in the rat carotid body. *The Biochemical*
2372 *journal* 272: 743-747, 1990.
- 2373 101. D'Ippolito G, Diabira S, Howard GA, Roos BA, and Schiller PC. Low oxygen tension inhibits
2374 osteogenic differentiation and enhances stemness of human MIAMI cells. *Bone* 39: 513-
2375 522, 2006.
- 2376 102. Daniel Y, Fait G, Lessing JB, Jaffa A, Gull I, Shenav M, Peyser MR, and Kupferminc MJ.
2377 Umbilical cord blood acid-base values in uncomplicated term vaginal breech deliveries.
2378 *Acta Obstet Gynecol Scand* 77: 182-185, 1998.
- 2379 103. Dardzinski BJ, and Sotak CH. Rapid tissue oxygen tension mapping using 19F inversion-
2380 recovery echo-planar imaging of perfluoro-15-crown-5-ether. *Magn Reson Med* 32: 88-97,
2381 1994.
- 2382 104. Das RHJ, van Osch GJVM, Kreukniet M, Oostra J, Weinans H, and Jahr H. Effects of
2383 individual control of pH and hypoxia in chondrocyte culture. *J Orthop Res* 28: 537-545,
2384 2010.
- 2385 105. Degrossoli A, Arrais-Silva WW, Colhone MC, Gadelha FR, Joazeiro PP, and Giorgio S. The
2386 influence of low oxygen on macrophage response to Leishmania infection. *Scand J*
2387 *Immunol* 74: 165-175, 2011.

- 2388 106. del Peso L, Castellanos MC, Temes E, Martín-Puig S, Cuevas Y, Olmos G, and Landázuri
2389 MO. The von Hippel Lindau/hypoxia-inducible factor (HIF) pathway regulates the
2390 transcription of the HIF-proline hydroxylase genes in response to low oxygen. *Journal of*
2391 *Biological Chemistry* 278: 48690-48695, 2003.
- 2392 107. Deninger AJ, Eberle B, Ebert M, Grossmann T, Heil W, Kauczor H-U, Lauer L, Markstaller
2393 K, Otten E, and Schmiedeskamp J. Quantification of regional intrapulmonary oxygen partial
2394 pressure evolution during apnea by ³He MRI. *Journal of Magnetic Resonance* 141: 207-
2395 216, 1999.
- 2396 108. Di Marco G, Lanza M, Pieruccini M, and Campagna S. A luminescent iridium (III)
2397 cyclometallated complex immobilized in a polymeric matrix as a solid-state oxygen sensor.
2398 *Advanced Materials* 8: 576-580, 1996.
- 2399 109. Dickinson J, Eriksen NL, Meyer BA, and Parisi VM. The effect of preterm birth on umbilical
2400 cord blood gases. *Obstetrics & Gynecology* 79: 575-578, 1992.
- 2401 110. Dijkhuizen P, Buursma A, Fongers TME, Gerding AM, Oeseburg B, and Zijlstra WG. The
2402 oxygen binding capacity of human haemoglobin. *Pflügers Archiv* 369: 223-231, 1977.
- 2403 111. Dings J, Meixensberger J, Jäger A, and Roosen K. Clinical experience with 118 brain
2404 tissue oxygen partial pressure catheter probes. *Neurosurgery* 43: 1082-1095, 1998.
- 2405 112. Dionne KE. Oxygen transport to respiring myocytes. *Journal of Biological Chemistry* 265:
2406 15400-15402, 1990.
- 2407 113. Dionne KE, Colton CK, and Yarmush ML. Effect of oxygen on isolated pancreatic tissue.
2408 *ASAIO Journal* 35: 739-741, 1989.
- 2409 114. Dmitriev RI, Borisov SM, Kondrashina AV, Pakan JMP, Anilkumar U, Prehn JHM, Zhdanov
2410 AV, McDermott KW, Klimant I, and Papkovsky DB. Imaging oxygen in neural cell and tissue
2411 models by means of anionic cell-permeable phosphorescent nanoparticles. *Cell Mol Life*
2412 *Sci* 72: 367-381, 2015.
- 2413 115. Dmitriev RI, and Papkovsky DB. Optical probes and techniques for O₂ measurement in live
2414 cells and tissue. *Cell Mol Life Sci* 69: 2025-2039, 2012.
- 2415 116. Dmitriev RI, Zhdanov AV, Jasione G, and Papkovsky DB. Assessment of cellular oxygen
2416 gradients with a panel of phosphorescent oxygen-sensitive probes. *Anal Chem* 84: 2930-
2417 2938, 2012.
- 2418 117. Domm C, Schünke M, Christesen K, and Kurz B. Redifferentiation of dedifferentiated
2419 bovine articular chondrocytes in alginate culture under low oxygen tension. *Osteoarthritis*
2420 *and Cartilage* 10: 13-22, 2002.
- 2421 118. Domm C, Schünke M, Steinhagen J, Freitag S, and Kurz B. Influence of various alginate
2422 brands on the redifferentiation of dedifferentiated bovine articular chondrocytes in alginate
2423 bead culture under high and low oxygen tension. *Tissue Eng* 10: 1796-1805, 2004.
- 2424 119. Dröge W. Free radicals in the physiological control of cell function. *Physiological reviews*
2425 82: 47-95, 2002.
- 2426 120. Duan L-J, Zhang-Benoit Y, and Fong G-H. Endothelium-intrinsic requirement for Hif-2alpha
2427 during vascular development. *Circulation* 111: 2227-2232, 2005.
- 2428 121. Duchen MR, and Biscoe TJ. Relative mitochondrial membrane potential and [Ca²⁺] i in
2429 type I cells isolated from the rabbit carotid body. *The Journal of physiology* 450: 33-61,
2430 1992.
- 2431 122. Duling BR. Microvascular responses to alterations in oxygen tension. *Circulation research*
2432 31: 481-489, 1972.
- 2433 123. Duling BR, and Berne RM. Longitudinal gradients in periarteriolar oxygen tension. A
2434 possible mechanism for the participation of oxygen in local regulation of blood flow. *Circ*
2435 *Res* 27: 669-678, 1970.
- 2436 124. Duling BR, Kuschinsky W, and Wahl M. Measurements of the perivascular PO₂ in the
2437 vicinity of the pial vessels of the cat. *Pflügers Arch* 383: 29-34, 1979.
- 2438 125. Dunn JF, Grinberg O, Roche M, Nwaigwe CI, Hou HG, and Swartz HM. Noninvasive
2439 assessment of cerebral oxygenation during acclimation to hypobaric hypoxia. *Journal of*
2440 *Cerebral Blood Flow & Metabolism* 20: 1632-1635, 2000.
- 2441 126. Dvorak A, Tilley AE, Shaykhiev R, Wang R, and Crystal RG. Do airway epithelium air-liquid
2442 cultures represent the in vivo airway epithelium transcriptome? *Am J Respir Cell Mol Biol*
2443 44: 465-473, 2011.

- 2444 127. Eberle B, Weiler N, Markstaller K, Kauczor H-U, Deninger A, Ebert M, Grossmann T, Heil
2445 W, Lauer LO, and Roberts TPL. Analysis of intrapulmonary O₂ concentration by MR
2446 imaging of inhaled hyperpolarized helium-3. *Journal of Applied Physiology* 87: 2043-2052,
2447 1999.
- 2448 128. Ebert BL, Firth JD, and Ratcliffe PJ. Hypoxia and mitochondrial inhibitors regulate
2449 expression of glucose transporter-1 via distinct Cis-acting sequences. *J Biol Chem* 270:
2450 29083-29089, 1995.
- 2451 129. El Awad B, Kreft B, Wolber EM, Hellwig-Bürgel T, Metzen E, Fandrey J, and Jelkmann W.
2452 Hypoxia and interleukin-1 β stimulate vascular endothelial growth factor production in
2453 human proximal tubular cells. *Kidney Int* 58: 43-50, 2000.
- 2454 130. El Sabbahy M, and Vaidya VS. Ischemic kidney injury and mechanisms of tissue repair.
2455 *Wiley interdisciplinary reviews Systems biology and medicine* 3: 606-618, 2011.
- 2456 131. Ellsworth ML, and Pittman RN. Arterioles supply oxygen to capillaries by diffusion as well
2457 as by convection. *Am J Physiol* 258: H1240-1243, 1990.
- 2458 132. Emerling BM, Weinberg F, Snyder C, Burgess Z, Mutlu GM, Viollet B, Budinger GRS, and
2459 Chandel NS. Hypoxic activation of AMPK is dependent on mitochondrial ROS but
2460 independent of an increase in AMP/ATP ratio. *Free Radic Biol Med* 46: 1386-1391, 2009.
- 2461 133. Engerman RL, Pfaffenbach D, and Davis MD. Cell turnover of capillaries. *Laboratory*
2462 *investigation; a journal of technical methods and pathology* 17: 738-743, 1967.
- 2463 134. Epstein AC, Gleadle JM, McNeill LA, Hewitson KS, O'Rourke J, Mole DR, Mukherji M,
2464 Metzen E, Wilson MI, and Dhanda A. C. elegans EGL-9 and mammalian homologs define a
2465 family of dioxygenases that regulate HIF by prolyl hydroxylation. *Cell* 107: 43-54, 2001.
- 2466 135. Ernst A, Alkass K, Bernard S, Salehpour M, Perl S, Tisdale J, Possnert G, Druid H, and
2467 Frisén J. Neurogenesis in the striatum of the adult human brain. *Cell* 156: 1072-1083,
2468 2014.
- 2469 136. Esipova TV, Karagodov A, Miller J, Wilson DF, Busch TM, and Vinogradov SA. Two new
2470 "protected" oxyphors for biological oximetry: properties and application in tumor imaging.
2471 *Anal Chem* 83: 8756-8765, 2011.
- 2472 137. Etherington PJ, Winlove P, Taylor P, Paleolog E, and Miotla JM. VEGF release is
2473 associated with reduced oxygen tensions in experimental inflammatory arthritis. *Clin Exp*
2474 *Rheumatol* 20: 799-805, 2002.
- 2475 138. Evans NT, and Naylor PF. The dynamics of changes in dermal oxygen tension. *Respir*
2476 *Physiol* 2: 61-72, 1966.
- 2477 139. Evans NT, and Naylor PF. The oxygen tension gradient across human epidermis. *Respir*
2478 *Physiol* 3: 38-42, 1967.
- 2479 140. Evans NT, and Naylor PF. Steady states of oxygen tension in human dermis. *Respir*
2480 *Physiol* 2: 46-60, 1966.
- 2481 141. Evans RG, Smith DW, Khan Z, Ngo JP, and Gardiner BS. Letter to the editor:" The
2482 plausibility of arterial-to-venous oxygen shunting in the kidney: it all depends on radial
2483 geometry". *American Journal of Physiology-Renal Physiology* 309: F179-F180, 2015.
- 2484 142. Ezashi T, Das P, and Roberts RM. Low O₂ tensions and the prevention of differentiation of
2485 hES cells. *Proc Natl Acad Sci U S A* 102: 4783-4788, 2005.
- 2486 143. Falchuk KH, Goetzl EJ, and Kulka JP. Respiratory gases of synovial fluids. An approach to
2487 synovial tissue circulatory-metabolic imbalance in rheumatoid arthritis. *Am J Med* 49: 223-
2488 231, 1970.
- 2489 144. Falstie-Jensen N, Spaun E, Brøchner-Mortensen J, and Falstie-Jensen S. The influence of
2490 epidermal thickness on transcutaneous oxygen pressure measurements in normal persons.
2491 *Scand J Clin Lab Invest* 48: 519-523, 1988.
- 2492 145. Famulla S, Schlich R, Sell H, and Eckel J. Differentiation of human adipocytes at
2493 physiological oxygen levels results in increased adiponectin secretion and isoproterenol-
2494 stimulated lipolysis. *Adipocyte* 1: 132-181, 2012.
- 2495 146. Fan J, Cai H, Yang S, Yan L, and Tan W. Comparison between the effects of normoxia and
2496 hypoxia on antioxidant enzymes and glutathione redox state in ex vivo culture of CD34(+)
2497 cells. *Comp Biochem Physiol B Biochem Mol Biol* 151: 153-158, 2008.
- 2498 147. Faubert B, Boily G, Izreig S, Griss T, Samborska B, Dong Z, Dupuy F, Chambers C, Fuerth
2499 BJ, Viollet B, Mamer OA, Avizonis D, DeBerardinis RJ, Siegel PM, and Jones RG. AMPK is

- a negative regulator of the Warburg effect and suppresses tumor growth in vivo. *Cell Metab* 17: 113-124, 2013.
148. Federspiel WJ, and Popel AS. A theoretical analysis of the effect of the particulate nature of blood on oxygen release in capillaries. *Microvasc Res* 32: 164-189, 1986.
 149. Fehrer C, Brunauer R, Laschober G, Unterluggauer H, Reitingner S, Kloss F, Güllly C, Gassner R, and Lepperdinger G. Reduced oxygen tension attenuates differentiation capacity of human mesenchymal stem cells and prolongs their lifespan. *Aging Cell* 6: 745-757, 2007.
 150. Feola M, Azar D, and Wiener L. Improved oxygenation of ischemic myocardium by hemodilution with stroma-free hemoglobin solution. *Chest* 75: 369-375, 1979.
 151. Fercher A, Borisov SM, Zhdanov AV, Klimant I, and Papkovsky DB. Intracellular O₂ sensing probe based on cell-penetrating phosphorescent nanoparticles. *ACS Nano* 5: 5499-5508, 2011.
 152. Ferrell WR, and Najafipour H. Changes in synovial PO₂ and blood flow in the rabbit knee joint due to stimulation of the posterior articular nerve. *J Physiol* 449: 607-617, 1992.
 153. Fick A. V. On liquid diffusion. *The London, Edinburgh, and Dublin Philosophical Magazine and Journal of Science* 10: 30-39, 1855.
 154. Fiegl M, Samudio I, Clise-Dwyer K, Burks JK, Mnjoyan Z, and Andreeff M. CXCR4 expression and biologic activity in acute myeloid leukemia are dependent on oxygen partial pressure. *Blood* 113: 1504-1512, 2009.
 155. Fischer B, and Bavister BD. Oxygen tension in the oviduct and uterus of rhesus monkeys, hamsters and rabbits. *J Reprod Fertil* 99: 673-679, 1993.
 156. Fischer MC, Spector ZZ, Ishii M, Yu J, Emami K, Itkin M, and Rizi R. Single-acquisition sequence for the measurement of oxygen partial pressure by hyperpolarized gas MRI. *Magnetic resonance in medicine* 52: 766-773, 2004.
 157. Fisher EM, Khan M, Salisbury R, and Kuppusamy P. Noninvasive monitoring of small intestinal oxygen in a rat model of chronic mesenteric ischemia. *Cell biochemistry and biophysics* 67: 451-459, 2013.
 158. Forristal CE, Christensen DR, Chinnery FE, Petruzzelli R, Parry KL, Sanchez-Elsner T, and Houghton FD. Environmental oxygen tension regulates the energy metabolism and self-renewal of human embryonic stem cells. *PLoS One* 8: e62507, 2013.
 159. Forstner H, and Gnaiger E editors. *Polarographic oxygen sensors*. Springer, 1983, p. 321-333.
 160. Forsyth NR, Kay A, Hampson K, Downing A, Talbot R, and McWhir J. Transcriptome alterations due to physiological normoxic (2% O₂) culture of human embryonic stem cells. *Regen Med* 3: 817-833, 2008.
 161. Forsyth NR, Musio A, Vezzoni P, Simpson AHRW, Noble BS, and McWhir J. Physiologic oxygen enhances human embryonic stem cell clonal recovery and reduces chromosomal abnormalities. *Cloning Stem Cells* 8: 16-23, 2006.
 162. Forsythe JA, Jiang B-H, Iyer NV, Agani F, Leung SW, Koos RD, and Semenza GL. Activation of vascular endothelial growth factor gene transcription by hypoxia-inducible factor 1. *Molecular and cellular biology* 16: 4604-4613, 1996.
 163. Foster ME, Laycock JRD, Silver IA, and Leaper DJ. Hypovolaemia and healing in colonic anastomoses. *British journal of surgery* 72: 831-834, 1985.
 164. Fox MD, and Raichle ME. Spontaneous fluctuations in brain activity observed with functional magnetic resonance imaging. *Nature reviews Neuroscience* 8: 700-711, 2007.
 165. Foy BD, Rotem A, Toner M, Tompkins RG, and Yarmush ML. A device to measure the oxygen uptake rate of attached cells: importance in bioartificial organ design. *Cell transplantation* 3: 515-527, 1993.
 166. Fraker CA, Cechin S, Álvarez-Cubela S, Echeverri F, Bernal A, Poo R, Ricordi C, Inverardi L, and Domínguez-Bendala J. A physiological pattern of oxygenation using perfluorocarbon-based culture devices maximizes pancreatic islet viability and enhances β -cell function. *Cell Transplant* 22: 1723-1733, 2013.
 167. Fu Q, Colgan SP, and Shelley CS. Hypoxia: The Force that Drives Chronic Kidney Disease. *Clin Med Res* 14: 15-39, 2016.

- 2555 168. Fu XW, Wang D, Nurse CA, Dinauer MC, and Cutz E. NADPH oxidase is an O₂ sensor in
2556 airway chemoreceptors: evidence from K⁺ current modulation in wild-type and oxidase-
2557 deficient mice. *Proceedings of the National Academy of Sciences* 97: 4374-4379, 2000.
- 2558 169. Fujibayashi Y, Cutler C, Anderson C, McCarthy D, Jones L, Sharp T, Yonekura Y, and
2559 Welch M. Comparative studies of Cu-64-ATSM and C-11-acetate in an acute myocardial
2560 infarction model: ex vivo imaging of hypoxia in rats. *Nuclear medicine and biology* 26: 117-
2561 121, 1999.
- 2562 170. Furuta GT, Turner JR, Taylor CT, Hershberg RM, Comerford K, Narravula S, Podolsky DK,
2563 and Colgan SP. Hypoxia-inducible factor 1-dependent induction of intestinal trefoil factor
2564 protects barrier function during hypoxia. *J Exp Med* 193: 1027-1034, 2001.
- 2565 171. Futralan D, Huang C-T, Schmidt-Wolf IGH, Larsson M, and Messmer D. Effect of oxygen
2566 levels on the physiology of dendritic cells: implications for adoptive cell therapy. *Mol Med*
2567 17: 910-916, 2011.
- 2568 172. Garcia-Ochoa F, and Gomez E. Bioreactor scale-up and oxygen transfer rate in microbial
2569 processes: an overview. *Biotechnol Adv* 27: 153-176, 2009.
- 2570 173. Garreta E, Melo E, Navajas D, and Farré R. Low oxygen tension enhances the generation
2571 of lung progenitor cells from mouse embryonic and induced pluripotent stem cells. *Physiol*
2572 *Rep* 2: 2014.
- 2573 174. Garris DR, and Mitchell JA. Intrauterine oxygen tension during the estrous cycle in the
2574 guinea pig: its relation to uterine blood volume and plasma estrogen and progesterone
2575 levels. *Biol Reprod* 21: 149-159, 1979.
- 2576 175. Gey GO. An Improved Technic for Massive Tissue Culture. *Am J Cancer* 17: 752-756,
2577 1933.
- 2578 176. Gibbons J, Hewitt E, and Gardner DK. Effects of oxygen tension on the establishment and
2579 lactate dehydrogenase activity of murine embryonic stem cells. *Cloning and stem cells* 8:
2580 117-122, 2006.
- 2581 177. Gimble JM, Bunnell BA, Frazier T, Rowan B, Shah F, Thomas-Porch C, and Wu X.
2582 Adipose-derived stromal/stem cells: a primer. *Organogenesis* 9: 3-10, 2013.
- 2583 178. Ginouvès A, Ilc K, Macías N, Pouysségur J, and Berra E. PHDs overactivation during
2584 chronic hypoxia "desensitizes" HIF α and protects cells from necrosis. *Proc Natl Acad*
2585 *Sci U S A* 105: 4745-4750, 2008.
- 2586 179. Giulivi C, Hochstein P, and Davies KJ. Hydrogen peroxide production by red blood cells.
2587 *Free Radical Biology and Medicine* 16: 123-129, 1994.
- 2588 180. Glover LE, Bowers BE, Saeedi B, Ehrentraut SF, Campbell EL, Bayless AJ, Dobrinskikh E,
2589 Kendrick AA, Kelly CJ, Burgess A, Miller L, Kominsky DJ, Jedlicka P, and Colgan SP.
2590 Control of creatine metabolism by HIF is an endogenous mechanism of barrier regulation in
2591 colitis. *Proc Natl Acad Sci U S A* 110: 19820-19825, 2013.
- 2592 181. Gnaiger E, Lassnig B, Kuznetsov A, Rieger G, and Margreiter R. Mitochondrial oxygen
2593 affinity, respiratory flux control and excess capacity of cytochrome c oxidase. *J Exp Biol*
2594 201: 1129-1139, 1998.
- 2595 182. Golub AS, Barker MC, and Pittman RN. Microvascular oxygen tension in the rat mesentery.
2596 *Am J Physiol Heart Circ Physiol* 294: H21-28, 2008.
- 2597 183. Golub AS, Barker MC, and Pittman RN. PO₂ profiles near arterioles and tissue oxygen
2598 consumption in rat mesentery. *Am J Physiol Heart Circ Physiol* 293: H1097-1106, 2007.
- 2599 184. Golub AS, and Pittman RN. Erythrocyte-associated transients in PO₂ revealed in capillaries
2600 of rat mesentery. *Am J Physiol Heart Circ Physiol* 288: H2735-2743, 2005.
- 2601 185. Golub AS, and Pittman RN. PO₂ measurements in the microcirculation using
2602 phosphorescence quenching microscopy at high magnification. *Am J Physiol Heart Circ*
2603 *Physiol* 294: H2905-2916, 2008.
- 2604 186. Gomes Sobrinho DB, Oliveira JBA, Petersen CG, Mauri AL, Silva LFI, Massaro FC, Baruffi
2605 RLR, Cavagna M, and Franco JG. IVF/ICSI outcomes after culture of human embryos at
2606 low oxygen tension: a meta-analysis. *Reprod Biol Endocrinol* 9: 143, 2011.
- 2607 187. Goossens GH, Bizzarri A, Venter N, Essers Y, Cleutjens JP, Konings E, Jocken JWE,
2608 Cajlakovic M, Ribitsch V, Clément K, and Blaak EE. Increased adipose tissue oxygen
2609 tension in obese compared with lean men is accompanied by insulin resistance, impaired
2610 adipose tissue capillarization, and inflammation. *Circulation* 124: 67-76, 2011.

- 2611 188. Goossens GH, and Blaak EE. Adipose tissue dysfunction and impaired metabolic health in
2612 human obesity: a matter of oxygen? *Front Endocrinol (Lausanne)* 6: 55, 2015.
- 2613 189. Grahl N, Puttikamonkul S, Macdonald JM, Gamcsik MP, Ngo LY, Hohl TM, and Cramer
2614 RA. In vivo hypoxia and a fungal alcohol dehydrogenase influence the pathogenesis of
2615 invasive pulmonary aspergillosis. *PLoS Pathog* 7: e1002145, 2011.
- 2616 190. Grainger CI, Greenwell LL, Lockley DJ, Martin GP, and Forbes B. Culture of Calu-3 cells at
2617 the air interface provides a representative model of the airway epithelial barrier. *Pharm Res*
2618 23: 1482-1490, 2006.
- 2619 191. Granger DN, Kvietys PR, Korthuis RJ, and Premen AJ. Microcirculation of the intestinal
2620 mucosa. *Comprehensive Physiology* 2011.
- 2621 192. GRANT JL, and SMITH B. Bone marrow gas tensions, bone marrow blood flow, and
2622 erythropoiesis in man. *Ann Intern Med* 58: 801-809, 1963.
- 2623 193. Graven KK, Bellur D, Klahn BD, Lowrey SL, and Amberger E. HIF-2alpha regulates
2624 glyceraldehyde-3-phosphate dehydrogenase expression in endothelial cells. *Biochim*
2625 *Biophys Acta* 1626: 10-18, 2003.
- 2626 194. Gregory IC. The oxygen and carbon monoxide capacities of fetal and adult blood. *J Physiol*
2627 236: 625-634, 1974.
- 2628 195. Griffith OW, and Meister A. Glutathione: interorgan translocation, turnover, and metabolism.
2629 *Proc Natl Acad Sci U S A* 76: 5606-5610, 1979.
- 2630 196. Grimshaw MJ, and Mason RM. Bovine articular chondrocyte function in vitro depends upon
2631 oxygen tension. *Osteoarthritis Cartilage* 8: 386-392, 2000.
- 2632 197. Grinnell F. Fibroblast biology in three-dimensional collagen matrices. *Trends in cell biology*
2633 13: 264-269, 2003.
- 2634 198. Gruden G, Thomas S, Burt D, Lane S, Chusney G, Sacks S, and Viberti G. Mechanical
2635 stretch induces vascular permeability factor in human mesangial cells: mechanisms of
2636 signal transduction. *Proc Natl Acad Sci U S A* 94: 12112-12116, 1997.
- 2637 199. Guarino RD, Dike LE, Haq TA, Rowley JA, Pitner JB, and Timmins MR. Method for
2638 determining oxygen consumption rates of static cultures from microplate measurements of
2639 pericellular dissolved oxygen concentration. *Biotechnology and bioengineering* 86: 775-
2640 787, 2004.
- 2641 200. Guarino RD, Dike LE, Haq TA, Rowley JA, Pitner JB, and Timmins MR. Method for
2642 determining oxygen consumption rates of static cultures from microplate measurements of
2643 pericellular dissolved oxygen concentration. *Biotechnol Bioeng* 86: 775-787, 2004.
- 2644 201. Gullichsen E, Nelimarkka O, Halkola L, and Niinikoski J. Renal oxygenation in endotoxin
2645 shock in dogs. *Crit Care Med* 17: 547-550, 1989.
- 2646 202. Gundry SR, Wang N, Sciolaro CM, Van Arsdell GS, Razzouk AJ, Hill AC, and Bailey LL.
2647 Uniformity of perfusion in all regions of the human heart by warm continuous retrograde
2648 cardioplegia. *Ann Thorac Surg* 61: 33-35, 1996.
- 2649 203. GUNTHER H, AUMULLER G, KUNKE SVP, and THEWS G. Die Sauerstoffversorgung der
2650 Niere. 1. *Verteilung der O₂-Drucke in der Rattenniere unter Normbedingungen Resp Exp*
2651 *Med* 163: 251-264, 1974.
- 2652 204. Guo R, Xu X, Lu Y, and Xie X. Physiological oxygen tension reduces hepatocyte
2653 dedifferentiation in in vitro culture. *Sci Rep* 7: 5923, 2017.
- 2654 205. Gustafsson U, Persson JK, Suneson A, and Kjellström BT. Microvascular lung tissue
2655 oxygenation--a methodological study in the pig. *Annals of the Academy of Medicine,*
2656 *Singapore* 28: 3-7, 1999.
- 2657 206. Guzy RD, Hoyos B, Robin E, Chen H, Liu L, Mansfield KD, Simon MC, Hammerling U, and
2658 Schumacker PT. Mitochondrial complex III is required for hypoxia-induced ROS production
2659 and cellular oxygen sensing. *Cell Metab* 1: 401-408, 2005.
- 2660 207. Guzy RD, and Schumacker PT. Oxygen sensing by mitochondria at complex III: the
2661 paradox of increased reactive oxygen species during hypoxia. *Exp Physiol* 91: 807-819,
2662 2006.
- 2663 208. Haas B, Chrusciel S, Fayad-Kobeissi S, Dubois-Randé J-L, Azuaje F, Boczkowski J,
2664 Motterlini R, and Foresti R. Permanent culture of macrophages at physiological oxygen
2665 attenuates the antioxidant and immunomodulatory properties of dimethyl fumarate. *J Cell*
2666 *Physiol* 230: 1128-1138, 2015.

- 2667 209. Haase VH. Hypoxia-inducible factors in the kidney. *Am J Physiol Renal Physiol* 291: F271-
2668 281, 2006.
- 2669 210. Haddad H, Windgassen D, Ramsborg CG, Paredes CJ, and Papoutsakis ET. Molecular
2670 understanding of oxygen-tension and patient-variability effects on ex vivo expanded T cells.
2671 *Biotechnology and bioengineering* 87: 437-450, 2004.
- 2672 211. Hagen T, Taylor CT, Lam F, and Moncada S. Redistribution of intracellular oxygen in
2673 hypoxia by nitric oxide: effect on HIF1alpha. *Science* 302: 1975-1978, 2003.
- 2674 212. Haisjackl M, Germann R, Hasibeder W, Schwarz B, Salak N, Pajk W, Bonatti J,
2675 Nussbaumer W, Klima G, and Kox W. Mucosal tissue oxygenation of the porcine jejunum
2676 during normothermic cardiopulmonary bypass. *British journal of anaesthesia* 82: 738-745,
2677 1999.
- 2678 213. Haisjackl M, Luz G, Sparr H, Germann R, Salak N, Friesenecker B, Deusch E, Meusburger
2679 S, and Hasibeder W. The effects of progressive anemia on jejunal mucosal and serosal
2680 tissue oxygenation in pigs. *Anesth Analg* 84: 538-544, 1997.
- 2681 214. Hajjar DP, Farber IC, and Smith SC. Oxygen tension within the arterial wall: relationship to
2682 altered bioenergetic metabolism and lipid accumulation. *Arch Biochem Biophys* 262: 375-
2683 380, 1988.
- 2684 215. Halliwell B. Oxidative stress in cell culture: an under-appreciated problem? *FEBS Lett* 540:
2685 3-6, 2003.
- 2686 216. Hamedani H, Kadlecsek SJ, Ishii M, Emami K, Kuzma NN, Xin Y, Rossman M, and Rizi RR.
2687 A variability study of regional alveolar oxygen tension measurement in humans using
2688 hyperpolarized (3) He MRI. *Magn Reson Med* 70: 1557-1566, 2013.
- 2689 217. Hamedani H, Shaghaghi H, Kadlecsek SJ, Xin Y, Han B, Siddiqui S, Rajaei J, Ishii M,
2690 Rossman M, and Rizi RR. Vertical gradients in regional alveolar oxygen tension in supine
2691 human lung imaged by hyperpolarized 3He MRI. *NMR Biomed* 27: 1439-1450, 2014.
- 2692 218. Hannah S, Mecklenburgh K, Rahman I, Bellingan GJ, Greening A, Haslett C, and Chilvers
2693 ER. Hypoxia prolongs neutrophil survival in vitro. *FEBS Lett* 372: 233-237, 1995.
- 2694 219. Hara S, Hamada J, Kobayashi C, Kondo Y, and Imura N. Expression and characterization
2695 of hypoxia-inducible factor (HIF)-3alpha in human kidney: suppression of HIF-mediated
2696 gene expression by HIF-3alpha. *Biochem Biophys Res Commun* 287: 808-813, 2001.
- 2697 220. Hardie DG, Hawley SA, and Scott JW. AMP-activated protein kinase--development of the
2698 energy sensor concept. *J Physiol* 574: 7-15, 2006.
- 2699 221. Hardie DG, Ross FA, and Hawley SA. AMPK: a nutrient and energy sensor that maintains
2700 energy homeostasis. *Nat Rev Mol Cell Biol* 13: 251-262, 2012.
- 2701 222. Harman D. Aging: a theory based on free radical and radiation chemistry. *J Gerontol* 11:
2702 298-300, 1956.
- 2703 223. Harms FA, Bodmer SIA, Raat NJH, Stolker RJ, and Mik EG. Validation of the
2704 protoporphyrin IX-triplet state lifetime technique for mitochondrial oxygen measurements in
2705 the skin. *Opt Lett* 37: 2625-2627, 2012.
- 2706 224. Harms FA, de Boon WM, Balestra GM, Bodmer SI, Johannes T, Stolker RJ, and Mik EG.
2707 Oxygen-dependent delayed fluorescence measured in skin after topical application of 5-
2708 aminolevulinic acid. *Journal of biophotonics* 4: 731-739, 2011.
- 2709 225. Harms FA, Voorbeijtel WJ, Bodmer SIA, Raat NJH, and Mik EG. Cutaneous respirometry
2710 by dynamic measurement of mitochondrial oxygen tension for monitoring mitochondrial
2711 function in vivo. *Mitochondrion* 13: 507-514, 2013.
- 2712 226. Harper SL, Pitts VH, Granger DN, and Kviety PR. Pancreatic tissue oxygenation during
2713 secretory stimulation. *American Journal of Physiology-Gastrointestinal and Liver*
2714 *Physiology* 250: G316-G322, 1986.
- 2715 227. Harrison JS, Rameshwar P, Chang V, and Bandari P. Oxygen saturation in the bone
2716 marrow of healthy volunteers. *Blood* 99: 394-394, 2002.
- 2717 228. He G, Shankar RA, Chzhan M, Samouilov A, Kuppusamy P, and Zweier JL. Noninvasive
2718 measurement of anatomic structure and intraluminal oxygenation in the gastrointestinal
2719 tract of living mice with spatial and spectral EPR imaging. *Proc Natl Acad Sci U S A* 96:
2720 4586-4591, 1999.
- 2721 229. He L, Dinger B, Sanders K, Hoidal J, Obeso A, Stensaas L, Fidone S, and Gonzalez C.
2722 Effect of p47phox gene deletion on ROS production and oxygen sensing in mouse carotid
2723 body chemoreceptor cells. *Am J Physiol Lung Cell Mol Physiol* 289: L916-924, 2005.

2724 230. Heistad DD, Armstrong ML, and Amundsen S. Blood flow through vasa vasorum in arteries
2725 and veins: effects of luminal PO₂. *Am J Physiol* 250: H434-442, 1986.

2726 231. Hellums JD. The resistance to oxygen transport in the capillaries relative to that in the
2727 surrounding tissue. *Microvasc Res* 13: 131-136, 1977.

2728 232. Hemann MT, and Greider CW. Wild-derived inbred mouse strains have short telomeres.
2729 *Nucleic Acids Res* 28: 4474-4478, 2000.

2730 233. Henderson JH, Ginley NM, Caplan AI, Niyibizi C, and Dennis JE. Low oxygen tension
2731 during incubation periods of chondrocyte expansion is sufficient to enhance postexpansion
2732 chondrogenesis. *Tissue Eng Part A* 16: 1585-1593, 2010.

2733 234. Hendgen-Cotta UB, Kelm M, and Rassaf T. Myoglobin functions in the heart. *Free Radic*
2734 *Biol Med* 73: 252-259, 2014.

2735 235. Henry W. Experiments on the quantity of gases absorbed by water, at different
2736 temperatures, and under different pressures. *Philosophical Transactions of the Royal*
2737 *Society of London* 93: 29-276, 1803.

2738 236. Herold U, Jakob H, Kamler M, Thiele R, Tochtermann U, Weinmann J, Motsch J, Gebhard
2739 MM, and Hagl S. Interruption of bronchial circulation leads to a severe decrease in
2740 peribronchial oxygen tension in standard lung transplantation technique. *Eur J Cardiothorac*
2741 *Surg* 13: 176-183, 1998.

2742 237. Heughan C, Niinikoski J, and Hunt TK. Oxygen tensions in lesions of experimental
2743 atherosclerosis of rabbits. *Atherosclerosis* 17: 361-367, 1973.

2744 238. Hewitson KS, McNeill LA, Riordan MV, Tian YM, Bullock AN, Welford RW, Elkins JM,
2745 Oldham NJ, Bhattacharya S, Gleadle JM, Ratcliffe PJ, Pugh CW, and Schofield CJ.
2746 Hypoxia-inducible factor (HIF) asparagine hydroxylase is identical to factor inhibiting HIF
2747 (FIH) and is related to the cupin structural family. *J Biol Chem* 277: 26351-26355, 2002.

2748 239. Heywood HK, and Lee DA. Bioenergetic reprogramming of articular chondrocytes by
2749 exposure to exogenous and endogenous reactive oxygen species and its role in the
2750 anabolic response to low oxygen. *J Tissue Eng Regen Med* 2016.

2751 240. Heywood HK, and Lee DA. Low oxygen reduces the modulation to an oxidative phenotype
2752 in monolayer-expanded chondrocytes. *J Cell Physiol* 222: 248-253, 2010.

2753 241. Hirao M, Hashimoto J, Yamasaki N, Ando W, Tsuboi H, Myoui A, and Yoshikawa H.
2754 Oxygen tension is an important mediator of the transformation of osteoblasts to osteocytes.
2755 *J Bone Miner Metab* 25: 266-276, 2007.

2756 242. Hirao M, Tamai N, Tsumaki N, Yoshikawa H, and Myoui A. Oxygen tension regulates
2757 chondrocyte differentiation and function during endochondral ossification. *J Biol Chem* 281:
2758 31079-31092, 2006.

2759 243. Hirsilä M, Koivunen P, Günzler V, Kivirikko KI, and Myllyharju J. Characterization of the
2760 human prolyl 4-hydroxylases that modify the hypoxia-inducible factor. *J Biol Chem* 278:
2761 30772-30780, 2003.

2762 244. Hirst DG, Denekamp J, and Hobson B. Proliferation studies of the endothelial and smooth
2763 muscle cells of the mouse mesentery after irradiation. *Cell Tissue Kinet* 13: 91-104, 1980.

2764 245. Hobbhahn J, Conzen PF, Goetz A, Seidl G, Gonschior P, Brendel W, and Peter K.
2765 Myocardial surface PO₂--an indicator of myocardial tissue oxygenation? *Cardiovasc Res*
2766 23: 529-540, 1989.

2767 246. Hodson L. Adipose tissue oxygenation: Effects on metabolic function. *Adipocyte* 3: 75-80,
2768 2014.

2769 247. Hoffman WE, Charbel FT, and Edelman G. Brain tissue oxygen, carbon dioxide, and pH in
2770 neurosurgical patients at risk for ischemia. *Anesth Analg* 82: 582-586, 1996.

2771 248. Hoffman WE, Charbel FT, Edelman G, and Ausman JI. Brain tissue oxygenation in patients
2772 with cerebral occlusive disease and arteriovenous malformations. *Br J Anaesth* 78: 169-
2773 171, 1997.

2774 249. Holmquist-Mengelbier L, Fredlund E, Löfstedt T, Noguera R, Navarro S, Nilsson H, Pietras
2775 A, Vallon-Christersson J, Borg A, Gradin K, Poellinger L, and Pålman S. Recruitment of
2776 HIF-1α and HIF-2α to common target genes is differentially regulated in
2777 neuroblastoma: HIF-2α promotes an aggressive phenotype. *Cancer Cell* 10: 413-423,
2778 2006.

- 2779 250. Holzer C, and Maier P. Maintenance of periportal and pericentral oxygen tensions in
2780 primary rat hepatocyte cultures: influence on cellular DNA and protein content monitored by
2781 flow cytometry. *Journal of cellular physiology* 133: 297-304, 1987.
- 2782 251. Holzwarth C, Vaegler M, Gieseke F, Pfister SM, Handgretinger R, Kerst G, and Müller I.
2783 Low physiologic oxygen tensions reduce proliferation and differentiation of human
2784 multipotent mesenchymal stromal cells. *BMC Cell Biol* 11: 11, 2010.
- 2785 252. Honig CR, and Gayeski TE. Precapillary O₂ loss and arteriovenous O₂ diffusion shunt are
2786 below limit of detection in myocardium. *Adv Exp Med Biol* 248: 591-599, 1989.
- 2787 253. Hoogsteen IJ, Lok J, Marres HAM, Takes RP, Rijken PFJW, van der Kogel AJ, and
2788 Kaanders JHAM. Hypoxia in larynx carcinomas assessed by pimonidazole binding and the
2789 value of CA-IX and vascularity as surrogate markers of hypoxia. *Eur J Cancer* 45: 2906-
2790 2914, 2009.
- 2791 254. Horak P, Crawford AR, Vadysirisack DD, Nash ZM, DeYoung MP, Sgroi D, and Ellisen LW.
2792 Negative feedback control of HIF-1 through REDD1-regulated ROS suppresses
2793 tumorigenesis. *Proc Natl Acad Sci U S A* 107: 4675-4680, 2010.
- 2794 255. Horie N, So K, Moriya T, Kitagawa N, Tsutsumi K, Nagata I, and Shinohara K. Effects of
2795 oxygen concentration on the proliferation and differentiation of mouse neural stem cells in
2796 vitro. *Cell Mol Neurobiol* 28: 833-845, 2008.
- 2797 256. Hosford PS, Millar J, Ramage AG, and Marina N. Abnormal oxygen homeostasis in the
2798 nucleus tractus solitarii of the spontaneously hypertensive rat. *Exp Physiol* 2017.
- 2799 257. Hu C-J, Wang L-Y, Chodosh LA, Keith B, and Simon MC. Differential roles of hypoxia-
2800 inducible factor 1 α (HIF-1 α) and HIF-2 α in hypoxic gene regulation. *Molecular and cellular*
2801 *biology* 23: 9361-9374, 2003.
- 2802 258. Huang Z, Fujiwara K, Minamide R, Hasegawa K, and Yoshikawa K. Necdin Controls
2803 Proliferation and Apoptosis of Embryonic Neural Stem Cells in an Oxygen Tension-
2804 Dependent Manner. *The Journal of Neuroscience* 33: 10362-10373, 2013.
- 2805 259. Ikejiri A, Nagai S, Goda N, Kurebayashi Y, Osada-Oka M, Takubo K, Suda T, and Koyasu
2806 S. Dynamic regulation of Th17 differentiation by oxygen concentrations. *Int Immunol* 24:
2807 137-146, 2012.
- 2808 260. Intaglietta M, Johnson PC, and Winslow RM. Microvascular and tissue oxygen distribution.
2809 *Cardiovascular research* 32: 632-643, 1996.
- 2810 261. Ishii T, Itoh K, Takahashi S, Sato H, Yanagawa T, Katoh Y, Bannai S, and Yamamoto M.
2811 Transcription factor Nrf2 coordinately regulates a group of oxidative stress-inducible genes
2812 in macrophages. *J Biol Chem* 275: 16023-16029, 2000.
- 2813 262. Ishikawa Y, and Ito T. Kinetics of hemopoietic stem cells in a hypoxic culture. *European*
2814 *journal of haematology* 40: 126-129, 1988.
- 2815 263. Ivanov KP, Derry AN, Vovenko EP, Samoilov MO, and Semionov DG. Direct
2816 measurements of oxygen tension at the surface of arterioles, capillaries and venules of the
2817 cerebral cortex. *Pflugers Arch* 393: 118-120, 1982.
- 2818 264. Jacobi CA, Zieren HU, Müller JM, Adili F, and Pichlmaier H. Anastomotic tissue oxygen
2819 tension during esophagectomy in patients with esophageal carcinoma. *Eur Surg Res* 28:
2820 26-31, 1996.
- 2821 265. Jacobi CA, Zieren HU, Zieren J, and Müller JM. Is tissue oxygen tension during
2822 esophagectomy a predictor of esophagogastric anastomotic healing? *J Surg Res* 74: 161-
2823 164, 1998.
- 2824 266. Jamieson D, and Van den Brenk HAS. Electrode size and tissue pO₂ measurement in rats
2825 exposed to air or high pressure oxygen. *Journal of applied physiology* 20: 514-518, 1965.
- 2826 267. Janne d'Othée B, Rachmuth G, Munasinghe J, and Lang EV. The effect of
2827 hyperoxygenation on T1 relaxation time in vitro. *Acad Radiol* 10: 854-860, 2003.
- 2828 268. Jansson L, Barbu A, Bodin B, Drott CJ, Espes D, Gao X, Grapensparr L, Källskog Ö, Lau J,
2829 Liljebäck H, Palm F, Quach M, Sandberg M, Strömberg V, Ullsten S, and Carlsson P-O.
2830 Pancreatic islet blood flow and its measurement. *Ups J Med Sci* 121: 81-95, 2016.
- 2831 269. Jaszczak P. Skin oxygen tension, skin oxygen consumption, and skin blood flow measured
2832 by a tc-pO₂ electrode. *Acta Physiol Scand Suppl* 603: 53-57, 1991.
- 2833 270. Jauniaux E, Gulbis B, and Burton GJ. The human first trimester gestational sac limits rather
2834 than facilitates oxygen transfer to the foetus--a review. *Placenta* 24 Suppl A: S86-93, 2003.

- 2835 271. Jauniaux E, Watson A, and Burton G. Evaluation of respiratory gases and acid-base
2836 gradients in human fetal fluids and uteroplacental tissue between 7 and 16 weeks'
2837 gestation. *Am J Obstet Gynecol* 184: 998-1003, 2001.
- 2838 272. Jauniaux E, Watson AL, Hempstock J, Bao YP, Skepper JN, and Burton GJ. Onset of
2839 maternal arterial blood flow and placental oxidative stress. A possible factor in human early
2840 pregnancy failure. *Am J Pathol* 157: 2111-2122, 2000.
- 2841 273. Jayaraman S, Song Y, Vetrivel L, Shankar L, and Verkman AS. Noninvasive in vivo
2842 fluorescence measurement of airway-surface liquid depth, salt concentration, and pH. *J*
2843 *Clin Invest* 107: 317-324, 2001.
- 2844 274. Jensen MD, Wallach DF, and Sherwood P. Diffusion in tissue cultures on gas-permeable
2845 and impermeable supports. *Journal of theoretical biology* 56: 443-458, 1976.
- 2846 275. Jiang J, Nakashima T, Liu KJ, Goda F, Shima T, and Swartz HM. Measurement of PO₂ in
2847 liver using EPR oximetry. *J Appl Physiol (1985)* 80: 552-558, 1996.
- 2848 276. Jiang Y-Z, Wang K, Li Y, Dai C-F, Wang P, Kendzierski C, Chen D-B, and Zheng J.
2849 Enhanced Cellular Responses and Distinct Gene Profiles in Human Fetoplacental Artery
2850 Endothelial Cells under Chronic Low Oxygen. *Biol Reprod* 2013.
- 2851 277. Jiang Y-Z, Wang K, Li Y, Dai C-F, Wang P, Kendzierski C, Chen D-B, and Zheng J.
2852 Transcriptional and functional adaptations of human endothelial cells to physiological
2853 chronic low oxygen. *Biol Reprod* 88: 114, 2013.
- 2854 278. Johnson LG, Dickman KG, Moore KL, Mandel LJ, and Boucher RC. Enhanced Na⁺
2855 transport in an air-liquid interface culture system. *American Journal of Physiology-Lung*
2856 *Cellular and Molecular Physiology* 264: L560-L565, 1993.
- 2857 279. Jurrus ER, and Weiss HS. In vitro tissue oxygen tensions in the rabbit aortic arch.
2858 *Atherosclerosis* 28: 223-232, 1977.
- 2859 280. Kabon B, Nagele A, Reddy D, Eagon C, Fleshman JW, Sessler DI, and Kurz A. Obesity
2860 decreases perioperative tissue oxygenation. *Anesthesiology* 100: 274-280, 2004.
- 2861 281. Kamga C, Krishnamurthy S, and Shiva S. Myoglobin and mitochondria: a relationship
2862 bound by oxygen and nitric oxide. *Nitric Oxide* 26: 251-258, 2012.
- 2863 282. Kamler M, Nowak K, Bock M, Herold U, Motsch J, Hagl S, Gebhard MM, and Jakob H.
2864 Bronchial artery revascularization restores peribronchial tissue oxygenation after lung
2865 transplantation. *J Heart Lung Transplant* 23: 763-766, 2004.
- 2866 283. Karanjawala ZE, Murphy N, Hinton DR, Hsieh CL, and Lieber MR. Oxygen metabolism
2867 causes chromosome breaks and is associated with the neuronal apoptosis observed in
2868 DNA double-strand break repair mutants. *Curr Biol* 12: 397-402, 2002.
- 2869 284. Karhausen J, Furuta GT, Tomaszewski JE, Johnson RS, Colgan SP, and Haase VH.
2870 Epithelial hypoxia-inducible factor-1 is protective in murine experimental colitis. *J Clin*
2871 *Invest* 114: 1098-1106, 2004.
- 2872 285. Kaser DJ. On developing a thesis for Reproductive Endocrinology and Infertility fellowship:
2873 a case study of ultra-low (2%) oxygen tension for extended culture of human embryos. *J*
2874 *Assist Reprod Genet* 34: 303-308, 2017.
- 2875 286. Kaser DJ, Bogale B, Sarda V, Farland LV, and Racowsky C. Randomized controlled trial of
2876 low (5%) vs. ultralow (2%) oxygen tension for in vitro development of human embryos.
2877 *Fertility and Sterility* 106: e4, 2016.
- 2878 287. Katopodi T, Tew SR, Clegg PD, and Hardingham TE. The influence of donor and hypoxic
2879 conditions on the assembly of cartilage matrix by osteoarthritic human articular
2880 chondrocytes on Hyalograft matrices. *Biomaterials* 30: 535-540, 2009.
- 2881 288. Kaufman DL, and Mitchell JA. Alterations in intrauterine oxygen tension during the estrous
2882 cycle in the rat and hamster and its regulation by ovarian steroid hormones: a comparative
2883 study. *Adv Exp Med Biol* 277: 745-750, 1990.
- 2884 289. Kay AG, Dale TP, Akram KM, Mohan P, Hampson K, Maffulli N, Spiteri MA, El Haj AJ, and
2885 Forsyth NR. BMP2 repression and optimized culture conditions promote human bone
2886 marrow-derived mesenchymal stem cell isolation. *Regen Med* 10: 109-125, 2015.
- 2887 290. Keeley TP, Siow RCM, Jacob R, and Mann GE. A PP2A-mediated feedback mechanism
2888 controls Ca(2+)-dependent NO synthesis under physiological oxygen. *FASEB J* 31: 5172-
2889 5183, 2017.

- 2890 291. Keeley TP, Siow RCM, Jacob R, and Mann GE. Reduced SERCA activity underlies
2891 dysregulation of Ca(2+) homeostasis under atmospheric O2 levels. *FASEB J* 32: 2531-
2892 2538, 2018.
- 2893 292. Kelly CJ, and Colgan SP. Breathless in the Gut: Implications of Luminal O2 for Microbial
2894 Pathogenicity. *Cell Host Microbe* 19: 427-428, 2016.
- 2895 293. Kelly CJ, Glover LE, Campbell EL, Kominsky DJ, Ehrentauf SF, Bowers BE, Bayless AJ,
2896 Saeedi BJ, and Colgan SP. Fundamental role for HIF-1 α in constitutive expression of
2897 human β defensin-1. *Mucosal immunology* 6: 1110-1118, 2013.
- 2898 294. Kelly CJ, Zheng L, Campbell EL, Saeedi B, Scholz CC, Bayless AJ, Wilson KE, Glover LE,
2899 Kominsky DJ, and Magnuson A. Crosstalk between microbiota-derived short-chain fatty
2900 acids and intestinal epithelial HIF augments tissue barrier function. *Cell host & microbe* 17: 662-671, 2015.
- 2902 295. Kerger H, Torres Filho IP, Rivas M, Winslow RM, and Intaglietta M. Systemic and
2903 subcutaneous microvascular oxygen tension in conscious Syrian golden hamsters. *Am J*
2904 *Physiol* 268: H802-810, 1995.
- 2905 296. Kessler M, and Lubbers DW. Aufbau und Anwendungsmöglichkeit verschiedener PO2-
2906 Elektroden. In: *Pflugers Archiv Fur Die Gesamte Physiologie Des Menschen Und Der*
2907 *Tiere* 1966, p. R82.
- 2908 297. Khan M, Kutala VK, Wisel S, Chacko SM, Kuppusamy ML, Kwiatkowski P, and Kuppusamy
2909 P editors. *Oxygen Transport to Tissue XXIX*. Springer, 2008, p. 45-52.
- 2910 298. Khaw KS, Wang CC, Ngan Kee WD, Pang CP, and Rogers MS. Effects of high inspired
2911 oxygen fraction during elective caesarean section under spinal anaesthesia on maternal
2912 and fetal oxygenation and lipid peroxidation. *Br J Anaesth* 88: 18-23, 2002.
- 2913 299. Kietzmann T, Hirsch-Ernst KI, Kahl GF, and Jungermann K. Mimicry in primary rat
2914 hepatocyte cultures of the in vivo perivenous induction by phenobarbital of cytochrome P-
2915 450 2B1 mRNA: role of epidermal growth factor and perivenous oxygen tension. *Mol*
2916 *Pharmacol* 56: 46-53, 1999.
- 2917 300. Kim T-S, Misumi S, Jung C-G, Masuda T, Isobe Y, Furuyama F, Nishino H, and Hida H.
2918 Increase in dopaminergic neurons from mouse embryonic stem cell-derived neural
2919 progenitor/stem cells is mediated by hypoxia inducible factor-1 α . *J Neurosci Res* 86:
2920 2353-2362, 2008.
- 2921 301. Kimberger O, Fleischmann E, Brandt S, Kugener A, Kabon B, Hiltebrand L, Krejci V, and
2922 Kurz A. Supplemental oxygen, but not supplemental crystalloid fluid, increases tissue
2923 oxygen tension in healthy and anastomotic colon in pigs. *Anesth Analg* 105: 773-779, 2007.
- 2924 302. Kinnala PJ, Kuttala KT, Grönroos JM, Havia TV, Nevalainen TJ, and Niinikoski JH.
2925 Pancreatic tissue perfusion in experimental acute pancreatitis. *European Journal of*
2926 *Surgery* 167: 689-694, 2001.
- 2927 303. Kinnala PJ, Kuttala KT, Grönroos JM, Havia TV, Nevalainen TJ, and Niinikoski JHA.
2928 Splanchnic and pancreatic tissue perfusion in experimental acute pancreatitis. *Scand J*
2929 *Gastroenterol* 37: 845-849, 2002.
- 2930 304. Kitzmann JP, Pepper AR, Gala-Lopez B, Pawlick R, Kin T, O'Gorman D, Mueller KR,
2931 Gruessner AC, Avgoustiniatos ES, Karatzas T, Szot GL, Posselt AM, Stock PG, Wilson JR,
2932 Shapiro AM, and Papas KK. Human islet viability and function is maintained during high-
2933 density shipment in silicone rubber membrane vessels. *Transplant Proc* 46: 1989-1991,
2934 2014.
- 2935 305. Knotzer H, Pajk W, Maier S, Ladurner R, Kleinsasser A, Wenzel V, Dünser MW, Ulmer H,
2936 and Hasibeder WR. Arginine vasopressin reduces intestinal oxygen supply and mucosal
2937 tissue oxygen tension. *Am J Physiol Heart Circ Physiol* 289: H168-173, 2005.
- 2938 306. Knowles HJ, Mole DR, Ratcliffe PJ, and Harris AL. Normoxic stabilization of hypoxia-
2939 inducible factor-1 α by modulation of the labile iron pool in differentiating U937
2940 macrophages: effect of natural resistance-associated macrophage protein 1. *Cancer Res*
2941 66: 2600-2607, 2006.
- 2942 307. Koay EJ, and Athanasiou KA. Hypoxic chondrogenic differentiation of human embryonic
2943 stem cells enhances cartilage protein synthesis and biomechanical functionality.
2944 *Osteoarthritis Cartilage* 16: 1450-1456, 2008.

- 2945 308. Kofoed H, Sjøntoft E, Siemssen SO, and Olesen HP. Bone marrow circulation after
2946 osteotomy. Blood flow, pO₂, pCO₂, and pressure studied in dogs. *Acta Orthop Scand* 56:
2947 400-403, 1985.
- 2948 309. Komatsu H, Barriga A, Medrano L, Omori K, Kandeel F, and Mullen Y. Oxygenated thawing
2949 and rewarming alleviate rewarming injury of cryopreserved pancreatic islets. *Biochem*
2950 *Biophys Res Commun* 486: 817-823, 2017.
- 2951 310. Komatsu H, Cook C, Wang C-H, Medrano L, Lin H, Kandeel F, Tai Y-C, and Mullen Y.
2952 Oxygen environment and islet size are the primary limiting factors of isolated pancreatic
2953 islet survival. *PLoS One* 12: e0183780, 2017.
- 2954 311. Koros WJ, Wang J, and Felder RM. Oxygen permeation through FEP Teflon and Kapton
2955 polyimide. *Journal of Applied Polymer Science* 26: 2805-2809, 1981.
- 2956 312. Korsbäck C, and Höckerstedt K. Small bowel and liver pO₂ during vasopressin infusion into
2957 the superior mesenteric artery. *Ann Chir Gynaecol* 73: 50-53, 1984.
- 2958 313. Kotaska K, Urinowska R, Klapkova E, Prusa R, Rob L, and Binder T. Re-evaluation of cord
2959 blood arterial and venous reference ranges for pH, pO₂, pCO₂, according to spontaneous
2960 or cesarean delivery. *Journal of Clinical Laboratory Analysis* 24: 300-304, 2010.
- 2961 314. Kovačič B. Culture systems: low-oxygen culture. *Methods Mol Biol* 912: 249-272, 2012.
- 2962 315. Krieger JA, Landsiedel JC, and Lawrence DA. Differential<i>in vitro</i> effects of
2963 physiological and atmospheric oxygen tension on normal human peripheral blood
2964 mononuclear cell proliferation, cytokine and immunoglobulin production. *International*
2965 *journal of immunopharmacology* 18: 545-552, 1996.
- 2966 316. Krogh A. The number and distribution of capillaries in muscles with calculations of the
2967 oxygen pressure head necessary for supplying the tissue. *J Physiol* 52: 409-415, 1919.
- 2968 317. Kumar A, Dailey LA, Swedrowska M, Siow R, Mann GE, Vizcay-Barrena G, Arno M,
2969 Mudway IS, and Forbes B. Quantifying the magnitude of the oxygen artefact inherent in
2970 culturing airway cells under atmospheric oxygen versus physiological levels. *FEBS Lett*
2971 590: 258-269, 2016.
- 2972 318. Kunath U, and Uckmann C. Der Sauerstoffpartialdruck in der Magenfunduswand in
2973 Abhängigkeit von der arteriellen Blutzufuhr. *Langenbeck's Archives of Surgery* 348: 191-
2974 199, 1979.
- 2975 319. Kunisaki Y, Bruns I, Scheiermann C, Ahmed J, Pinho S, Zhang D, Mizoguchi T, Wei Q,
2976 Lucas D, Ito K, Mar JC, Bergman A, and Frenette PS. Arteriolar niches maintain
2977 haematopoietic stem cell quiescence. *Nature* 502: 637-643, 2013.
- 2978 320. Kusuma S, Peijnenburg E, Patel P, and Gerecht S. Low oxygen tension enhances
2979 endothelial fate of human pluripotent stem cells. *Arteriosclerosis, thrombosis, and vascular*
2980 *biology* 34: 913-920, 2014.
- 2981 321. Laderoute KR. The interaction between HIF-1 and AP-1 transcription factors in response to
2982 low oxygen. *Semin Cell Dev Biol* 16: 502-513, 2005.
- 2983 322. Lando D, Peet DJ, Gorman JJ, Whelan DA, Whitelaw ML, and Bruick RK. FIH-1 is an
2984 asparaginyl hydroxylase enzyme that regulates the transcriptional activity of hypoxia-
2985 inducible factor. *Genes Dev* 16: 1466-1471, 2002.
- 2986 323. Lando D, Peet DJ, Whelan DA, Gorman JJ, and Whitelaw ML. Asparagine hydroxylation of
2987 the HIF transactivation domain a hypoxic switch. *Science* 295: 858-861, 2002.
- 2988 324. Lane N. *Oxygen: the molecule that made the world*. OUP Oxford, 2002.
- 2989 325. Lash JM, and Bohlen HG. Perivascular and tissue PO₂ in contracting rat spinotrapezius
2990 muscle. *Am J Physiol* 252: H1192-1202, 1987.
- 2991 326. Le Q-T, Chen E, Salim A, Cao H, Kong CS, Whyte R, Donington J, Cannon W, Wakelee H,
2992 Tibshirani R, Mitchell JD, Richardson D, O'Byrne KJ, Koong AC, and Giaccia AJ. An
2993 evaluation of tumor oxygenation and gene expression in patients with early stage non-small
2994 cell lung cancers. *Clin Cancer Res* 12: 1507-1514, 2006.
- 2995 327. Leary TS, Klinck JR, Hayman G, Friend P, Jamieson NV, and Gupta AK. Measurement of
2996 liver tissue oxygenation after orthotopic liver transplantation using a multiparameter sensor.
2997 A pilot study. *Anaesthesia* 57: 1128-1133, 2002.
- 2998 328. Lecoq J, Parpaleix A, Roussakis E, Ducros M, Goulam Houssen Y, Vinogradov SA, and
2999 Charpak S. Simultaneous two-photon imaging of oxygen and blood flow in deep cerebral
3000 vessels. *Nat Med* 17: 893-898, 2011.

- 3001 329. Lee CM, Genetos DC, You Z, and Yellowley CE. Hypoxia regulates PGE(2) release and
3002 EP1 receptor expression in osteoblastic cells. *J Cell Physiol* 212: 182-188, 2007.
- 3003 330. Lee ES, Bauer GE, Caldwell MP, and Santilli SM. Association of artery wall hypoxia and
3004 cellular proliferation at a vascular anastomosis. *Journal of Surgical Research* 91: 32-37,
3005 2000.
- 3006 331. Lee Y-A, Kim JY, Hong S-J, Lee S-H, Yoo MC, Kim KS, and Yang H-I. Synovial
3007 proliferation differentially affects hypoxia in the joint cavities of rheumatoid arthritis and
3008 osteoarthritis patients. *Clin Rheumatol* 26: 2023-2029, 2007.
- 3009 332. Lee Y-A, Kim JY, Hong S-J, Lee S-H, Yoo MC, Kim KS, and Yang H-I. Synovial
3010 proliferation differentially affects hypoxia in the joint cavities of rheumatoid arthritis and
3011 osteoarthritis patients. *Clin Rheumatol* 26: 2023-2029, 2007.
- 3012 333. Lei XG, Zhu J-H, Cheng W-H, Bao Y, Ho Y-S, Reddi AR, Holmgren A, and Arnér ESJ.
3013 Paradoxical Roles of Antioxidant Enzymes: Basic Mechanisms and Health Implications.
3014 *Physiol Rev* 96: 307-364, 2016.
- 3015 334. Leichtweiss H-P, Lübbers DW, Weiss CH, Baumgärtl H, and Reschke W. The oxygen
3016 supply of the rat kidney: Measurements of intrarenal pO₂. *Pflügers Archiv* 309: 328-349,
3017 1969.
- 3018 335. Lengner CJ, Gimelbrant AA, Erwin JA, Cheng AW, Guenther MG, Welstead GG,
3019 Alagappan R, Frampton GM, Xu P, and Muffat J. Derivation of pre-X inactivation human
3020 embryonic stem cells under physiological oxygen concentrations. *Cell* 141: 872-883, 2010.
- 3021 336. Lennon DP, Edmison JM, and Caplan AI. Cultivation of rat marrow-derived mesenchymal
3022 stem cells in reduced oxygen tension: effects on in vitro and in vivo osteochondrogenesis. *J*
3023 *Cell Physiol* 187: 345-355, 2001.
- 3024 337. Leonard MO, Cottell DC, Godson C, Brady HR, and Taylor CT. The role of HIF-1 alpha in
3025 transcriptional regulation of the proximal tubular epithelial cell response to hypoxia. *J Biol*
3026 *Chem* 278: 40296-40304, 2003.
- 3027 338. LEVY MN, and IMPERIAL ES. Oxygen shunting in renal cortical and medullary capillaries.
3028 *Am J Physiol* 200: 159-162, 1961.
- 3029 339. Li H, Hou H, Sucheta A, Williams BB, Lariviere JP, Khan MN, Lesniewski PN, Gallez B, and
3030 Swartz HM. Implantable resonators--a technique for repeated measurement of oxygen at
3031 multiple deep sites with in vivo EPR. *Adv Exp Med Biol* 662: 265-272, 2010.
- 3032 340. Li Q, Sun B, Wang X, Jin Z, Zhou Y, Dong L, Jiang L-H, and Rong W. A crucial role for
3033 hydrogen sulfide in oxygen sensing via modulating large conductance calcium-activated
3034 potassium channels. *Antioxid Redox Signal* 12: 1179-1189, 2010.
- 3035 341. Li S, Oreffo ROC, Sengers BG, and Tare RS. The effect of oxygen tension on human
3036 articular chondrocyte matrix synthesis: integration of experimental and computational
3037 approaches. *Biotechnol Bioeng* 111: 1876-1885, 2014.
- 3038 342. Li T-S, Cheng K, Malliaras K, Matsushita N, Sun B, Marbán L, Zhang Y, and Marbán E.
3039 Expansion of human cardiac stem cells in physiological oxygen improves cell production
3040 efficiency and potency for myocardial repair. *Cardiovasc Res* 89: 157-165, 2011.
- 3041 343. Li T-S, and Marbán E. Physiological levels of reactive oxygen species are required to
3042 maintain genomic stability in stem cells. *Stem Cells* 28: 1178-1185, 2010.
- 3043 344. Li W-C, Ruan X-Z, Zhang H-M, and Zeng Y-J. Biomechanical properties of different
3044 segments of human umbilical cord vein and its value for clinical application. *Journal of*
3045 *Biomedical Materials Research Part B: Applied Biomaterials* 76: 93-97, 2006.
- 3046 345. Lillegard JB, Fisher JE, Nedredal G, Luebke-Wheeler J, Bao J, Wang W, Amoiti B, and
3047 Nyberg SL. Normal atmospheric oxygen tension and the use of antioxidants improve
3048 hepatocyte spheroid viability and function. *J Cell Physiol* 226: 2987-2996, 2011.
- 3049 346. Lind Due V, Bonde J, Kann T, and Perner A. Extremely low oxygen tension in the rectal
3050 lumen of human subjects. *Acta anaesthesiologica scandinavica* 47: 372-372, 2003.
- 3051 347. Link G, Clark KE, and Lang U. Umbilical blood flow during pregnancy: evidence for
3052 decreasing placental perfusion. *Am J Obstet Gynecol* 196: 489.e481-487, 2007.
- 3053 348. Lippitsch ME, Pusterhofer J, Leiner MJ, and Wolfbeis OS. Fibre-optic oxygen sensor with
3054 the fluorescence decay time as the information carrier. *Analytica Chimica Acta* 205: 1-6,
3055 1988.

349. Liss P, Nygren A, Revsbech NP, and Ulfendahl HR. Intrarenal oxygen tension measured by a modified Clark electrode at normal and low blood pressure and after injection of x-ray contrast media. *Pflügers Archiv European Journal of Physiology* 434: 705-711, 1997.
350. Liu KJ, Bacic G, Hoopes PJ, Jiang J, Du H, Ou LC, Dunn JF, and Swartz HM. Assessment of cerebral pO₂ by EPR oximetry in rodents: effects of anesthesia, ischemia, and breathing gas. *Brain Res* 685: 91-98, 1995.
351. Liu Y, Cox SR, Morita T, and Kourembanas S. Hypoxia regulates vascular endothelial growth factor gene expression in endothelial cells. Identification of a 5' enhancer. *Circ Res* 77: 638-643, 1995.
352. Lloyd BB, Cunningham DJC, and Goode RC. Depression of hypoxic hyperventilation in man by sudden inspiration of carbon monoxide. *Arterial Chemoreceptors* 409: 145-148, 1968.
353. Locke R, Hauser CJ, and Shoemaker WC. The use of surface oximetry to assess bowel viability. *Archives of Surgery* 119: 1252-1256, 1984.
354. Lodge KM, Thompson AA, Chilvers ER, and Condliffe AM. Hypoxic regulation of neutrophil function and consequences for *Staphylococcus aureus* infection. *Microbes and infection* 19: 166-176, 2017.
355. Löfstedt T, Fredlund E, Holmquist-Mengelbier L, Pietras A, Ovenberger M, Poellinger L, and Pählman S. Hypoxia inducible factor-2 α in cancer. *Cell Cycle* 6: 919-926, 2007.
356. Lopci E, Grassi I, Chiti A, Nanni C, Cicoria G, Toschi L, Fonti C, Lodi F, Mattioli S, and Fanti S. PET radiopharmaceuticals for imaging of tumor hypoxia: a review of the evidence. *American journal of nuclear medicine and molecular imaging* 4: 365, 2014.
357. Lord EM, Harwell L, and Koch CJ. Detection of hypoxic cells by monoclonal antibody recognizing 2-nitroimidazole adducts. *Cancer Res* 53: 5721-5726, 1993.
358. Lösse B, Schuchhardt S, and Niederle N. The oxygen pressure histogram in the left ventricular myocardium of the dog. *Pflugers Arch* 356: 121-132, 1975.
359. Louis NA, Hamilton KE, Canny G, Shekels LL, Ho SB, and Colgan SP. Selective induction of mucin-3 by hypoxia in intestinal epithelia. *J Cell Biochem* 99: 1616-1627, 2006.
360. Lu C, Rollins M, Hou H, Swartz HM, Hopf H, Miclau T, and Marcucio RS. Tibial fracture decreases oxygen levels at the site of injury. *Iowa Orthop J* 28: 14-21, 2008.
361. Lu C, Saless N, Wang X, Sinha A, Decker S, Kazakia G, Hou H, Williams B, Swartz HM, and Hunt TK. The role of oxygen during fracture healing. *Bone* 52: 220-229, 2013.
362. Lübbers DW, and Baumgärtl H. Heterogeneities and profiles of oxygen pressure in brain and kidney as examples of the pO₂ distribution in the living tissue. *Kidney Int* 51: 372-380, 1997.
363. Lund-Olesen K. Oxygen tension in synovial fluids. *Arthritis Rheum* 13: 769-776, 1970.
364. Lyons DG, Parpaleix A, Roche M, and Charpak S. Mapping oxygen concentration in the awake mouse brain. *Elife* 5: 2016.
365. Maas DH, Storey BT, and Mastroianni L. Oxygen tension in the oviduct of the rhesus monkey (*Macaca mulatta*). *Fertil Steril* 27: 1312-1317, 1976.
366. MacCraith BD, McDonagh CM, O'Keeffe G, Keyes ET, Vos JG, O'Kelly B, and McGilp JF. Fibre optic oxygen sensor based on fluorescence quenching of evanescent-wave excited ruthenium complexes in sol-gel derived porous coatings. *Analyst* 118: 385-388, 1993.
367. Mahnke A, Meier RJ, Schatz V, Hofmann J, Castiglione K, Schleicher U, Wolfbeis OS, Bogdan C, and Jantsch J. Hypoxia in *Leishmania major* skin lesions impairs the NO-dependent leishmanicidal activity of macrophages. *J Invest Dermatol* 134: 2339-2346, 2014.
368. Maier P, Saad B, and Schawalder HP. Effect of periportal- and centrilobular-equivalent oxygen tension on liver specific functions in long-term rat hepatocyte cultures. *Toxicol In Vitro* 8: 423-435, 1994.
369. Maines MD. The heme oxygenase system: a regulator of second messenger gases. *Annu Rev Pharmacol Toxicol* 37: 517-554, 1997.
370. Malek AM, Alper SL, and Izumo S. Hemodynamic shear stress and its role in atherosclerosis. *Jama* 282: 2035-2042, 1999.
371. Mamchaoui K, and Saumon G. A method for measuring the oxygen consumption of intact cell monolayers. *Am J Physiol Lung Cell Mol Physiol* 278: L858-863, 2000.

3112 372. Manalo DJ, Rowan A, Lavoie T, Natarajan L, Kelly BD, Shui QY, Garcia JGN, and
3113 Semenza GL. Transcriptional regulation of vascular endothelial cell responses to hypoxia
3114 by HIF-1. *Blood* 105: 659-669, 2005.

3115 373. Mansfield KD, Simon MC, and Keith B. Hypoxic reduction in cellular glutathione levels
3116 requires mitochondrial reactive oxygen species. *J Appl Physiol* 97: 1358-1366, 2004.

3117 374. Markway BD, Tan G-K, Brooke G, Hudson JE, Cooper-White JJ, and Doran MR. Enhanced
3118 chondrogenic differentiation of human bone marrow-derived mesenchymal stem cells in low
3119 oxygen environment micropellet cultures. *Cell Transplant* 19: 29-42, 2010.

3120 375. Marshall C, Mamary AJ, Verhoeven AJ, and Marshall BE. Pulmonary artery NADPH-
3121 oxidase is activated in hypoxic pulmonary vasoconstriction. *American journal of respiratory
3122 cell and molecular biology* 15: 633-644, 1996.

3123 376. Martin GC, Green RS, and Holzman IR. Acidosis in newborns with nuchal cords and
3124 normal Apgar scores. *J Perinatol* 25: 162-165, 2005.

3125 377. Martinez I, Nedredal GI, Øie CI, Warren A, Johansen O, Le Couteur DG, and Smedsrød B.
3126 The influence of oxygen tension on the structure and function of isolated liver sinusoidal
3127 endothelial cells. *Comp Hepatol* 7: 4, 2008.

3128 378. Masson N, Singleton RS, Sekirnik R, Trudgian DC, Ambrose LJ, Miranda MX, Tian Y-M,
3129 Kessler BM, Schofield CJ, and Ratcliffe PJ. The FIH hydroxylase is a cellular peroxide
3130 sensor that modulates HIF transcriptional activity. *EMBO Rep* 13: 251-257, 2012.

3131 379. Mastrogiannaki M, Matak P, Keith B, Simon MC, Vaultont S, and Peyssonnaud C. HIF-2 α ,
3132 but not HIF-1 α , promotes iron absorption in mice. *The Journal of clinical investigation* 119:
3133 1159, 2009.

3134 380. Mastroianni L, and Jones R. OXYGEN TENSION WITHIN THE RABBIT FALLOPIAN
3135 TUBE. *J Reprod Fertil* 9: 99-102, 1965.

3136 381. Mathis C, Poussin C, Weisensee D, Gebel S, Hengstermann A, Sewer A, Belcastro V,
3137 Xiang Y, Ansari S, Wagner S, Hoeng J, and Peitsch MC. Human bronchial epithelial cells
3138 exposed in vitro to cigarette smoke at the air-liquid interface resemble bronchial epithelium
3139 from human smokers. *Am J Physiol Lung Cell Mol Physiol* 304: L489-503, 2013.

3140 382. McCallum WD, and McAreavey DR. Human umbilical vessel diameters and blood gas
3141 tensions in the first two minutes after delivery. *Gynecologic and Obstetric Investigation* 7:
3142 201-212, 1976.

3143 383. McGovern NN, Cowburn AS, Porter L, Walmsley SR, Summers C, Thompson AAR, Anwar
3144 S, Willcocks LC, Whyte MKB, Condliffe AM, and Chilvers ER. Hypoxia selectively inhibits
3145 respiratory burst activity and killing of *Staphylococcus aureus* in human neutrophils. *J
3146 Immunol* 186: 453-463, 2011.

3147 384. McLimans WF, Blumenson LE, and Tunnah KV. Kinetics of gas diffusion in mammalian cell
3148 culture systems. II. Theory. *Biotechnology and Bioengineering* 10: 741-763, 1968.

3149 385. McNulty PH, King N, Scott S, Hartman G, McCann J, Kozak M, Chambers CE, Demers LM,
3150 and Sinoway LI. Effects of supplemental oxygen administration on coronary blood flow in
3151 patients undergoing cardiac catheterization. *Am J Physiol Heart Circ Physiol* 288: H1057-
3152 1062, 2005.

3153 386. Meier J, Pape A, Kleen M, Hutter J, Kemming G, and Habler O. Regional blood flow during
3154 hyperoxic haemodilution. *Clin Physiol Funct Imaging* 25: 158-165, 2005.

3155 387. Meister A, and Anderson ME. Glutathione. *Annu Rev Biochem* 52: 711-760, 1983.

3156 388. Mellstrom A, Månsson P, Jonsson K, and Hartmann M. Measurements of subcutaneous
3157 tissue PO₂ reflect oxygen metabolism of the small intestinal mucosa during hemorrhage
3158 and resuscitation. An experimental study in pigs. *Eur Surg Res* 42: 122-129, 2009.

3159 389. Metzen M, Wolff W, Fandrey F, and Jelkmann J. Pericellular PO₂ and O₂ consumption in
3160 monolayer cell cultures. *Respiration Physiology* 100: 101 - 106, 1995.

3161 390. Metzger H, and Heuber S. Local oxygen tension and spike activity of the cerebral grey
3162 matter of the rat and its response to short intervals of O₂ deficiency or CO₂ excess.
3163 *Pflugers Arch* 370: 201-209, 1977.

3164 391. Meyer EG, Buckley CT, Thorpe SD, and Kelly DJ. Low oxygen tension is a more potent
3165 promoter of chondrogenic differentiation than dynamic compression. *J Biomech* 43: 2516-
3166 2523, 2010.

- 3167 392. Michelakis ED, Hampl V, Nsair A, Wu X, Harry G, Haromy A, Gurtu R, and Archer SL.
3168 Diversity in mitochondrial function explains differences in vascular oxygen sensing. *Circ*
3169 *Res* 90: 1307-1315, 2002.
- 3170 393. Michiels C, Arnould T, and Remacle J. Endothelial cell responses to hypoxia: initiation of a
3171 cascade of cellular interactions. *Biochim Biophys Acta* 1497: 1-10, 2000.
- 3172 394. Mignon C, Uzunbajakava NE, Raafs B, Botchkareva NV, and Tobin DJ.
3173 Photobiomodulation of human dermal fibroblasts in vitro: decisive role of cell culture
3174 conditions and treatment protocols on experimental outcome. *Sci Rep* 7: 2797, 2017.
- 3175 395. Mik EG, Johannes T, and Ince C. Monitoring of renal venous PO₂ and kidney oxygen
3176 consumption in rats by a near-infrared phosphorescence lifetime technique. *Am J Physiol*
3177 *Renal Physiol* 294: F676-681, 2008.
- 3178 396. Miller GW, Mugler JP, Altes TA, Cai J, Mata JF, de Lange EE, Tobias WA, Cates GD, and
3179 Brookeman JR. A short-breath-hold technique for lung pO₂ mapping with ³He MRI. *Magn*
3180 *Reson Med* 63: 127-136, 2010.
- 3181 397. Millman JR, Tan JH, and Colton CK. The effects of low oxygen on self-renewal and
3182 differentiation of embryonic stem cells. *Current opinion in organ transplantation* 14: 694-
3183 700, 2009.
- 3184 398. Mimura I, and Nangaku M. The suffocating kidney: tubulointerstitial hypoxia in end-stage
3185 renal disease. *Nat Rev Nephrol* 6: 667-678, 2010.
- 3186 399. Ming G, and Zhenhao D. Prediction of oxygen solubility in pure water and brines up to high
3187 temperatures and pressures. *Geochimica et Cosmochimica Acta* 74: 5631-5640, 2010.
- 3188 400. Mitchell JA, and Yochim JM. Intrauterine oxygen tension during the estrous cycle in the rat:
3189 its relation to uterine respiration and vascular activity. *Endocrinology* 83: 701-705, 1968.
- 3190 401. Mitchell JA, and Yochim JM. Measurement of intrauterine oxygen tension in the rat and its
3191 regulation by ovarian steroid hormones. *Endocrinology* 83: 691-700, 1968.
- 3192 402. Mohyeldin A, Garzón-Muvdi T, and Quiñones-Hinojosa A. Oxygen in stem cell biology: a
3193 critical component of the stem cell niche. *Cell Stem Cell* 7: 150-161, 2010.
- 3194 403. Mondragon-Teran P, Baboo JZ, Mason C, Lye GJ, and Veraitch FS. The full spectrum of
3195 physiological oxygen tensions and step-changes in oxygen tension affects the neural
3196 differentiation of mouse embryonic stem cells. *Biotechnol Prog* 27: 1700-1708, 2011.
- 3197 404. Mondragon-Teran P, Lye GJ, and Veraitch FS. Lowering oxygen tension enhances the
3198 differentiation of mouse embryonic stem cells into neuronal cells. *Biotechnol Prog* 25: 1480-
3199 1488, 2009.
- 3200 405. Moore JA, and Ethier CR. Oxygen mass transfer calculations in large arteries. *J Biomech*
3201 *Eng* 119: 469-475, 1997.
- 3202 406. Morin SJ. Oxygen tension in embryo culture: does a shift to 2% O₂ in extended culture
3203 represent the most physiologic system? *J Assist Reprod Genet* 34: 309-314, 2017.
- 3204 407. Morosin M, Vignati C, Novi A, Salvioni E, Veglia F, Alimento M, Merli G, Sciomer S,
3205 Sinagra G, and Agostoni P. The alveolar to arterial oxygen partial pressure difference is
3206 associated with pulmonary diffusing capacity in heart failure patients. *Respir Physiol*
3207 *Neurobiol* 233: 1-6, 2016.
- 3208 408. Morote-Garcia JC, Rosenberger P, Nivillac NMI, Coe IR, and Eltzschig HK. Hypoxia-
3209 inducible factor-dependent repression of equilibrative nucleoside transporter 2 attenuates
3210 mucosal inflammation during intestinal hypoxia. *Gastroenterology* 136: 607-618, 2009.
- 3211 409. Morrison SJ, Csete M, Groves AK, Melega W, Wold B, and Anderson DJ. Culture in
3212 reduced levels of oxygen promotes clonogenic sympathoadrenal differentiation by isolated
3213 neural crest stem cells. *J Neurosci* 20: 7370-7376, 2000.
- 3214 410. Moss AJ, Samuelson P, Angell C, and Minken SL. Polarographic evaluation of transmural
3215 oxygen availability in intact muscular arteries. *J Atheroscler Res* 8: 803-810, 1968.
- 3216 411. Muller M, Padberg W, Schindler E, Sticher J, Osmer C, Friemann S, and Hempelmann G.
3217 Renocortical tissue oxygen pressure measurements in patients undergoing living donor
3218 kidney transplantation. *Anesthesia & Analgesia* 87: 474-476, 1998.
- 3219 412. Müller M, Schück R, Erkens U, Sticher J, Haase C, and Hempelmann G. [Effects of lumbar
3220 peridural anesthesia on tissue pO₂ of the large intestine in man]. *Anesthesiol Intensivmed*
3221 *Notfallmed Schmerzther* 30: 108-110, 1995.
- 3222 413. Mulligan-Kehoe MJ, and Simons M. Vasa vasorum in normal and diseased arteries.
3223 *Circulation* 129: 2557-2566, 2014.

3224 414. Murphy CL, and Polak JM. Control of human articular chondrocyte differentiation by
3225 reduced oxygen tension. *J Cell Physiol* 199: 451-459, 2004.

3226 415. Murphy CL, and Sambanis A. Effect of oxygen tension and alginate encapsulation on
3227 restoration of the differentiated phenotype of passaged chondrocytes. *Tissue Eng* 7: 791-
3228 803, 2001.

3229 416. Najafipour H, and Ferrell WR. Comparison of synovial PO₂ and sympathetic
3230 vasoconstrictor responses in normal and acutely inflamed rabbit knee joints. *Exp Physiol*
3231 80: 209-220, 1995.

3232 417. Nakamura M, Yamabe H, Osawa H, Nakamura N, Shimada M, Kumasaka R, Murakami R,
3233 Fujita T, Osanai T, and Okumura K. Hypoxic conditions stimulate the production of
3234 angiogenin and vascular endothelial growth factor by human renal proximal tubular
3235 epithelial cells in culture. *Nephrol Dial Transplant* 21: 1489-1495, 2006.

3236 418. Nastri CO, Nóbrega BN, Teixeira DM, Amorim J, Diniz LMM, Barbosa MWP, Giorgi VSI,
3237 Pileggi VN, and Martins WP. Low versus atmospheric oxygen tension for embryo culture in
3238 assisted reproduction: a systematic review and meta-analysis. *Fertil Steril* 106: 95-
3239 104.e117, 2016.

3240 419. Neumann HP, Bender BU, Berger DP, Laubenberger J, Schultze-seemann W, Wetterauer
3241 U, FERSTL FJ, Herbst EW, Schwarzkopf G, and Hes FJ. Prevalence, morphology and
3242 biology of renal cell carcinoma in von Hippel-Lindau disease compared to sporadic renal
3243 cell carcinoma. *The Journal of urology* 160: 1248-1254, 1998.

3244 420. Newby D, Marks L, and Lyall F. Dissolved oxygen concentration in culture medium:
3245 assumptions and pitfalls. *Placenta* 26: 353-357, 2005.

3246 421. Ng S, March S, Galstian A, Hanson K, Carvalho T, Mota MM, and Bhatia SN. Hypoxia
3247 promotes liver-stage malaria infection in primary human hepatocytes in vitro. *Dis Model*
3248 *Mech* 7: 215-224, 2014.

3249 422. Ngo JP, Kar S, Kett MM, Gardiner BS, Pearson JT, Smith DW, Ludbrook J, Bertram JF,
3250 and Evans RG. Vascular geometry and oxygen diffusion in the vicinity of artery-vein pairs in
3251 the kidney. *Am J Physiol Renal Physiol* 307: F1111-1122, 2014.

3252 423. Nicolaije C, Koedam M, and van Leeuwen JPTM. Decreased oxygen tension lowers
3253 reactive oxygen species and apoptosis and inhibits osteoblast matrix mineralization through
3254 changes in early osteoblast differentiation. *J Cell Physiol* 227: 1309-1318, 2012.

3255 424. Nicolaije C, van de Peppel J, and van Leeuwen JPTM. Oxygen-induced transcriptional
3256 dynamics in human osteoblasts are most prominent at the onset of mineralization. *J Cell*
3257 *Physiol* 228: 1863-1872, 2013.

3258 425. Nicolls MR, and Zamora MR. Bronchial blood supply after lung transplantation without
3259 bronchial artery revascularization. *Curr Opin Organ Transplant* 15: 563-567, 2010.

3260 426. Nie X, Laforest R, Elvington A, Randolph GJ, Zheng J, Voller T, Abendschein DR, Lapi SE,
3261 and Woodard PK. PET/MRI of Hypoxic Atherosclerosis Using 64Cu-ATSM in a Rabbit
3262 Model. *Journal of Nuclear Medicine* 57: 2006-2011, 2016.

3263 427. Nie X, Randolph GJ, Elvington A, Bandara N, Zheleznyak A, Gropler RJ, Woodard PK, and
3264 Lapi SE. Imaging of hypoxia in mouse atherosclerotic plaques with (64)Cu-ATSM. *Nucl*
3265 *Med Biol* 43: 534-542, 2016.

3266 428. Niinikoski J, Heughan C, and Hunt TK. Oxygen tensions in the aortic wall of normal rabbits.
3267 *Atherosclerosis* 17: 353-359, 1973.

3268 429. Nöldge-Schomburg GF, Priebe HJ, Armbruster K, Pannen B, Haberstroh J, and Geiger K.
3269 Different effects of early endotoxaemia on hepatic and small intestinal oxygenation in pigs.
3270 *Intensive Care Med* 22: 795-804, 1996.

3271 430. Nombela-Arrieta C, Pivarnik G, Winkel B, Canty KJ, Harley B, Mahoney JE, Park S-Y, Lu J,
3272 Protopopov A, and Silberstein LE. Quantitative imaging of haematopoietic stem and
3273 progenitor cell localization and hypoxic status in the bone marrow microenvironment. *Nat*
3274 *Cell Biol* 15: 533-543, 2013.

3275 431. Nowak K, Kamler M, Bock M, Motsch J, Hagl S, Jakob H, and Gebhard MM. Bronchial
3276 artery revascularization affects graft recovery after lung transplantation. *Am J Respir Crit*
3277 *Care Med* 165: 216-220, 2002.

3278 432. O'Connor JPB, Jackson A, Buonaccorsi GA, Buckley DL, Roberts C, Watson Y, Cheung S,
3279 McGrath DM, Naish JH, Rose CJ, Dark PM, Jayson GC, and Parker GJM. Organ-specific

effects of oxygen and carbogen gas inhalation on tissue longitudinal relaxation times. *Magn Reson Med* 58: 490-496, 2007.

433. O'Connor PM, Anderson WP, Kett MM, and Evans RG. RENAL PREGLOMERULAR ARTERIAL-VEIN O₂ SHUNTING IS A STRUCTURAL ANTI-OXIDANT DEFENCE MECHANISM OF THE RENAL CORTEX. *Clinical and Experimental Pharmacology and Physiology* 33: 637-641, 2006.

434. O'Connor PM, Anderson WP, Kett MM, and Evans RG. Simultaneous measurement of pO₂ and perfusion in the rabbit kidney in vivo. *Adv Exp Med Biol* 599: 93-99, 2007.

435. O'Driscoll SW, Fitzsimmons JS, and Commisso CN. Role of oxygen tension during cartilage formation by periosteum. *J Orthop Res* 15: 682-687, 1997.

436. Ogawa S, Lee TM, Kay AR, and Tank DW. Brain magnetic resonance imaging with contrast dependent on blood oxygenation. *Proc Natl Acad Sci U S A* 87: 9868-9872, 1990.

437. Olbryt M, Habryka A, Student S, Jarzab M, Tyszkiewicz T, and Lisowska KM. Global gene expression profiling in three tumor cell lines subjected to experimental cycling and chronic hypoxia. *PLoS One* 9: e105104, 2014.

438. Olsson R, and Carlsson P-O editors. *Oxygen Transport to Tissue XXVII*. Springer, 2006, p. 263-268.

439. Ortiz-Prado E, Natah S, Srinivasan S, and Dunn JF. A method for measuring brain partial pressure of oxygen in unanesthetized unrestrained subjects: The effect of acute and chronic hypoxia on brain tissue PO₂. *Journal of neuroscience methods* 193: 217-225, 2010.

440. Ottosen LDM, Hindkjær J, Husth M, Petersen DE, Kirk J, and Ingerslev HJ. Observations on intrauterine oxygen tension measured by fibre-optic microsensors. *Reproductive biomedicine online* 13: 380-385, 2006.

441. Palacios-Callender M, Hollis V, Mitchison M, Frakich N, Unitt D, and Moncada S. Cytochrome c oxidase regulates endogenous nitric oxide availability in respiring cells: a possible explanation for hypoxic vasodilation. *Proc Natl Acad Sci U S A* 104: 18508-18513, 2007.

442. Pandian RP, Parinandi NL, Ilangoan G, Zweier JL, and Kuppusamy P. Novel particulate spin probe for targeted determination of oxygen in cells and tissues. *Free Radic Biol Med* 35: 1138-1148, 2003.

443. Papandreou I, Cairns RA, Fontana L, Lim AL, and Denko NC. HIF-1 mediates adaptation to hypoxia by actively downregulating mitochondrial oxygen consumption. *Cell Metab* 3: 187-197, 2006.

444. Park S-K, Dadak AM, Haase VH, Fontana L, Giaccia AJ, and Johnson RS. Hypoxia-induced gene expression occurs solely through the action of hypoxia-inducible factor 1 α (HIF-1 α): role of cytoplasmic trapping of HIF-2 α . *Mol Cell Biol* 23: 4959-4971, 2003.

445. Parpaleix A, Goulam Houssen Y, and Charpak S. Imaging local neuronal activity by monitoring PO₂ transients in capillaries. *Nat Med* 19: 241-246, 2013.

446. Parrinello S, Samper E, Krtolica A, Goldstein J, Melov S, and Campisi J. Oxygen sensitivity severely limits the replicative lifespan of murine fibroblasts. *Nat Cell Biol* 5: 741-747, 2003.

447. Pasarica M, Sereda OR, Redman LM, Albarado DC, Hymel DT, Roan LE, Rood JC, Burk DH, and Smith SR. Reduced adipose tissue oxygenation in human obesity: evidence for rarefaction, macrophage chemotaxis, and inflammation without an angiogenic response. *Diabetes* 58: 718-725, 2009.

448. Patrick A, Seluanov M, Hwang C, Tam J, Khan T, Morgenstern A, Wiener L, Vazquez JM, Zafar H, and Wen R. Sensitivity of primary fibroblasts in culture to atmospheric oxygen does not correlate with species lifespan. *Aging* 8: 2016.

449. Pattappa G, Thorpe SD, Jegard NC, Heywood HK, de Bruijn JD, and Lee DA. Continuous and uninterrupted oxygen tension influences the colony formation and oxidative metabolism of human mesenchymal stem cells. *Tissue Eng Part C Methods* 19: 68-79, 2013.

450. Pearlstein DP, Ali MH, Mungai PT, Hynes KL, Gewertz BL, and Schumacker PT. Role of mitochondrial oxidant generation in endothelial cell responses to hypoxia. *Arteriosclerosis, thrombosis, and vascular biology* 22: 566-573, 2002.

- 3335 451. Pedersen M, Dissing TH, Mørkenborg J, Stødkilde-Jørgensen H, Hansen LH, Pedersen
3336 LB, Grenier N, and Frøkiaer J. Validation of quantitative BOLD MRI measurements in
3337 kidney: application to unilateral ureteral obstruction. *Kidney Int* 67: 2305-2312, 2005.
- 3338 452. Persson PB, Ehmke H, Kirchheim HR, Janssen B, Baumann JE, Just A, and Nafz B.
3339 Autoregulation and non-homeostatic behaviour of renal blood flow in conscious dogs. *J*
3340 *Physiol* 462: 261-273, 1993.
- 3341 453. Pettersen EO, Larsen LH, Ramsing NB, and Ebbesen P. Pericellular oxygen depletion
3342 during ordinary tissue culturing, measured with oxygen microsensors. *Cell Prolif* 38: 257-
3343 267, 2005.
- 3344 454. Pezzulo AA, Starner TD, Scheetz TE, Traver GL, Tilley AE, Harvey B-G, Crystal RG,
3345 McCray PB, and Zabner J. The air-liquid interface and use of primary cell cultures are
3346 important to recapitulate the transcriptional profile of in vivo airway epithelia. *Am J Physiol*
3347 *Lung Cell Mol Physiol* 300: L25-31, 2011.
- 3348 455. Pinder AG, and James PE. When does low oxygen become hypoxia? Implications for nitrite
3349 reduction. *Circulation research* 104: e25-e26, 2009.
- 3350 456. Pittman RN. Oxygen gradients in the microcirculation. *Acta Physiol (Oxf)* 202: 311-322,
3351 2011.
- 3352 457. Pittman RN. Oxygen transport and exchange in the microcirculation. *Microcirculation* 12:
3353 59-70, 2005.
- 3354 458. Pittman RN. *Regulation of Tissue Oxygenation*. San Rafael (CA): Morgan & Claypool Life
3355 Sciences, 2011.
- 3356 459. Pittman RN, and Duling BR. Effects of altered carbon dioxide tension on hemoglobin
3357 oxygenation in hamster cheek pouch microvessels. *Microvasc Res* 13: 211-224, 1977.
- 3358 460. Pittman RN, and Duling BR. Measurement of percent oxyhemoglobin in the
3359 microvasculature. *J Appl Physiol* 38: 321-327, 1975.
- 3360 461. Pittman RN, and Duling BR. A new method for the measurement of percent
3361 oxyhemoglobin. *J Appl Physiol* 38: 315-320, 1975.
- 3362 462. Place TL, Domann FE, and Case AJ. Limitations of oxygen delivery to cells in culture: An
3363 underappreciated problem in basic and translational research. *Free Radic Biol Med* 113:
3364 311-322, 2017.
- 3365 463. Pohlmann A, Arakelyan K, Hentschel J, Cantow K, Flemming B, Ladwig M, Waiczies S,
3366 Seeliger E, and Niendorf T. Detailing the relation between renal T2* and renal tissue pO2
3367 using an integrated approach of parametric magnetic resonance imaging and invasive
3368 physiological measurements. *Invest Radiol* 49: 547-560, 2014.
- 3369 464. Portron S, Merceron C, Gauthier O, Lesoeur J, Sourice S, Masson M, Fellah BH, Geffroy
3370 O, Lallemand E, Weiss P, Guicheux J, and Vinatier C. Effects of in vitro low oxygen tension
3371 preconditioning of adipose stromal cells on their in vivo chondrogenic potential: application
3372 in cartilage tissue repair. *PLoS One* 8: e62368, 2013.
- 3373 465. Postigo L, Heredia G, Illsley NP, Torricos T, Dolan C, Echalar L, Tellez W, Maldonado I,
3374 Brimacombe M, Balanza E, Vargas E, and Zamudio S. Where the O2 goes to: preservation
3375 of human fetal oxygen delivery and consumption at high altitude. *J Physiol* 587: 693-708,
3376 2009.
- 3377 466. Powers DE, Millman JR, Bonner-Weir S, Rappel MJ, and Colton CK. Accurate control of
3378 oxygen level in cells during culture on silicone rubber membranes with application to stem
3379 cell differentiation. *Biotechnol Prog* 26: 805-818, 2010.
- 3380 467. Powers DE, Millman JR, Huang RB, and Colton CK. Effects of oxygen on mouse
3381 embryonic stem cell growth, phenotype retention, and cellular energetics. *Biotechnol*
3382 *Bioeng* 101: 241-254, 2008.
- 3383 468. Prabhakar NR, and Semenza GL. Oxygen sensing and homeostasis. *Physiology* 30: 340-
3384 348, 2015.
- 3385 469. Prasad SM, Czepiel M, Cetinkaya C, Smigielska K, Weli SC, Lysdahl H, Gabrielsen A,
3386 Petersen K, Ehlers N, Fink T, Minger SL, and Zachar V. Continuous hypoxic culturing
3387 maintains activation of Notch and allows long-term propagation of human embryonic stem
3388 cells without spontaneous differentiation. *Cell Prolif* 42: 63-74, 2009.
- 3389 470. Prytherch Z, Job C, Marshall H, Oreffo V, Foster M, and Bérubé K. Tissue-specific stem
3390 cell differentiation in an in vitro airway model. *Macromolecular bioscience* 11: 1467-1477,
3391 2011.

3392 471. Puente BN, Kimura W, Muralidhar SA, Moon J, Amatruda JF, Phelps KL, Grinsfelder D,
3393 Rothermel BA, Chen R, Garcia JA, Santos CX, Thet S, Mori E, Kinter MT, Rindler PM,
3394 Zacchigna S, Mukherjee S, Chen DJ, Mahmoud AI, Giacca M, Rabinovitch PS,
3395 Aroumougame A, Shah AM, Szveda LI, and Sadek HA. The oxygen-rich postnatal
3396 environment induces cardiomyocyte cell-cycle arrest through DNA damage response. *Cell*
3397 157: 565-579, 2014.

3398 472. Pugh CW, and Ratcliffe PJ. Regulation of angiogenesis by hypoxia: role of the HIF system.
3399 *Nat Med* 9: 677-684, 2003.

3400 473. Purpura KA, George SH, Dang SM, Choi K, Nagy A, and Zandstra PW. Soluble Flt-1
3401 Regulates Flk-1 Activation to Control Hematopoietic and Endothelial Development in an
3402 Oxygen-Responsive Manner. *Stem Cells* 26: 2832-2842, 2008.

3403 474. Raleigh JA, Chou SC, Arteel GE, and Horsman MR. Comparisons among pimonidazole
3404 binding, oxygen electrode measurements, and radiation response in C3H mouse tumors.
3405 *Radiat Res* 151: 580-589, 1999.

3406 475. Ramírez MÁ, Pericuesta E, Yáñez-Mó M, Palasz A, and Gutiérrez-Adán A. Effect of long-
3407 term culture of mouse embryonic stem cells under low oxygen concentration as well as on
3408 glycosaminoglycan hyaluronan on cell proliferation and differentiation. *Cell Prolif* 44: 75-85,
3409 2011.

3410 476. Ratcliffe PJ. Oxygen sensing and hypoxia signalling pathways in animals: the implications
3411 of physiology for cancer. *J Physiol* 591: 2027-2042, 2013.

3412 477. Rausch ME, Weisberg S, Vardhana P, and Tortoriello DV. Obesity in C57BL/6J mice is
3413 characterized by adipose tissue hypoxia and cytotoxic T-cell infiltration. *Int J Obes (Lond)*
3414 32: 451-463, 2008.

3415 478. Readnower RD, Brainard RE, Hill BG, and Jones SP. Standardized bioenergetic profiling of
3416 adult mouse cardiomyocytes. *Physiol Genomics* 44: 1208-1213, 2012.

3417 479. Redfors B, Bragadottir G, Sellgren J, Swärd K, and Ricksten S-E. Acute renal failure is
3418 NOT an acute renal successa clinical study on the renal oxygen supply/demand
3419 relationship in acute kidney injury. *Critical care medicine* 38: 1695-1701, 2010.

3420 480. Reeve HL, Michelakis E, Nelson DP, Weir EK, and Archer SL. Alterations in a redox
3421 oxygen sensing mechanism in chronic hypoxia. *Journal of Applied Physiology* 90: 2249-
3422 2256, 2001.

3423 481. Reusch P, Wagdy H, Reusch R, Wilson E, and Ives HE. Mechanical strain increases
3424 smooth muscle and decreases nonmuscle myosin expression in rat vascular smooth
3425 muscle cells. *Circ Res* 79: 1046-1053, 1996.

3426 482. Reuther MS, Briggs KK, Schumacher BL, Masuda K, Sah RL, and Watson D. In vivo
3427 oxygen tension in human septal cartilage increases with age. *Laryngoscope* 122: 2407-
3428 2410, 2012.

3429 483. Reykdal S, Abboud C, and Liesveld J. Effect of nitric oxide production and oxygen tension
3430 on progenitor preservation in ex vivo culture. *Exp Hematol* 27: 441-450, 1999.

3431 484. Richman AI, Su EY, and Ho G. Reciprocal relationship of synovial fluid volume and oxygen
3432 tension. *Arthritis Rheum* 24: 701-705, 1981.

3433 485. Ricksten S-E, Bragadottir G, and Redfors B. Renal oxygenation in clinical acute kidney
3434 injury. *Critical Care* 17: 221, 2013.

3435 486. Riley RJ, and Johnson JW. Collecting and analyzing cord blood gases. *Clin Obstet Gynecol*
3436 36: 13-23, 1993.

3437 487. Rivera BK, Naidu SK, Subramanian K, Joseph M, Hou H, Khan N, Swartz HM, and
3438 Kuppusamy P. Real-time, in vivo determination of dynamic changes in lung and heart
3439 tissue oxygenation using EPR oximetry. *Adv Exp Med Biol* 812: 81-86, 2014.

3440 488. Rodesch F, Simon P, Donner C, and Jauniaux E. Oxygen measurements in endometrial
3441 and trophoblastic tissues during early pregnancy. *Obstet Gynecol* 80: 283-285, 1992.

3442 489. Römers LH, Bakker C, Dollée N, Hoeks SE, Lima A, Raat NJ, Johannes T, Stolker RJ, and
3443 Mik EG. Cutaneous mitochondrial PO₂, but not tissue oxygen saturation, is an early
3444 indicator of the physiologic limit of hemodilution in the Pig. *The Journal of the American*
3445 *Society of Anesthesiologists* 125: 124-132, 2016.

3446 490. Rosen P, Boulton M, Moriarty P, Khaliq A, and McLeod D. Effect of varying oxygen
3447 concentrations on the proliferation of retinal microvascular cells in vitro. *Exp Eye Res* 53:
3448 597-601, 1991.

3449 491. Rosenberger C, Mandriota S, Jürgensen JS, Wiesener MS, Hörstrup JH, Frei U, Ratcliffe
3450 PJ, Maxwell PH, Bachmann S, and Eckardt K-U. Expression of hypoxia-inducible factor-1 α
3451 and-2 α in hypoxic and ischemic rat kidneys. *Journal of the American Society of Nephrology*
3452 13: 1721-1732, 2002.

3453 492. Rosenberger P, Schwab JM, Mirakaj V, Masekowsky E, Mager A, Morote-Garcia JC, Unertl
3454 K, and Eltzschig HK. Hypoxia-inducible factor-dependent induction of netrin-1 dampens
3455 inflammation caused by hypoxia. *Nat Immunol* 10: 195-202, 2009.

3456 493. Ross C, Alston M, Bickenbach JR, and Aykin-Burns N. Oxygen tension changes the rate of
3457 migration of human skin keratinocytes in an age-related manner. *Experimental dermatology*
3458 20: 58-63, 2011.

3459 494. Roy S, Khanna S, Bickerstaff AA, Subramanian SV, Atalay M, Bierl M, Pendyala S, Levy D,
3460 Sharma N, Venojarvi M, Strauch A, Orosz CG, and Sen CK. Oxygen sensing by primary
3461 cardiac fibroblasts: a key role of p21(Waf1/Cip1/Sdi1). *Circ Res* 92: 264-271, 2003.

3462 495. Roy S, Tripathy M, Mathur N, Jain A, and Mukhopadhyay A. Hypoxia improves expansion
3463 potential of human cord blood-derived hematopoietic stem cells and marrow repopulation
3464 efficiency. *Eur J Haematol* 88: 396-405, 2012.

3465 496. Rumsey WL, Pawlowski M, Lejavardi N, and Wilson DF. Oxygen pressure distribution in
3466 the heart in vivo and evaluation of the ischemic" border zone". *American Journal of*
3467 *Physiology-Heart and Circulatory Physiology* 266: H1676-H1680, 1994.

3468 497. Rumsey WL, Vanderkooi JM, and Wilson DF. Imaging of phosphorescence: a novel
3469 method for measuring oxygen distribution in perfused tissue. *Science* 241: 1649-1652,
3470 1988.

3471 498. Saeedi BJ, Kao DJ, Kitzenberg DA, Dobrinskikh E, Schwisow KD, Masterson JC, Kendrick
3472 AA, Kelly CJ, Bayless AJ, Kominsky DJ, Campbell EL, Kuhn KA, Furuta GT, Colgan SP,
3473 and Glover LE. HIF-dependent regulation of claudin-1 is central to intestinal epithelial tight
3474 junction integrity. *Mol Biol Cell* 26: 2252-2262, 2015.

3475 499. Sahaf B, Atkuri K, Heydari K, Malipatlolla M, Rappaport J, Regulier E, Herzenberg LA, and
3476 Herzenberg LA. Culturing of human peripheral blood cells reveals unsuspected lymphocyte
3477 responses relevant to HIV disease. *Proc Natl Acad Sci U S A* 105: 5111-5116, 2008.

3478 500. Sakadžić S, Mandeville ET, Gagnon L, Musacchia JJ, Yaseen MA, Yucel MA, Lefebvre J,
3479 Lesage F, Dale AM, Eikermann-Haerter K, Ayata C, Srinivasan VJ, Lo EH, Devor A, and
3480 Boas DA. Large arteriolar component of oxygen delivery implies a safe margin of oxygen
3481 supply to cerebral tissue. *Nat Commun* 5: 5734, 2014.

3482 501. Sakadžić S, Roussakis E, Yaseen MA, Mandeville ET, Srinivasan VJ, Arai K, Ruvinskaya
3483 S, Devor A, Lo EH, Vinogradov SA, and Boas DA. Two-photon high-resolution
3484 measurement of partial pressure of oxygen in cerebral vasculature and tissue. *Nat Methods*
3485 7: 755-759, 2010.

3486 502. Sakadžić S, Roussakis E, Yaseen MA, Mandeville ET, Srinivasan VJ, Arai K, Ruvinskaya
3487 S, Wu W, Devor A, Lo EH, Vinogradov SA, and Boas DA. Cerebral blood oxygenation
3488 measurement based on oxygen-dependent quenching of phosphorescence. *J Vis Exp*
3489 2011.

3490 503. Salama R, Masson N, Simpson P, Sciesielski LK, Sun M, Tian Y-M, Ratcliffe PJ, and Mole
3491 DR. Heterogeneous Effects of Direct Hypoxia Pathway Activation in Kidney Cancer. *PLoS*
3492 *One* 10: e0134645, 2015.

3493 504. Samanta D, and Semenza GL. Maintenance of redox homeostasis by hypoxia-inducible
3494 factors. *Redox Biol* 13: 331-335, 2017.

3495 505. Santilli SM, Fiegel VD, and Knighton DR. Alloxan diabetes alters the rabbit transarterial wall
3496 oxygen gradient. *J Vasc Surg* 18: 227-233, 1993.

3497 506. Santilli SM, Fiegel VD, and Knighton DR. Changes in the aortic wall oxygen tensions of
3498 hypertensive rabbits. Hypertension and aortic wall oxygen. *Hypertension* 19: 33-39, 1992.

3499 507. Santilli SM, Stevens RB, Anderson JG, Payne WD, and Caldwell MD. Transarterial wall
3500 oxygen gradients at the dog carotid bifurcation. *Am J Physiol* 268: H155-161, 1995.

3501 508. Santilli SM, Tretinyak AS, and Lee ES. Transarterial wall oxygen gradients at the
3502 deployment site of an intra-arterial stent in the rabbit. *Am J Physiol Heart Circ Physiol* 279:
3503 H1518-1525, 2000.

509. Santilli SM, Wernsing SE, and Lee ES. Transarterial wall oxygen gradients at a prosthetic vascular graft to artery anastomosis in the rabbit. *Journal of vascular surgery* 31: 1229-1239, 2000.

510. Santolucito JA, and Whitcomb E. Effect of paraoxon on erythrocyte metabolism as measured by oxygen uptake in vitro. *Br J Pharmacol* 42: 298-302, 1971.

511. Sato Y, Endo H, Okuyama H, Takeda T, Iwahashi H, Imagawa A, Yamagata K, Shimomura I, and Inoue M. Cellular hypoxia of pancreatic beta-cells due to high levels of oxygen consumption for insulin secretion in vitro. *J Biol Chem* 286: 12524-12532, 2011.

512. Schiller ZA, Schiele NR, Sims JK, Lee K, and Kuo CK. Adipogenesis of adipose-derived stem cells may be regulated via the cytoskeleton at physiological oxygen levels in vitro. *Stem Cell Res Ther* 4: 79, 2013.

513. Schipani E, Ryan HE, Didrickson S, Kobayashi T, Knight M, and Johnson RS. Hypoxia in cartilage: HIF-1alpha is essential for chondrocyte growth arrest and survival. *Genes & development* 15: 2865-2876, 2001.

514. Schödel J, Mole DR, and Ratcliffe PJ. Pan-genomic binding of hypoxia-inducible transcription factors. *Biol Chem* 394: 507-517, 2013.

515. Schödel J, Oikonomopoulos S, Ragoussis J, Pugh CW, Ratcliffe PJ, and Mole DR. High-resolution genome-wide mapping of HIF-binding sites by ChIP-seq. *Blood* 117: e207-217, 2011.

516. Schofield CJ, and Ratcliffe PJ. Oxygen sensing by HIF hydroxylases. *Nature reviews Molecular cell biology* 5: 343-354, 2004.

517. Schofield CJ, and Ratcliffe PJ. Signalling hypoxia by HIF hydroxylases. *Biochemical and biophysical research communications* 338: 617-626, 2005.

518. Schrobback K, Klein TJ, Crawford R, Upton Z, Malda J, and Leavesley DI. Effects of oxygen and culture system on in vitro propagation and redifferentiation of osteoarthritic human articular chondrocytes. *Cell Tissue Res* 347: 649-663, 2012.

519. Schurek HJ, Jost U, Baumgärtl H, Bertram H, and Heckmann U. Evidence for a preglomerular oxygen diffusion shunt in rat renal cortex. *Am J Physiol* 259: F910-915, 1990.

520. Schwanhäusser B, Busse D, Li N, Dittmar G, Schuchhardt J, Wolf J, Chen W, and Selbach M. Global quantification of mammalian gene expression control. *Nature* 473: 337-342, 2011.

521. Sekine K, Kagawa Y, Maeyama E, Ota H, Haraguchi Y, Matsuura K, and Shimizu T. Oxygen consumption of human heart cells in monolayer culture. *Biochem Biophys Res Commun* 452: 834-839, 2014.

522. Semenza GL. Oxygen sensing, hypoxia-inducible factors, and disease pathophysiology. *Annu Rev Pathol* 9: 47-71, 2014.

523. Semenza GL. Regulation of hypoxia-induced angiogenesis: a chaperone escorts VEGF to the dance. *J Clin Invest* 108: 39-40, 2001.

524. Setschenow J. Über die konstitution der salzlösungen auf grund ihres verhaltens zu kohlendensäure. *Zeitschrift für Physikalische Chemie* 4: 117-125, 1889.

525. Seylaz J, and Pinard E. Continuous measurement of gas partial pressures in intracerebral tissue. *Journal of applied physiology: respiratory, environmental and exercise physiology* 44: 528-533, 1978.

526. Sezai S, Sakurabayashi S, Yamamoto Y, Morita T, Hirano M, and Oka H. Hepatic arterial and portal venous oxygen content and extraction in liver cirrhosis. *Liver* 13: 31-35, 1993.

527. Sharan M, Vovenko EP, Vadapalli A, Popel AS, and Pittman RN. Experimental and theoretical studies of oxygen gradients in rat pial microvessels. *J Cereb Blood Flow Metab* 28: 1597-1604, 2008.

528. Sheehy EJ, Buckley CT, and Kelly DJ. Oxygen tension regulates the osteogenic, chondrogenic and endochondral phenotype of bone marrow derived mesenchymal stem cells. *Biochem Biophys Res Commun* 417: 305-310, 2012.

529. Sheridan WG, Lowndes RH, and Young HL. Intraoperative tissue oximetry in the human gastrointestinal tract. *The American Journal of Surgery* 159: 314-319, 1990.

530. Sheridan WG, Lowndes RH, and Young HL. Tissue oxygen tension as a predictor of colonic anastomotic healing. *Dis Colon Rectum* 30: 867-871, 1987.

3560 531. Shibata M, Ichioka S, Ando J, and Kamiya A. Microvascular and interstitial PO₂
3561 measurements in rat skeletal muscle by phosphorescence quenching. *J Appl Physiol*
3562 (1985) 91: 321-327, 2001.

3563 532. Shibata M, and Kamiya A. Microvascular and interstitial pO₂ measurements in the skeletal
3564 muscle by phosphorescence quenching technique. *Proceedings of the First Joint*
3565 *BMES/EMBS Conference* 2: 806-vol, 1999.

3566 533. Shimada H, Hashimoto Y, Nakada A, Shigeno K, and Nakamura T. Accelerated generation
3567 of human induced pluripotent stem cells with retroviral transduction and chemical inhibitors
3568 under physiological hypoxia. *Biochem Biophys Res Commun* 417: 659-664, 2012.

3569 534. Shonat RD, and Johnson PC. Oxygen tension gradients and heterogeneity in venous
3570 microcirculation: a phosphorescence quenching study. *Am J Physiol* 272: H2233-2240,
3571 1997.

3572 535. Shonat RD, Wilson DF, Riva CE, and Pawlowski M. Oxygen distribution in the retinal and
3573 choroidal vessels of the cat as measured by a new phosphorescence imaging method.
3574 *Appl Opt* 31: 3711-3718, 1992.

3575 536. Shweiki D, Itin A, Soffer D, and Keshet E. Vascular endothelial growth factor induced by
3576 hypoxia may mediate hypoxia-initiated angiogenesis. *Nature* 359: 843-845, 1992.

3577 537. Silvola JM, Saraste A, Forsback S, Laine VJO, Saukko P, Heinonen SE, Ylä-Herttuala S,
3578 Roivainen A, and Knuuti J. Detection of hypoxia by [18F] EF5 in atherosclerotic plaques in
3579 mice. *Arteriosclerosis, thrombosis, and vascular biology* 31: 1011-1015, 2011.

3580 538. Simmen HP, and Blaser J. Analysis of pH and pO₂ in abscesses, peritoneal fluid, and
3581 drainage fluid in the presence or absence of bacterial infection during and after abdominal
3582 surgery. *Am J Surg* 166: 24-27, 1993.

3583 539. Simon MC, and Keith B. The role of oxygen availability in embryonic development and stem
3584 cell function. *Nature reviews Molecular cell biology* 9: 285, 2008.

3585 540. Sinaasappel M, Itersen Mv, and Ince C. Microvascular oxygen pressure in the pig intestine
3586 during haemorrhagic shock and resuscitation. *The Journal of physiology* 514: 245-253,
3587 1999.

3588 541. Sinagowitz E, Golsong M, Wilms H, and Halbfass HJ. In vivo determination of local tissue
3589 pO₂ in renal cortex in kidney transplantation. In: *Chirurgisches Forum fur experimentelle*
3590 *und klinische Forschung* 1977, p. 299-302.

3591 542. Siow RC, Sato H, and Mann GE. Heme oxygenase-carbon monoxide signalling pathway in
3592 atherosclerosis: anti-atherogenic actions of bilirubin and carbon monoxide? *Cardiovasc*
3593 *Res* 41: 385-394, 1999.

3594 543. Skolasinska K, Harbig K, Lübbers DW, and Wodick R. PO₂ and microflow histograms of
3595 the beating heart in response to changes in arterial pO₂. *Basic Res Cardiol* 73: 307-319,
3596 1978.

3597 544. Smith RH, Guilbeau EJ, and Reneau DD. The oxygen tension field within a discrete volume
3598 of cerebral cortex. *Microvasc Res* 13: 233-240, 1977.

3599 545. Sobhanifar S, Aquino-Parsons C, Stanbridge EJ, and Olive P. Reduced expression of
3600 hypoxia-inducible factor-1α in perinecrotic regions of solid tumors. *Cancer Res* 65:
3601 7259-7266, 2005.

3602 546. Soini HO, Takala J, Nordin AJ, Mäkisalo HJ, and Höckerstedt KA. Peripheral and liver
3603 tissue oxygen tensions in hemorrhagic shock. *Crit Care Med* 20: 1330-1334, 1992.

3604 547. Solodushko V, Parker JC, and Fouty B. Pulmonary microvascular endothelial cells form a
3605 tighter monolayer when grown in chronic hypoxia. *American journal of respiratory cell and*
3606 *molecular biology* 38: 491, 2008.

3607 548. Soothill PW, Nicolaidis KH, Rodeck CH, and Campbell S. Effect of gestational age on fetal
3608 and intervillous blood gas and acid-base values in human pregnancy. *Fetal Ther* 1: 168-
3609 175, 1986.

3610 549. Sowter HM, Raval RR, Moore JW, Ratcliffe PJ, and Harris AL. Predominant role of
3611 hypoxia-inducible transcription factor (Hif)-1α versus Hif-2α in regulation of the
3612 transcriptional response to hypoxia. *Cancer Res* 63: 6130-6134, 2003.

3613 550. Spence VA, and Beck JS. Transcutaneous measurement of PO₂ and PCO₂ in the dermis
3614 at the site of the tuberculin reaction in healthy human subjects. *J Pathol* 155: 289-293,
3615 1988.

3616 551. Spence VA, and Walker WF. Measurement of oxygen tension in human skin. *Medical and*
3617 *biological engineering* 14: 159-165, 1976.

3618 552. Spencer JA, Ferraro F, Roussakis E, Klein A, Wu J, Runnels JM, Zaher W, Mortensen LJ,
3619 Alt C, Turcotte R, Yusuf R, Côté D, Vinogradov SA, Scadden DT, and Lin CP. Direct
3620 measurement of local oxygen concentration in the bone marrow of live animals. *Nature*
3621 2014.

3622 553. Stacpoole SR, Webber DJ, Bilican B, Compston A, Chandran S, and Franklin RJ. Neural
3623 precursor cells cultured at physiologically relevant oxygen tensions have a survival
3624 advantage following transplantation. *Stem cells translational medicine* 2: 464-472, 2013.

3625 554. Stacpoole SRL, Bilican B, Webber DJ, Luzhynskaya A, He XL, Compston A, Karadottir R,
3626 Franklin RJM, and Chandran S. Derivation of neural precursor cells from human ES cells at
3627 3% O₂ is efficient, enhances survival and presents no barrier to regional specification and
3628 functional differentiation. *Cell Death Differ* 18: 1016-1023, 2011.

3629 555. Stacpoole SRL, Webber DJ, Bilican B, Compston A, Chandran S, and Franklin RJM.
3630 Neural precursor cells cultured at physiologically relevant oxygen tensions have a survival
3631 advantage following transplantation. *Stem Cells Transl Med* 2: 464-472, 2013.

3632 556. Steinberg GR, and Kemp BE. AMPK in health and disease. *Physiological reviews* 89: 1025-
3633 1078, 2009.

3634 557. Steptoe PC, Edwards RG, and Purdy JM. Human blastocysts grown in culture. *Nature* 229:
3635 132-133, 1971.

3636 558. Stevens ED. Use of plastic materials in oxygen-measuring systems. *J Appl Physiol* (1985)
3637 72: 801-804, 1992.

3638 559. Stevens KM. Oxygen requirements for liver cells in vitro. *Nature* 206: 199-199, 1965.

3639 560. Stücker M, Struk PA, Hoffmann K, Schulze L, Röchling A, and Lübbers DW. The
3640 transepidermal oxygen flux from the environment is in balance with the capillary oxygen
3641 supply. *J Invest Dermatol* 114: 533-540, 2000.

3642 561. Studer L, Csete M, Lee SH, Kabbani N, Walikonis J, Wold B, and McKay R. Enhanced
3643 proliferation, survival, and dopaminergic differentiation of CNS precursors in lowered
3644 oxygen. *J Neurosci* 20: 7377-7383, 2000.

3645 562. Subczynski WK, Hopwood LE, and Hyde JS. Is the mammalian cell plasma membrane a
3646 barrier to oxygen transport? *The Journal of general physiology* 100: 69-87, 1992.

3647 563. Sun X, Voloboueva LA, Stary CM, and Giffard RG. Physiologically normal 5% O₂ supports
3648 neuronal differentiation and resistance to inflammatory injury in neural stem cell cultures. *J*
3649 *Neurosci Res* 93: 1703-1712, 2015.

3650 564. Swirski FK, Nahrendorf M, Etzrodt M, Wildgruber M, Cortez-Retamozo V, Panizzi P,
3651 Figueiredo J-L, Kohler RH, Chudnovskiy A, Waterman P, Aikawa E, Mempel TR, Libby P,
3652 Weissleder R, and Pittet MJ. Identification of splenic reservoir monocytes and their
3653 deployment to inflammatory sites. *Science* 325: 612-616, 2009.

3654 565. Sylvester JT, Shimoda LA, Aaronson PI, and Ward JPT. Hypoxic pulmonary
3655 vasoconstriction. *Physiol Rev* 92: 367-520, 2012.

3656 566. Synnestvedt K, Furuta GT, Comerford KM, Louis N, Karhausen J, Eltzschig HK, Hansen
3657 KR, Thompson LF, and Colgan SP. Ecto-5'-nucleotidase (CD73) regulation by hypoxia-
3658 inducible factor-1 mediates permeability changes in intestinal epithelia. *J Clin Invest* 110:
3659 993-1002, 2002.

3660 567. Takahashi E, Endoh H, and Doi K. Intracellular gradients of O₂ supply to mitochondria in
3661 actively respiring single cardiomyocyte of rats. *Am J Physiol* 276: H718-724, 1999.

3662 568. Takahashi E, Endoh H, and Doi K. Visualization of myoglobin-facilitated mitochondrial O₂
3663 delivery in a single isolated cardiomyocyte. *Biophys J* 78: 3252-3259, 2000.

3664 569. Takahashi R, Kobayashi C, Kondo Y, Nakatani Y, Kudo I, Kunitomo M, Imura N, and Hara
3665 S. Subcellular localization and regulation of hypoxia-inducible factor-2alpha in vascular
3666 endothelial cells. *Biochem Biophys Res Commun* 317: 84-91, 2004.

3667 570. Thermann M, Jostarndt L, Eberhard F, Richter H, and Sass W. [Oxygen supply of the
3668 human small intestine in mechanical ileus]. *Langenbecks Arch Chir* 363: 179-184, 1985.

3669 571. Thomas DD, Liu X, Kantrow SP, and Lancaster JR. The biological lifetime of nitric oxide:
3670 implications for the perivascular dynamics of NO and O₂. *Proceedings of the National*
3671 *Academy of Sciences of the United States of America* 98: 355-360, 2001.

- 3672 572. Thomas SR. The biomedical applications of fluorine-19 NMR. *Magnetic resonance imaging*
3673 2: 1536-1552, 1988.
- 3674 573. Thomas SR, Pratt RG, Millard RW, Samaratunga RC, Shiferaw Y, McGoron AJ, and Tan
3675 KK. In vivo PO₂ imaging in the porcine model with perfluorocarbon F-19 NMR at low field.
3676 *Magn Reson Imaging* 14: 103-114, 1996.
- 3677 574. Thompson AA, Binham J, Plant T, Whyte MK, and Walmsley SR. Hypoxia, the HIF pathway
3678 and neutrophilic inflammatory responses. *Biol Chem* 394: 471-477, 2013.
- 3679 575. Thompson CB. Into Thin Air: How We Sense and Respond to Hypoxia. *Cell* 167: 9-11,
3680 2016.
- 3681 576. Thorp JA, Trobough T, Evans R, Hedrick J, and Yeast JD. The effect of maternal oxygen
3682 administration during the second stage of labor on umbilical cord blood gas values: a
3683 randomized controlled prospective trial. *Am J Obstet Gynecol* 172: 465-474, 1995.
- 3684 577. Thulborn KR, Waterton JC, Matthews PM, and Radda GK. Oxygenation dependence of the
3685 transverse relaxation time of water protons in whole blood at high field. *Biochimica et*
3686 *Biophysica Acta (BBA)-General Subjects* 714: 265-270, 1982.
- 3687 578. Tiede LM, Cook EA, Morsey B, and Fox HS. Oxygen matters: tissue culture oxygen levels
3688 affect mitochondrial function and structure as well as responses to HIV viroproteins. *Cell*
3689 *Death Dis* 2: e246, 2011.
- 3690 579. Tilles AW, Berthiaume F, Yarmush ML, Tompkins RG, and Toner M. Bioengineering of liver
3691 assist devices. *J Hepatobiliary Pancreat Surg* 9: 686-696, 2002.
- 3692 580. Timpson CJ, Carter CC, and Olmsted III J. Mechanism of quenching of electronically
3693 excited ruthenium complexes by oxygen. *The Journal of Physical Chemistry* 93: 4116-
3694 4120, 1989.
- 3695 581. Tokuda Y, Crane S, Yamaguchi Y, Zhou L, and Falanga V. The levels and kinetics of
3696 oxygen tension detectable at the surface of human dermal fibroblast cultures. *J Cell Physiol*
3697 182: 414-420, 2000.
- 3698 582. Tordjman J editor. *Physiology and Physiopathology of Adipose Tissue*. Springer, 2013, p.
3699 67-75.
- 3700 583. Torres Filho IP, and Intaglietta M. Microvessel PO₂ measurements by phosphorescence
3701 decay method. *Am J Physiol* 265: H1434-1438, 1993.
- 3702 584. Torres Filho IP, Kerger H, and Intaglietta M. pO₂ measurements in arteriolar networks.
3703 *Microvasc Res* 51: 202-212, 1996.
- 3704 585. Torres Filho IP, Leunig M, Yuan F, Intaglietta M, and Jain RK. Noninvasive measurement
3705 of microvascular and interstitial oxygen profiles in a human tumor in SCID mice.
3706 *Proceedings of the National Academy of Sciences* 91: 2081-2085, 1994.
- 3707 586. Trayhurn P. Hypoxia and adipose tissue function and dysfunction in obesity. *Physiological*
3708 *reviews* 93: 1-21, 2013.
- 3709 587. Trepiana J, Meijide S, Navarro R, Hernández ML, Ruiz-Sanz JI, and Ruiz-Larrea MB.
3710 Influence of oxygen partial pressure on the characteristics of human hepatocarcinoma
3711 cells. *Redox Biol* 12: 103-113, 2017.
- 3712 588. Treuhaft PS, and McCarty DJ. Synovial fluid pH, lactate, oxygen and carbon dioxide partial
3713 pressure in various joint diseases. *Arthritis Rheum* 14: 475-484, 1971.
- 3714 589. Treuhaft PS, and MCCarty DJ. Synovial fluid pH, lactate, oxygen and carbon dioxide partial
3715 pressure in various joint diseases. *Arthritis Rheum* 14: 475-484, 1971.
- 3716 590. Tripathi A, Bydder GM, Hughes JM, Pennock JM, Goatcher A, Orr JS, Steiner RE, and
3717 Greenspan RH. Effect of oxygen tension on NMR spin-lattice relaxation rate of blood in
3718 vivo. *Invest Radiol* 19: 174-178, 1984.
- 3719 591. Tsai AG, Friesenecker B, Mazzoni MC, Kerger H, Buerk DG, Johnson PC, and Intaglietta
3720 M. Microvascular and tissue oxygen gradients in the rat mesentery. *Proceedings of the*
3721 *National Academy of Sciences* 95: 6590-6595, 1998.
- 3722 592. Tsai AG, Friesenecker B, Mazzoni MC, Kerger H, Buerk DG, Johnson PC, and Intaglietta
3723 M. Microvascular and tissue oxygen gradients in the rat mesentery. *Proc Natl Acad Sci U S*
3724 *A* 95: 6590-6595, 1998.
- 3725 593. Tsai AG, Johnson PC, and Intaglietta M. Is the distribution of tissue pO₂ homogeneous?
3726 *Antioxid Redox Signal* 9: 979-984, 2007.
- 3727 594. Tsai AG, Johnson PC, and Intaglietta M. Oxygen gradients in the microcirculation.
3728 *Physiological reviews* 83: 933-963, 2003.

3729 595. Tuncay OC, Ho D, and Barker MK. Oxygen tension regulates osteoblast function. *American*
3730 *Journal of Orthodontics and Dentofacial Orthopedics* 105: 457-463, 1994.

3731 596. Turner J, Quek L-E, Titmarsh D, Krömer JO, Kao L-P, Nielsen L, Wolvetang E, and
3732 Cooper-White J. Metabolic profiling and flux analysis of MEL-2 human embryonic stem
3733 cells during exponential growth at physiological and atmospheric oxygen concentrations.
3734 *PLoS One* 9: e112757, 2014.

3735 597. Tuuli MG, Longtine MS, and Nelson DM. Review: Oxygen and trophoblast biology--a
3736 source of controversy. *Placenta* 32 Suppl 2: S109-118, 2011.

3737 598. Tygstrup N, Winkler K, Mellemgaard K, and Andreassen M. Determination of the hepatic
3738 arterial blood flow and oxygen supply in man by clamping the hepatic artery during surgery.
3739 *Journal of Clinical Investigation* 41: 447, 1962.

3740 599. Uchida T, Rossignol F, Matthay MA, Mounier R, Couette S, Clottes E, and Clerici C.
3741 Prolonged hypoxia differentially regulates hypoxia-inducible factor (HIF)-1alpha and HIF-
3742 2alpha expression in lung epithelial cells: implication of natural antisense HIF-1alpha. *J Biol*
3743 *Chem* 279: 14871-14878, 2004.

3744 600. Ugolini GS, Pavesi A, Rasponi M, Fiore GB, Kamm R, and Soncini M. Human cardiac
3745 fibroblasts adaptive responses to controlled combined mechanical strain and oxygen
3746 changes in vitro. *eLife* 6: e22847, 2017.

3747 601. Utting JC, Robins SP, Brandao-Burch A, Orriss IR, Behar J, and Arnett TR. Hypoxia inhibits
3748 the growth, differentiation and bone-forming capacity of rat osteoblasts. *Exp Cell Res* 312:
3749 1693-1702, 2006.

3750 602. V=avere AL, and Lewis JS. Cu--ATSM: A radiopharmaceutical for the PET imaging of
3751 hypoxia. *Dalton Transactions* 4893-4902, 2007.

3752 603. Vadapalli A, Pittman RN, and Popel AS. Estimating oxygen transport resistance of the
3753 microvascular wall. *Am J Physiol Heart Circ Physiol* 279: H657-671, 2000.

3754 604. Vajpayee N, Graham SS, and Bem S. Basic examination of blood and bone marrow.
3755 *Henrys clinical diagnosis and management by laboratory methods* 22: 509-535, 2011.

3756 605. Valenzuela P, and Guizarro R. The effects of time on pH and gas values in the blood
3757 contained in the umbilical cord. *Acta Obstet Gynecol Scand* 85: 1307-1309, 2006.

3758 606. Valorani MG, Montelatici E, Germani A, Biddle A, D'Alessandro D, Strollo R, Patrizi MP,
3759 Lazzari L, Nye E, Otto WR, Pozzilli P, and Alison MR. Pre-culturing human adipose tissue
3760 mesenchymal stem cells under hypoxia increases their adipogenic and osteogenic
3761 differentiation potentials. *Cell Prolif* 45: 225-238, 2012.

3762 607. van Uden P, Kenneth NS, and Rocha S. Regulation of hypoxia-inducible factor-1alpha by
3763 NF-kappaB. *Biochem J* 412: 477-484, 2008.

3764 608. van Wagensveld BA, van Gulik TM, Gabeler EE, van der Kleij AJ, Obertop H, and Gouma
3765 DJ. Intrahepatic tissue pO₂ during continuous or intermittent vascular inflow occlusion in a
3766 pig liver resection model. *Eur Surg Res* 30: 13-25, 1998.

3767 609. Vanden Hoek TL, Becker LB, Shao Z, Li C, and Schumacker PT. Reactive oxygen species
3768 released from mitochondria during brief hypoxia induce preconditioning in cardiomyocytes.
3769 *J Biol Chem* 273: 18092-18098, 1998.

3770 610. Vanderkooi JM, Maniara G, Green TJ, and Wilson DF. An optical method for measurement
3771 of dioxygen concentration based upon quenching of phosphorescence. *J Biol Chem* 262:
3772 5476-5482, 1987.

3773 611. VanderMeer TJ, Wang H, and Fink MP. Endotoxemia causes ileal mucosal acidosis in the
3774 absence of mucosal hypoxia in a normodynamic porcine model of septic shock. *Critical*
3775 *care medicine* 23: 1217-1226, 1995.

3776 612. Vassilaki N, Kalliampakou KI, Kotta-Loizou I, Befani C, Liakos P, Simos G, Mentis AF,
3777 Kalliaropoulos A, Doumba PP, Smirlis D, Foka P, Bauhofer O, Poenisch M, Windisch MP,
3778 Lee ME, Koskinas J, Bartenschlager R, and Mavromara P. Low oxygen tension enhances
3779 hepatitis C virus replication. *J Virol* 87: 2935-2948, 2013.

3780 613. Vaupel P, Braunbeck W, and Thews G. Respiratory gas exchange and pO₂-distribution in
3781 splenic tissue. *Adv Exp Med Biol* 37A: 401-406, 1973.

3782 614. Vaupel P, Frinak S, Müller-Klieser W, and Manz R. The end of a postulate: There are no
3783 hostile metabolic conditions within the normal spleen. *Bibl Anat* 20: 403-406, 1981.

3784 615. Victor VM, Nuñez C, D'Ocón P, Taylor CT, Esplugues JV, and Moncada S. Regulation of
3785 oxygen distribution in tissues by endothelial nitric oxide. *Circ Res* 104: 1178-1183, 2009.

- 3786 616. Villarruel SM, Boehm CA, Pennington M, Bryan JA, Powell KA, and Muschler GF. The
3787 effect of oxygen tension on the in vitro assay of human osteoblastic connective tissue
3788 progenitor cells. *J Orthop Res* 26: 1390-1397, 2008.
- 3789 617. Villeneuve L, Tiede LM, Morsey B, and Fox HS. Quantitative proteomics reveals oxygen-
3790 dependent changes in neuronal mitochondria affecting function and sensitivity to rotenone.
3791 *J Proteome Res* 12: 4599-4606, 2013.
- 3792 618. Vink RG, Roumans NJ, Čajlaković M, Cleutjens JPM, Boekschoten MV, Fazelzadeh P,
3793 Vogel MAA, Blaak EE, Mariman EC, van Baak MA, and Goossens GH. Diet-induced weight
3794 loss decreases adipose tissue oxygen tension with parallel changes in adipose tissue
3795 phenotype and insulin sensitivity in overweight humans. *Int J Obes (Lond)* 2017.
- 3796 619. Viticchiè G, Agostini M, Lena AM, Mancini M, Zhou H, Zolla L, Dinsdale D, Saintigny G,
3797 Melino G, and Candi E. p63 supports aerobic respiration through hexokinase II. *Proc Natl*
3798 *Acad Sci U S A* 112: 11577-11582, 2015.
- 3799 620. Vorp DA, Lee PC, Wang DH, Makaroun MS, Nemoto EM, Ogawa S, and Webster MW.
3800 Association of intraluminal thrombus in abdominal aortic aneurysm with local hypoxia and
3801 wall weakening. *J Vasc Surg* 34: 291-299, 2001.
- 3802 621. Vorp DA, Wang DH, Webster MW, and Federspiel WJ. Effect of intraluminal thrombus
3803 thickness and bulge diameter on the oxygen diffusion in abdominal aortic aneurysm.
3804 *Journal of biomechanical engineering* 120: 579-583, 1998.
- 3805 622. Vovenko E. Distribution of oxygen tension on the surface of arterioles, capillaries and
3806 venules of brain cortex and in tissue in normoxia: an experimental study on rats. *Pflugers*
3807 *Arch* 437: 617-623, 1999.
- 3808 623. Vovenko EP. Transmural oxygen tension gradients in rat cerebral cortex arterioles.
3809 *Neurosci Behav Physiol* 39: 363-370, 2009.
- 3810 624. Vretzakis G, Ferdi E, Papaziogas B, Dragoumanis C, Pneumatikos J, Tsangaris I,
3811 Tsakiridis K, and Konstantinou F. Coronary sinus venoarterial CO2 difference in different
3812 hemodynamic states. *Acta Anaesthesiol Belg* 55: 221-227, 2004.
- 3813 625. Wagenführ L, Meyer AK, Braunschweig L, Marrone L, and Storch A. Brain oxygen tension
3814 controls the expansion of outer subventricular zone-like basal progenitors in the developing
3815 mouse brain. *Development* 142: 2904-2915, 2015.
- 3816 626. Walker A, Maddern L, Day E, Renou P, Talbot J, and Wood C. Fetal scalp tissue oxygen
3817 tension measurements in relation to maternal dermal oxygen tension and fetal heart rate. *J*
3818 *Obstet Gynaecol Br Commonw* 78: 1-12, 1971.
- 3819 627. Walmsley SR, Cowburn AS, Clatworthy MR, Morrell NW, Roper EC, Singleton V, Maxwell
3820 P, Whyte MK, and Chilvers ER. Neutrophils from patients with heterozygous germline
3821 mutations in the von Hippel Lindau protein (pVHL) display delayed apoptosis and enhanced
3822 bacterial phagocytosis. *Blood* 108: 3176-3178, 2006.
- 3823 628. Walmsley SR, Print C, Farahi N, Peyssonnaud C, Johnson RS, Cramer T, Sobolewski A,
3824 Condliffe AM, Cowburn AS, Johnson N, and Chilvers ER. Hypoxia-induced neutrophil
3825 survival is mediated by HIF-1 α -dependent NF-kappaB activity. *J Exp Med* 201: 105-
3826 115, 2005.
- 3827 629. Wang F, Thirumangalathu S, and Loeken MR. Establishment of new mouse embryonic
3828 stem cell lines is improved by physiological glucose and oxygen. *Cloning Stem Cells* 8:
3829 108-116, 2006.
- 3830 630. Wang GL, Jiang BH, Rue EA, and Semenza GL. Hypoxia-inducible factor 1 is a basic-helix-
3831 loop-helix-PAS heterodimer regulated by cellular O2 tension. *Proc Natl Acad Sci U S A* 92:
3832 5510-5514, 1995.
- 3833 631. Wang H, Flach H, Onizawa M, Wei L, McManus MT, and Weiss A. Negative regulation of
3834 Hif1 α expression and TH17 differentiation by the hypoxia-regulated microRNA miR-210.
3835 *Nat Immunol* 15: 393-401, 2014.
- 3836 632. Wang W, Winlove CP, and Michel CC. Oxygen partial pressure in outer layers of skin of
3837 human finger nail folds. *J Physiol* 549: 855-863, 2003.
- 3838 633. Ward J. Oxygen sensors in context. *Biochimica et Biophysica Acta (BBA)-Bioenergetics*
3839 1777: 1-14, 2008.
- 3840 634. Warnecke C, Zaborowska Z, Kurreck J, Erdmann VA, Frei U, Wiesener M, and Eckardt K-
3841 U. Differentiating the functional role of hypoxia-inducible factor (HIF)-1 α and HIF-

2alpha (EPAS-1) by the use of RNA interference: erythropoietin is a HIF-2alpha target gene in Hep3B and Kelly cells. *FASEB J* 18: 1462-1464, 2004.

635. Waypa GB, Chandel NS, and Schumacker PT. Model for hypoxic pulmonary vasoconstriction involving mitochondrial oxygen sensing. *Circ Res* 88: 1259-1266, 2001.

636. Waypa GB, Guzy R, Mungai PT, Mack MM, Marks JD, Roe MW, and Schumacker PT. Increases in mitochondrial reactive oxygen species trigger hypoxia-induced calcium responses in pulmonary artery smooth muscle cells. *Circ Res* 99: 970-978, 2006.

637. Weidling J, Sameni S, Lakey JRT, and Botvinick E. Method measuring oxygen tension and transport within subcutaneous devices. *J Biomed Opt* 19: 087006, 2014.

638. Weinberg F, Hamanaka R, Wheaton WW, Weinberg S, Joseph J, Lopez M, Kalyanaraman B, Mutlu GM, Budinger GRS, and Chandel NS. Mitochondrial metabolism and ROS generation are essential for Kras-mediated tumorigenicity. *Proc Natl Acad Sci U S A* 107: 8788-8793, 2010.

639. Weiner CP, Sipes SL, and Wenstrom K. The effect of fetal age upon normal fetal laboratory values and venous pressure. *Obstet Gynecol* 79: 713-718, 1992.

640. Weinmann M, Jendrosseck V, Güner D, Goecke B, and Belka C. Cyclic exposure to hypoxia and reoxygenation selects for tumor cells with defects in mitochondrial apoptotic pathways. *FASEB J* 18: 1906-1908, 2004.

641. Weir EK, and Archer SL. The mechanism of acute hypoxic pulmonary vasoconstriction: the tale of two channels. *FASEB J* 9: 183-189, 1995.

642. Welch WJ, Baumgärtl H, Lübbers D, and Wilcox CS. Nephron pO₂ and renal oxygen usage in the hypertensive rat kidney. *Kidney Int* 59: 230-237, 2001.

643. Westfall SD, Sachdev S, Das P, Hearne LB, Hannink M, Roberts RM, and Ezashi T. Identification of oxygen-sensitive transcriptional programs in human embryonic stem cells. *Stem Cells Dev* 17: 869-881, 2008.

644. Whalen WJ, Nair P, and Ganfield RA. Measurements of oxygen tension in tissues with a micro oxygen electrode. *Microvasc Res* 5: 254-262, 1973.

645. Whitcutt MJ, Adler KB, and Wu R. A biphasic chamber system for maintaining polarity of differentiation of culture respiratory tract epithelial cells. *In Vitro Cellular & Developmental Biology-Plant* 24: 420-428, 1988.

646. White M, Rouleau JL, Ruddy TD, De Marco T, Moher D, and Chatterjee K. Decreased coronary sinus oxygen content: a predictor of adverse prognosis in patients with severe congestive heart failure. *J Am Coll Cardiol* 18: 1631-1637, 1991.

647. White RA, Nolan L, Harley D, Long J, Klein S, Tremper K, Nelson R, Tabrisky J, and Shoemaker W. Noninvasive evaluation of peripheral vascular disease using transcutaneous oxygen tension. *Am J Surg* 144: 68-75, 1982.

648. Wiener L, Santamore WP, Venkataswamy A, Plzak L, and Templeton J. Postoperative monitoring of myocardial oxygen tension: experience in 51 coronary artery bypass patients. *Clin Cardiol* 5: 431-435, 1982.

649. Wild JM, Fichele S, Woodhouse N, Paley MNJ, Kasuboski L, and van Beek EJR. 3D volume-localized pO₂ measurement in the human lung with ³He MRI. *Magn Reson Med* 53: 1055-1064, 2005.

650. Wilkening RB, and Meschia G. Current topic: comparative physiology of placental oxygen transport. *Placenta* 13: 1-15, 1992.

651. Wilkinson PL, Graham BH, Moyers JR, Hamilton WK, Ports TA, Ulliyot DJ, and Chatterjee K. Changes in mixed venous and coronary sinus P50 secondary to anesthesia and cardiac disease. *Anesth Analg* 59: 751-758, 1980.

652. Williams SEJ, Wootton P, Mason HS, Bould J, Iles DE, Riccardi D, Peers C, and Kemp PJ. Hemoxygenase-2 is an oxygen sensor for a calcium-sensitive potassium channel. *Science* 306: 2093-2097, 2004.

653. Wilson DF, Erecińska M, Drown C, and Silver IA. The oxygen dependence of cellular energy metabolism. *Archives of Biochemistry and Biophysics* 195: 485-493, 1979.

654. Winbury MM, Howe BB, and Weiss JR. Effect of nitroglycerin and dipyridamole on epicardial and endocardial oxygen tension--further evidence for redistribution of myocardial blood flow. *J Pharmacol Exp Ther* 176: 184-199, 1971.

655. Winegrad S, Henrion D, Rappaport L, and Samuel JL. Self-protection by cardiac myocytes against hypoxia and hyperoxia. *Circ Res* 85: 690-698, 1999.

3899 656. Winter JD, Estrada M, and Cheng H-LM. Normal tissue quantitative T1 and T2* MRI
3900 relaxation time responses to hypercapnic and hyperoxic gases. *Acad Radiol* 18: 1159-
3901 1167, 2011.

3902 657. Wittenberg JB. Myoglobin-facilitated oxygen diffusion: role of myoglobin in oxygen entry
3903 into muscle. *Physiol Rev* 50: 559-636, 1970.

3904 658. Wittenberg JB. On optima: the case of myoglobin-facilitated oxygen diffusion. *Gene* 398:
3905 156-161, 2007.

3906 659. Wolff M, Fandrey J, and Jelkmann W. Microelectrode measurements of pericellular PO₂ in
3907 erythropoietin-producing human hepatoma cell cultures. *American Journal of Physiology-
3908 Cell Physiology* 265: C1266-C1270, 1993.

3909 660. Wölflle D, Schmidt H, and Jungermann K. Short-term modulation of glycogen metabolism,
3910 glycolysis and gluconeogenesis by physiological oxygen concentrations in hepatocyte
3911 cultures. *Eur J Biochem* 135: 405-412, 1983.

3912 661. Wolinsky H, and Glagov S. Nature of species differences in the medial distribution of aortic
3913 vasa vasorum in mammals. *Circ Res* 20: 409-421, 1967.

3914 662. Wong AP, Bear CE, Chin S, Pasceri P, Thompson TO, Huan L-J, Ratjen F, Ellis J, and
3915 Rossant J. Directed differentiation of human pluripotent stem cells into mature airway
3916 epithelia expressing functional CFTR protein. *Nat Biotechnol* 30: 876-882, 2012.

3917 663. Wood IS, Stezhka T, and Trayhurn P. Modulation of adipokine production, glucose uptake
3918 and lactate release in human adipocytes by small changes in oxygen tension. *Pflugers
3919 Arch* 462: 469-477, 2011.

3920 664. Worlitzsch D, Tarran R, Ulrich M, Schwab U, Cekici A, Meyer KC, Birrer P, Bellon G,
3921 Berger J, Weiss T, Botzenhart K, Yankaskas JR, Randell S, Boucher RC, and Döring G.
3922 Effects of reduced mucus oxygen concentration in airway Pseudomonas infections of cystic
3923 fibrosis patients. *J Clin Invest* 109: 317-325, 2002.

3924 665. Xie P, Sun Y, Ouyang Q, Hu L, Tan Y, Zhou X, Xiong B, Zhang Q, Yuan D, Pan Y, Liu T,
3925 Liang P, Lu G, and Lin G. Physiological oxygen prevents frequent silencing of the DLK1-
3926 DIO3 cluster during human embryonic stem cells culture. *Stem Cells* 32: 391-401, 2014.

3927 666. Xie Y, Zhang J, Lin Y, Gaeta X, Meng X, Wisidagama DRR, Cinkornpumin J, Koehler CM,
3928 Malone CS, Teitell MA, and Lowry WE. Defining the role of oxygen tension in human neural
3929 progenitor fate. *Stem Cell Reports* 3: 743-757, 2014.

3930 667. Yamakawa M, Liu LX, Date T, Belanger AJ, Vincent KA, Akita GY, Kuriyama T, Cheng SH,
3931 Gregory RJ, and Jiang C. Hypoxia-inducible factor-1 mediates activation of cultured
3932 vascular endothelial cells by inducing multiple angiogenic factors. *Circ Res* 93: 664-673,
3933 2003.

3934 668. Yan H-M, Ramachandran A, Bajt ML, Lemasters JJ, and Jaeschke H. The oxygen tension
3935 modulates acetaminophen-induced mitochondrial oxidant stress and cell injury in cultured
3936 hepatocytes. *Toxicol Sci* 117: 515-523, 2010.

3937 669. Yanagi K, Miyoshi H, and Ohshima N. Improvement of metabolic performance of
3938 hepatocytes cultured in vitro in a packed-bed reactor for use as a bioartificial liver. *ASAIO
3939 journal* 44: M436-M440, 1998.

3940 670. Yang Y, Xu Y, Ding C, Khoudja RY, Lin M, Awonuga AO, Dai J, Puscheck EE, Rappolee
3941 DA, and Zhou C. Comparison of 2, 5, and 20 % O₂ on the development of post-thaw
3942 human embryos. *J Assist Reprod Genet* 33: 919-927, 2016.

3943 671. Yarmush ML, Toner M, Dunn JC, Rotem A, Hubel A, and Tompkins RG. Hepatic tissue
3944 engineering. Development of critical technologies. *Ann N Y Acad Sci* 665: 238-252, 1992.

3945 672. Yarmush ML, Toner M, Dunn JC, Rotem A, Hubel A, and Tompkins RG. Hepatic tissue
3946 engineering. Development of critical technologies. *Ann N Y Acad Sci* 665: 238-252, 1992.

3947 673. Ye J, Gao Z, Yin J, and He Q. Hypoxia is a potential risk factor for chronic inflammation and
3948 adiponectin reduction in adipose tissue of ob/ob and dietary obese mice. *Am J Physiol
3949 Endocrinol Metab* 293: E1118-1128, 2007.

3950 674. Yedwab GA, Paz G, Homonnai TZ, David MP, and Kraicer PF. The temperature, pH, and
3951 partial pressure of oxygen in the cervix and uterus of women and uterus of rats during the
3952 cycle. *Fertility and sterility* 27: 304-309, 1976.

3953 675. Yeomans ER, Hauth JC, Gilstrap LC, and Strickland DM. Umbilical cord pH, PCO₂, and
3954 bicarbonate following uncomplicated term vaginal deliveries. *Am J Obstet Gynecol* 151:
3955 798-800, 1985.

- 3956 676. Yin J, Gao Z, He Q, Zhou D, Guo Z, and Ye J. Role of hypoxia in obesity-induced disorders
3957 of glucose and lipid metabolism in adipose tissue. *Am J Physiol Endocrinol Metab* 296:
3958 E333-342, 2009.
- 3959 677. Yochim JM, and Mitchell JA. Intrauterine oxygen tension in the rat during progestation: its
3960 possible relation to carbohydrate metabolism and the regulation of nidation. *Endocrinology*
3961 83: 706-713, 1968.
- 3962 678. Yoshida Y, Takahashi K, Okita K, Ichisaka T, and Yamanaka S. Hypoxia enhances the
3963 generation of induced pluripotent stem cells. *Cell Stem Cell* 5: 237-241, 2009.
- 3964 679. Yu BP. Cellular defenses against damage from reactive oxygen species. *Physiological*
3965 *reviews* 74: 139-162, 1994.
- 3966 680. Yu J-x, Kodibagkar VD, Cui W, and Mason RP. 19F: a versatile reporter for non-invasive
3967 physiology and pharmacology using magnetic resonance. *Current medicinal chemistry* 12:
3968 819-848, 2005.
- 3969 681. Yu J, Ishii M, Law M, Woodburn JM, Emami K, Kadlecsek S, Vahdat V, Guyer RA, and Rizi
3970 RR. Optimization of scan parameters in pulmonary partial pressure oxygen measurement
3971 by hyperpolarized ³He MRI. *Magnetic resonance in medicine* 59: 124-131, 2008.
- 3972 682. Yu J, Rajaei S, Ishii M, Law M, Emami K, Woodburn JM, Kadlecsek S, Vahdat V, and Rizi
3973 RR. Measurement of pulmonary partial pressure of oxygen and oxygen depletion rate with
3974 hyperpolarized helium-3 MRI: a preliminary reproducibility study on pig model. *Acad Radiol*
3975 15: 702-712, 2008.
- 3976 683. Yuan G, Vasavda C, Peng Y-J, Makarenko VV, Raghuraman G, Nanduri J, Gadalla MM,
3977 Semenza GL, Kumar GK, Snyder SH, and Prabhakar NR. Protein kinase G-regulated
3978 production of H₂S governs oxygen sensing. *Sci Signal* 8: ra37, 2015.
- 3979 684. Zagórski Z, Gossler B, and Naumann GO. Effect of low oxygen tension on the growth of
3980 bovine corneal endothelial cells in vitro. *Ophthalmic Res* 21: 440-442, 1989.
- 3981 685. Zahm AM, Bucaro MA, Ayyaswamy PS, Srinivas V, Shapiro IM, Adams CS, and
3982 Mukundakrishnan K. Numerical modeling of oxygen distributions in cortical and cancellous
3983 bone: oxygen availability governs osteonal and trabecular dimensions. *Am J Physiol Cell*
3984 *Physiol* 299: C922-929, 2010.
- 3985 686. Zahm AM, Bucaro MA, Srinivas V, Shapiro IM, and Adams CS. Oxygen tension regulates
3986 preosteocyte maturation and mineralization. *Bone* 43: 25-31, 2008.
- 3987 687. Zäll S, Milocco I, and Ricksten SE. Effects of adenosine on myocardial blood flow and
3988 metabolism after coronary artery bypass surgery. *Anesthesia & Analgesia* 73: 689-
3989 695, 1991.
- 3990 688. Zauner A, Bullock R, Di X, and Young HF. Brain oxygen, CO₂, pH, and temperature
3991 monitoring: evaluation in the feline brain. *Neurosurgery* 37: 1168-1176; discussion 1176-
3992 1167, 1995.
- 3993 689. Zeitouni NE, Dersch P, Naim HY, and von Köckritz-Blickwede M. Hypoxia Decreases
3994 Invasin-Mediated Yersinia enterocolitica Internalization into Caco-2 Cells. *PLoS One* 11:
3995 e0146103, 2016.
- 3996 690. Zeitouni NE, Fandrey J, Naim HY, and von Köckritz-Blickwede M. Measuring oxygen levels
3997 in Caco-2 cultures. *Hypoxia (Auckl)* 3: 53-66, 2015.
- 3998 691. Zemlenyi T, Crawford DW, and Cole MA. Adaptation to arterial wall hypoxia demonstrated
3999 in vivo with oxygen microcathodes. *Atherosclerosis* 76: 173-179, 1989.
- 4000 692. Zhang C, Bélanger S, Pouliot P, and Lesage F. Measurement of Local Partial Pressure of
4001 Oxygen in the Brain Tissue under Normoxia and Epilepsy with Phosphorescence Lifetime
4002 Microscopy. *PLoS One* 10: e0135536, 2015.
- 4003 693. Zhang JL, Morrell G, Rusinek H, Warner L, Vivier P-H, Cheung AK, Lerman LO, and Lee
4004 VS. Measurement of renal tissue oxygenation with blood oxygen level-dependent MRI and
4005 oxygen transit modeling. *Am J Physiol Renal Physiol* 306: F579-587, 2014.
- 4006 694. Zhang Y, Xie C, Wang H, Foss RM, Clare M, George EV, Li S, Katz A, Cheng H, Ding Y,
4007 Tang D, Reeves WH, and Yang L-J. Irisin exerts dual effects on browning and
4008 adipogenesis of human white adipocytes. *Am J Physiol Endocrinol Metab* 311: E530-541,
4009 2016.
- 4010 695. Zhao F, Sellgren K, and Ma T. Low-oxygen pretreatment enhances endothelial cell growth
4011 and retention under shear stress. *Tissue Eng Part C Methods* 15: 135-146, 2009.

4012 696. Zheng L, Kelly CJ, and Colgan SP. Physiologic hypoxia and oxygen homeostasis in the
4013 healthy intestine. A Review in the Theme: Cellular Responses to Hypoxia. *Am J Physiol*
4014 *Cell Physiol* 309: C350-360, 2015.

4015 697. Zhou L, Dosanjh A, Chen H, and Karasek M. Divergent effects of extracellular oxygen on
4016 the growth, morphology, and function of human skin microvascular endothelial cells. *J Cell*
4017 *Physiol* 182: 134-140, 2000.

4018 698. Zhu J, Aja S, Kim E-K, Park MJ, Ramamurthy S, Jia J, Hu X, Geng P, and Ronnett GV.
4019 Physiological oxygen level is critical for modeling neuronal metabolism in vitro. *J Neurosci*
4020 *Res* 90: 422-434, 2012.

4021 699. Zorov DB, Juhaszova M, and Sollott SJ. Mitochondrial reactive oxygen species (ROS) and
4022 ROS-induced ROS release. *Physiological reviews* 94: 909-950, 2014.

4023 700. Zscharnack M, Poesel C, Galle J, and Bader A. Low oxygen expansion improves
4024 subsequent chondrogenesis of ovine bone-marrow-derived mesenchymal stem cells in
4025 collagen type I hydrogel. *Cells Tissues Organs* 190: 81-93, 2009.

4026

4027

4028

4029

4030

4031

4032

4033

4034

4035

4036

4037

4038

4039

4040

4041

4042

4043

Figure Legends

Figure 1. Timeline of O₂-related research publications

(*Main graph*) Number of PubMed entries in which the keyword oxygen is mentioned within the title or abstract over the past 76 years. Arrows indicate important events relevant to the scientific study of oxygen in the context of medical science. (*Pie chart*) Distribution of PubMed entries in which 'oxygen' is mentioned in either the title or abstract between 01/01/2010 and 31/12/2017. ROS – reactive oxygen species

Figure 2. Techniques to determine tissue and cellular PO₂

(A) Diagram of the two common types of O₂-sensitive electrodes, the Clark and Whalen type. Both are connected to an external power supply and galvanometer to record changes in current due to reduction of O₂ at the cathode. (B) The basis for hemoglobin saturation measurements. The binding of O₂ to hemoglobin is associated with a change in its spectral properties, which are measured at various wavelengths to determine the ratio of oxyhemoglobin to total hemoglobin. (C) *Top*, the excitation (solid)/emission spectra (dashed) spectra for Pt^{II}-porphyrin based phosphorescent probes, with a structural schematic provided in the inset. Adapted from (151). *Bottom*, schematics illustrating the basis for O₂ measurements by time-resolved fluorescence; *left*, After the initial excitation flash, phosphorescent emission decays at an exponential rate, with most O₂-sensitive complexes exhibiting lifetimes in the 10-1000μs range; *right*, the relationship between calculated probe lifetime and PO₂. (D) Representative images of ¹¹C-acetate and ⁶⁴Cu-ATSM loaded isolated hearts subjected to left-anterior descending artery occlusion, generating a region of ischaemia identified by the absence of flow (¹¹C +ve) and +ve ⁶⁴Cu-ATSM loading. Taken with permission from (169). (E) Immunohistochemical section of a squamous cell carcinoma stained to show pimonadazole (green) and carbonic anhydrase 9 (red), with blood vessels (white) and necrotic regions (enclosed in dashed white) identified. Taken with permission from (253).

Figure 3. Oxygen gradients in the respiratory system

Concentrations, in kPa, of O₂ (●, left axis), CO₂ (■, right axis) and H₂O (▲, right axis) from 'dry' atmosphere to the pulmonary venous circulation. Increases in PH₂O and PCO₂ in the respiratory tract reduce PO₂ proportionally, and venous admixture within the pulmonary vein reduces PO₂ further.

Figure 4. Oxygen gradients in the vascular system

(A) The relationship between PO₂ (●, right axis), area (●) and velocity (●) throughout the vasculature. Highlighted are the generally perceived vessels in which gaseous (red) and nutrient (blue) exchange takes place. Velocity and area are arbitrarily defined here, and average PO₂ is adapted from Tsai et al. (2003). (B) A standard oxyhemoglobin saturation curve, with the average PO₂ values within relevant blood vessels annotated.

Figure 5. Parameters of atmospheric O₂ levels within the cell culture environment

(A) An approximate O₂ unit conversion table with the multiplication factor required to convert current unit (row) into desired unit (column). (B) The atmospheric composition at sea level, at 1600m above sea level, and within a standard culture incubator (5% CO₂, 75% humidity). (C) The P_{H₂O} and PO₂ in pure water are plotted across a range of temperatures, and the concentration (cO₂) and solubility (S) of O₂ calculated based on the equations of Benson and Krause (32), as summarised by Forstner and Gnaiger (159). (D) An application of Fick's second law of diffusion to describe the time required for culture medium to equilibrate following exposure to an atmosphere of different O₂ content. Q=rate of diffusion, A=liquid surface area, D=diffusivity of O₂ in liquid, k=solubility of O₂ in liquid, Cs=saturating concentration, C=new concentration, d=liquid depth.

Figure 6. Predicting pericellular PO₂ in cell monolayers

(A) Parameters critical in predicting pericellular PO₂ in cultured cells. The value of V (O₂ consumption rate) can be simplified by considering a zero-order relationship between V and PO₂, as described by Yarmush et al. (672) or modelled using Michaelis-Menton kinetics as described by Powers et al. (466). As we know O₂ consumption is affected by O₂ availability, predictions will have more accuracy if V is modelled using the latter. (B) Illustration of the relationship between pericellular PO₂ and cellular O₂ consumption, with commonly used cell types annotated according to published values. Cell types with high O₂ consumption such as cardiomyocytes or hepatocytes can initiate a 'self-inflicted' hypoxia when ambient PO₂ is low. *Abbreviations:* P=pericellular PO₂; P_s=PO₂ at gas/liquid interface; d=fluid height; V=O₂ consumption rate (V_{max}); p=cell density; D=O₂ diffusivity in liquid; k=O₂ solubility in liquid; A=surface area at gas/liquid interface

Figure 7. Oxygen distribution in the lung

(A) An illustration depicting the known distribution of PO₂ in the mammalian lung, combining experimentally derived values with theoretical values derived from established physiology. Pulmonary arterial PO₂ (PaO₂) is usually slightly lower than alveoli PO₂ as outlined in the equation $PaO_2 = PO_2(\text{alveoli}) - 1 \text{ kPa}$ and discussed in Section III-A. (B) Whole lung PO₂ mapping using ³He-based MRI scanning in healthy volunteers and in patients with chronic obstructive pulmonary disease (COPD). Taken with permission from Miller et al. (2010) (396). (C) Peribronchial PO₂ values determined using microelectrode penetration upon (*left*) ligation of the bronchial artery (BA) or bronchial collaterals in dog (adapted with permission from (282)), and (*right*) increases in forced inspiratory PO₂ (FiO₂), adapted from Herold et al. (1998) (236). Both examples illustrate the dependence of peribronchial PO₂ on bronchial artery perfusion rather than the bronchi themselves. (D) Comparison between conventional cell culture, in which the monolayer is completely submerged in medium, and air-liquid interface culture used to maintain differentiated primary

epithelial cells. Transwell® chambers are used to elevate the monolayer, exposing the apical surface to the atmosphere whilst maintaining basolateral access to medium through a microporous membrane.

Figure 8. Oxygen distribution in the arterial wall

(A) Illustration of known distribution of PO_2 in the wall of large arteries such as the aorta, carotid and femoral arteries, combining experimentally derived values with theoretical values obtained from established physiology. (B) Representative trace obtained when a microelectrode is advanced in 5µm increments through the wall of the rabbit thoracic aorta. Redrawn with permission from Niinikoski et al. (1973). (C) Graphical PO_2 profiles through the walls of small (*top*) and large (*bottom*) arteries, illustrating the effect that the vasa vasorum has on adventitial PO_2 . *endothelium

Figure 9. Oxygen distribution in the microvasculature

(A) An idealised microvascular network. (B) Reported PO_2 values plotted against the vessel diameter in microvascular experimental preparations. Results are separated according to tissue, and coded according to the measurement technique employed: □ indicate microelectrode penetration, Δ derived from measurements of hemoglobin saturation, where PO_2 was interpolated based on known species Hb dissociation curves, and ○ phosphorescence quenching microscopy. Adapted from (594).

Figure 10. Effects of physiological normoxia on human endothelial cells

Experimental data describing the careful definition of cellular oxygenation *in vitro* and the subsequent characterization of cellular function and phenotype during long-term culture under these conditions. (A) Intracellular PO_2 in HUVEC monolayers cultured in 96-well plates (100µL volume) at a PO_2 of 18 kPa and then exposed acutely to 5 kPa, measured using MitoXpress INTRA in an O_2 -regulated plate reader. This illustrates that the PO_2 in the medium is only moderately higher than cytosolic, and both parameters rapidly change upon changes in ambient PO_2 . (B) Intracellular PO_2 in HUVEC monolayers as a function of the ambient PO_2 , defined by a 4-parameter sigmoidal fit. Dashed lines indicate the conditions in which HUVEC were subsequently cultured. (C) HIF-1α protein levels in HUVEC cultured for 5 days at the indicated PO_2 in an O_2 -regulated workstation, and corrected for the resulting intracellular PO_2 determined in B. Plotting against intracellular PO_2 results in P_{50} values more likely to be observed in the vasculature *in vivo*. (D) Expression of a Nrf2 regulated antioxidant defense protein, NAD(P)H-quinone oxidoreductase 1 (NQO1), in HUVEC cultured at a PO_2 of 18 or 5 kPa for 1-5 days and then challenged with the electrophile diethylmaleate (DEM, 100µM for 24h). These data illustrate the difference between cellular phenotypes when cells are exposed acutely (24h) or chronically (5 days) to lower O_2 . (E) Phosphorylation of endothelial nitric oxide synthase (eNOS) in response to histamine (10µM, 2 min) stimulation in HUVEC cultured at a PO_2 of 18 or 5 kPa for 5 days, demonstrating a more rapid

decline in phosphorylation over time in cells cultured under physiological normoxia.. (F) Intracellular Ca^{2+} mobilization in response to histamine, measured using Fura-2AM. Lower plateau $[\text{Ca}^{2+}]_i$ at physiological normoxia are reversed by treatment with the sarco/endoplasmic reticulum Ca^{2+} ATPase inhibitor cyclopiazonic acid (CPA). Panels A, B and D are replotted from Chapple et al. 2016 (75) and panels C, E are taken from Keeley et al. 2017 (290), and panel F is taken from Keeley et al. 2017b (291).

Figure 11. Oxygen distribution in the adult heart

Illustration depicting the PO_2 within the heart, summarizing published studies for different species with known values established in physiology. Individual myocardial PO_2 values are further summarized in the adjacent graph, separated according to technique used; \square microelectrode penetration, \triangle derived from measurements of myohemoglobin saturation, where PO_2 was interpolated based on known species Hb dissociation curves, \circ phosphorescence quenching microscopy and \diamond implanted EPR probes. Values are colour-coded to highlight those taken at superficial sites (red) or single cell intracellular measurements (blue).

Figure 12. O_2 distribution in the brain

Illustration depicting the reported PO_2 distribution within the brain, with PO_2 values concerning microvascular or grey matter arranged according to reported depth of measurement. In some cases, depth was estimated based on the methodological description. Studies marked with a \circ were conducted using 2-photon PQM (define), whilst those marked with a \square used ESR.

Figure 13. O_2 distribution in the liver

Illustration of the reported PO_2 distribution in the liver. Note, blood entering the sinusoids is a 3:1 mixture of portal venous and hepatic arterial blood, thus sinusoidal O_2 concentrations can be estimated based on known values for the source vessels ($\text{PO}_2 \sim 8$ kPa).

Figure 14. O_2 distribution in the kidney

Anatomical illustration of known PO_2 values in the kidney, derived from a number of different experimental models, species and techniques. *Bottom left*, a representative trace obtained from invading an O_2 -sensitive microelectrode into the rat kidney following the illustrated path. Depths corresponding to the cortex and medulla are highlighted. Adapted with permission from (362). *Bottom right*, PO_2 values within an individual rat nephron, adapted with permission from (642).

Figure 15. O_2 distribution in the gastrointestinal tract

A, Data from a number of studies (see text for more discussion and references) investigating PO_2 distribution in the gastrointestinal tract. Values are separated into those taken from the stomach, small and large intestines, and further divided according to anatomical/cellular location (lumen,

4198 mucosa or serosa). Symbols are coded according to technique employed; □ microelectrode, △
4199 approximate based on pimonidazole staining, ▽ suffusion, ○ phosphorescence quenching
4200 microscopy and ◇ EPR. **B**, Immunohistochemical images of the colon wall stained with the
4201 hypoxia-specific probe pimonidazole. Images are taken using either fluorescence (left) or bright
4202 field (right) microscopes. Taken with permission from (294) and (157), respectively.

4203

4204 **Figure 16. Oxygen distribution in bone and cartilage**

4205 **(A)** Distribution of O₂ within a typical synovial joint. **(B)** Representative image highlighting the
4206 passage of a microvessel (yellow) from the outer bone (blue) into the marrow (black). Intravascular
4207 PO₂ was determined at 2 different points: within the bone (red arrow and dot) and within the
4208 marrow (green arrow and dot). IV – intravascular. Adapted with permission from (552).

4209

4210 **Figure 17. Oxygen distribution in the skin**

4211 **(A)** Concept of transcutaneous measurement of blood gas concentrations. Heating the skin causes
4212 vasodilation and enhances O₂ delivery to the epidermis, where it diffuses towards the
4213 measurement electrodes. **(B)** Distribution of published PO₂ values in the dermis and subcutaneous
4214 tissues, as well as transcutaneous measurements. Symbols are coded according to technique
4215 used: □ microelectrode, ○ phosphorescence quenching microscopy. *Skin was heated to 41°C in
4216 this study. # Paraffin oil was applied to the skin to prevent O₂ diffusion from the atmosphere,
4217 +Subcutaneous microvascular measurements using Oxyphor G4. **(C)** An example of a PO₂ profile
4218 generating by electrode penetration of the skin, adapted with permission from Baumgärtl et
4219 al. (27).

4220

4221 **Figure 18. Oxygen distribution in the oviduct and uterus**

4222 Reported values for intrauterine and oviduct PO₂ across mammalian species. Intrauterine values
4223 are separated according to menstrual cycle stage. In Rhesus monkeys, ovulation is associated
4224 with large fluctuations in oviduct PO₂ (365), hence the pre-ovulation value is labeled appropriately.

4225

4226
4227

Table 1-1 Permeability of commonly used plastic culture surfaces

Surface	D (10 ⁻⁵ cm ² sec ⁻¹)	k (10 ⁻⁹ mol cm ⁻³ mmHg ⁻¹)	Reference
Medium	3.3	1.2	(371, 389)
	2	1.2	(672)
	2.8	1.3	(112, 466)
Polystyrene	0.01	8.6	(466)
PDMS	2.2	12.2	(466)
Teflon	0.03	5.1	(311)

4228 *Abbreviations:* PDMS, polydimethylsiloxane; Teflon, polytetrafluoroethylene; D, O₂ diffusivity;
4229 k, O₂ solubility coefficient
4230

4231
4232 **Table 1-2 Equations used to predict pericellular PO₂ *in vitro***

Equation	Reference
$h = k [(P_s - P)/V]$	(559)
$-DdP/dx = V_p P / [k(K_m + P)]$	(672)
Solved: $\theta = 0.5 [1 - \alpha - \beta_M + [(1 + \alpha + \beta_M)^2 - 4\alpha]^{0.5}]$	
$P = P_s - (V_p/60D)(760/k)(h/A)$	(389)
$-DdP/dx = -Dk(P_x - P_s)/h$	(371)
$1 - \theta = [F_v + (1 - F_v)(\theta/\beta_v + \theta)](\theta/\beta_M + \theta)\alpha^*$ (Solved)	(466)
$p = [(P - P_s)DA]/Vh$	(596)

4249 *Abbreviations:* P= pericellular PO₂; P_s=PO₂ at gas/liquid interface; d=fluid height; V=O₂ consumption rate
4250 (V_{max}); p=cell density; D=O₂ diffusivity in liquid; k=O₂ solubility in liquid; K_m=PO₂ when O₂ consumption is
4251 0.5max; A=surface area; $\theta = P/P_s$; $\alpha = dV_p/DkP_s$; $\beta_M = K_m/P_s$; $F_v = V_{max,0}/V_{max,\infty}$; $\beta_v = K_v/P_s$ (where K_v is a
4252 fitted constant describing dV/dP_s)
4253
4254
4255

4256 **Table 1-3 Pericellular PO₂ levels under standard culture conditions**
4257
4258

Cell type	Method	PO ₂ (kPa)		Reference
		Ambient*	Pericellular	
Rat hepatocytes	electrode	18	8	(250)
		13	5.8	
		4	1.5	
HepG2/3B	electrode	18	<0.1	(659)
HepG2/3B	electrode	18	<0.1	(389)
			<0.1	
BAEC	electrode	18	10.4	(389)
HUVEC	Fibre-optic probe	21	19-20	(2)
hEPC		5	3.4	
		1	0.7	
HASMC	ESR	21	18.9	(442)
HUVEC	MitoXpress	18.5	~17	(75)
		5	3.5	
hiPSC-CM	electrode	21	10.4	(521)
HASMC			16.4	
HCF			18.6	
HMVEC			17.9	
Rat-CM			14.9	
mESC	Fibre-optic probe	2	2	(404)
hESC iPSC	Fibre-optic probe	21	4-5	(2)
		5	1.5	
		1	0.4	
MEF	MitoXpress	21	8.1	(151)
		10	3.8	
hESC	Fibre-optic probe	21	15	(320)
		5	≤1	
Rat mesangial LLC-PK ₁	electrode	18	14.7 <0.1	(389)
Type II alveolar	electrode	18	13.3	(371)
Dermal fibroblasts	electrode	18	12	(581)
		2	0	
T-47D	electrode	21	1-18	(453)
MIN6 (β cells)	Pimonidazole	20	-	(511)
PANC-1	HIF-1α	10	-	
		7	+	
		5	++	
		3	++	
		0	+++	
Trophoblast	electrode	21	<1	(77)
hESC	Fibre-optic probe	21	15	(320)
		5	≤1	
PMN	Oxodish	21	0-14	(64)
		4	<1	
RAW 264.7	Patch probe	20	~8	(690)
		5	~1.5	
Caco-2	Patch probe	19	~4-5	(114)
		1	<0.1	
Cortical neurons	MitoXpress	18-20	14-16	(250)

4259 *Unless clearly defined, ambient PO₂ was determined to be either 21 or 18 kPa based on the
4260 inclusion/absence of 5% CO₂ and humidification. *Abbreviations:* BAEC, bovine aortic endothelial cells;
4261 HUVEC, human umbilical vein endothelial cells; HMVEC, human cardiac microvascular endothelial cells;
4262 HASMC, human aortic smooth muscle cells; hEPC, human endothelial progenitor cells; hiPSC-CM, human
4263 induced pluripotent stem cells-cardiomyocyte differentiated;; mESC, mouse embryonic stem cells ; hPSC,
4264 human pluripotent stem cells; HCF, human cardiac fibroblasts; Rat-CM, rat cardiomyocytes; PMN, peripheral
4265 blood mononuclear cells
4266

Table 1-4 The effects of culture at physiological normoxia on endothelial cell physiology

Species	Cell type	PO ₂ (kPa)	Time (d)	Summary*	Reference
Human	HUVEC	5 (12 shear)	3	<ul style="list-style-type: none"> ↑ growth (BrdU) ↑ expression of membrane and ECM proteins CD105, CD31, fibronectin, laminin and type VI collagen Different morphology after 24 h shear stress (20 dyne/cm²) (more spindle-like, elongated) • ↑ NO and PGI₂ production with shear stress, ↔□ with 20% vs 12% O₂ 	(695)
	EPC HUVEC	5, 1	3	<ul style="list-style-type: none"> dissolved medium O₂ level much lower in ESC, iPSC and EPC cultures than HUVEC • ↑ traditional hypoxia-sensitive genes (VEGF, Glut1, EPO) 	(2)
	HUVEC HUAEC	3	up to 25	<ul style="list-style-type: none"> ↑ FGF and VEGF stimulated growth and migration Putting non-adapted cells in 3% O₂ for 1 day ↑ effects of FGF and VEGF, and putting adapted cells in 21% O₂ did not reverse the effect of adaptation of growth. ↓ cell surface area compared to non-adapted once adhered • Micro-array analysis showed 41-74 up-regulated and 21-86 down-regulated genes (all HIF regulated), (HUVEC-HUAEC). 	(276) (277)
	HUVEC	5 (5 shear)	3	<ul style="list-style-type: none"> ↔□ protein/mRNA expression following shear between 5 and 20% O₂. ↓ apoptosis gene expression (Bcl), no additive effect of 5-FU • ↑ permeability with 5-FU, reversed by resveratrol. 	(1)
	HUVEC	5	1, >5	<ul style="list-style-type: none"> Culture at 5 kPa ambient PO₂ results in intracellular PO₂ of ~3.5 kPa in HUVEC monolayers ↓ Induction of antioxidant defense proteins (HO-1, NQO1) by electrophilic agents ↔ induction of glutathione-related proteins (GCLC, GCLM, xCT) but no change in [GSH]_i ↑ Bach1 protein and siRNA-mediated knockdown rescued HO-1 induction at 5 kPa O₂ ↓ proliferation 	(75)
	HUVEC	5, 1	>5	<ul style="list-style-type: none"> IC₅₀ for HIF-1α stabilization is 2.3 kPa O₂ when plotted against intracellular PO₂ ↑ PP2A-C protein and co-localization with eNOS mediated rapid dephosphorylation in response to Ca²⁺ dependent stimuli, but not laminar shear stress. PP2A-C protein levels show bell-shaped relationship with ambient PO₂, peaking at 5 kPa NO bioavailability inversely proportional to PO₂ • Culture at physiological normoxia induced phenotype distinct from that under hyperoxic (room air) and hypoxic (1 kPa O₂) conditions. 	(290)
	HUVEC	5	>5	<ul style="list-style-type: none"> ↓plateau phase [Ca²⁺]_i in cells at 5 kPa O₂, rescued by co-treatment with SERCA-inhibitor CPA. • Cells at 5 kPa O₂ more resistant to Ca²⁺ overload due to mitochondrial 'sparing' by increased SERCA activity. 	(291)
	HPMVEC ST1.6R	5	12	<ul style="list-style-type: none"> Confluent monolayers contained 30% fewer cells, but formed a tighter barrier as measured by TER. • ↑ cortical actin levels 	(547)
	HDMVEC	5	14	<ul style="list-style-type: none"> ↑ Basal and stimulated growth (PMA and IL-1β) • ↑ ECM proteins (type VI collagen) 	(697)

Bovine	Corneal EC	6	4	<ul style="list-style-type: none"> • \uparrow $[H^3]$-thymidine incorporation and cell count 	(684)
	BRMVEC	95, 40, 20, 10 5	4	<ul style="list-style-type: none"> • Endothelial cells more sensitive to effects of oxygen compared with pericytes and fibroblasts from same vessel 	(490)
Rat	Liver sinusoidal EC	5	5	<p> \downarrow basal apoptosis (MTT and Annexin V/PI) \leftrightarrow \square morphology of confluent monolayer, or fenestrated characteristics \downarrow endocytotic capacity during culture significantly less at 5% \downarrow ICAM-1 and IL-6 expression/production (pro-inflammatory) and \uparrow IL-10 production (anti-inflammatory) (only measured after 48 h) \uparrow H_2O_2 basal production (DCF), treatment with catalase reverses effects on apoptosis <ul style="list-style-type: none"> • \leftrightarrow \square NO release (Griess reaction) </p>	(377)

4268 *Abbreviations:* HUVEC, human umbilical vein endothelial cells; ECM, extracellular matrix; NO, nitric oxide; PGI₂, prostacyclin; EPC, endothelial progenitor cells;
4269 iPSC, inducible pluripotent stem cells; ESC, embryonic stem cells; VEGF, vascular endothelial growth factor; Glut1, glucose transporter 1; EPO, erythropoietin;
4270 HUAEC, human umbilical artery endothelial cells; FGF, fibroblast growth factor; 5-FU, 5-fluorouracil; HO-1, heme-oxygenase 1; NQO1, NADPH-quinone
4271 oxidoreductase 1; GCLC/M, glutamate-cysteine ligase catalytic/modulatory subunit; xCT, cystine-glutamate antiporter system X; GSH, glutathione; PP2A-C, protein
4272 phosphatase 2A catalytic subunit; SERCA, sarco/endoplasmic reticulum Ca²⁺ ATPase; CPA, cyclopiazonic acid; HPMVEC, human pulmonary microvascular
4273 endothelial cells; TER, transendothelial resistance; HDMVEC, human dermal microvascular endothelial cells; PMA, phorbol 12-myristate 13-acetate; IL-1 β ,
4274 interleukin 1 β ; BRMVEC, bovine retinal microvascular endothelial cells; ICAM-1, intracellular adhesion molecule 1; DCF, dichlorofluorescein; MTT, 3-(4,5-
4275 Dimethylthiazol-2-yl)-2,5-Diphenyltetrazolium Bromide; PI, propidium iodide.
4276

Table 1-5 The effects of culture at physiological normoxia on circulating cell physiology

Species	Cell Type	PO ₂ (kPa)	Time (d)	Summary	Reference
Human	PBMC	5	1-5 d	<ul style="list-style-type: none"> • ↑unstimulated and Con A stimulated proliferation, no effect on PHA stimulation • ↑early expression of lymphocyte marker CD69 • ↓basal and H₂O₂ induced ROS production (DCF) • Altered released cytokine profile following stimulation with Con A or LPS 	(315)
	PBMC	5	15	<ul style="list-style-type: none"> • Gene expression array revealed higher expression of genes important for lymphocyte biology, immune function and cell-cycle progression. • ↓expression of genes involved in stress response, cell death and cellular repair. 	(210)
	PBMC	5	5 d	<ul style="list-style-type: none"> • Proliferation stimulated by antigen CD8/CD28 crosslinking, or Con A, was ↑at 5%, but no effect on phytohemagglutinin-stimulated proliferation. • Unstimulated cell viability unaffected by adaptation to 5% 	(16)
	Negatively enriched T cells PBMC	5	3 d	<ul style="list-style-type: none"> • ↓GSH and GSH:GSSG following culture (vs fresh), less reduction at 5% • ↓proliferation • ↑CD8/CD28 stimulated NO and ROS production • ↑lymphocyte marker CD69 	(17)
	PBMC	5	>6 d	<ul style="list-style-type: none"> • HIV-transactivator of transcription (Tat) protein induces apoptosis at 20%, but proliferation at 5% O₂ • Tat can be used to prime cells for HIV infection as well as other methods, only at 5% O₂ 	(499)
	PBMC	5	7 d	<ul style="list-style-type: none"> • <i>in vitro</i> culture ↑SOD1-3, CAT, GPx mRNA. At 5% O₂, ↓CAT and GPx mRNA vs room air • ↑GPx activity, no change in CAT or SOD activity. • ↑Intracellular GSH, though overall decrease during culture. • ↓superoxide and hydrogen peroxide 	(146)
	PBMC-matured dendritic cells	5	duration of culture	<ul style="list-style-type: none"> • ↔□ total cell yield • ↓endocytosis of dextran-FITC • ↑LPS-induced IL-12 (p70) and T-cell activation during co-culture 	(171)
Mouse	CD4+ T cells	5, 1	36 h	<ul style="list-style-type: none"> • ↑Th17 specific differentiation at 5%, ↓ all subset differentiation at 1% • No effect of 5% on proliferation, 1% ↓ • Increased mTORC1 activity at 5% O₂ 	(259)
	Primary splenocytes Splenocyte-differentiated T Cells	2.5	6 d	<ul style="list-style-type: none"> • ↑CD4:CD8, but dramatically higher killing (lytic) potential of CD8+ cells at 5%, with ↑density of CD25 surface antigen. • ↓cell death 	(61)
	macrophage line J774	6	24 h	<ul style="list-style-type: none"> • ↓ <i>Leishmania amazonensis</i> (intracellular parasite) infection at 5% • ↔□ NO or ROS production 	(105)

4278 *Abbreviations:* PBMC, peripheral blood mononuclear cells; con A, concanavalin A; PHA, phytohaemagglutinin; DCF, dichlorofluoroscein; LPS, lipopolysaccharide;
4279 GSH, glutathione (reduced); GSSG, glutathione (oxidised); NO, nitric oxide; ROS, reactive oxygen species; HIV, human immunodeficiency virus; SOD, superoxide
4280 dismutase; CAT, catalase; GPx, glutathione peroxidase; mTORC, mammalian target of rapamycin, FITC, fluorescein isothiocyanate; IL-12, interleukin 12.
4281

Table 1-6 The effects of culture at physiological normoxia on intestinal cell physiology

Cell Type	PO ₂ (kPa)	Time (h)	Summary	Reference
T84 Caco-2 B	2.6	0-48	<ul style="list-style-type: none"> • Intestinal epithelial cells maintain barrier resistance under hypoxia, whereas oral epithelia and endothelial cells increase permeability • ↑ ITF mRNA by 4 h, maintained at protein level for 48 h, and is HIF-1 dependent • Anti-ITF antibody attenuates hypoxia-induced ↑ resistance in Caco-2 cells. Addition of ITF to endothelial cells ↑ resistance during hypoxia. • ITF is induced <i>in vivo</i> by hypoxia (8% O₂, 4 h) • Hypoxia <i>in vivo</i> associated with increased permeability relative to normoxic controls. Possibly under pathological hypoxia <i>in vivo</i>. 	(170)
Caco-2	2.6	0-96	<ul style="list-style-type: none"> • ↑ MRD1 mRNA (18 h) and protein (maintained at 96 h, peak at 48 h) in hypoxia, dependent on HIF-1 • Increase in protein translated to increased surface expression and function (drug efflux) 	(93)
T84 Caco-2	2.6	0-96	<ul style="list-style-type: none"> • ↑ CD79 and CD339 mRNA (18 h) and protein (maintained at 96 h, peak at 48 h) in hypoxia, dependent on HIF-1. • Both proteins are ecto-5'-nucleases responsible for metabolizing 5'-AMP to adenosine, which activates A2B receptors and ↑ barrier integrity 	(566)
T84 ModeK	2.6	0-48	<ul style="list-style-type: none"> • ↑ MUC3 selectively by hypoxia: mRNA (maintained by 24 h) and protein (peaked at 24 h and declined afterwards). Probably HIF-1 mediated. • MUC3 interacts with ITF at the apical surface of epithelial cells 	(359)
T84 Caco-2	2	0-48	<ul style="list-style-type: none"> • Hypoxia ↓ adenosine uptake • ↓ ENT1 and 2 mRNA and protein during hypoxia, maintained at 48 h and HIF-1 dependent • siRNA against ENT2 decreased adenosine uptake, therefore explaining first observation. • Hypoxia <i>in vivo</i> associated with increased permeability relative to normoxic controls. Possibly under pathological hypoxia <i>in vivo</i> 	(408)
T84 Caco-2	2	0-48	<ul style="list-style-type: none"> • Time-dependent increased Netrin-1 protein during hypoxia, dependent on HIF-1 activity • Endogenous netrin-1 reduces monocyte transepithelial migration via activation of the adenosine A2B receptor on the monocyte. This reduces inflammatory activation and therefore protects the epithelial barrier during inflammation. 	(492)
T84 Caco-2	1	0-24	<ul style="list-style-type: none"> • HIF-1 conditional KO reduced expression of DEFB1 in mouse intestine and Caco-2 cells • Exposure to hypoxia ↑ HIF-1, although basal levels were observed • No change in DEFB1 protein during hypoxia, despite ↑ HIF and dependence on it. • HIF-1 siRNA reduces hBD-1 soluble protein excreted, which would ↑ Bacterial load in intestine • In human bowel scrapings (epithelial-enriched), expression of DEFB1 mRNA correlated linearly with GLUT1 (HIF target), and hBD-1 staining was most prominent at apical edge of colonic mucosa 	(293)

Caco-2 T84	1	0-48	<ul style="list-style-type: none"> • Enzymes involved in creatine metabolism regulated specifically by HIF-2 during hypoxia. • Induction of CKM and CKB maintained at 48 h (protein) and abolished with HIF-2 siRNA • CKM and CKB enzymes are localised to the apical surface of polarised epithelium, and enriched at the adherens junction. • HIF-2 dependent CK induction maintains barrier integrity and protects against inflammation. • Inhibition of CK strongly decreases resistance under hypoxic conditions 	(180)
Caco-2	1	0-144	<ul style="list-style-type: none"> • Measurements of medium PO₂ using optical sensor spots immobilised onto standard 24WPs, gas-permeable 24WP and Transwell inserts • Medium PO₂ reached 4 kPa after 6 days post-confluence in standard 24WP, whereas it was only ~15 kPa in gas permeable plates and in inserts. • Despite low O₂ levels, no HIF-1 stabilisation was observed under standard conditions in normal plates • Medium volume was 1ml: very high for 24-well plate, large depth would lead to O₂ depletion 	(690)
Caco-2	1	24	<ul style="list-style-type: none"> • Hypoxic pre-incubation significantly reduced bacterial internalisation. • This was dependent on β-1 integrin, the protein levels of which were decreased by hypoxic exposure in correlation with increased HIF-1, though no definitive siRNA experiment was performed. • Hypoxia reduces bacterial infection by down-regulating β1 integrin. 	(689)

Abbreviations: ITF, Intestinal Trefoil Factor; HIF, hypoxia-inducible factor; MRD1, multidrug resistance protein 1; MUC, mucin; ENT, equilibrative nucleoside transporter; DEFB1; β defensin gene; hBD-1, human β -defensin; GLUT1, glucose transporter 1; CKM/B, creatine kinase M/B;

4287 **Table 1-7 The effects of culture at physiological normoxia on bone cell physiology**

Species	Cell type	PO ₂ (kPa)	Time	Comments	Reference
Human	SV-HFO (human osteoblastic cell line)	2	3 wk	<ul style="list-style-type: none"> • ↓ mineralisation due to less differentiation and maturation of extracellular matrix components (collagen) • ↓ROS (mitoSOX and DCF) and lower expression of SOD1/2 and CAT 	(423)
		2	3 wk	<ul style="list-style-type: none"> • Microarray of cells cultured at 2 kPa for various phases of differentiation • Impact most prominent during early phase when mineralisation begins to occur 	(424)
Mouse	MC3T3-E1 preosteoblast Calvarial organ culture	5	35 d	<ul style="list-style-type: none"> • Earlier and greater Ca²⁺ mineralisation • ↑ ALP staining and earlier • ↑Osteocalcin expression initially, but declined by 35 d • ↑Cx43 expression at cell-cell junctions and whole cell lysates • ↑Osteocyte markers (Dmp1, Mepe and Fgf23) • ↑osteocyte population (cells expressing Dmp1 and Mepe) in organoid cultures 	(241)
	MC3T3-E1 preosteoblast	2, 5	72 h	<ul style="list-style-type: none"> • 2 kPa strongly associated with HIF stabilisation (PMZD staining and HRE luciferase), not observed at 5 kPa • ↑PGE₂ production and EP1 receptor expression at 2 kPa 	(329)
	MLOA5 (preosteoblast) MLOY4 (osteocyte)	2, 5	7 d	<ul style="list-style-type: none"> • ↓PO₂ associated with ↓ALP activity and mineral deposition • no change in viability • ↑HIF stabilisation at 2 kPa preserves cell function under hypoxia 	(686)
Rat	Calvarial osteoblasts	10	7 d	<ul style="list-style-type: none"> • Compared to hyperoxia (90% O₂), ↑proliferation • No change in ALP activity 	(595)
	Primary osteoblasts	0.2-20	18 d	<ul style="list-style-type: none"> • ↓bone module formation with ↓PO₂ • at 2 kPa O₂, ↓proliferation but no change in apoptosis • Delayed osteoblast differentiation markers (osteocalcin and PLOD) and ↓collagen production. 	(601)
Rabbit	Periosteal organ culture	1-90	6 wk	<ul style="list-style-type: none"> • Highest growth and chondrogenesis at 15 kPa • ↓collagen synthesis at very high and very low O₂ levels • Culture in a 'sealed 'jar' apparatus 	(435)

4288 *Abbreviations:* ALP, alkaline phosphatase; PLOD, procollagen lysine, 2-oxoglutarate, 5-dioxygenase; Cx43, connexin 43; Dmp1, dentin matrix protein 1; Mepe,
4289 matrix extracellular phosphoglycoprotein; Fgf23, fibroblast growth factor 23; PMZD, pimonidazole; HRE, hypoxia-responsive element; PGE₂, prostaglandin E₂; EP1,
4290 prostaglandin E receptor 1; HIF, hypoxia-inducible factor; ROS, reactive oxygen species; DCF, dichlorofluorescein; SOD, superoxide dismutase; CAT, catalase; SV-
4291 HFO, SV40-transformed Human Fetal Osteoblastic cells

4292

Table 1-8 The effects of culture at physiological normoxia on chondrocyte physiology

Species	Cell Type	PO ₂ (kPa)	Time	Comments	Reference
Human	Chondrocytes	5	4 wk	<ul style="list-style-type: none"> • ↑ collagen II, aggrecan and SOX9 mRNA in 3D culture • ↑ proliferation and GAG synthesis • no change in pH or glucose consumption • Redifferentiated phenotype only achieved when 5 kPa O₂ and 3D culture combined 	(414)
	Meniscus cells Chondrocytes	5	2 wk	<ul style="list-style-type: none"> • no change in collagen I mRNA • ↑ Collagen II and SOX9 mRNA in meniscus cells but not chondrocytes 	(4)
		5	3 wk	<ul style="list-style-type: none"> • ↑ GAG and hyaline-cartilage like matrix deposition • ↑ Collagen II, aggrecan and SOX9 protein expression 	(287)
		5	5 d	<ul style="list-style-type: none"> • no change in aggrecan or Col I mRNA expression, or in DNA content, lactate production or glucose consumption • ↑ VEGF production and mRNA levels at pH 7.4 and 5 kPa O₂ 	(104)
		5	4 wk	<ul style="list-style-type: none"> • no change in growth or DNA content • ↑ CD44 and CD105 expression • ↑ Pellet volume and GAG content • no change in col1/2 mRNA expression, but ↑ aggrecan mRNA 	(518)
		20	NA	<ul style="list-style-type: none"> • Modeling O₂ consumption and PO₂ profiles in 3D alginate chondrocyte cultures • PO₂ <8 kPa makes chondrocytes favor proteoglycan synthesis over collagen 	(341)
Bovine	Chondrocytes	3-60	6 d	<ul style="list-style-type: none"> • ↓ DNA content with ↓ PO₂ • ↓ Sulphate incorporation, as indicative of GAG synthesis, with ↓ PO₂ • ↑ Proteoglycan aggregation with ↓ PO₂ 	(86)
		0.1, 5, 10, 20	7 d	<ul style="list-style-type: none"> • no change in viability or proliferation, which didn't actually occur • no change in aggrecan expression • ↑ pellet volume peaking at 10 kPa O₂, indicative of ↑ collagen synthesis • no change in pH until 0.1 kPa • ↓ rRNA yield at 0.1 kPa. Suggested that chondrocytes are particularly robust in withstanding hypoxia relative to other cell types 	(196)
		5	4 wk	<ul style="list-style-type: none"> • no change in growth, viability or pH • no change in Collagen I mRNA • ↑ Collagen II and aggrecan mRNA • ↑ matrix collagen and GAG content during 3D culture. • Culture at 5 kPa exacerbated redifferentiation during 3D culture • All culture performed on orbital shakers so pericellular PO₂ was also ~5 kPa 	(415)

Bovine		5	3 wk	<ul style="list-style-type: none"> • ↓ Collagen I mRNA during redifferentiation • ↑ Collagen II, XI and aggrecan mRNA during redifferentiation • ↑ Collagen staining in 3D beads, especially towards the periphery where PO₂ would be highest 	(117)
		5	3 wk	<ul style="list-style-type: none"> • ↓ Collagen I and ↑ Collagen II/aggrecan mRNA and staining during redifferentiation • ↑ sulfate and proline incorporation, indicative of GAG and proteoglycan synthesis 	(118)
		2, 5	14 d	<ul style="list-style-type: none"> • ↓ proliferation at both O₂ levels but no change in protein content • ↑ O₂ consumption during monolayer culture which was proportional to PO₂ • ↑ ROS at 20 kPa • Differences in cellular phenotype between 2 and 5 kPa 	(240)
		2, 5	9 d	<ul style="list-style-type: none"> • ↑ mitochondrial mass during culture , more pronounced at 20 kPa than 2. Associated with ↑ oxidative phosphorylation • ↑ ROS and O₂ consumption at 20 kPa which could be restored to fresh/ 2 kPa values but treatment with NAC • ↑ GAG accumulation in 3D culture at 5 kPa 	(239)
Mouse	C3H10T1/2 E14.5 murine forearm limb	5	7 d	<ul style="list-style-type: none"> • ↑ BMP-2 induced GAG synthesis with concomitant ↓ ALP activity and alizarin red staining, indicating less osteoblastic differentiation. • No change in adipocyte differentiation • No change in proliferation • ↑ Col2a1 mRNA expression and ↓ Col10a1 mRNA expression, mediated by ↑ p-p38 and HDAC4 activity. • Enlarged matrix area in forelimbs cultured at 5 kPa O₂ • 5 kPa O₂ promotes chondrogenic differentiation but not terminally. 	(242)
Rabbit	Chondrocyte	5	3 wk	<ul style="list-style-type: none"> • ↑ proliferation • ↑ Collagen II mRNA but no change in aggrecan or collagen I • ↑ aggregation with more collagen and GAG deposition. • Culture at 5 kPa O₂ during the expansion phase more pronounced than during the 3D phase 	(233)

4294 *Abbreviations:* GAG, glycosaminoglycan; ROS, reactive oxygen species; NAC, N-acetyl cysteine; BMP-2, bone morphogenic protein 2; ALP, alkaline phosphatase;
4295 ColX, collagen X; HDAC4, histone deacetylase 4; VEGF, vascular endothelial growth factor.

4296

4297 **Table 1-9 The effects of culture at physiological normoxia on marrow-derived stem cells**

Species	Cell type	PO ₂ (kPa)	Time	Comments	References
Human	MSC	1	1-3 wk	<ul style="list-style-type: none"> • ↓proliferation • ↓adipogenic and chondrogenic differentiation 	(251)
	MSC in pellet culture	2	14 d	<ul style="list-style-type: none"> • ↑sulphated GAG, collagen and proteoglycan formation, with more homogenous surface distribution. More chondrogenic 	(374)
	haemopoietic	5	10 d	<ul style="list-style-type: none"> • ↑CD34+ CD38- expansion due to ↑proliferation, not ↓apoptosis • ↑myeloid-committed cells (CD33+ CD14+) with ↑colony forming potential • ↑subsequent cell engraftment in irradiated mice 	(495)
	MSC	5, 2	thawing and duration of culture	<ul style="list-style-type: none"> • ↓colony numbers and cell yield at 5% specifically, but ↓colony and individual cell size at 2%. • ↑bone-marrow specific markers (CD44, 73 and 105) at both 5 and 2 kPa • ↓cellular senescence at 5 and 2% • ↓O₂ consumption (microelectrode) and ↑lactate production, with ↓proportion of ATP generated by oxidative phosphorylation (azide sensitive) • ↑ chondrogenic differentiation at 5% specifically 	(449)
	Haemopoietic (CD44+ progenitor)	5	>7 d	<ul style="list-style-type: none"> • ↓NO production (Griess) • ↑proliferation and colony formation, with ↑progenitor cell production and proliferation 	(483)
	mesenchymal	3	up to 100 d	<ul style="list-style-type: none"> • ↑colony formation following isolation at 3 kPa • ↔□ hypoxia-associated genes, but 2313 differentially expressed genes related mostly to ageing (↓) and bone-marrow specific markers (↑) • ↓senescence over 100 d, with high population doubling times • ↓AGE accumulation and SA-β-gal+ cells, markers of senescence 	(149)
	MIAMI	3	15 d	<ul style="list-style-type: none"> • highest proliferation at 3 kPa • ↑embryonic and 'stem' genes OCT4, REX-1 and hTeRT • ↓osteoblast marker genes Runx and OCN • ↓ALP activity, mineral deposition and ECM-associated Ca²⁺ content • MIAMI cells less differentiation/mature than MSC. 	(101)
Porcine	Marrow nucleated cells	1,5,10	6 d	<ul style="list-style-type: none"> • Largest colonies formed with the highest density of cells at 5 kPa • Similar colonies formed between 1 and 20 kPa 	(616)
	MSC	5	42 d	<ul style="list-style-type: none"> • Agarose constructs contained increased GAG deposition, particularly within the core. • ↑Col2a1 and ↓Col1a1 relative to room air/ 	(391)

	MSC	5	expd/dif/both	<ul style="list-style-type: none"> • expansion at 5% results in larger colony formation and thus higher cell yield • Differentiation at 5%, even when following expansion at 20%, enhances the chondrogenic potential of MSC; more stable pellet/hydrogel with $\uparrow\text{Ca}^{2+}$ content and \downarrowcollagen X 	(528)
Rat	MSC	5	up to 21 d	<ul style="list-style-type: none"> • Enhanced calcium content and mineralisation at 5 kPa O_2 suggests cells more likely differentiate in response to stimulation at 5 kPa O_2 	(336)
Sheep	mesenchymal	5	up to 14 d	<ul style="list-style-type: none"> • \uparrowcolony size and number, \uparrowproliferation • \downarrowsenescence • \uparrowchondrogenic differentiation 	(700)

4298 *Abbreviations:* GAG, glycosaminoglycan; ColX, collagen X; MSC, mesenchymal stem cell; NO, nitric oxide; SA- β -gal, senescence associated β -
4299 galactosidase; AGE, advanced glycosylation end-products; OCT4, octamer-binding transcription factor 4; hTeRT, human telomerase reverse
4300 transcriptase; Runx; Runt-related transcription factor 1; OCN, osteocalcin; ALP, alkaline phosphatase; ECM, extracellular matrix; MIAMI, Marrow-
4301 isolated adult multilineage inducible cells; MSC, mesenchymal stem cells
4302

4303 **Table 1-10 The effects of culture at physiological normoxia on skin cell physiology**

Species	Cell Type	PO ₂ (kPa)	Time (d)	Comments	Reference
Human (Mouse)	82-6 and Bj (HCA2) MEF	3	60 (from isolation)	<ul style="list-style-type: none"> • MEF cultures did not undergo senescence at 3 kPa, but it could be induced by exposure to 20 kPa at early time points • At 3 kPa, MEFs behaved more like human fibroblasts • Changes in expression patterns of p53 regulatory proteins p19^{ARF} and p16 at 3 kPa. • ↑ Chromosomal breakage at 20 kPa in MEFs • MEF are particularly sensitive to oxygen metabolism damage, but at 3 kPa are just as robust as human fibroblasts 	(446)
	Keratinocyte	4	From isolation	<ul style="list-style-type: none"> • Comparison between cells from young and old donors • ↑migration (scratch) in young, but not old, cells. No change in proliferation • ↓ROS (DHE) independent of age • Scratching induces ROS production at leading edge, dissipation of which related to migration rate 	(493)
	Dermal Fibroblasts	2	>3 d	<ul style="list-style-type: none"> • No change in metabolic activity or morphology • ↓ inhibition of metabolic activity by blue light (450 nm) at 2 kPa, whereas NIR light (850 nm) stimulated metabolism only at 2 kPa 	(394)
	HCT116 Keratinocytes	5	4	<ul style="list-style-type: none"> • ↑ HIF protein at 5 kPa in HCT116, much less in keratinocytes (barely visible) • Accompanied by HRE-Luc activity and GLUT-1 mRNA increases in HCT116 cells • Inhibition of MAPK cascade with U0126 reduced HIF1 protein, as did treatment with doxorubicin • ↑ proliferation in HCT116 cells at 5 kPa, barely effected by HIF1 KO. • All observations consistent with 'self-inflicted hypoxia' due to O₂ consumption. Inhibition of MAPK or DNA damaging agents would reduce cellular activity (O₂ consumption), thereby increasing pericellular 	(68)
Mouse	Tail fibroblasts MEF	3	7.5	<ul style="list-style-type: none"> • Spontaneous chromosomal breaks at 20 kPa reduced at 3 kPa in cells with compromised chromosome stability (Ku86^{-/-}) • No change in cell proliferation • Some level of spontaneous instability even at 3 kPa, probably due to other sources of ROS 	(283) (78)
Rodent	Fibroblasts	3	30 d	<ul style="list-style-type: none"> • Fibroblasts from lab mouse strains are the only rodent cells to exhibit marked sensitivity to O₂ 	(448)

4304 *Abbreviations:* MEF, mouse embryonic fibroblasts; ROS, reactive oxygen species; DHE, dihydroethidium; HRE-Luc, luciferase conjugated hypoxia-responsive
 4305 element; GLUT-1, glucose transporter 1; MAPK, mitogen activated protein kinase

4306

4307 **Table 1-11 The effects of culture at physiological normoxia on adipose tissue resident cells**

Species	Cell type	PO ₂ (kPa)	Time (d)	Comments	Reference
Human	Adipocytes	15, 10, 5, 3, 1	1	<ul style="list-style-type: none"> Leptin, VEGF and IL-6 mRNA and secretion inversely proportional to PO₂ Adiponectin mRNA and secretion proportional to PO₂ Steepest part of sigmoid curves between 3-10 kPa, with 10 kPa often not different from room air Glucose uptake and GLUT transporter expression increased proportional to PO₂ and corresponds to increased lactate secretion 	(663)
	Adipocytes	10, 5	14	<ul style="list-style-type: none"> No change in differentiation (Oil red O staining), but decreased lipid droplet size proportional to PO₂ Increased triglyceride content at 10 kPa Increased expression and secretion of adiponectin, IL-6 and DPP4, with concomitant decreases in leptin secretion (adipokine secretion) Increased glycerol release and hormone sensitive lipase expression at 10 kPa (lipolysis) Conditioned medium from 10 kPa cells induced the lowest SMC proliferation 	(145)
	Adipose MSC	5	duration of induction	<ul style="list-style-type: none"> a combination of kinase chemical inhibitors and 5% O₂ is optimal for the induction of iPSCs from adipose-derived stem-cells 	(533)
	Adipose MSC	2	duration of culture	<ul style="list-style-type: none"> ↑proliferation ↑viability ↑adipogenic and osteogenic differentiation potential following pre-adaptation to low O₂ 	(606)
	Adipose MSC	5	21	<ul style="list-style-type: none"> ↓fatty acid binding protein 4 expression ↓glycerol-3-phosphate dehydrogenase activity and triglyceride content, markers of adipogenic differentiation effects of low O₂ abolished by cytoskeletal inhibitors cytochalasin D and blebbistatin 	(512)
Human Rabbit	Adipose stromal cells	5	21	<ul style="list-style-type: none"> culture at 5 kPa increases chondrogenic differentiation of stromal cells <i>in vitro</i> but does not increase subsequent chondrogenesis <i>in vivo</i> 	(464)

4308 *Abbreviations:* VEGF, vascular endothelial growth factor; IL-6, interleukin-6; GLUT, glucose transporter; DPP4; Dipeptidyl peptidase-4; SMC, smooth muscle cell;
 4309 iPSC, inducible pluripotent stem cell; MSC, mesenchymal stem cell

4310 **Table 1-12 The effects of physiological normoxia on embryonic stem cell physiology**

Species	Cell type	PO ₂ (kPa)	Time (d)	Comments	Reference
Human	ESC (H1)	5	12-15	<ul style="list-style-type: none"> • hESC differentiation in culture was inversely proportional to PO₂: little differentiation apparent when cultured at 1-4 kPa O₂ • Greater embryonic body formation under low O₂ • Phenomenon is not reversible, exposure to room air after low O₂ does not induce much more differentiation 	(142)
	ESC (H1, RH1 and H9)	2	14	<ul style="list-style-type: none"> • Clonal recovery was 4-12-fold higher at 2 kPa and cells were less differentiated • Switching back to room air reduced colony formation • Less spontaneous chromosomal alterations and perhaps longer telomeres 	(161)
	ESC (H1, RH1 and H9)	2	10 passages	<ul style="list-style-type: none"> • Genetic screen of cells cultured for 10 passages at 2 or 18 kPa O₂ • Between p0 and 10, no change in genome at room air, but robust genomic changes at 2 kPa 	(160)
	H1 and H9	4	7 (after multiple passages)	<ul style="list-style-type: none"> • Cultures at 4 kPa displayed less heterogeneity in their transcriptome • No change in the expression of pluripotency after culture at 20 kPa for 7 days, although a number of genes under the OCT4/NANOG/SOX2 triad are expressed much less 	(643)
	CLS1 / 2	1, 5, 10, 15	Up to 8 weeks	<ul style="list-style-type: none"> • Colony formation as inversely proportional to PO₂ • After 4 weeks, re-exposure to room air rapidly induced proliferation and differentiation, even in cultures kept at 5 kPa for 18 months • Colonies at 5 kPa O₂ homogenous and undifferentiated • Inhibition of notch signaling normalised differentiation 	(469)
	Blastocyst-derived	5	From thawing	<ul style="list-style-type: none"> • Cells thawed at 5 kPa O₂ and then exposed to room air for >3 d • No gross changes in genome after chronic culture at room air • Spontaneous differentiation reduced after exposure to room air • Exposure to room air induces irreversible X-chromosome inactivation 	(335)
	H9	5	6-12	<ul style="list-style-type: none"> • At room air, dissolved PO₂ ~15 kPa, and near 1 kPa at 5 kPa ambient • Decreased O₂ consumption at 5 kPa • Early vascular markers (CD42, KDR and CD56) increased at 5 kPa, with morphological evidence for increased endothelial differentiation • When differentiation was split into 2 parts; culture at 5 kPa was only required for the first 6 days • Culture at 5 kPa increases ROS formation (DCF) and inhibition with DPI abolished this and the increased EC differentiation 	(320)
	MEL-2 ESC	2	Up to 5	<ul style="list-style-type: none"> • No significant change in proliferation • ↑ Lactate and glucose consumption, and ↓ ammonia consumption 	(596)

				<ul style="list-style-type: none"> • ↑ production of alanine, and ↑ consumption of aspartate, asparagine and glycine. ↓ consumption of glutamine • Good information on O₂ diffusion and limitations <i>in vitro</i>. Intracellular PO₂ most certainly close to 0 kPa at 2 kPa ambient in ESC cultures 	
Human	Shef3 and Hues-7	5	Minimum of 3 passages	<ul style="list-style-type: none"> • No large change in amino acid utilisation or production • ↑ Glycine consumption • ↓ serine uptake 	(82)
	hESC and hiPSC	2	>5	<ul style="list-style-type: none"> • Genomic screen suggested culture at 2 kPa shifted cells towards neuronal lineages (expression of SOX1, HES5 and FOXG1), specifically towards glial differentiation vs neuronal • Effect was abolished by HIF-2 siRNA and HIF-α inhibition • HIF regulates MYC and thus LIN28/let-7, a key neuronal lineage regulator 	(666)
	Blastocyst-derived	5	From derivation/thawing	<ul style="list-style-type: none"> • Imprinted region DLK1-DIO3 frequently silenced during culture due to hyper-methylation • When lines were derived and maintained at 5 kPa, gene products from this regions (MEG3 and SNORD114-3) were still highly expressed • Re-exposure to room air caused rapid downregulation of these gene products and methylation of their promoters • Greater genomic stability when cultured and maintained at 5 kPa O₂ 	(665)
	Shef3 and Hues-7	5	Minimum of 3 passages	<ul style="list-style-type: none"> • ↑ GLUT3 expression and membrane localisation • GLUT3 mRNA positively correlates with OCT4 mRNA • Changes in GLUT3 expression may underlie changes in lactate/glucose consumption 	(83)
Mouse	D3	4	9	<ul style="list-style-type: none"> • mESC cultured at 4 kPa for 9 days and then back to room air for 5 more. Early culture at 4 kPa O₂ increased differentiated cardiomyocyte yield 	(30)
	stem cell (fresh)	5	28	<ul style="list-style-type: none"> • More outgrowths from blastocysts and increased proliferation with more alkaline phosphatase activity in outgrowths 	(176)
	stem cell (fresh)	5	from blastocyst isolation	<ul style="list-style-type: none"> • ↑ overall cellular yield • ↓ ROS production (measured using DCF fluorescence) • combination of low O₂ and physiological levels of glucose (100mg/dL) optimum for yield 	(629)
	CCE and D3 mESC	0, 1, 5, 20 and 40	Up to 25	<ul style="list-style-type: none"> • Mathematical modelling of PO₂ at the cell layer • ↑ proliferation at 5 kPa vs room air • Very low O₂ levels (<1 kPa) ↓ pluripotency genes (Oct4, Nanog, Sox2) and at 40 kPa 	(467)
	D3 mESC	3.5	12	<ul style="list-style-type: none"> • Greater degree of differentiation into dopaminergic neuronal precursor cells at low O₂ and with greater yield 	(300)

Mouse	iPSC (MEF)	5	up to 30	<ul style="list-style-type: none"> • ↑efficiency of pluripotency induction and ↑yield. Observed with both viral and non-viral transfection methods • no change in proliferation • ↑57.2% ESC-specific genes, ↓67.5% fibroblast-specific genes. Demonstrates efficiency in differentiation 	(678)
	R1	1, 2, 4, 8	7	<ul style="list-style-type: none"> • Production and secretion of Flt-1 and VEGF change temporally over 7 days and at low O₂, driving ESC into either hematopoietic or endothelial lineages at different time points • Colony formation greatest at 2-4 kPa O₂ and lowest at 1 and 20 kPa 	(473)
	E14Tg2a mESC	2	8	<ul style="list-style-type: none"> • Increased viability during 8 days of differentiation • ↑ neuronal stem cell differentiation. • Valuable data on dissolved PO₂ in culture 	(404)
	E14Tg2a mESC	2	8	<ul style="list-style-type: none"> • Highest number and diameter of neural bodies (rosettes) between 4-10 kPa O₂, with the greatest number of viable cells • Greatest number of neuronal precursor cells observed at 4 kPa O₂ • Increases from 2-4/6 kPa O₂ associated with ↑ total yield 	(403)
	R1 129/Sv (ESC) MAR B6D2 F1 (ESC)	5	3	<ul style="list-style-type: none"> • ↑apoptosis • ↑proliferation • ↑ROS generation (measured using DCF fluorescence) • ↓cardiomyocyte differentiation 	(475)
	E14Tg2A (ESC) iPSwt4F (iPSC)	5	up to 12	<ul style="list-style-type: none"> • ↑embryonic body formation • ↑expression of NKx2.1 and FOXA2, markers of endodermal and early lung epithelial lineages • ↑differentiation into early pulmonary lineages following stimulated differentiation 	(173)

Abbreviations: ESC, embryonic stem cell; ROS, reactive oxygen species; DCF, dichlorofluorescein; OCT4, octamer-binding transcription factor 4; Flt-1, vascular endothelial growth factor receptor 1; KDR, kinase insert domain receptor/vascular endothelial growth factor receptor 2; DPI, diphenyleneiodonium; EC, endothelial cell; NKx2.1, NK2 Homeobox 1; FOXA4, forkhead box protein A2; iPSC, inducible pluripotent stem cell; HES5, Hes Family BHLH Transcription Factor 5; FOXG1, forkhead box protein G1; HIF, hypoxia-inducible factor; MYC, v-Myc avian myelocytomatosis viral oncogene homolog; DLK1-DIO3, delta-like homolog 1- type III iodothyronine deiodinase gene cluster; GLUT, glucose transporter.

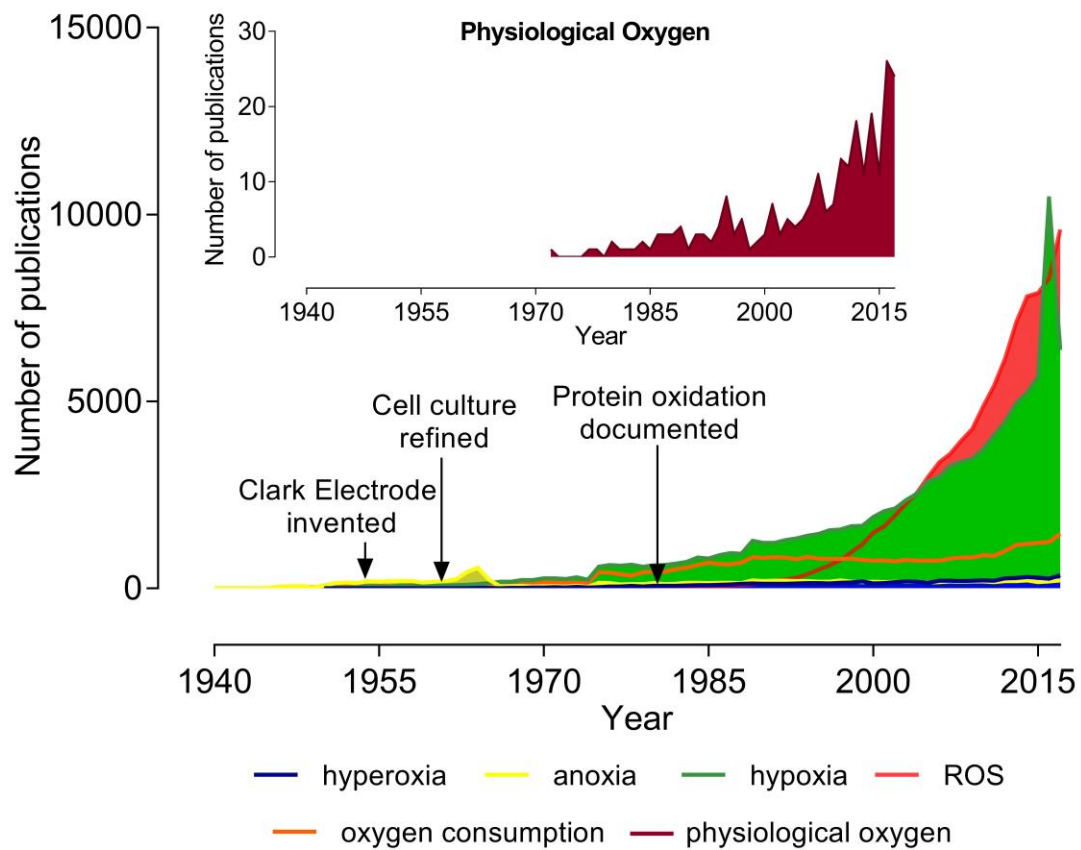


Figure 1

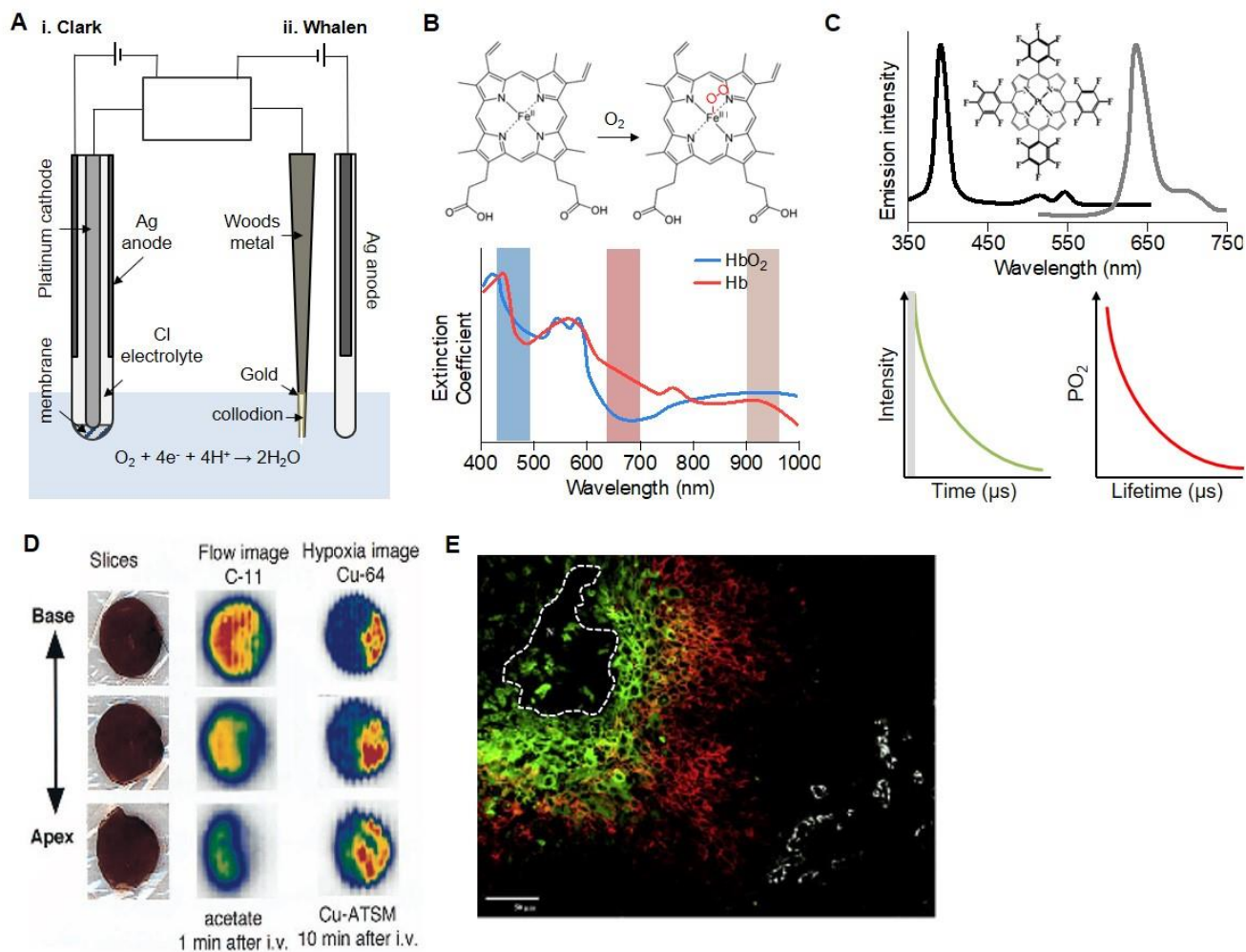


Figure 2

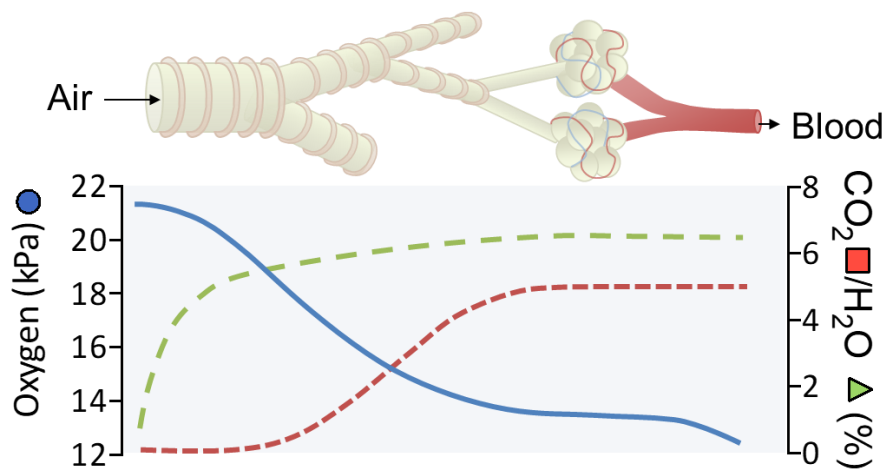


Figure 3

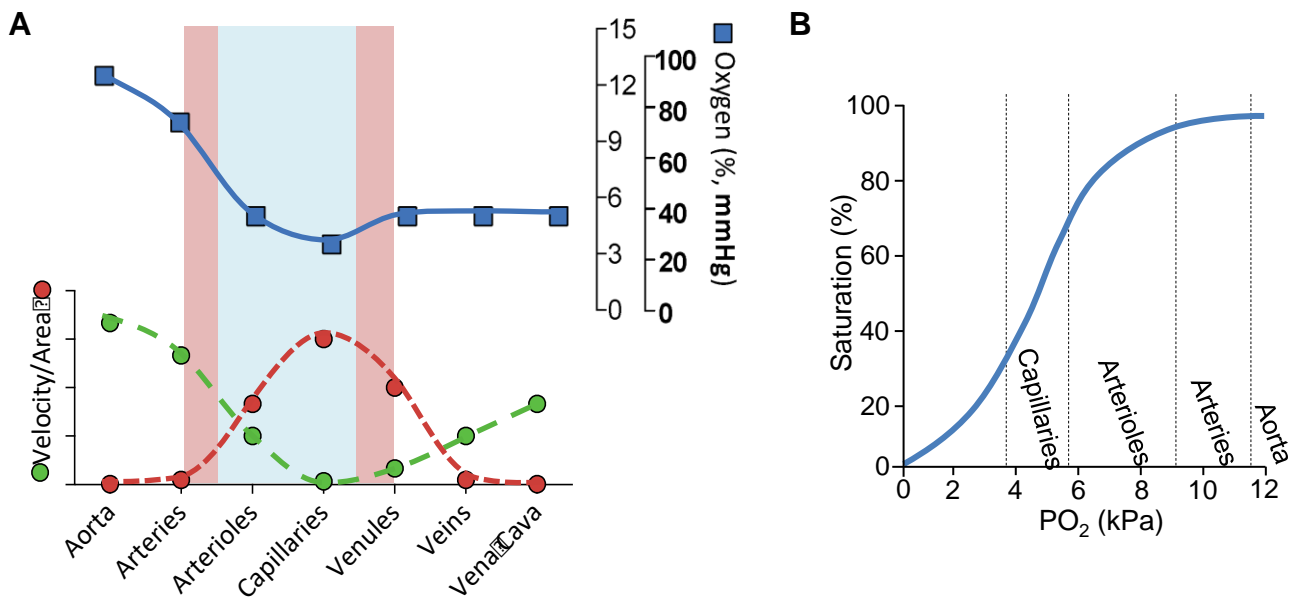


Figure 4

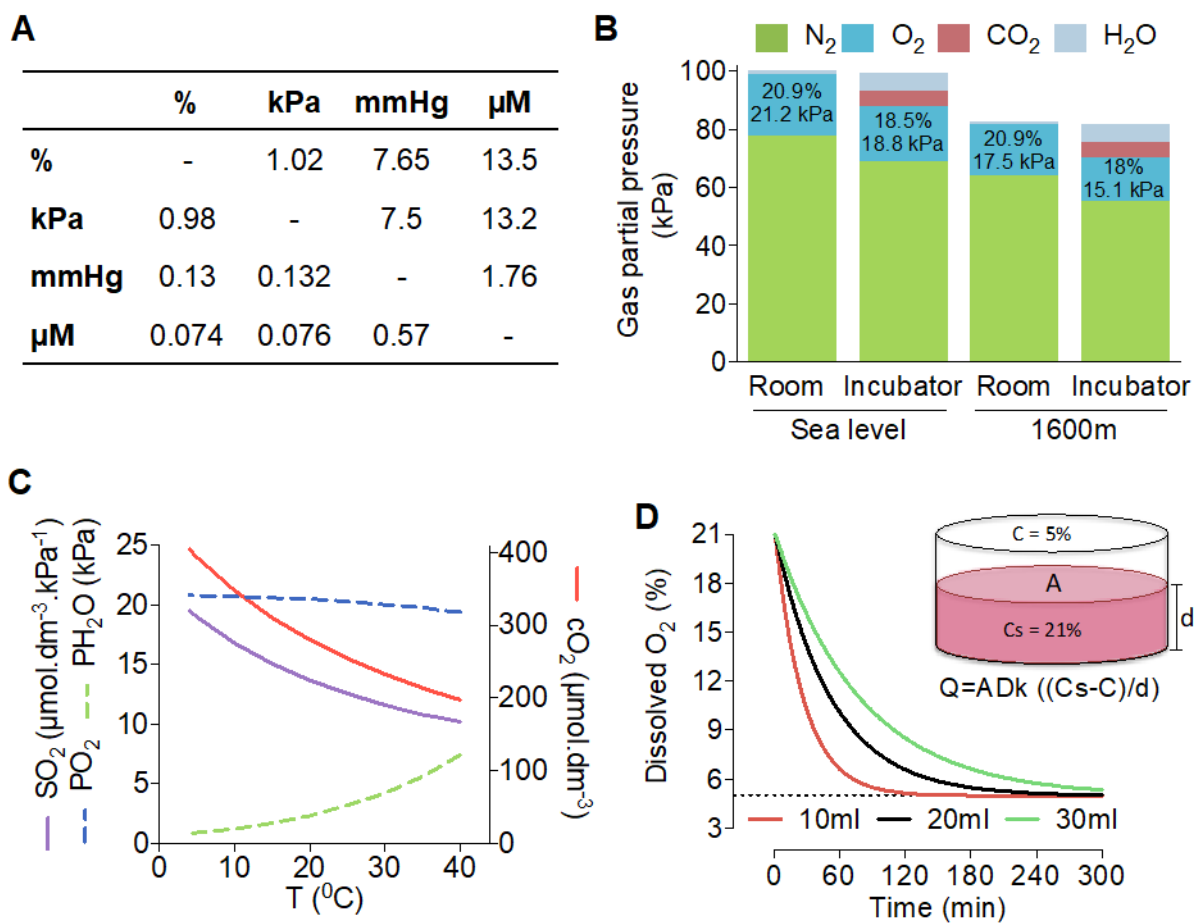


Figure 5

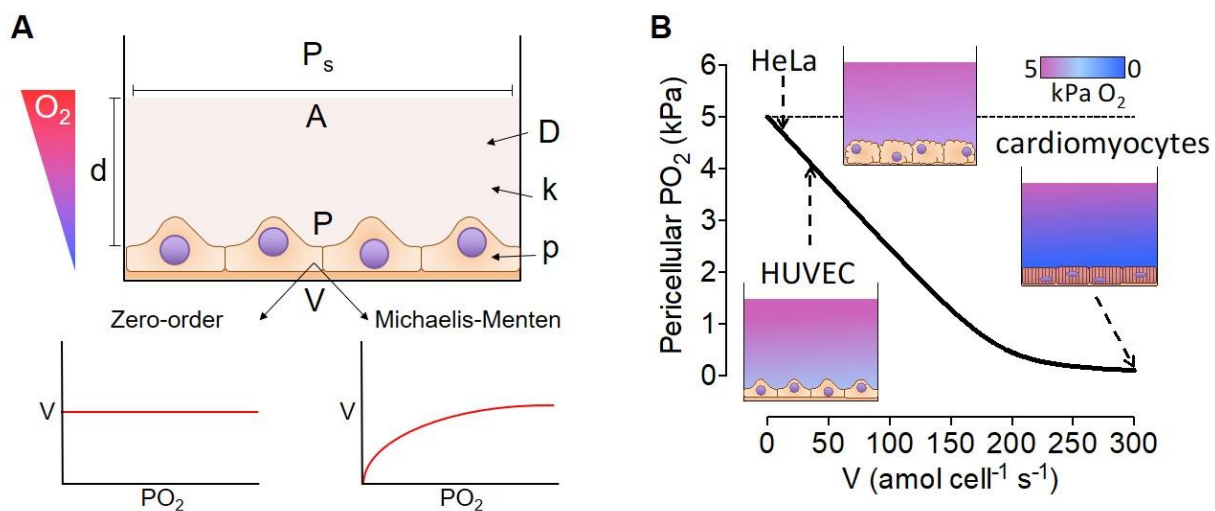


Figure 6

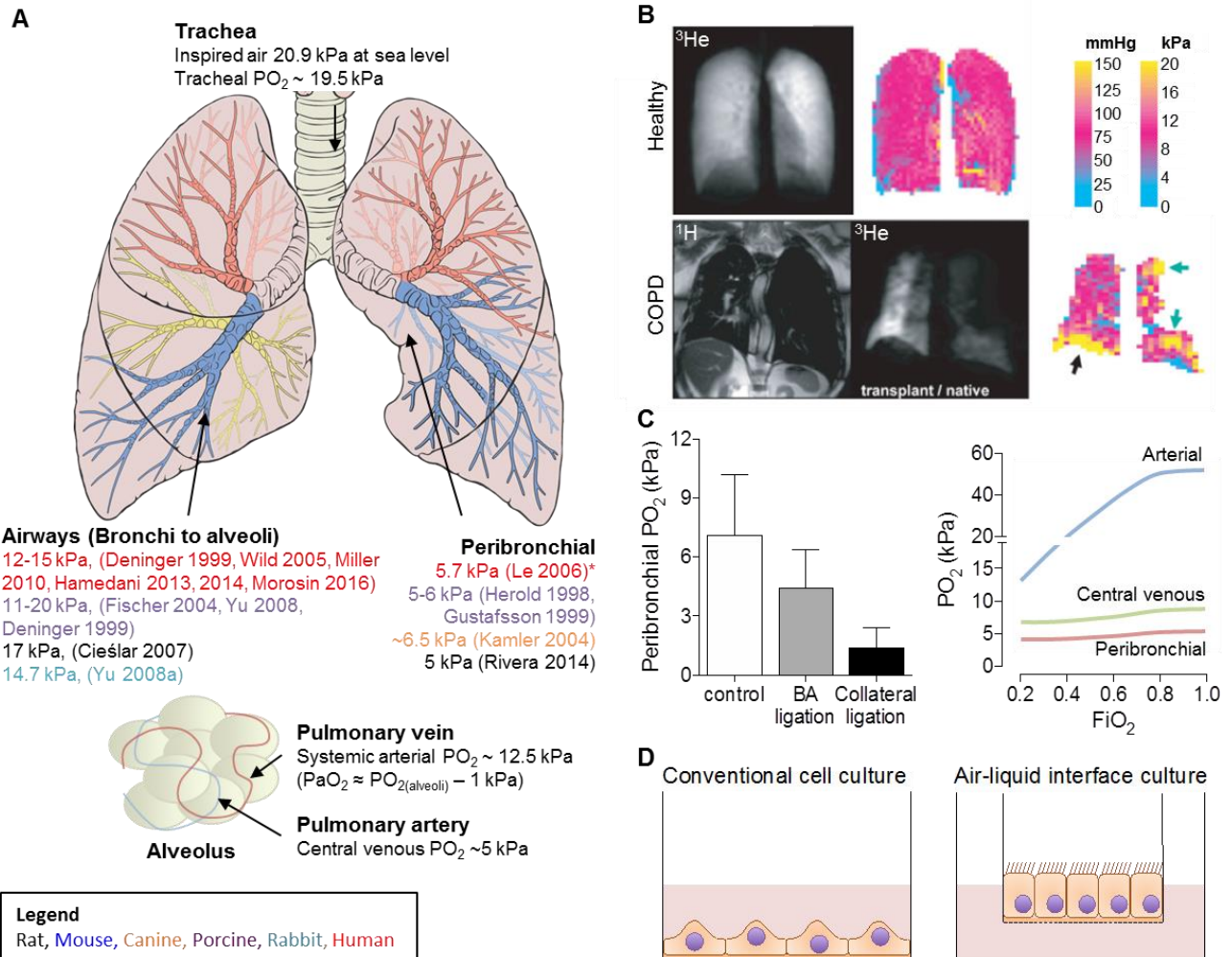
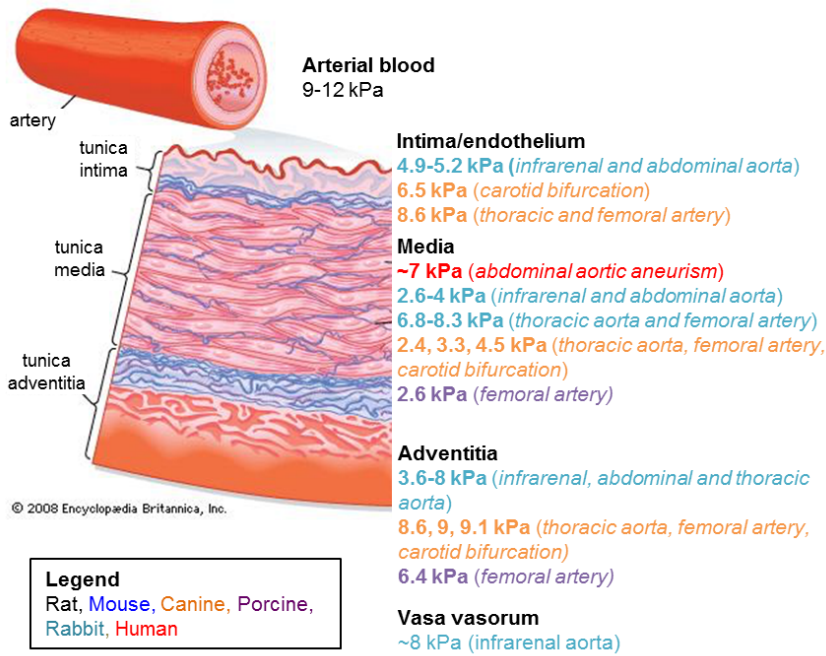
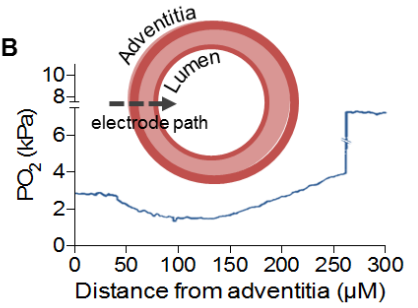


Figure 7

A



B



C

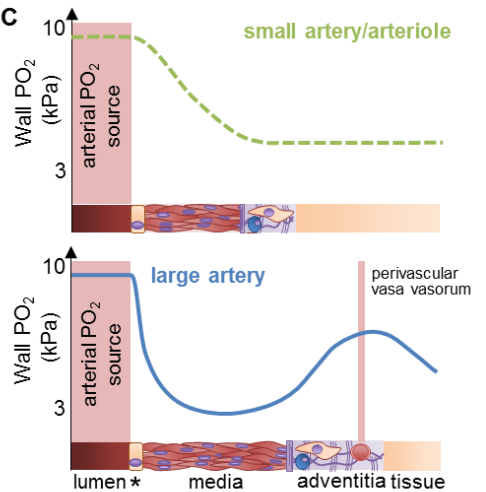


Figure 8

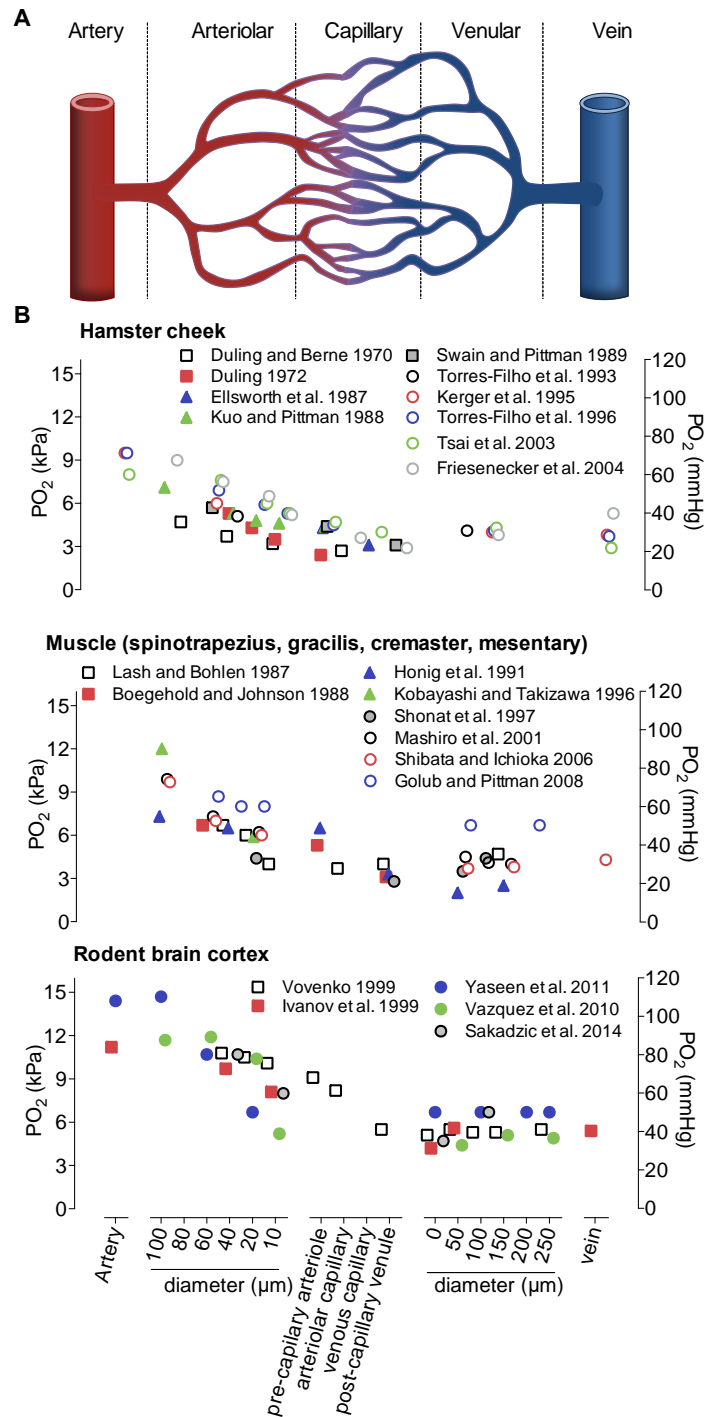


Figure 9

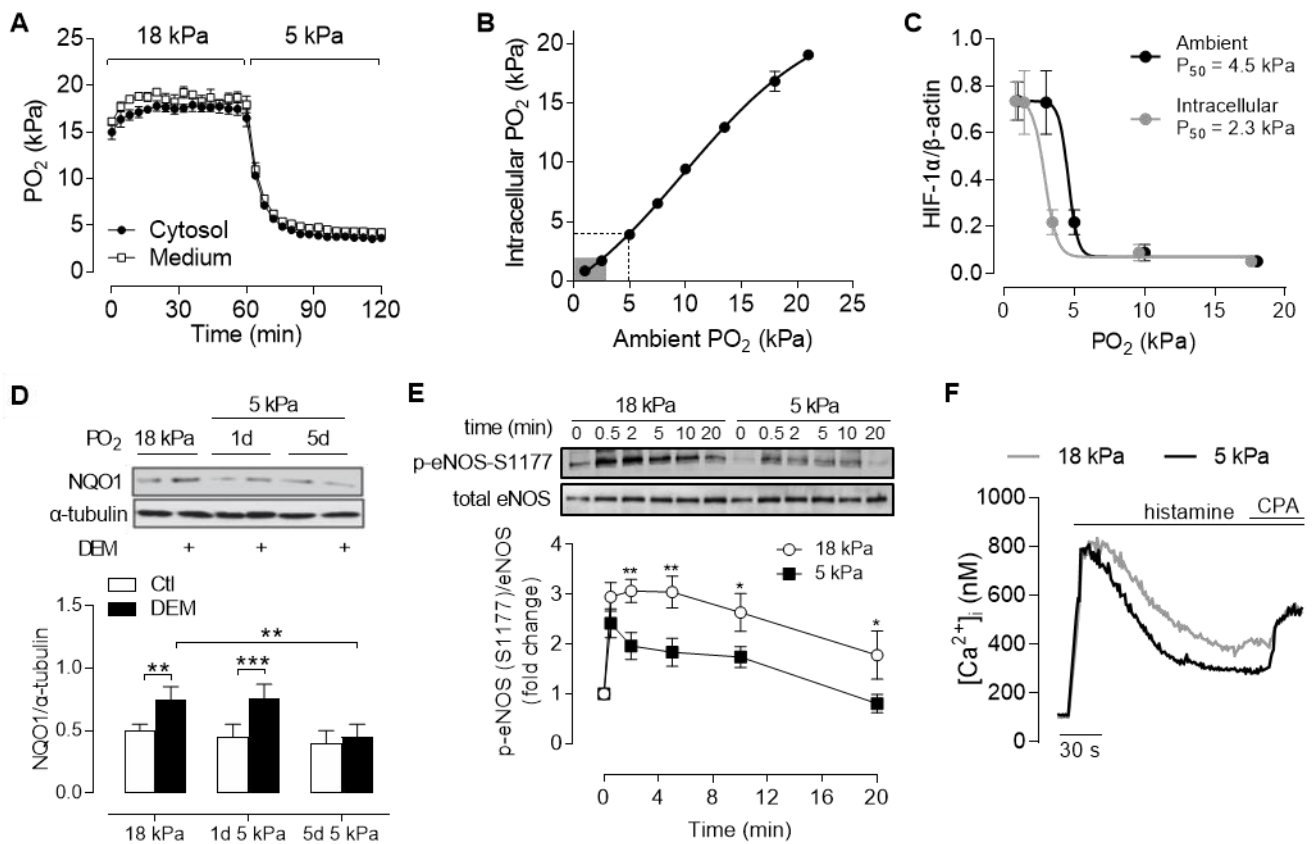


Figure 10

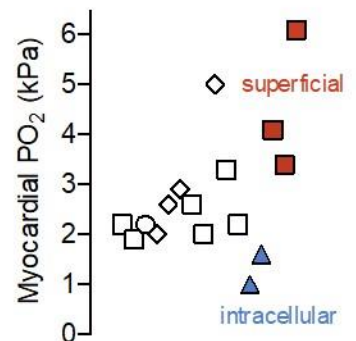
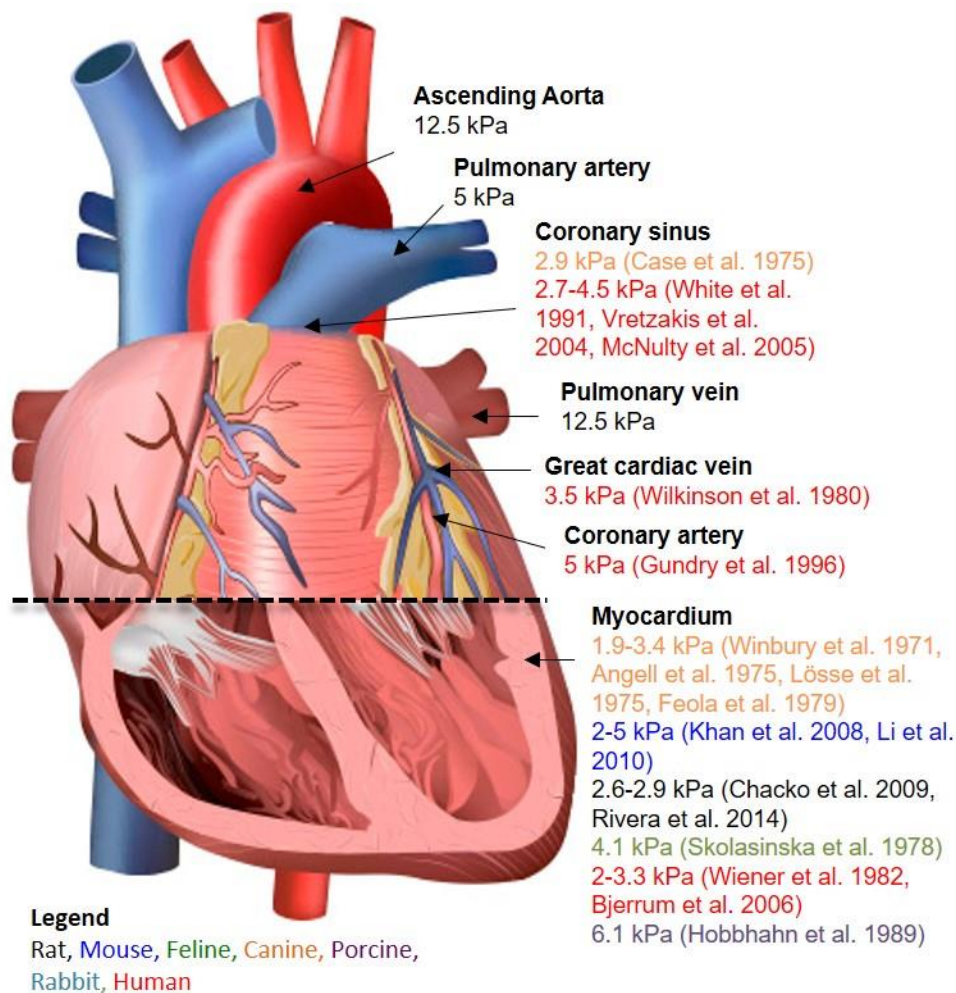


Figure 11

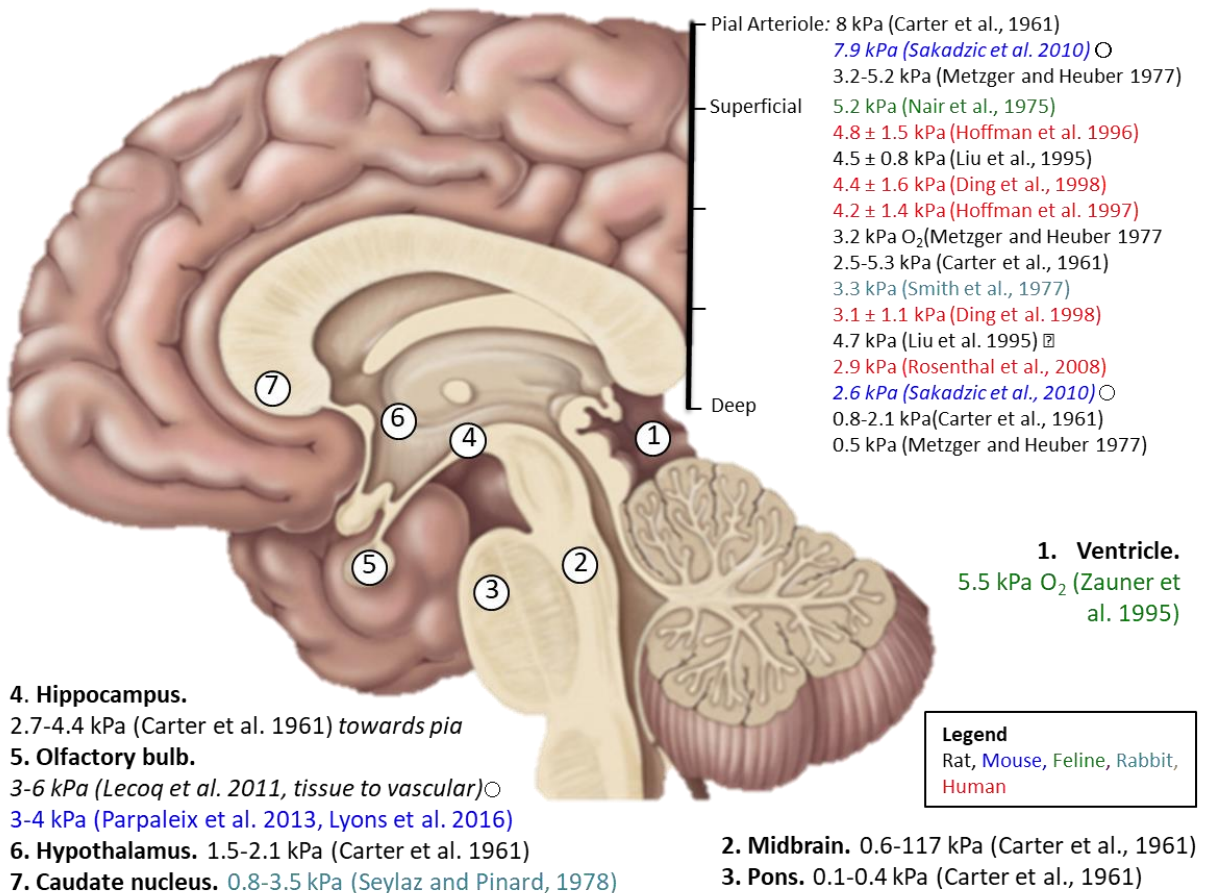


Figure 12

Parenchyma

3.9 kPa* (Soini et al., 1992)
4.7-5.6 kPa (Dardzinski and Sotak, 1994)
7.3 kPa (Leary et al., 2002)
4.1 kPa (Brooks et al., 2004)
4.5-5.5 kPa (Brooks et al., 2007)

Hepatic vein

4-4.7 kPa (Wolfe et al., 1983)
6.3 kPa (Sezai et al., 1993)
4 kPa (Tygstrup et al., 1962)

Hepatic artery

12.2 kPa (Sezai et al., 1993)

Portal vein

6.4 kPa (Tygstrup et al., 1962)
6.8 kPa (Sezai et al., 1993)
6.5-8 kPa (Wolfe et al., 1983)

Legend

Mouse
Porcine
Human

Portal triad

8.7 kPa (Wolfe et al., 1983)

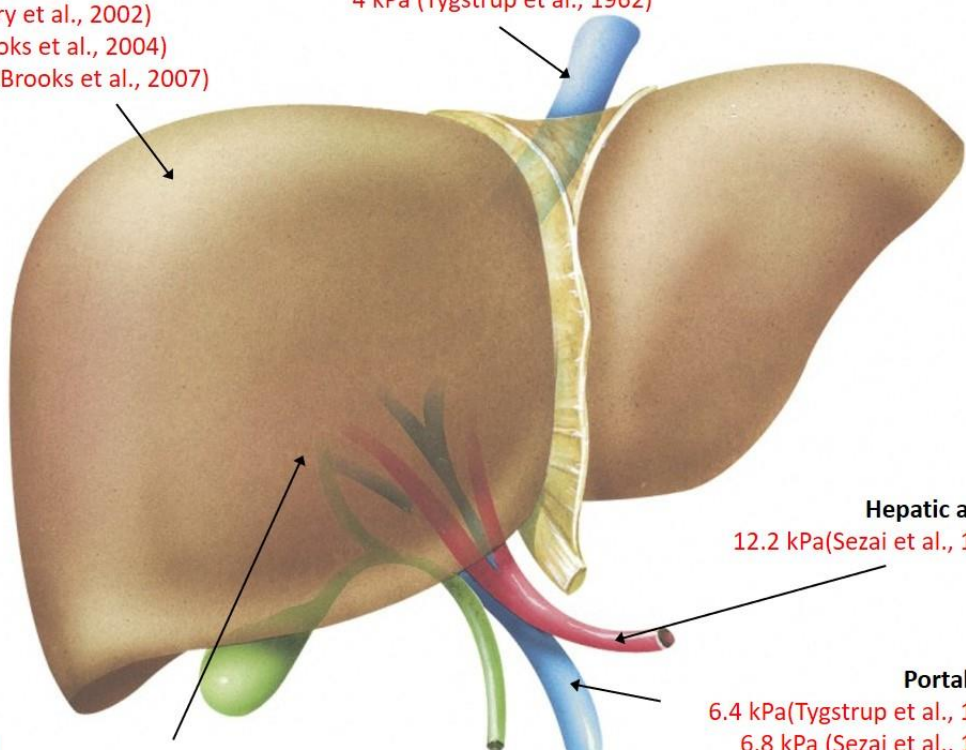


Figure 13

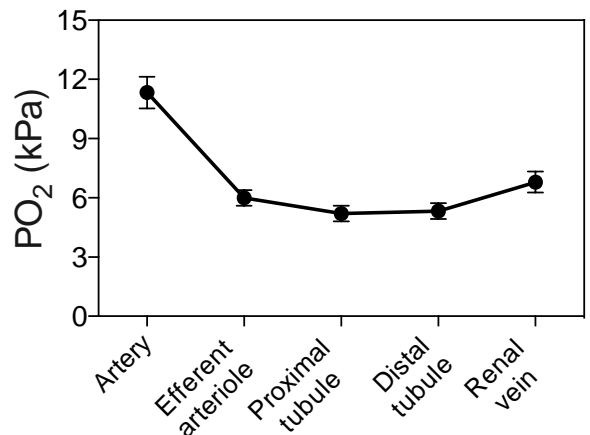
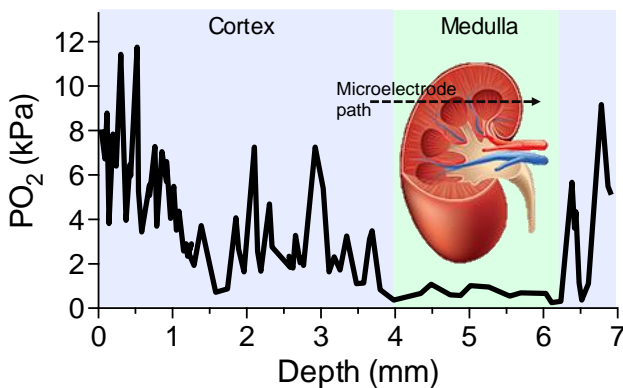
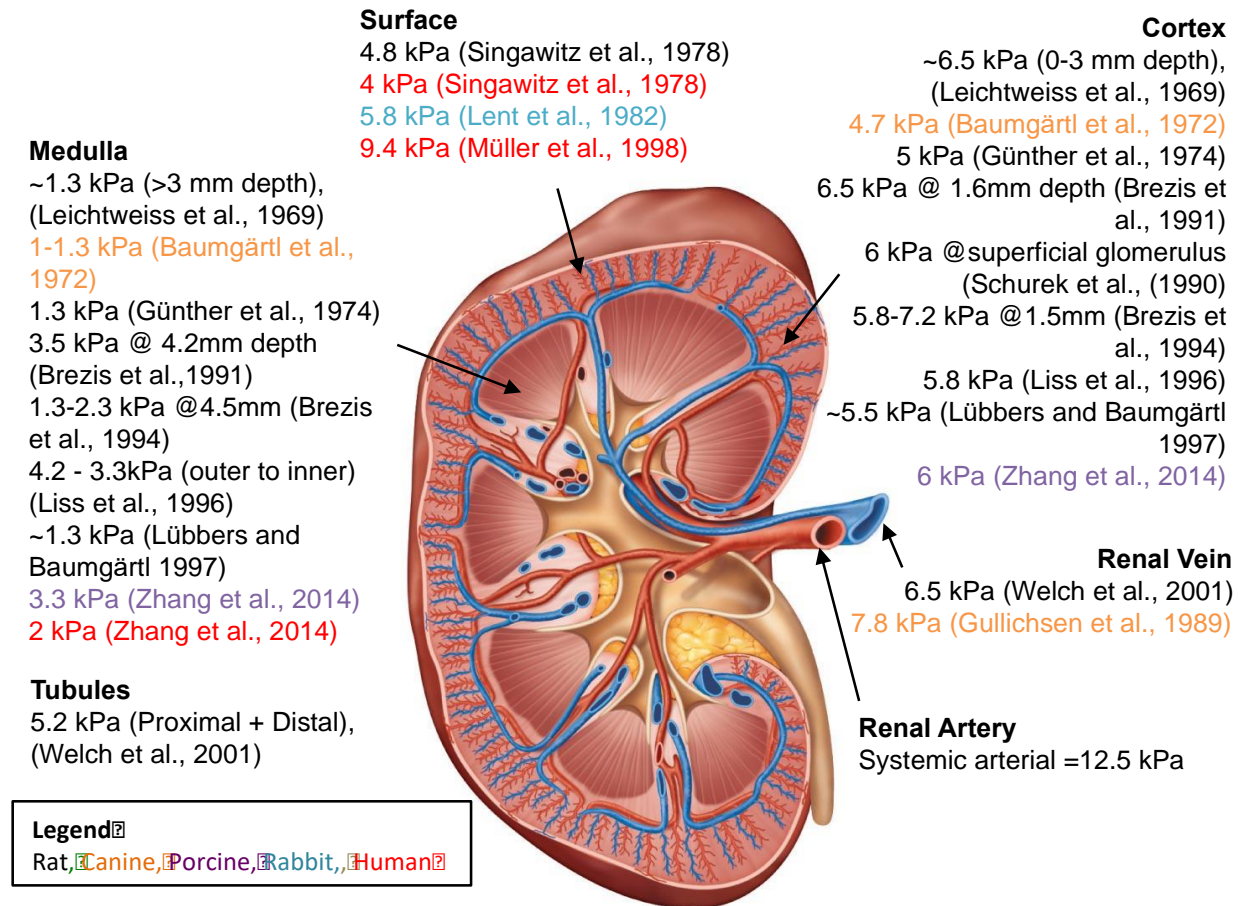


Figure 14

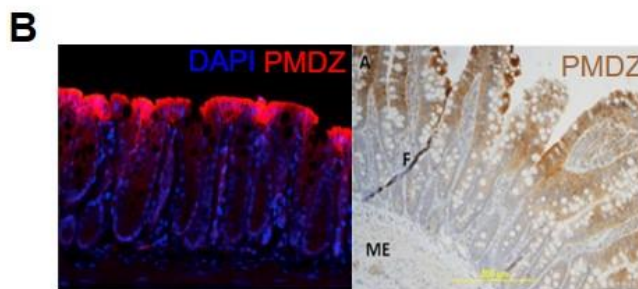
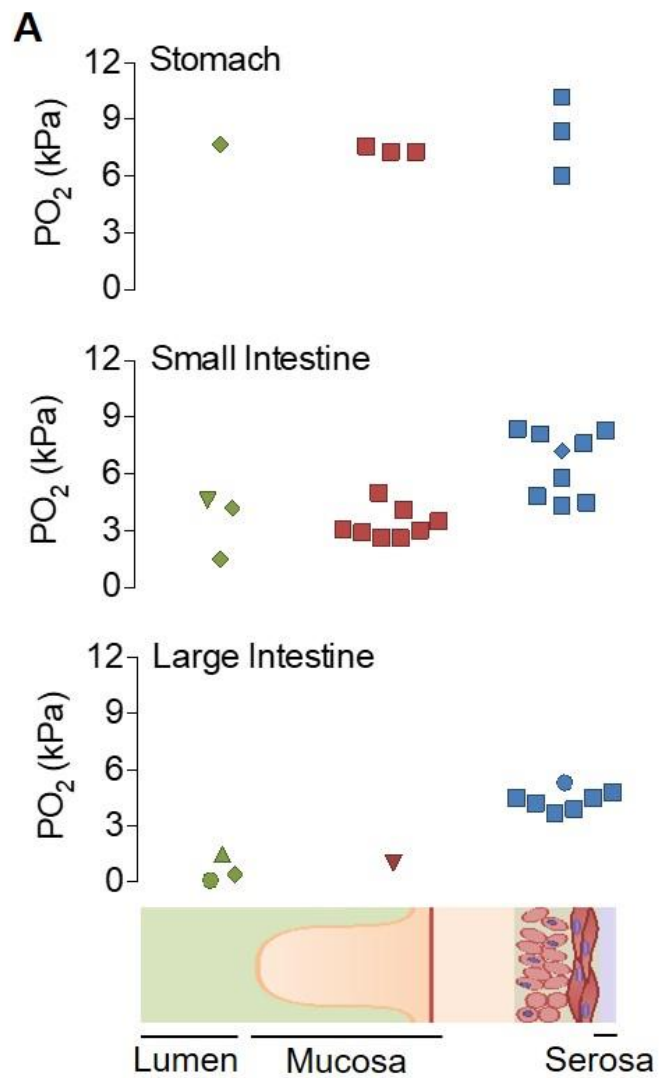


Figure 15

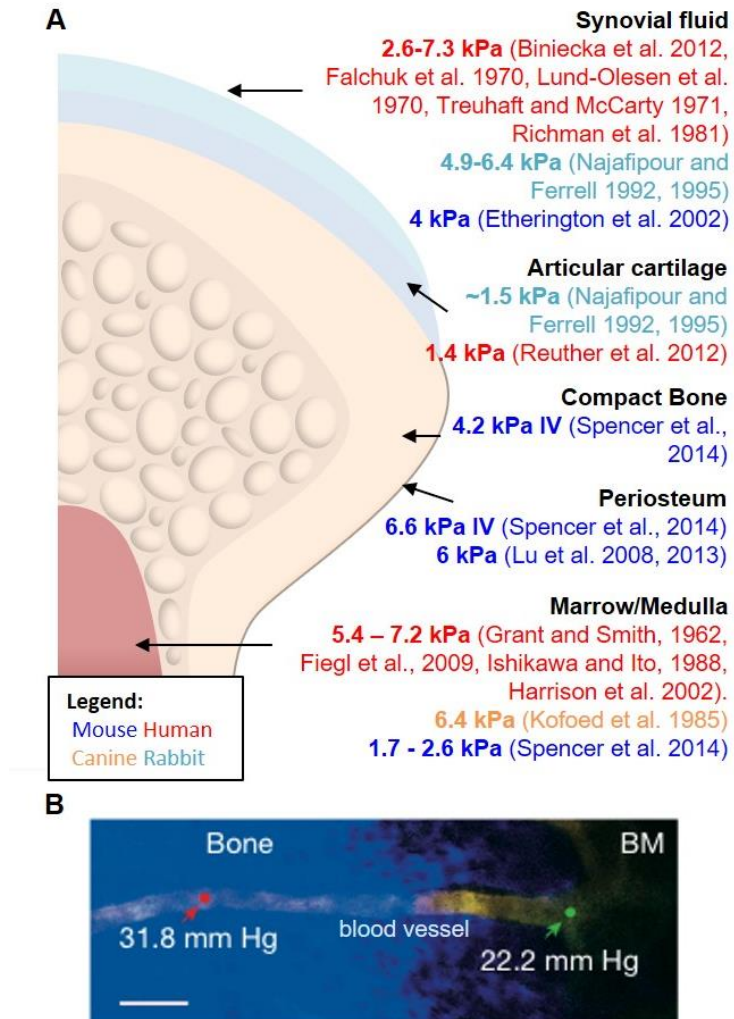


Figure 16

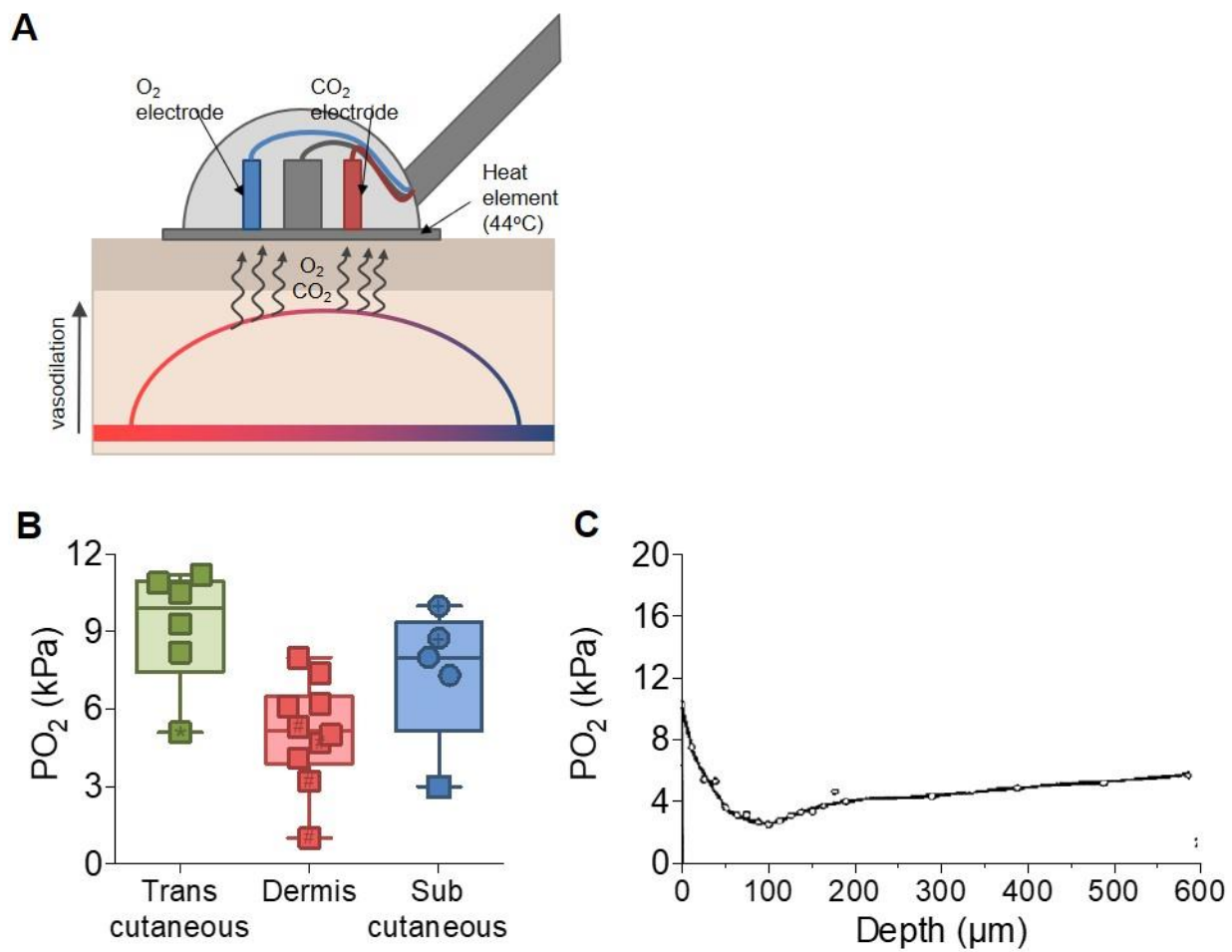


Figure 17

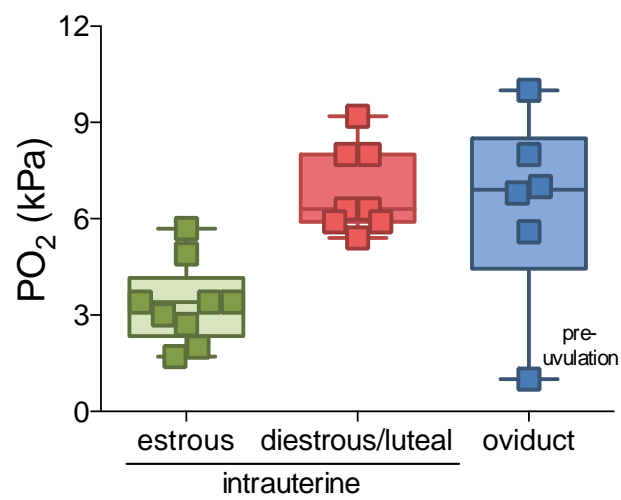


Figure 18